AD-A031 506 GENERAL ELECTRIC CO SYRACUSE N Y HEAVY MILITARY ELEC--ETC F/G 17/1
COMPUTER-AIDED DETECTION STUDY.(U)
JUL 66

UNCLASSIFIED NOBSR-93298

NL

1 OF 2
ADA031506

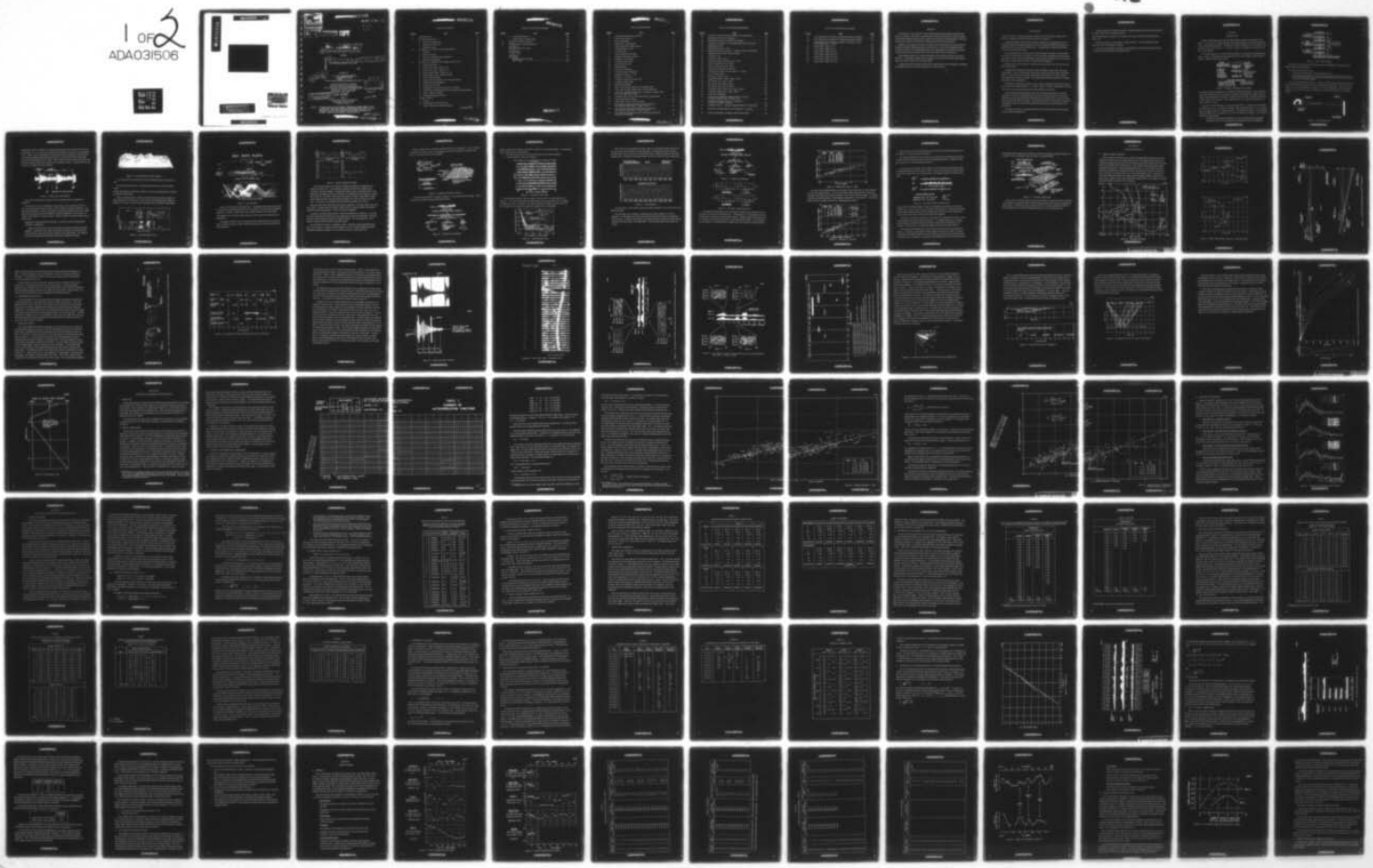

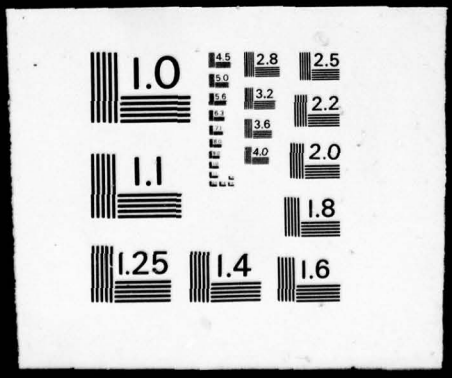

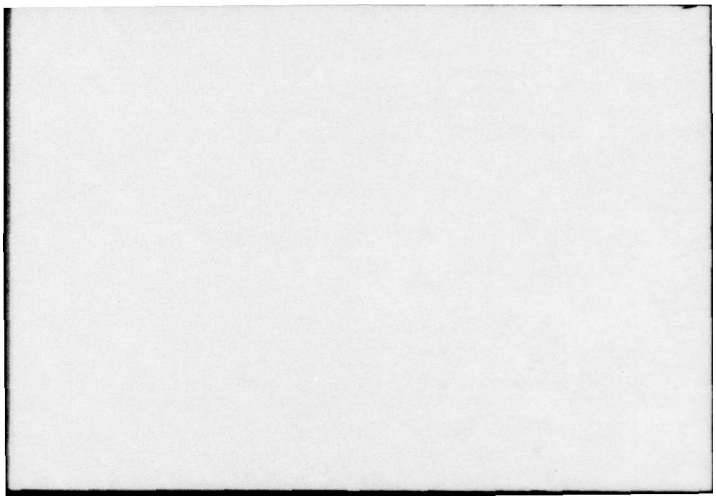

COMPUTER-AIDED DETECTION STUDY. (U)

(6)

FINAL
REPORT

(9) Final rept. for period ending 1 Jul 66.

FOR PERIOD ENDING 1 JULY 1966.

000244

C

(12) 173p.

FUNDED BY

U.S. NAVY BUREAU OF SHIPS
Contract NObsr-93298 (15) new

General Electric Company Requisition EH-88170

ADVANCE SONAR DEVELOPMENT
ADVANCE PROJECTS OPERATION
HEAVY MILITARY ELECTRONICS ~~DEPARTMENT~~ Systems
GENERAL ELECTRIC COMPANY
SYRACUSE, NEW YORK 13201

(11) July 1966

TABLE OF CONTENTS

660830-0285

TABLE OF CONTENTS (concluded)

LIST OF ILLUSTRATIONS

LIST OF ILLUSTRATIONS (continued)

LIST OF ILLUSTRATIONS (concluded)

ABSTRACT

A nominally one-year program to study single ping clustering techniques for advanced sonars is complete. Sonar data, recorded at sea, have been processed on a digital computer and the results studied to deduce both a model of the processor output and features of the data that might be useful as discrimminants between noise and target output signals.

Statistics of the output of the linear correlator have been collected for various intervals for about 200 pings, both bottom bounce and surface duct. Plots of the standard deviation versus the mean and of the standardized forms of the third and fourth moments show extremely high correlation for nontarget intervals for both modes and for various days.

The Rayleigh model is not a suitable description of the statistics of many of the output intervals. The statistics of these intervals appear to vary as much from one interval to the next in one return as they vary from ping to ping.

An energy detector has been simulated and its output plots have been studied in an attempt to establish the source of the reverberation as a function of time.

CONCLUSIONS

WE DO NOT HAVE A GOOD ANALYTICAL MODEL FOR THE LINEAR CORRELATOR OUTPUT, EITHER FOR NOISE INTERVALS OR FOR TARGETS.

An analytical model of the linear correlator, especially for nontarget intervals, is absolutely essential for detection studies, since it provides the essential relationship between false alarm rate and the threshold level. It appears that a simple model of good accuracy may not be easy to find.

We are optimistic that continued study of the character of the input to the correlator will reveal a useful model; for example, it may be possible to satisfactorily characterize the statistics of the correlator output when it is normalized with respect to the input amplitude and for various types or sources of reverberation background.

IT APPEARS THAT THE CAUSES OF THE GROSS FEATURES OF THE RETURN SIGNAL ARE UNDERSTOOD.

Considering the sidelobes of the beam pattern, the depth, bottom slope, and sound speed profile, it can be calculated that the scattered returns from the surface and bottom arrive at times which are concurrent with features of the data that are quite consistant from ping to ping; features incidently, which appear both within and outside the 10-second interval which has been studied.

We desire to classify the correlator input in order to determine if the output statistics are a function of the type of input; i.e., surface, bottom, or volume reverberation or noise.

THE MEAN AND STANDARD DEVIATION ARE STRONGLY RELATED.

For the nontarget intervals studied, the mean and standard deviation are strongly correlated. The ratio of standard deviation to mean is quite constant for all of the nontarget intervals for both surface duct and bottom bounce modes and for various time intervals in many of the surface duct pings. The data for various runs are somewhat clustered about absolute values of the mean and standard deviation which are quite different from one another.

The value of this ratio is approximately that which it would have been were the data to have a Rayleigh distribution.

For those cases where data from intervals containing target echoes have been processed, the value of this ratio is markedly different.

THE STANDARDIZED FORMS OF THE THIRD AND FOURTH MOMENTS ARE STRONGLY RELATED.

The same comment as above applies to these statistics. The only difference is that these are a little more abstract statistics.

In this case the Rayleigh distribution is represented by a point on the plot which lies on or quite near the regression line through the data.

SECTION I

INTRODUCTION

Computer-Aided Detection is the long range objective of the work described in this report. The intent is to study methods and develop techniques to assist the sonar operator to make detection decisions. An objective is to find methods to use the computer to do clerical work for the operator; i.e., for ways to reduce, consolidate, or summarize the data for the operator.

This report describes work toward the development of a single ping thresholding technique. Figure 1, illustrating the many aspects of the overall Computer-Aided Detection problem, indicates where this work fits.

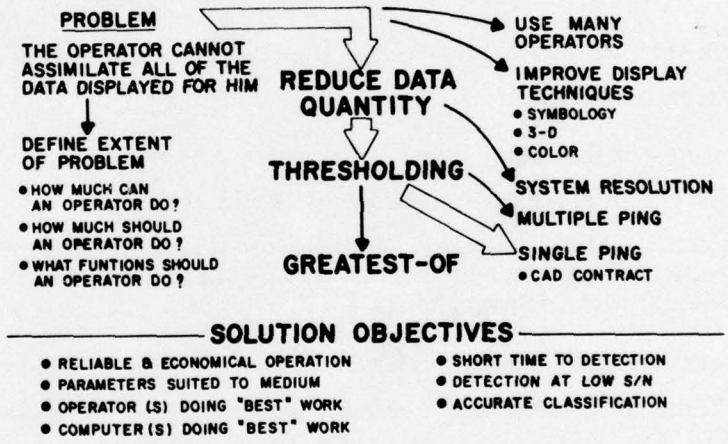

Figure 1. Computer-Aided Detection Problem

This effort concerns development of a single ping clustering technique. This technique is based upon the concept that the computer can consider (according to its design) the many outputs of signal processors relevant to a specific volume of sonar coverage and generate a single output for the operator, which might represent, for example the probability of a target within this volume.

Figure 2 is a block diagram of a computer-aided system. Although several different processors are shown, one might just as easily think of this approach as a way to combine the many doppler outputs of a single processor. This diagram is vague: it is not known at this time either what processors to use or how to combine their outputs. It is desired to illustrate the concept that:

> Arithmetic processing of measuremens made on the data output of the signal processor(s) can be used to reduce the total quantity of data to be displayed.

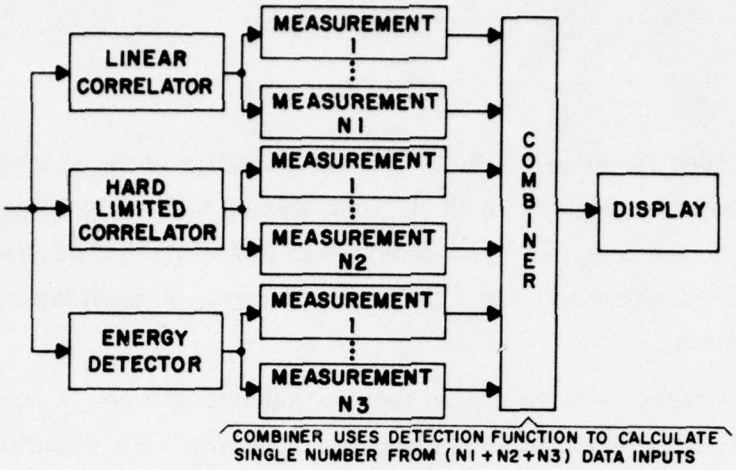

Figure 2. System Block Diagram

We believe that, by cleverly selecting the data to be displayed, the operator may be helped to make an early detection.

The objectives of this study are:

1. To analyze in depth certain recorded sonar data, and
2. With mathematical functions, to describe the statistical distribution of that data and computed parameters (discriminants) derived from that data for the two cases of with and without target signal.

The approach described is empirical. Actual AN/SQS-26 sonar outputs recorded at sea aboard USS Wilkinson working with a submarine target are being used. Most of the work centers around two experiments of December 1963. Both experiments were run as shown in Figure 3: the submarine made an octagonal run while the ship steamed on a straight course.

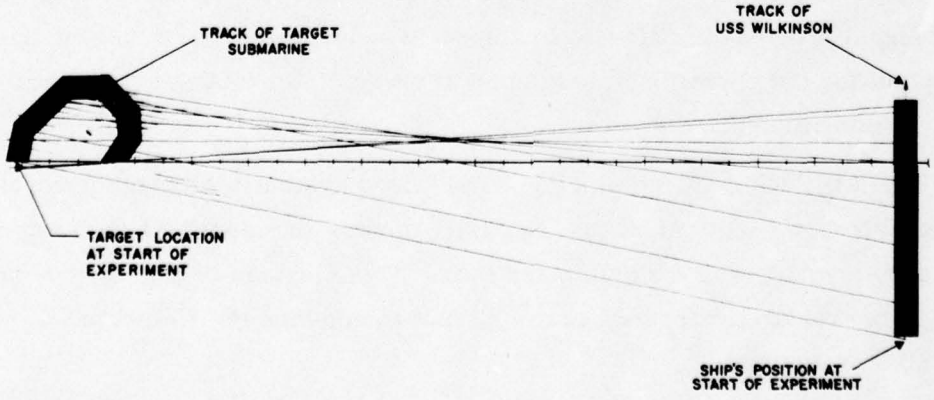

Figure 3. Plot of Experiment

During these runs the AN/SQS-26 was operated in the bottom bounce mode to allow coded transmission, but, at 0° depression angle to take advantage of the surface duct propagation mode. Figure 4 shows schematically an excerpt from the ping sequence, typically linear FM and Psuedo-Random FM (PRFM) interspersed, and shows the portion of the PRFM pings which were digitized for this study. These data have been processed on the IBM 7094 computer and plots of the output waveforms are available to study. An energy detector and the linear correlator have been simulated.

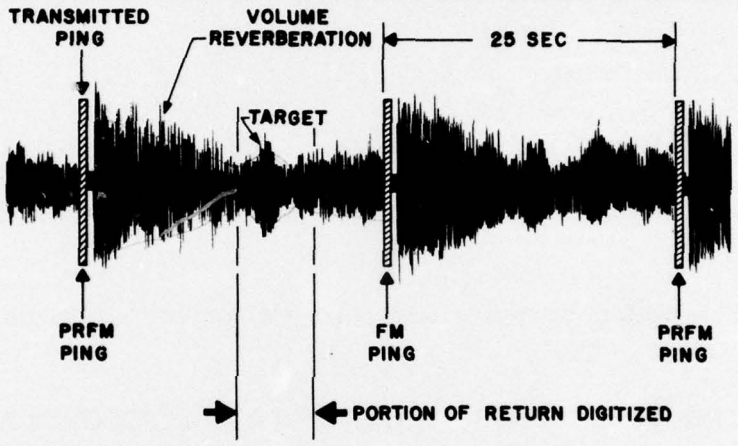

Figure 4. Excerpt from Ping Sequence

Plots of the energy detector output for the 200 digitized pings are presented in Appendix A.

The first two runs were separated by only two days; they were made in the same area, sound conditions were quite similar, and the weather was good on both days -- yet they look quite different. Some of the features of these ping sequences which have caused particular interest are the obvious difference in general appearance, the occurence of "bumps" and "wiggles" in consecutive pings, and the existence of possible bottom bounce target echoes.

THERE MAY BE SOME BOTTOM BOUNCE OR TRIANGULAR PATH ECHOES IN THE REEL 6 SEQUENCE.

Figure 5 is a picture of a three-dimensional model that was made of the Reel 6 sequence. The plots for this model were made so that they all have the same full scale value; this value was fairly low compared to the target peaks. This clips the tops from the target peaks and enhances the smaller wiggles and bumps.

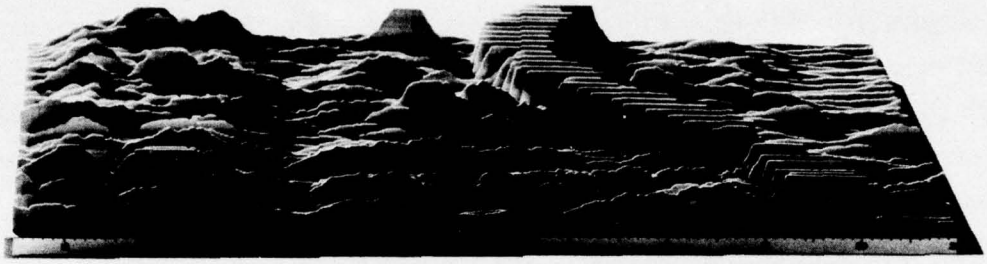

Figure 5. Three-Dimensional Model of Reel 6

It is obvious that the noise does not really vary greatly from one ping to the next.

The possible bottom bounce or triangular path echoes are in the back right corner.

THERE ARE RIDGES OR BUMPS AT ABOUT 13 AND 15 SECONDS WHICH APPEAR IN ALMOST EVERY PING.

Figure 6 illustrates this in another way and also shows that these ridges are quite prominent in the Reel 9 data. There seems little doubt that these ridges are generated by surface or bottom scattered energy from the sidelobes of the pattern.

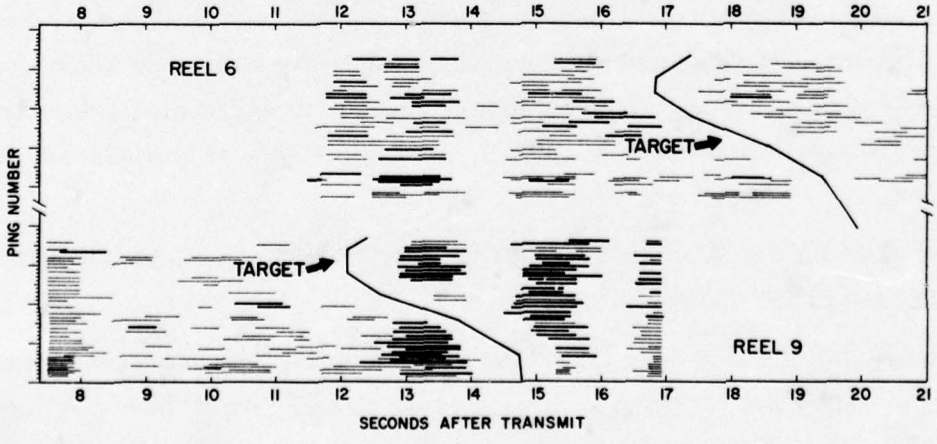

Figure 6. Composite Reels 6 and 9

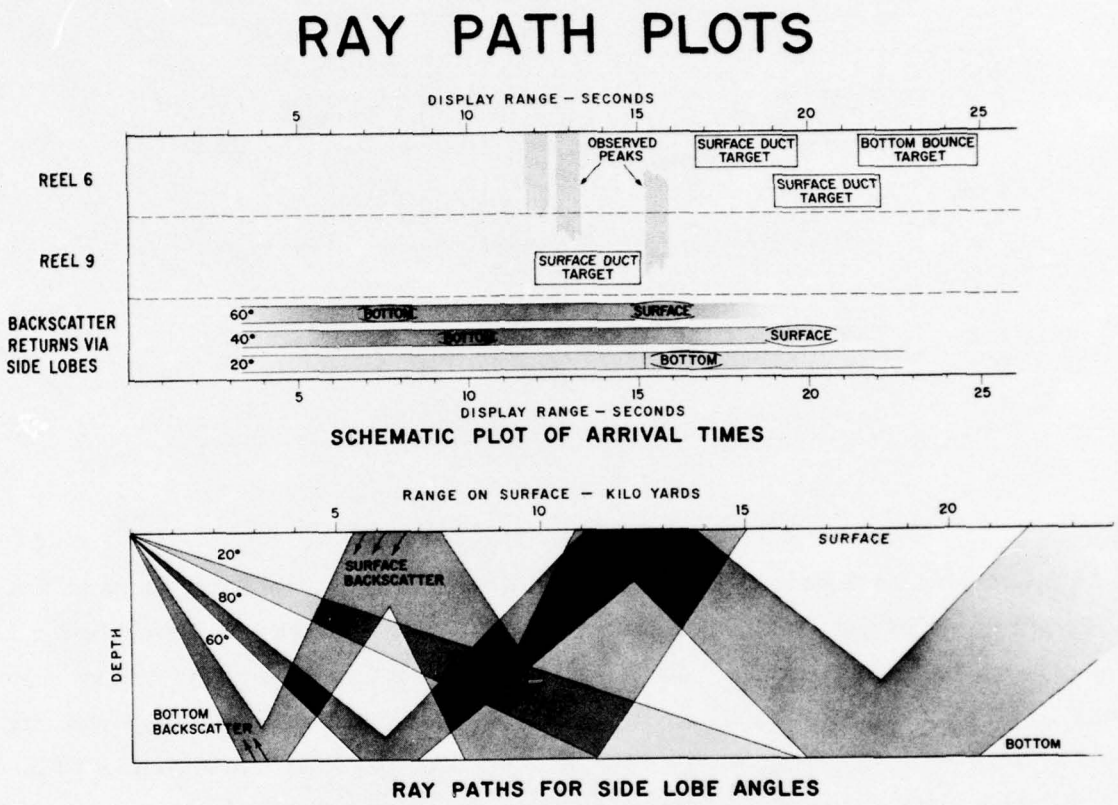

Figure 7. Ray Path Plots

Figure 7 illustrates how this might occur. Calculations based upon the data that we have, both on the radiation pattern of the AN/SQS-26 and on the sound propagation conditions, are able to confirm many of the ridges observed on the power plots.

THE SPREAD OF THE PEAK AMPLITUDES OF THE TARGET ECHOES IS QUITE DIFFERENT.

The graphs of Figure 8 show the amplitudes of the target peaks from the power plots, and also a measure of aspect which was scaled off our reconstructed plots of the experiments.

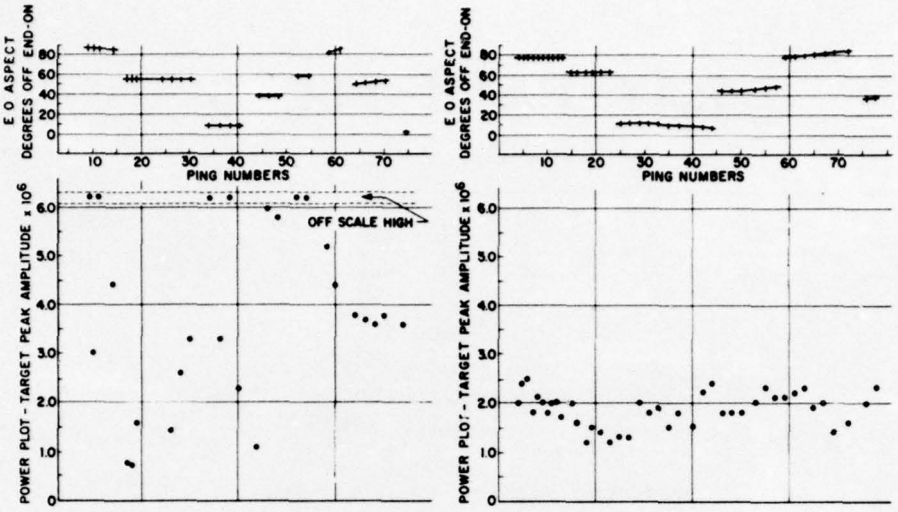

Figure 8. Target Amplitude and Aspect

A less obvious feature is the lack of correlation of target echo amplitude with a measure of target aspect. This measure of aspect was selected to enhance such a correlation, but none resulted. Considering the Reel 9 data, one observes that a more significant correlation would occur if the data were shifted five or six pings and, indeed, this is the case. Similarly, with a shift of five pings, the Reel 6 data display a significantly high correlation with this measure of aspect; this was not obvious, but is welcome. It remains to be understood why this estimate of aspect was "wrong."

There are other loose ends which have not been cleared up. This part of the work is the most recent. When the study was started, there was every reason to believe that answers would fall into place fairly easily -- that is not what has happened.

At the start, the data were processed with the simulated linear correlator. It was only as an aid to determine the target echo time that the power plots were generated. The power plots have since developed into quite an important adjunct. The main purpose is still to develop a useful model of the linear correlator output.

We had hoped to discover a relatively simple model that could be generally useful and, at the same time, could be accurate enough to serve as a basis for detection studies. Although investigation continues, it is not obvious that such a model does exist.

Figure 9 illustrates the computer simulation of the linear correlator. An AC correlator is simulated, having its output at the frequency of the sum of its inputs; the shift of this frequency from its nominal value is doppler.

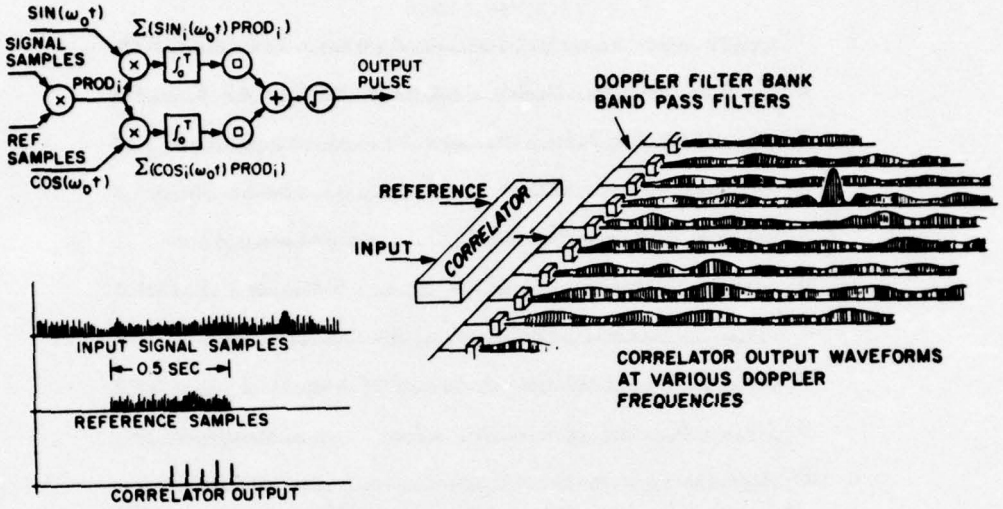

Figure 9. Computer Simulated Correlator

The first data processed as shown in Figure 10 were intervals from 10 pings. These intervals were selected to not include target returns.

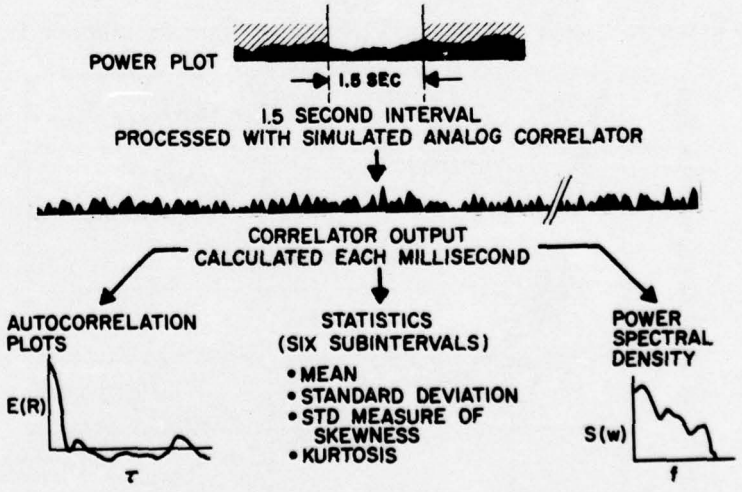

Figure 10. Preliminary Processing

Figure 11 shows the correlator output plots for these 10 1.5-second intervals. Two characteristics of the data are to be evaluated:

1. How often can the data be sampled and still have uncorrelated samples?
2. Are the statistics of the data stationary?

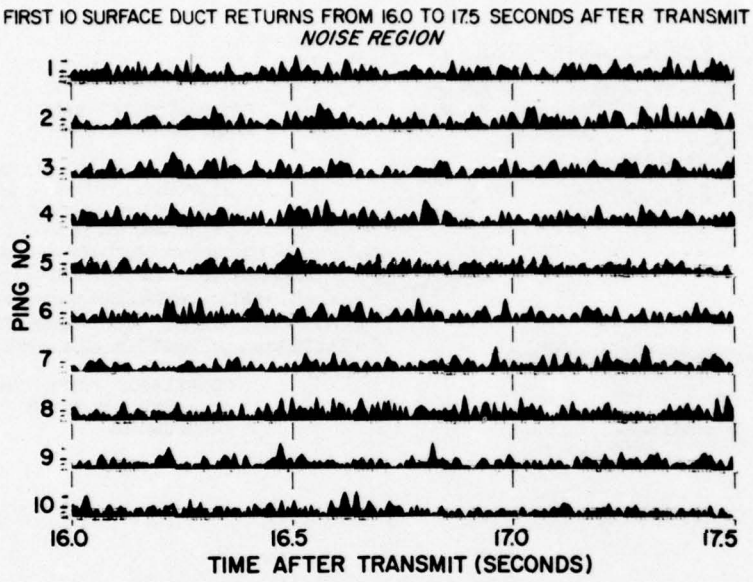

Figure 11. Correlator Output Plots

The autocorrelation plots shown in Figure 12 are for the 1.5-second intervals of Figure 11. The correlation coefficient drops rapidly until a lag of about 10 to 15 samples and after that varies considerably, but seldom exceeds the absolute value for a lag of 10. It was decided to use each tenth sample and consider them as independent.

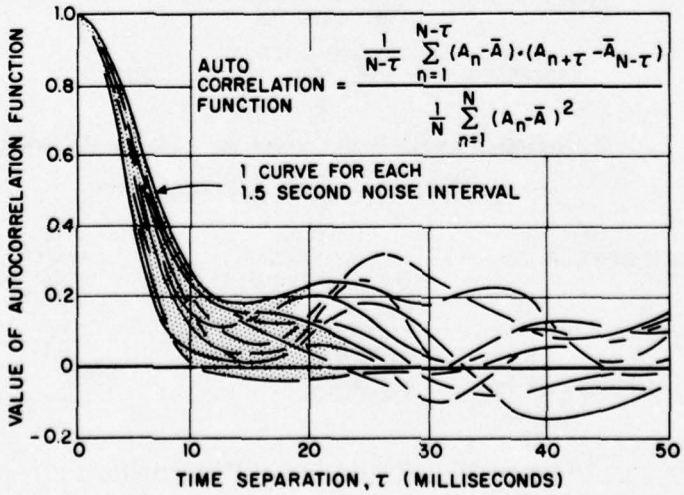

Figure 12. Autocorrelation Plots

Plots of the mean and standard deviation, Figure 13, for both the entire interval and for six quarter-second subintervals show that there is considerable variation in these statistics both within one interval and from ping to ping. Statistical tests show that these statistics are not stationary from ping to ping, and in some cases not within a single ping.

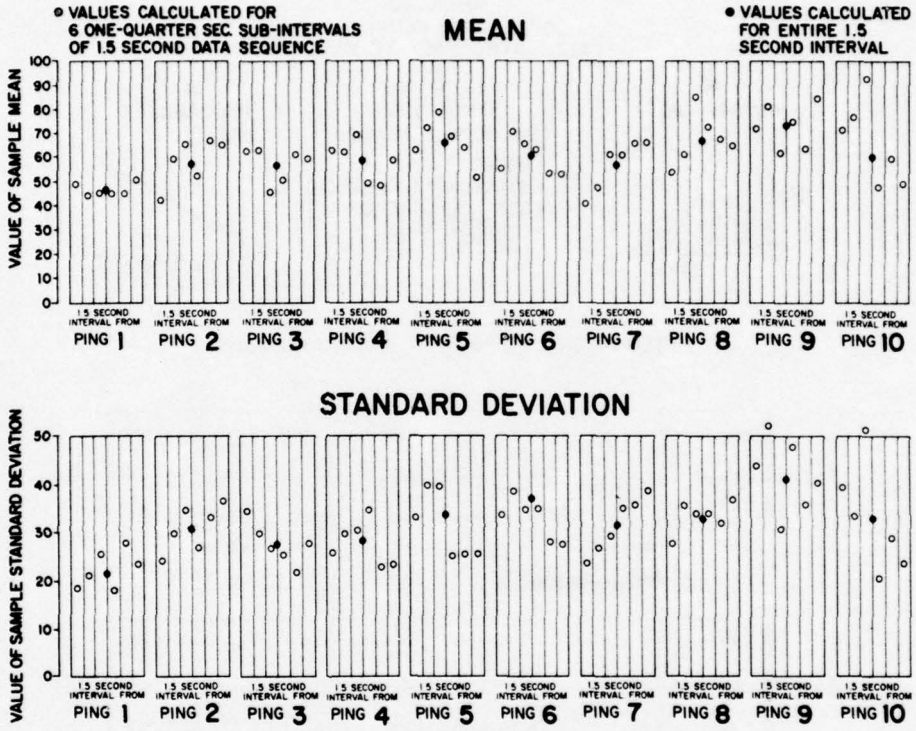

Figure 13. Noise Statistics

As noted earlier, power density spectra have been calculated, but so far they have not been interpreted.

The next step was to process, calculating every tenth sample (as shown in Figure 14), 1.5-second intervals from all of the 200 ping intervals which were digitized. These include, in addition to the surface duct sequences already mentioned, bottom bounce sequences from the January 1965 experiments. The next three figures summarize the results.

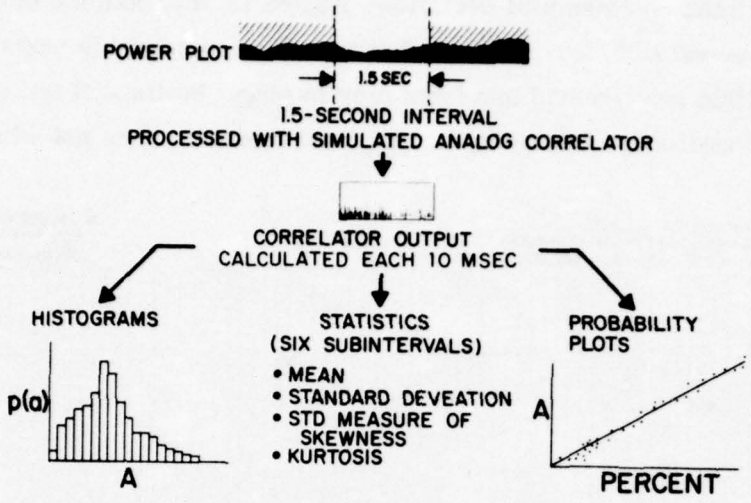

Figure 14. Production Processing

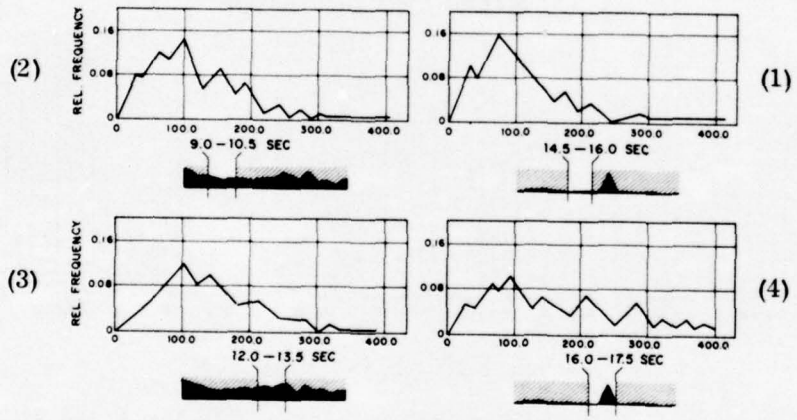

Figure 15. Correlator Output Histograms

The shape of the histogram of the 150 amplitude samples from one interval can be associated with power plot characteristics. The histograms with the highest mode and shortest high end tail are from featureless regions. Whenever peaks on the power plot are included, the middle becomes lower and the high end tail longer. This association has encouraged us to seek the physical significance of the features of the power plots.

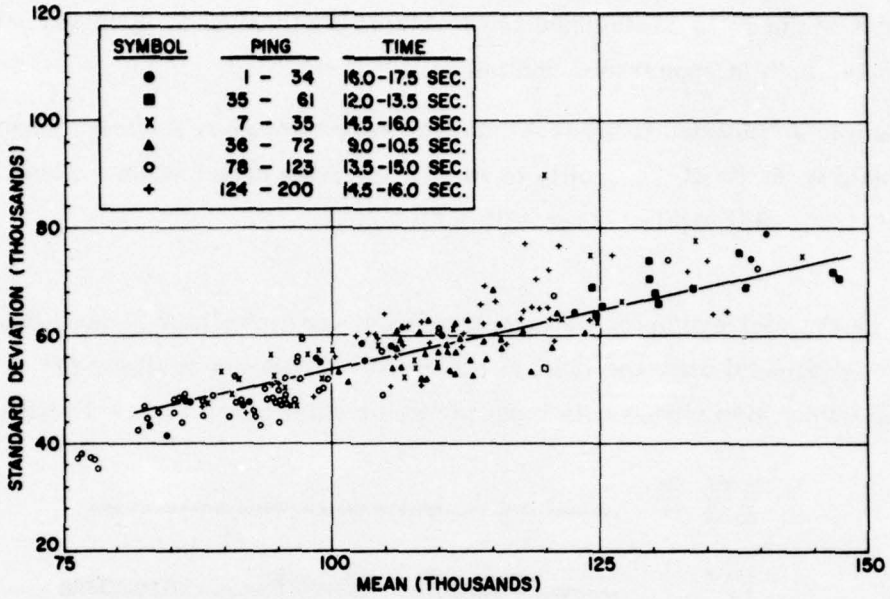

Figure 16. Standard Deviation vs. Mean

The ratio of the standard deviation to the mean is quite similar for all of the data that do not include target intervals. The various symbols shown associate with various ping sequences, both surface duct and bottom bounce, from which the data are taken. It is quite impressive that these statistics, from different experiments, look so similar. For a given mean, this ratio is higher for intervals containing target returns.

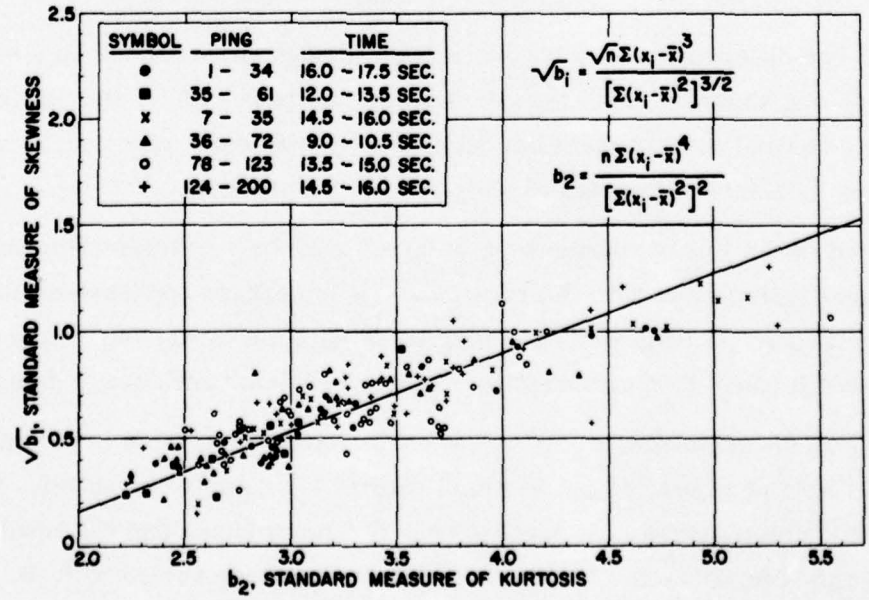

Figure 17. Skewness vs. Kurtosis

This plot of the ratio of standardized forms of the third and fourth moments is much like Figure 16, both in appearance and effect.

The sample amplitudes from each interval were plotted on Rayleigh paper so than an estimate could be made of the quality of fit to a Rayleigh distribution. About half of the data seemed to fit well and the other half did not.

It was known, for example, that the algebra of the correlator showed that the output is Rayleigh distributed when the input is noise. What was not realized for quite a while, was that the output also varies with input power or amplitude; Figure 18 illustrates this effect.

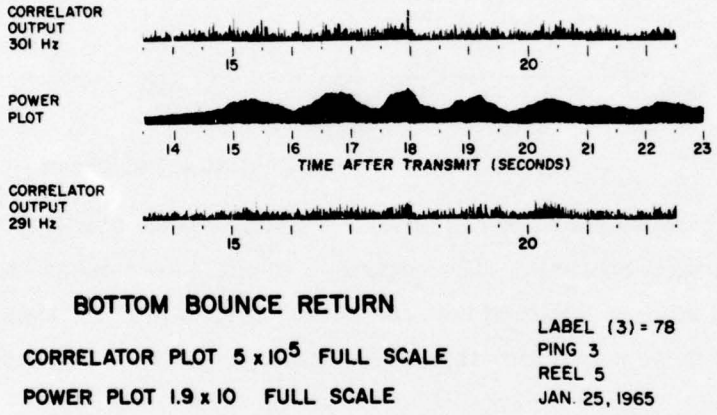

Figure 18. Correlator Outputs and Power Plot

It shows that two different doppler channels, even though uncorrelated on a sample by sample basis, can show the same overall shape as the power plot. Half-second averages of the doppler channel outputs correlate significantly with each other and significantly with a similar half-second average of the power plot amplitude.

The output of the linear correlator is a function of the amplitude at its input, as well as the degree of correlation with the reference. It is perhaps appropriate to question the advantage that might be gained by having these data measured separately as, for example, would be done by a combination clipper correlator and energy detector.

The current understanding of the output of the linear correlator is summarized in Figure 19. There is a noise output to which outputs for signals are added. Multipath requires that the signal ambiguity surface be added many times and the resultant output can become very complicated. Because the output amplitude varies with the input power,

the statistics for any interval are a function of both what is going on and how strongly it is received. This is a difficult situation to model in a general fashion.

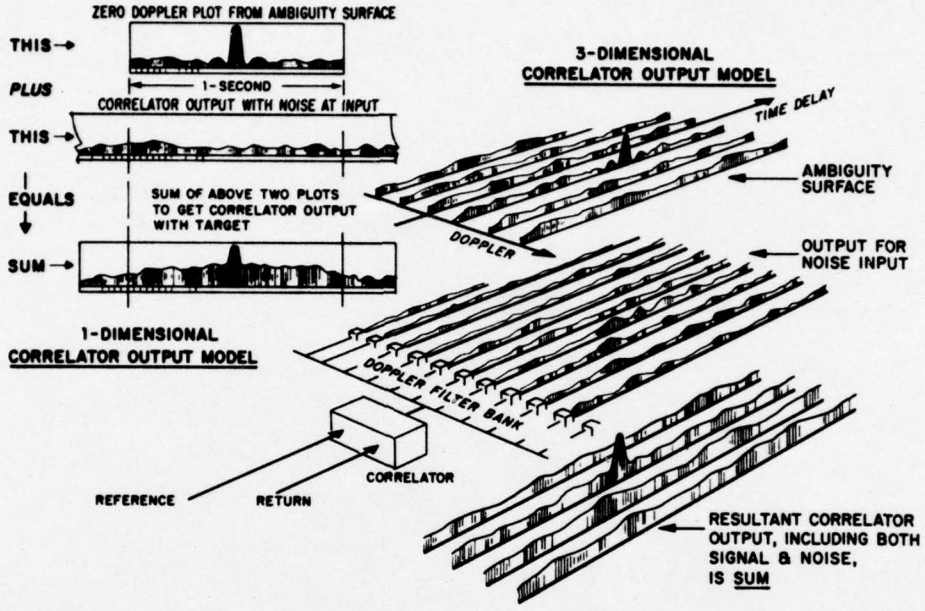

Figure 19. Correlator Output Model

So far only the correlator with noise and reverberation at the input has been considered. It is proposed to continue this study, emphasizing the bottom bounce mode and considering target echoes. Preliminary looks at target echoes show a fairly complicated structure, and a workable plan to collect meaningful statistics has not yet been formulated.

SECTION II

SONAR BACKGROUND

A. MEDIUM CHARACTERISTICS

Several medium characteristics have been investigated because they have a strong influence on both the noise and target signal returns. The bottom characteristics are particularly important since much of the returned energy which interferes with the target return is apparently bounced off the bottom, even when the target return itself comes through the surface duct. Information obtained from the U.S. Navy Underwater Sound Laboratory indicates that in the general area of this experiment (Alpha), the bottom is level, with three or four feet of silt over a fine sand subbottom layer. Apparently no record has been kept for the ship or target tracks during the collection of the Reel 6 or Reel 9 data. Figure 20 shows some fathometer readings taken in area Alpha on the same days that the Reel 6 and Reel 9 data were taken.

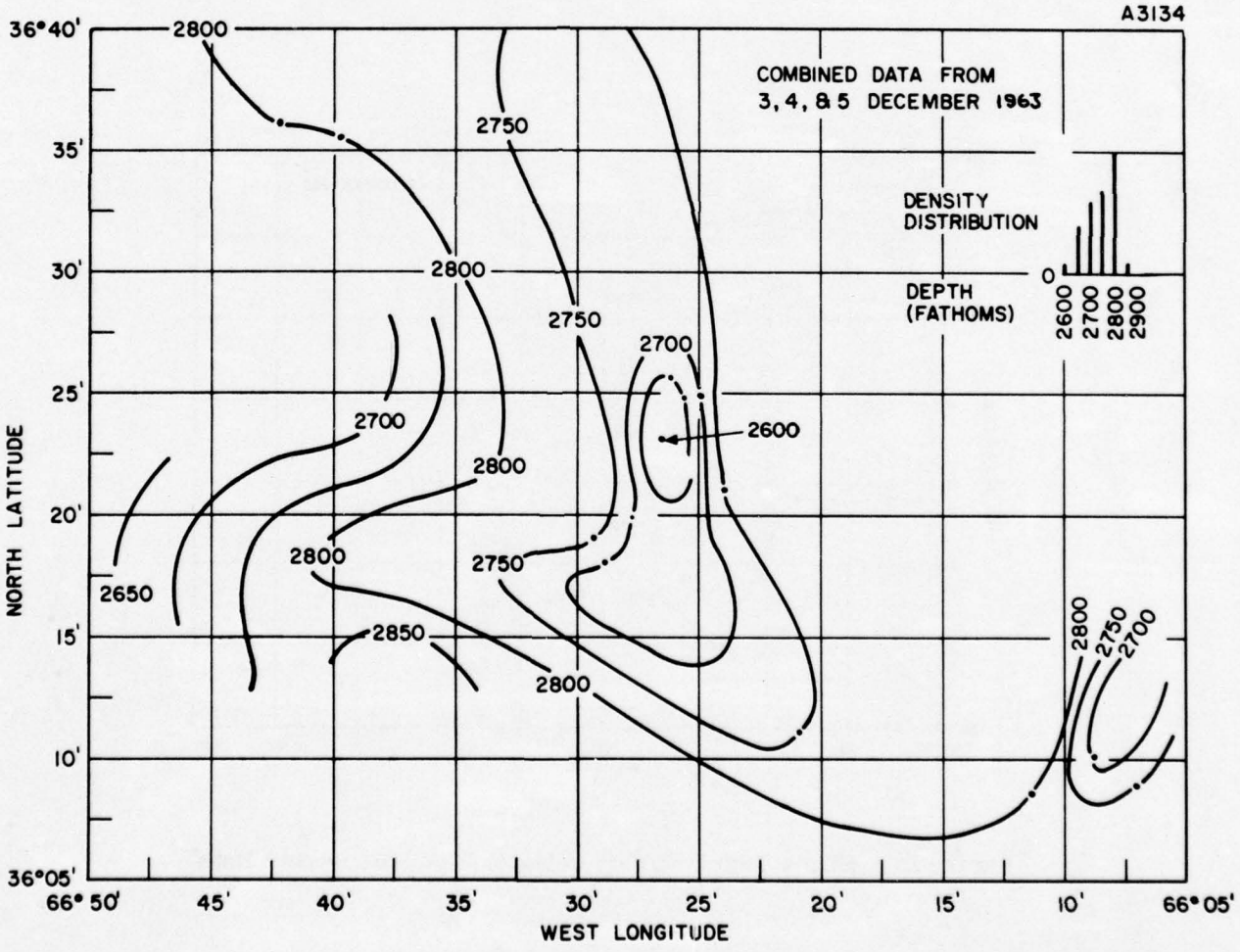

Figure 20. Fathometer Readings

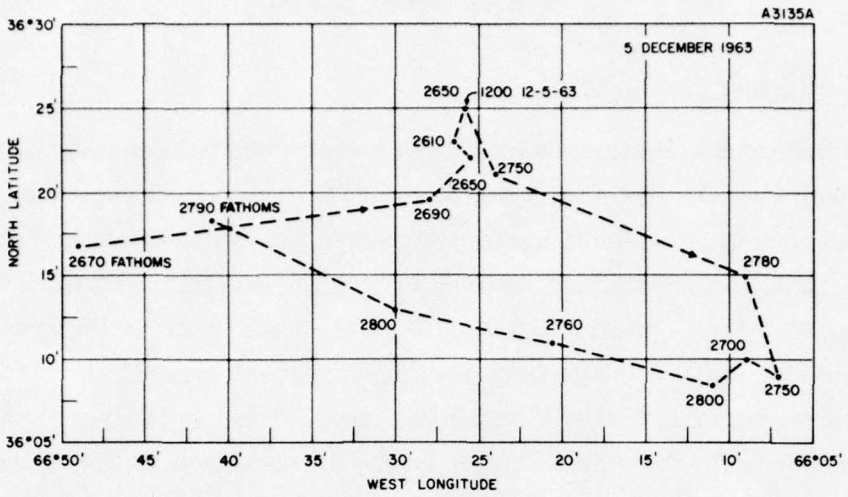

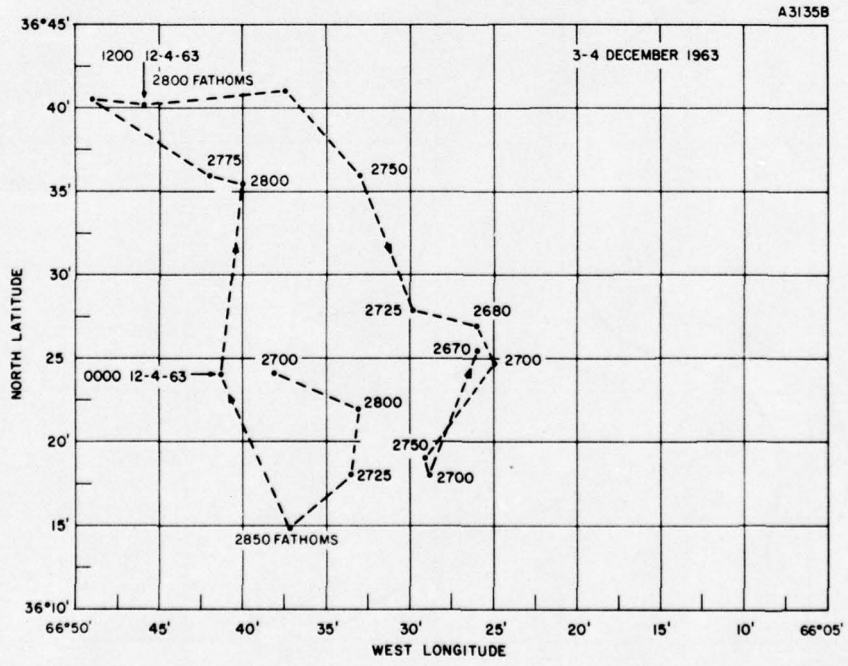

Figure 21. Ship's Track During Collection of Fathometer Data

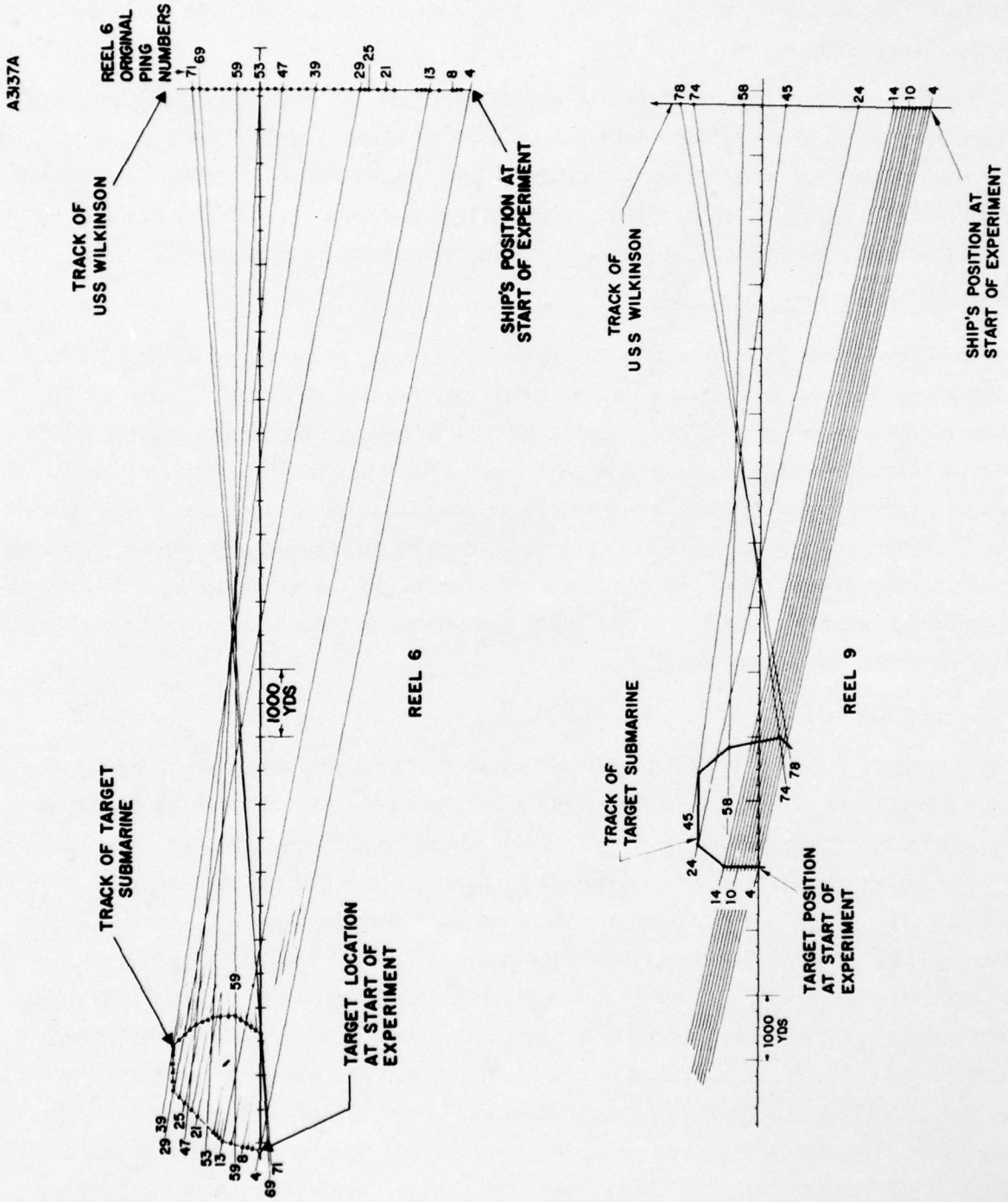

Figure 22. Track Plot Estimates Based on Power Plot Range Data

Figure 21 shows the ship's tracks during the times when the fathometer readings were taken. The set of estimated contour lines sketched in Figure 20 indicates a relatively flat bottom. The distribution of depth values indicates a general plain with low hills on a small percentage of the area.

Currents of several knots with nearby countercurrents are believed to exist in the general area. Wind speed during the tests was about 25 knots. While these surface conditions were not measured in such a way that their effects can be accurately calculated, they are extreme enough to affect the data (ship's track estimations, surface scatter, etc.) and thus their possible effect must be considered in evaluating the results.

B. EXPERIMENT TRACK PLOTS

It would be helpful to have track plots of both the target and destroyer during the data collecting runs for use in analyzing both the noise and target signal returns. Since ship position records were not available, track estimates were made (for the two surface duct runs) based on experiment planning notes and range data available from the power plots (Appendix A). In calculating these tracks it was assumed that the destroyer traveled straight at four knots and that the target traveled straight sides of its track at four knots. The ideal symmetrical octagonal course was compromised to agree with actual range data; the transition point from one leg to the next of the track was estimated from breaks in the slope of power plot range versus time relation.

C. REPEATING BUMPS

By drawing straight lines between simultaneous (in time) points on the two tracks and indicating bump regions from the power plot data (referencing zero time at the destroyer track point) a representation of ping-to-ping space location of these bumps is shown, for Reel 9, in Figure 23. Bumps are chosen in a somewhat subjective manner from the power plots in Figure A-2. Their locations are indicated by retaining segments of the lines connecting ship and target locations for each ping number. The bumps apparently caused by the target are purposely omitted from the display. Since the target is relatively strong in most of these pings it obscures noise bumps in its time region. An estimated target track is shown in Figure 23 to indicate this explanation for the absence of bumps in the target region. The amplitudes of the various bumps (not indicated in the figure) are shown in Figure A-2. Where parts of two or more segments are close together, the beams from these pings were looking at the same region of the ocean. Under some conditions bottom irregularities in that region would show up in several pings. Such irregularities apparently

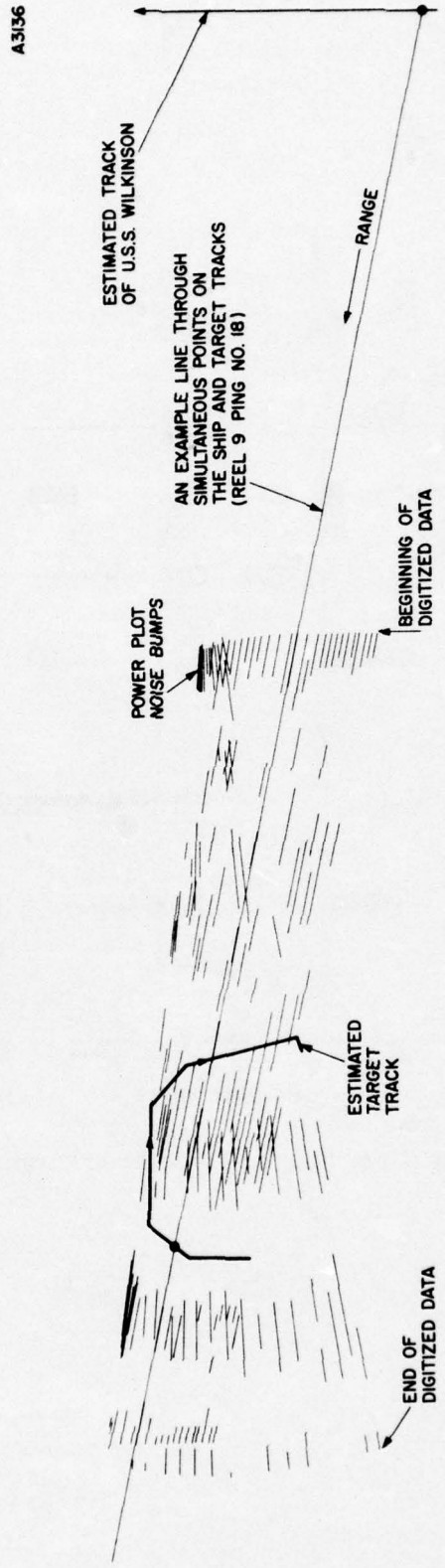

Figure 23. Power Plot Amplitude Bumps Shown in Relation to Ping-to-Ping Space Coverage (Reel 9 Data)

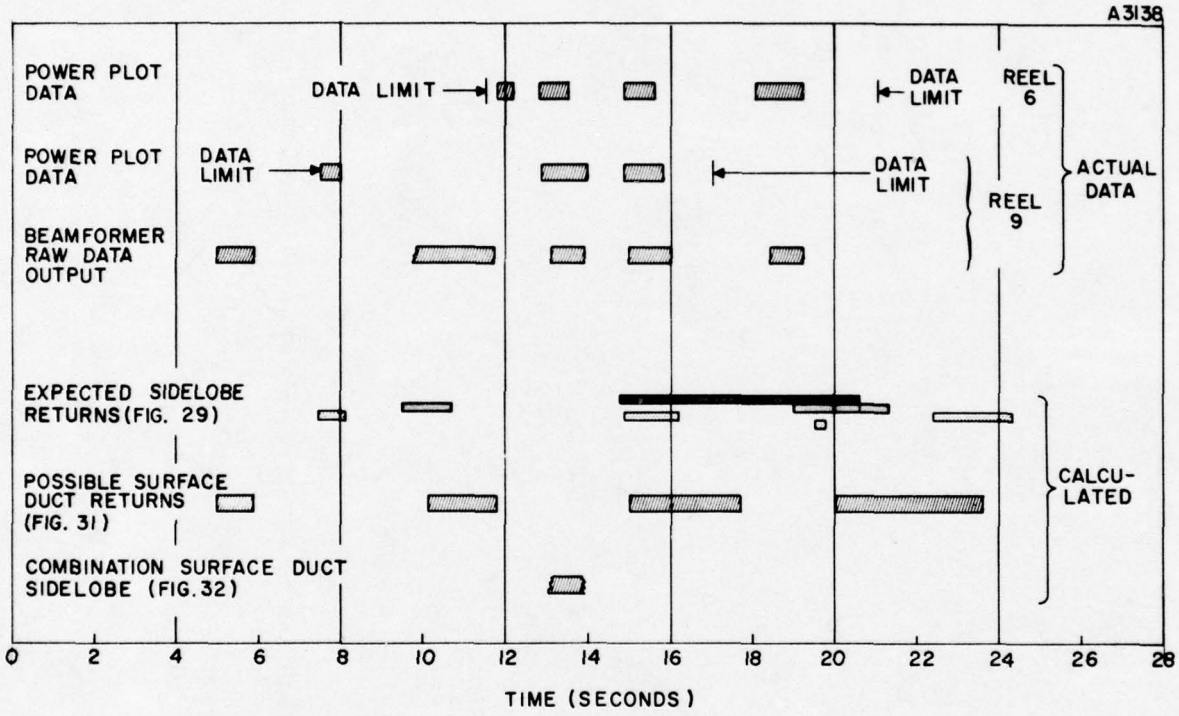

Figure 24. Consistent (from Ping to Ping) Reverberation Type Returns

do not show up in the data from either of these two reels. There is some indication of coinciding bumps but it appears that these are better correlated on a "time after transmit" basis alone. Figure 6 shows essentially the same data, but the lines connecting simultaneous points on the two tracks are laid out parallel to each other to show the time relationship of the bumps. Correlations such as these could be caused by sidelobe returns from medium boundaries which remain essentially the same from ping to ping (such as a level bottom).

The shaded areas in the upper half of Figure 24 show a condensed (over many pings) version of energy concentration as a function of time. Primarily because the time intervals over which data were digitized are limited, the beamformer raw data were photographed from the scope face display for several pings on Reel 9 to show data outside the digitized intervals. An example of the beamformer output is shown in Figure 25.

In addition to the time location of these bumps, their amplitude characteristics are valuable for their analysis. While the relative values of the signal amplitude over the entire ping (and from ping to ping) have been distorted by the AGC processing, the power plot characteristics over shorter time intervals and the correlator output are still of particular interest. Power plot outputs for Reel 6 data are shown in Figure 26. The full scale values for all the pings are the same; this clips the target signals but shows the lower valued noise regions in a more comparable form. Correlator output was calculated for several time intervals to help in searching for characteristics of these bump regions; these are shown in Figures 27 and 28 for time intervals in Reel 6 ping numbers 13, 14, 67, and 69. Power plot data are shown in the center of the figures to indicate the time regions for which correlator output is shown. The correlator output presentation is a grey scale map of correlator output over the time and frequency extents indicated; the data reduction details of producing these maps are described in a later part of this report. Features such as, for example, the generally parallel ridges and valleys running in a slanted direction from high frequency-early time to lower frequency-later time areas which appear in the four plots for the 13.2-second bump region are characteristic of this high reverberation interval.

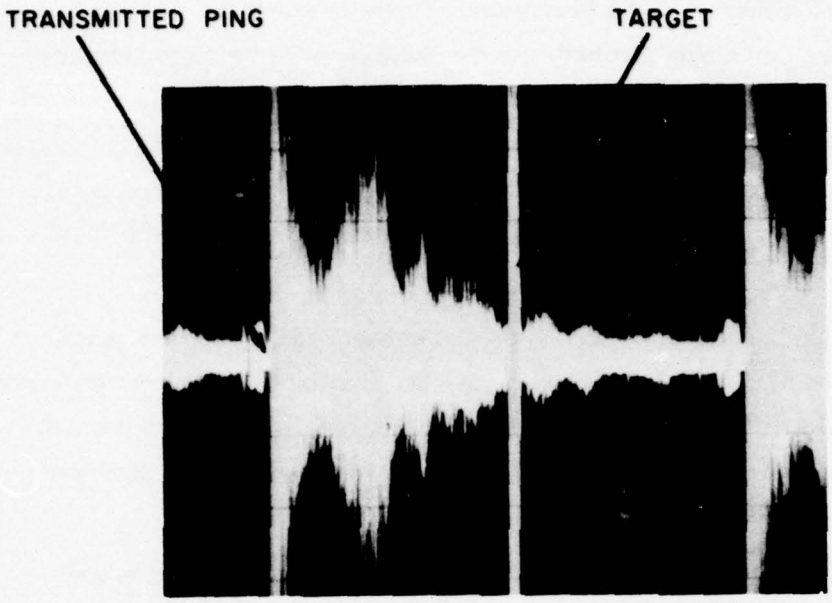

A3139

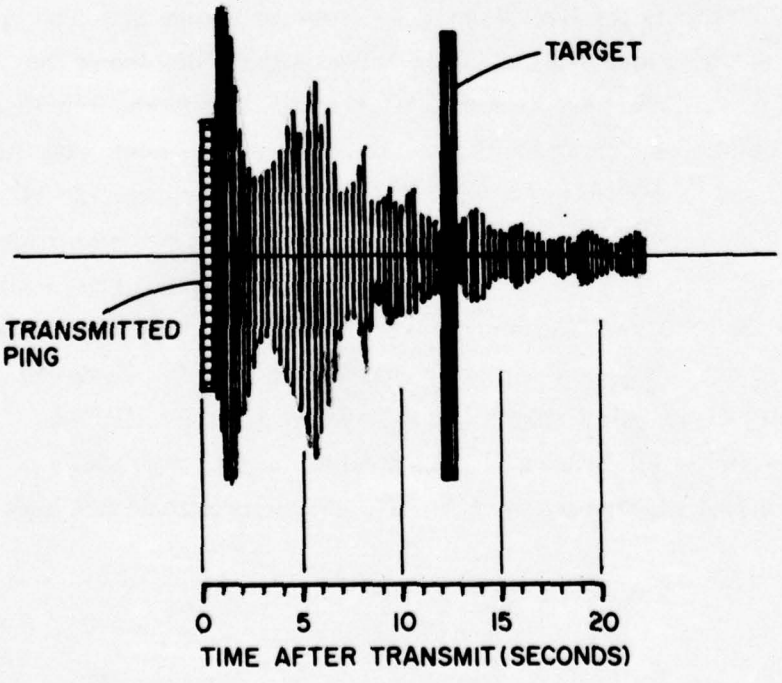

TYPICAL REEL 9 PING (COPY OF SCOPE PHOTOGRAPH OF SIGNAL AT BEAMFORMER OUTPUT)

Figure 25. Typical Beamformer Output

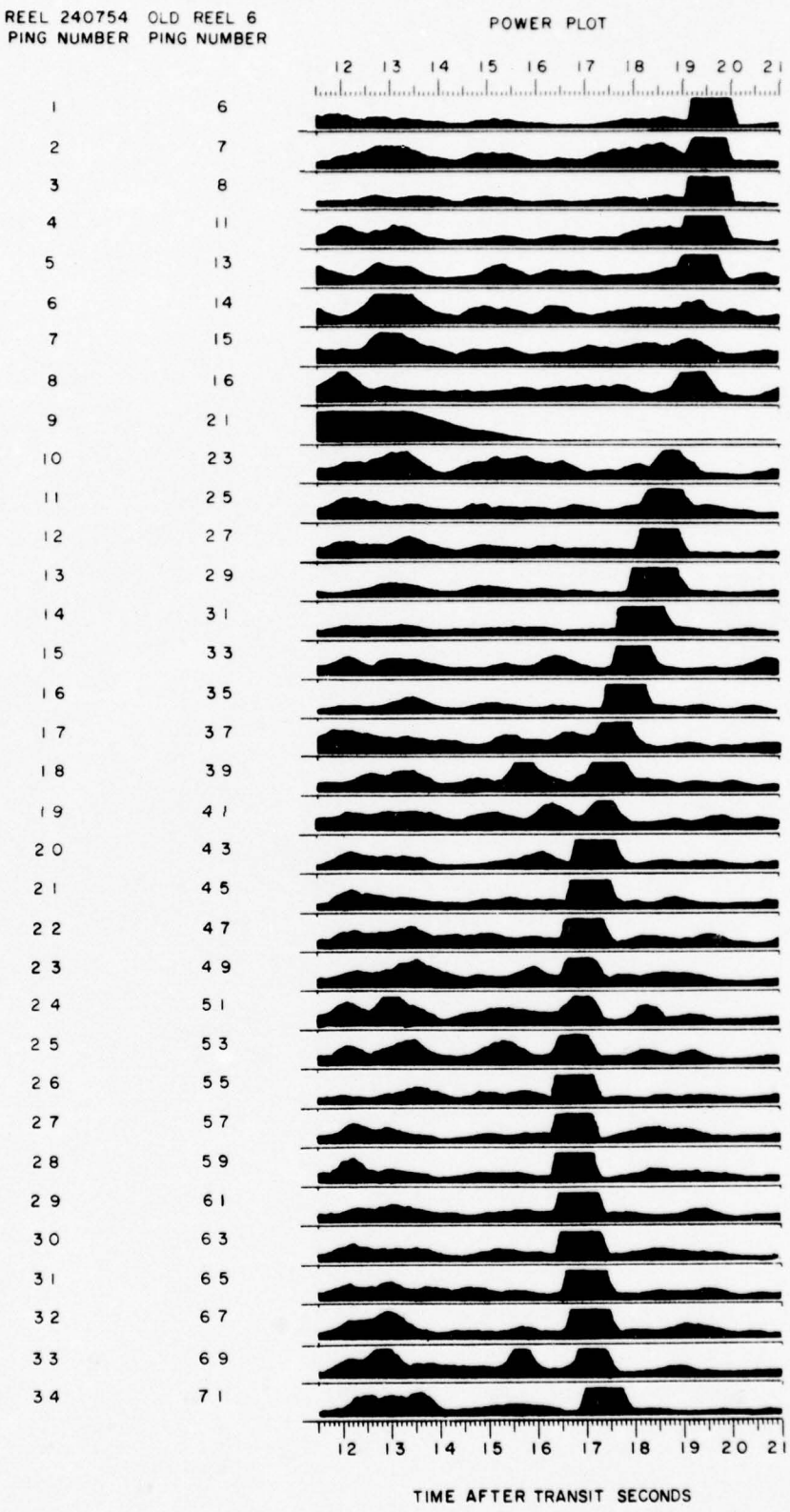

Figure 26. Power Plots, Reel 6, Full Scale Fixed

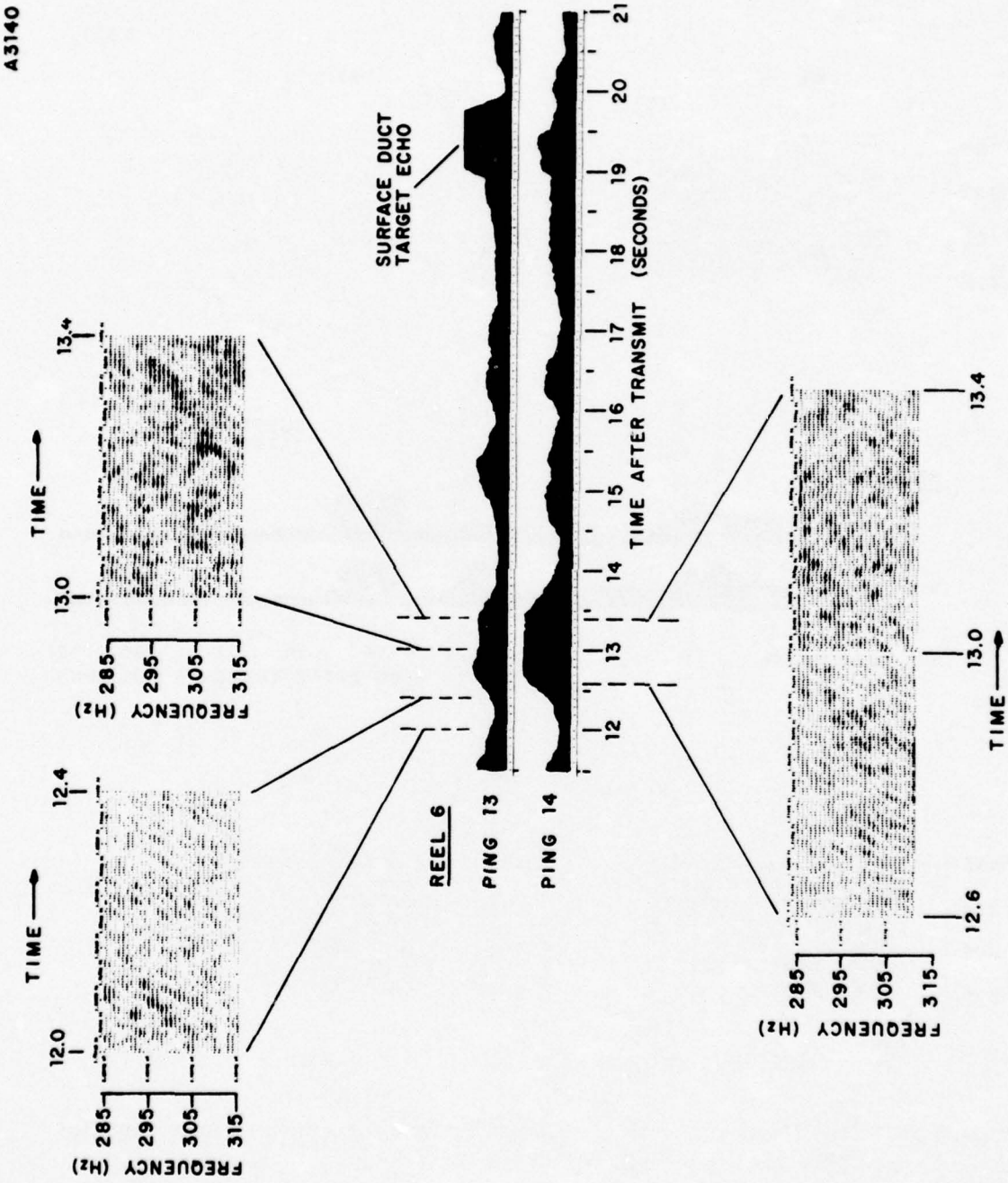

Figure 27. Grey Maps of Correlator Output Surface for Times of Reverberation Peaks (Reel 6, Pings 13 and 14)

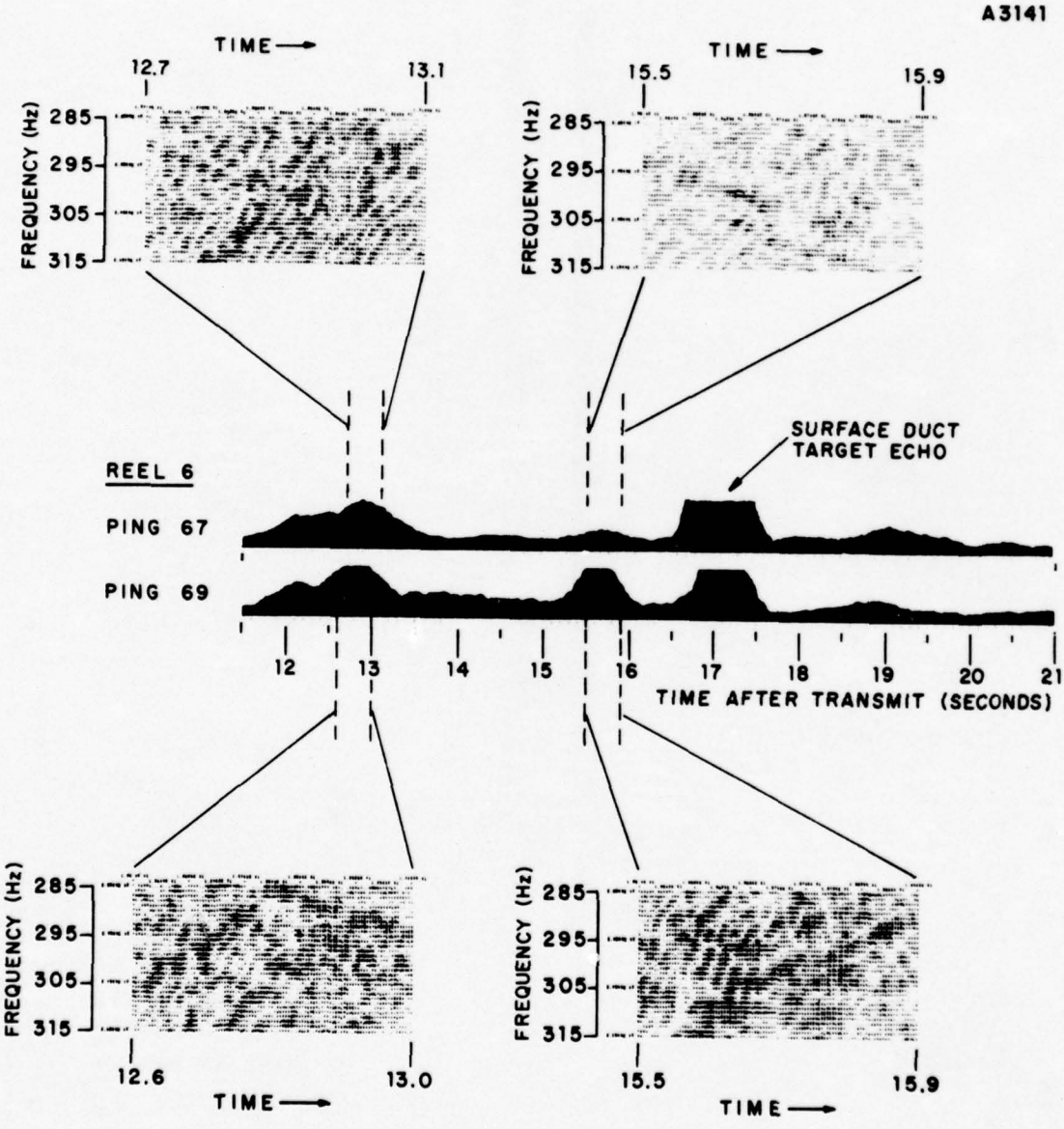

Figure 28. Grey Maps of Correlator Output Surface for Times of Reverberation Peaks (Reel 6, Pings 67 and 69)

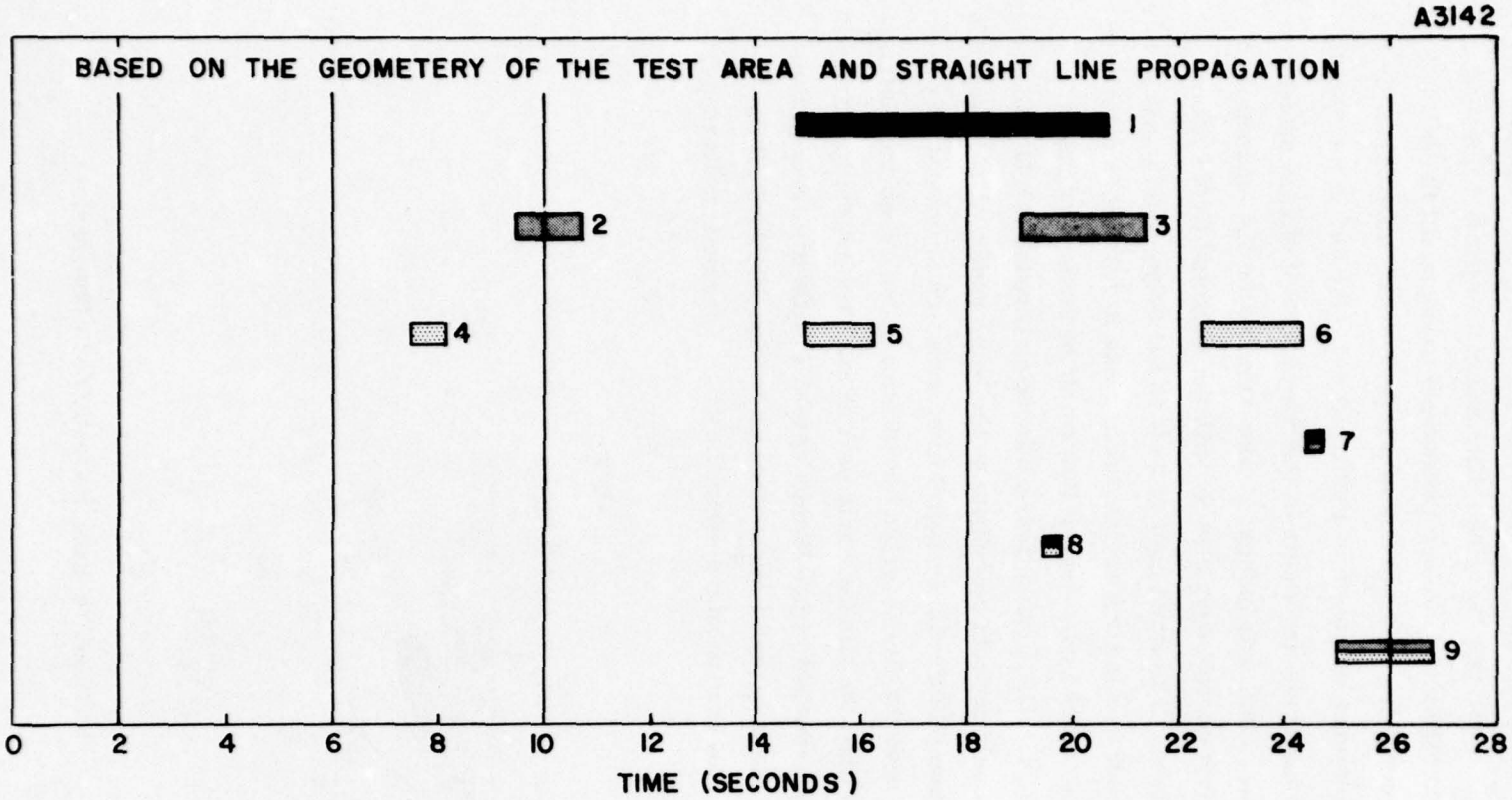

1. First bottom reflection through the 22° sidelobe
2. First bottom reflection through the 41° sidelobe
3. First surface reflection (bounced off the bottom) through the 41° sidelobe
4. First bottom reflection through the 60° sidelobe
5. First surface reflection (bounced off the bottom) through the 60° sidelobe
6. Second bottom reflection (bottom - surface - bottom and back) through the 60° sidelobe
7. Combination path (to the bottom through the 22° sidelobe then back through the 41° sidelobe surface - bottom and back or vice versa).
8. Combination path (to the bottom through the 22° sidelobe then back through the 60° sidelobe surface - bottom and back or vice versa).
9. Combination path (bottom to surface through the 41° sidelobe then returned bottom - surface - bottom and back through the 60° sidelobe).

Figure 29. Time Intervals of Expected Bottom and Surface Backscatter Through Beam Sidelobes

CONFIDENTIAL

If the physical sources of these bumps can be found, it may be helpful in characterizing the "noise" they represent. Some results of an initial attempt to predict the time intervals of sidelobe bottom backscatter and surface reflections (bounced off the bottom) are shown in Figure 29. The simplifying assumptions of a level bottom, approximately straight line propagation, and sidelobes as shown in Figure 30 are indicated in the sketch shown in Figure 7. These same intervals are shown in the fourth row of shaded areas in Figure 24 for comparison with the actual data bumps. The bump in the 7.8-second time region of the Reel 9 power plot data corresponds closely with the expected first bottom backscatter through the 60° sidelobe. The rapid gain dropoff on the scope display used for the beamformer raw data output in this time region would make it difficult to determine a bump in this interval; this is indicated by the jagged line cutoff of the shaded region ending at 11.5 seconds in Figure 24. The first bottom backscatter through the 41° sidelobe is shown in an interval where it could at least contribute to the bump ending at 11.7 seconds in the beamformer output. The bump in the 15.4-second interval which is consistent over all three data displays coincides with the first surface backscatter (bounced off the bottom) through the 60° sidelobe. It also lines up with the early part of the first bottom backscatter through the 22° sidelobe. The 18.7-second region bumps appear a little too early in time to be completely correlated with the proposed first surface reflection (bounced off the bottom) through the 41° sidelobe, but in view of the simplifications assumed, a discrepancy this large would not be surprising.

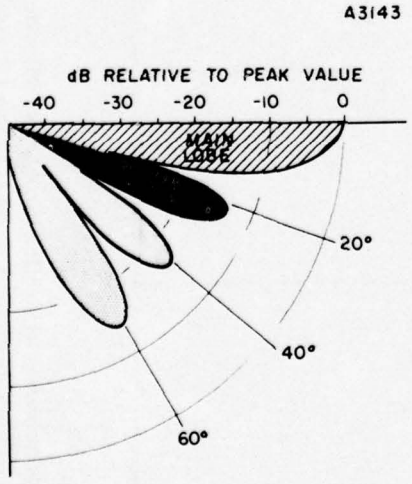

Figure 30. AN/SQS-26 Calculated Vertical Pattern (Zero Depression)

The 5.5-second region bump (which is strong and consistent over all four of the Reel 9 pings for which the raw data were photographed) is unique in that it has already died out considerably before a vertical return from the bottom ("depth sounder return") would be expected (about 6.8 seconds from a 5.6-kyd depth). It may be that this 5.5-second bump is the first surface backscatter through the surface duct as indicated in Figure 31. The time extents of the returns indicated in this figure are based on the length of a composite 5.5-second region return made up from the beamformer raw data output. The time intervals of arrival of surface reflections through this proposed surface duct are included in Figure 24. The second surface reflection corresponds closely with the last part (at least) of the 11-second region bump in the Reel 9 beamformer output.

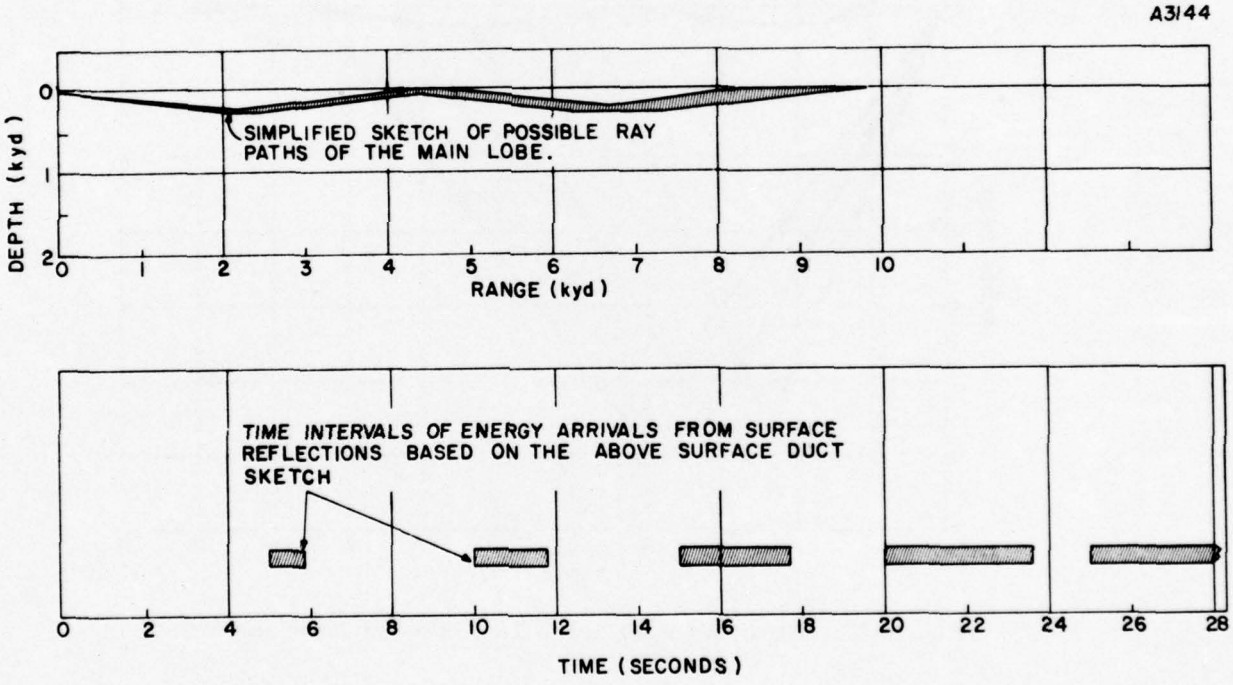

Figure 31. Estimated Surface Duct Propagation

This leaves unexplained the bump in the 13.5-second region which is consistently strong in all three of the real data outputs; it is of particular interest because the target moves through it in the Reel 9 data. Since the surface duct signal is relatively strong it may be that this bump is the triangular path surface reflection from the second surface reflection of the surface duct bounced off the bottom through the 60° sidelobe as sketched in Figure 32. This would have to come through about 7° off center of the sidelobe (about 6 dB down as shown in Figure 30); this is on a steep part of the sidelobe which may explain the short time extent of the bump.

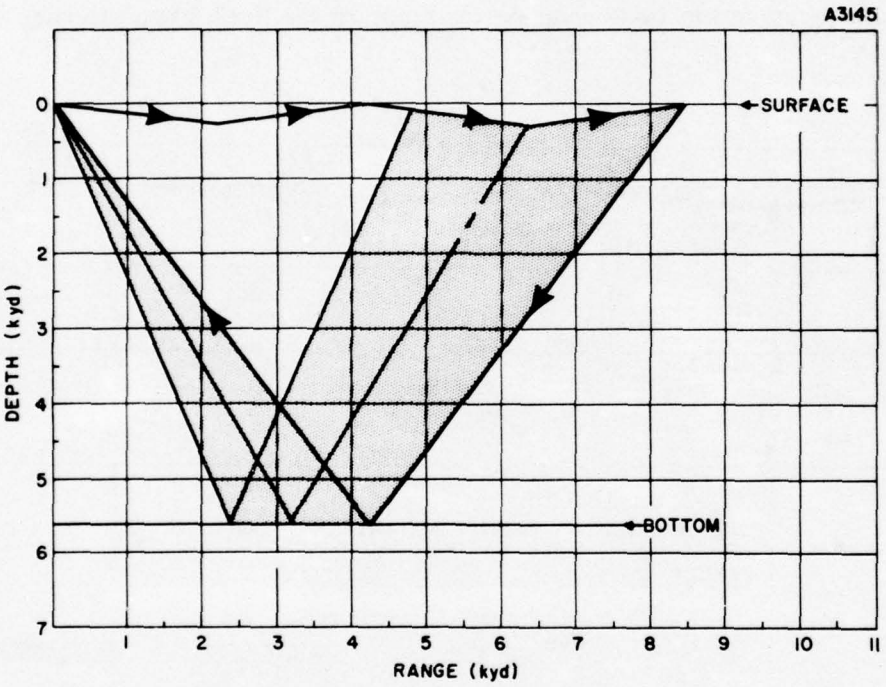

Figure 32. Reverberation in the 13.5-Second Time Region

More data will have to be considered before these tentative explanations of the energy concentrations can be confirmed. Particularly, the beamformer output from Reel 6 should be considered as well as that from more pings of Reel 9. More important is the usefulness of knowing the source of these different noise regions; comparison among the correlator output and other amplitude data is promising.

To get a better understanding of propagation characteristics it is planned to obtain computer calculated ray paths as functions of the velocity profile. A preliminary output of this effort, showing a surface duct as part of a split main lobe, is shown in Figure 33. The velocity profile used in this plot is based on BT data obtained from the U.S. Navy Underwater Sound Laboratory. The 0 to 700 foot depth BT data were taken at 0800, 3 December 1963, in the same general area that the experimental sonar data were taken. No BT data for greater depths were available for the area at that time, so the sound velocity used for greater depths were obtained from a representative curve for this area (Figure 34). The surface duct ray paths shown tend to support the possibility that the 5-second region noise bumps shown in Figure 32 are actually surface reflections coming through the surface duct.

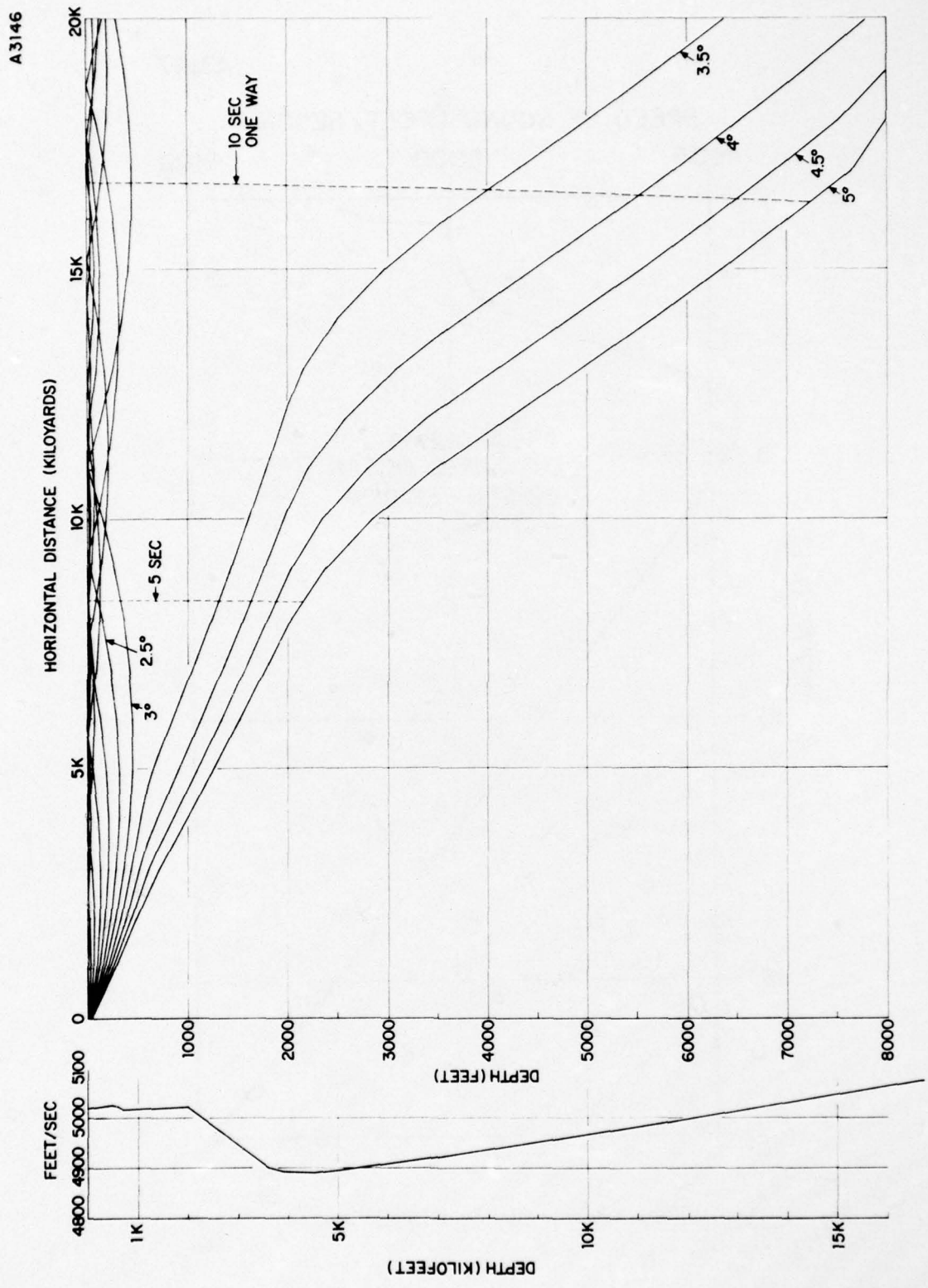

Figure 33. Computer Calculated Ray Plots Showing Split Beam Main Lobe

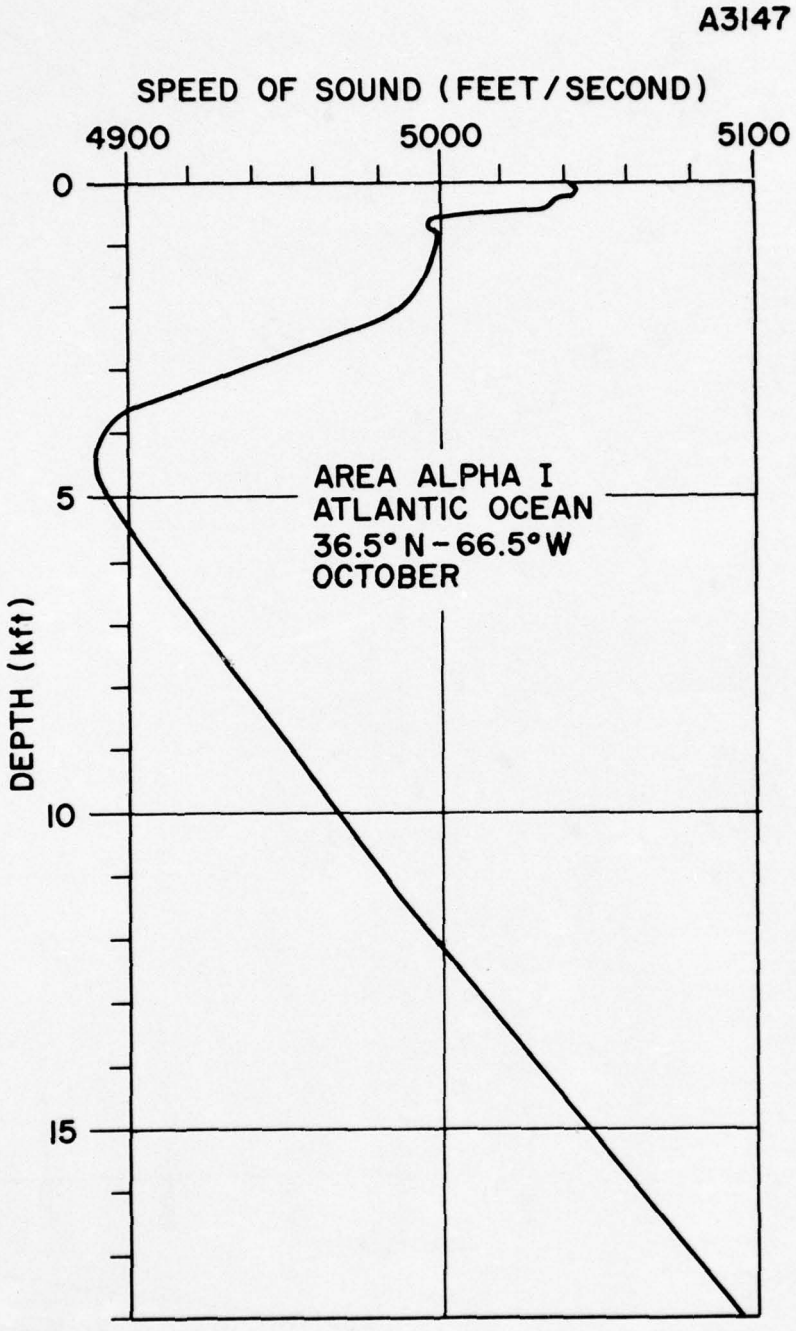

Figure 34. Sound Speed Profile

SECTION III

STATISTICAL ANALYSIS OF SONAR RETURNS

A. OBJECTIVE

The following section summarizes the initial efforts and results obtained from the study of the amplitudes of correlator output samples from (essentially) target-free portions of sonar returns. The investigation was based on the analyses of 1.5-second intervals from both surface duct and bottom bounce transmissions. The conclusions and properties discussed apply only to these data; extrapolation to other environmental conditions or to target intervals is not justified.

The purpose of the first stage of the investigation was to describe as many properties as possible of the correlator output and to attempt to model the output by a probability distribution.

B. SERIAL CORRELATION

The first step in the analysis of the sonar returns for the surface duct mode was to determine at what rate the correlator output should be (time) sampled so that uncorrelated observations could be obtained. This was accomplished by computing the autocorrelation matrix for a 1.5-second interval for pings* 1 to 10 for a time interval starting at 16.0 seconds. In addition, in order to study the stationarity of the return, each interval was divided into six subintervals and the autocorrelation function up to lag 50 was computed for each segment. There are a total of 1500 numbers in the 1.5-second interval and, hence, a total of 250 in each subinterval. An examination of the results indicates that the serial correlation function behaved erratically. It decreases monotonically until close to zero as the index increased from 1 to 10, but its behavior thereafter was erratic, differing from ping to ping, and sometimes increasing higher (in absolute value) than its value at the index of 10. Since it was desirable to have as low a correlation as possible so that the observations would be approximately uncorrelated (if not independent) to work with, in the selection of a probability model, a compromise sampling rate of every tenth value was used in the remaining study. There were only a few instances for a correlation index

---

* In this report, two numbering systems are used to refer to the sonar pings: (1) a number from 1 to 200 corresponding to the sequence of the data on the data tape, and (2) a number for the ping (and another for the reel) assigned at the time of recording. The power plots of Appendix A display both numbers.

greater than 10 that the absolute value of the serial correlation was greater than 0.30. Examination of the data also revealed that the returns were not stationary within the 1.5-second interval. The serial correlations for a given lag varied radically from one segment of the interval to another; these are shown in Table 1. The underlined entires indicate those intervals for which there were large differences in the autocorrelation function within a single ping.

The variability of the mean and standard deviation within and between pings was illustrated in Figure 13. Statistical analysis indicated that, for some of the pings, there was a significant difference between both the within ping means and standard deviations and the between ping means and standard deviations. This was the case for pings 7, 8, and 9. The means and standard deviations are given at the top of Table 1. The centered values give the overall ping values of these statistics; thus, we see for some of the pings that even a small segment is not stationary.

Subsequently, the serial correlation matrix for the bottom bounce pings was obtained. The correlation function did not drop as rapidly as in the case of the surface duct mode and behaved more erratically (see Reference 1, page 32); however, the same sampling rate was chosen as for the surface duct mode pings, although possibly every 15 would have been a somewhat better choice. The reasons for this choice were that it was felt that using the same sampling rate for the two modes would allow for a more meaningful comparison between the two, the desire to have a uniform procedure for handling the data, and that the initial statistical results on bottom bounce pings using the 1 in 10 sampling rate were similar to those from the surface duct mode.

C. SUMMARY OF DISTRIBUTIONAL PROPERITES

In order to investigate the statistical behavior of the sampled data, a computer program was written to calculate, for each interval (the data for each interval consist of 150 correlator amplitudes) the mean, standard deviation, standardized measure of skewness ($\sqrt{b_1}$), and standardized measure of kurtosis, b_2. In addition, histograms of the amplitudes of the correlator output were prepared for some of the pings. Intervals to be processed were obtained from 77 surface duct pings and 122 bottom bounce pings. The following time segments were sampled.

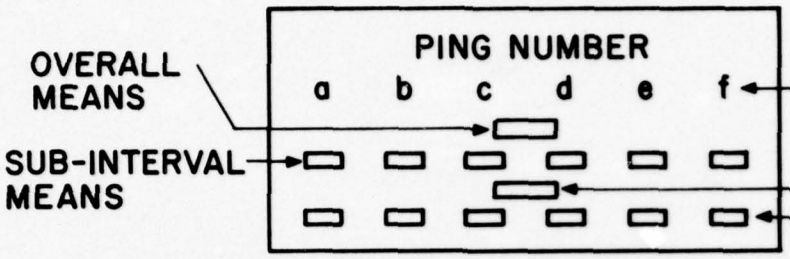

	PING 1						PING 2						PING 3						PING 4						PING 5					
	a	b	c	d	e	f	a	b	c	d	e	f	a	b	c	d	e	f	a	b	c	d	e	f	a	b	c	d	e	f
			47.2						58.7						57.0						58.2						66.5			
$\bar{x}$	49.5	44.8	46.7	45.8	46.1	50.1	41.4	59.9	65.6	52.4	67.7	65.3	62.0	62.5	46.7	50.5	60.6	59.4	62.2	61.1	69.3	49.6	48.5	58.2	6.28	72.8	79.7	68.5		
			21.7						30.6						27.5						27.9						33.9			
σ	18.7	21.8	25.2	17.8	27.6	23.8	24.5	28.8	34.6	26.4	22.4	36.7	34.1	29.3	26.9	25.6	21.7	27.4	26.6	29.5	30.9	34.4	22.7	23.1	3.28	39.9	39.2	30.0		
1	0.95	0.97	0.98	0.97	0.98	0.97	0.98	0.98	0.98	0.97	0.98	0.97	0.99	0.98	0.98	0.98	0.97	0.97	0.98	0.97	0.98	0.98	0.97	0.98	0.98	0.99	0.98	0.96		
2	0.80	0.88	0.82	0.89	0.93	0.89	0.94	0.92	0.94	0.90	0.91	0.90	0.95	0.91	0.94	0.93	0.90	0.90	0.91	0.88	0.90	0.94	0.87	0.91	0.92	0.95	0.93	0.85		
3	0.59	0.75	0.70	0.78	0.85	0.77	0.88	0.84	0.88	0.79	0.81	0.79	0.90	0.81	0.87	0.85	0.80	0.80	0.82	0.76	0.80	0.88	0.72	0.82	0.83	0.89	0.86	0.69		
4	0.36	0.60	0.57	0.64	0.75	0.64	0.80	0.73	0.80	0.65	0.69	0.67	0.84	0.70	0.78	0.76	0.67	0.69	0.71	0.61	0.68	0.80	0.55	0.70	0.71	0.82	0.77	0.50		
5	0.13	0.45	0.45	0.49	0.64	0.50	0.70	0.62	0.72	0.50	0.57	0.53	0.76	0.57	0.67	0.65	0.54	0.57	0.58	0.45	0.54	0.71	0.37	0.56	0.58	0.75	0.67	0.32		
6	-0.06	0.31	0.33	0.34	0.53	0.37	0.62	0.51	0.65	0.36	0.45	0.39	0.69	0.45	0.57	0.55	0.42	0.47	0.46	0.31	0.41	0.62	0.21	0.43	0.45	0.67	0.58	0.17		
7	-0.20	0.20	0.22	0.21	0.42	0.26	0.53	0.40	0.58	0.22	0.35	0.26	0.61	0.35	0.47	0.45	0.31	0.39	0.35	0.19	0.29	0.54	0.07	0.30	0.32	0.60	0.49	0.05		
8	-0.28	0.11	0.13	0.09	0.32	0.17	0.46	0.31	0.53	0.11	0.26	0.15	0.54	0.26	0.37	0.35	0.22	0.33	0.25	0.09	0.18	0.46	-0.04	0.19	0.19	0.54	0.40	-0.02		
9	-0.30	0.04	0.06	-0.02	0.23	0.12	0.39	0.23	0.49	0.03	0.19	0.06	0.48	0.19	0.28	0.26	0.15	0.30	0.17	0.03	0.10	0.40	-0.11	0.10	0.09	0.49	0.33	-0.05		
10	-0.27	-0.01	0.00	-0.10	0.16	0.10	0.33	0.17	0.47	-0.02	0.14	-0.00	0.43	0.14	0.21	0.18	0.11	0.28	0.10	0.00	0.04	0.34	-0.15	0.04	-0.00	0.44	0.28	-0.06		
11	-0.21	-0.04	-0.04	-0.16	0.10	0.09	0.27	0.13	0.46	-0.05	0.10	-0.05	0.38	0.10	0.16	0.11	0.07	0.26	0.04	0.00	0.01	0.30	-0.16	0.01	-0.07	0.41	0.23	-0.05		
12	-0.14	-0.07	-0.06	-0.26	0.05	0.10	0.23	0.11	0.45	-0.06	0.06	-0.08	0.34	0.08	0.12	0.04	0.03	0.23	-0.01	0.02	-0.01	0.27	-0.14	-0.03	0.12	0.38	0.20	-0.04		
13	-0.08	-0.08	-0.07	-0.23	0.02	0.12	0.19	0.11	0.45	-0.06	0.03	-0.09	0.31	0.08	0.10	-0.02	-0.01	0.19	-0.04	0.06	-0.00	0.24	-0.11	-0.04	-0.15	0.36	0.17	-0.04		
14	-0.05	-0.09	-0.07	-0.24	-0.01	0.14	0.15	0.12	0.45	-0.04		-0.09	0.28	0.08	0.10	-0.07	-0.07	0.14	-0.07	0.09	0.02	0.21	-0.07	-0.04	-0.15	0.34	0.16	-0.05		
15	-0.04	-0.10	-0.06	-0.24	-0.04	0.15	0.13	0.14	0.44	-0.03	-0.03	-0.08	0.26	0.08	0.10	-0.11	-0.13	0.09	-0.09	0.13	0.05	0.19	-0.03	-0.03	-0.15	0.32	0.16	-0.07		
16	-0.06	-0.10	-0.05	-0.24	-0.06	0.15	0.11	0.16	0.44	-0.02	-0.06	-0.07	0.23	0.08	0.12	-0.15	-0.19	0.03	-0.09	0.16	0.10	0.17	0.01	-0.02	-0.14	0.30	0.17	-0.09		
17	-0.09	-0.10	-0.03	-0.23	-0.07	0.13	0.10	0.18	0.44	-0.02	-0.08	-0.07	0.19	0.07	0.15	-0.19	-0.25	-0.03	-0.09	0.19	0.15	0.15	0.03	-0.01	-0.12	0.28	0.19	-0.10		
18	-0.12	-0.08	-0.02	-0.21	-0.09	0.10	0.09	0.18	0.43	-0.04	-0.10	-0.07	0.16	0.06	0.18	-0.21	-0.31	-0.07	-0.08	0.21	0.21	0.14	0.04	0.00	-0.10	0.25	0.20	-0.10		
19	-0.13	-0.05	-0.01	-0.20	-0.11	0.05	0.08	0.18	0.43	-0.06	-0.11	-0.08	0.12	0.04	0.21	-0.23	-0.36	-0.11	-0.06	0.22	0.26	0.12	0.02	0.01	-0.09	0.22	0.22	-0.07		
20	-0.13	-0.01	0.00	-0.19	-0.13	0.00	0.07	0.17	0.42	-0.09	-0.12	-0.10	0.07	0.10	0.23	-0.24	-0.38	-0.13	-0.04	0.23	0.31	0.10	-0.01	0.01	-0.09	0.20	0.23	-0.02		
21	-0.11	0.04	0.01	-0.19	-0.15	-0.05	0.06	0.15	0.41	-0.13	-0.11	-0.12	0.02	-0.02	0.26	-0.24	-0.40	-0.15	-0.03	0.22	0.34	0.09	-0.05	0.00	-0.09	0.17	0.23	0.04		
22	-0.07	0.09	0.02	-0.18	-0.18	-0.10	0.04	0.12	0.40	-0.18	-0.10	-0.14	-0.02	-0.06	0.27	-0.23	-0.39	-0.17	-0.02	0.21	0.35	0.08	-0.10	-0.00	-0.11	0.14	0.23	0.09		
23	-0.02	0.13	0.02	-0.18	-0.20	-0.14	0.03	0.09	0.40	-0.23	-0.07	-0.18	-0.07	-0.09	0.28	-0.22	-0.38	-0.19	-0.02	0.17	0.35	0.07	-0.15	-0.01	-0.13	0.12	0.22	0.13		
24	0.03	0.17	0.02	-0.19	-0.23	-0.16	0.00	0.07	0.39	-0.27	-0.50	-0.21	-0.11	-0.13	0.29	-0.19	-0.35	-0.22	-0.04	0.12	0.33	0.06	-0.20	-0.02	-0.16	0.09	0.20	0.13		
25	0.07	0.18	0.02	-0.19	-0.26	-0.18	-0.03	0.04	0.38	-0.32	-0.22	-0.25	-0.15	-0.17	0.28	-0.16	-0.32	-0.25	-0.06	0.06	0.30	0.06	-0.24	-0.02	-0.18	0.06	0.19	0.10		
26	0.09	0.18	0.02	-0.19	-0.28	-0.19	-0.06	0.02	0.37	-0.35	0.01	-0.28	-0.19	-0.20	0.27	-0.13	-0.30	-0.27	-0.10	-0.02	0.25	0.05	-0.27	-0.02	-0.20	0.04	0.17	0.03		
27	0.10	0.16	0.02	-0.18	-0.29	-0.19	-0.10	0.01	0.36	-0.37	0.03	-0.31	-0.22	-0.23	0.25	-0.10	-0.27	-0.29	-0.14	-0.10	0.20	0.05	-0.27	-0.01	-0.21	0.02	0.16	-0.05		
28	0.07	0.13	0.02	-0.17	-0.28	-0.19	-0.14	0.00	0.35	-0.38	0.06	-0.33	-0.24	-0.26	0.24	-0.07	-0.25	-0.30	-0.19	-0.18	0.15	0.04	-0.26	-0.00	-0.21	0.02	0.15	0.13		
29	0.02	0.09	0.10	-0.14	-0.27	-0.19	-0.18	-0.00	0.34	-0.37	0.08	-0.34	-0.26	-0.27	0.22	-0.05	-0.23	-0.29	-0.23	-0.25	0.10	0.05	-0.23	0.01	-0.19	-0.01	0.14	-0.21		
30	-0.05	0.06	0.11	-0.10	-0.24	-0.18	-0.22	0.46	0.32	-0.35	0.10	-0.34	-0.28	-0.28	0.21	-0.03	-0.20	-0.28	-0.28	-0.31	0.07	0.05	-0.19	0.03	-0.15	-0.02	0.14	-0.25		
31	-0.13	0.03	0.13	-0.07	-0.21	-0.17	-0.26	0.01	0.31	-0.31	0.12	-0.33	-0.29	-0.28	0.20	-0.02	-0.18	-0.27	-0.31	-0.34	0.05	0.06	-0.13	0.03	-0.10	-0.03	0.15	-0.27		
32	-0.20	0.01	0.15	-0.03	-0.16	-0.16	-0.30	0.02	0.29	-0.26	0.13	-0.31	-0.29	-0.26	0.19	-0.02	-0.15	-0.26	-0.33	-0.35	0.05	0.06	-0.06	0.04	-0.04	-0.03	0.17	-0.25		
33	-0.27	0.00	0.16	0.01	-0.10	-0.15	-0.33	0.03	0.28	-0.20	0.14	-0.28	-0.30	-0.24	0.18	-0.01	-0.12	-0.26	-0.34	-0.33	0.06	0.07	-0.35	0.03	0.03	-0.04	0.19	-0.21		
34	-0.31	0.00	0.17	0.03	-0.05	-0.13	-0.36	0.04	0.27	-0.13	0.15	-0.25	-0.31	-0.21	0.18	-0.01	-0.10	-0.27	-0.34	-0.28	0.08	0.08	0.05	0.01	0.09	-0.04	0.21	-0.15		
35	-0.33	0.00	0.18	0.05	0.11	-0.10	-0.38	0.05	0.26	-0.08	0.16	-0.22	-0.31	-0.18	0.17	-0.01	-0.08	-0.28	-0.33	-0.22	0.12	0.09	0.09	-0.02	-0.16	-0.05	0.23	-0.08		
36	-0.31	0.01	0.18	0.05	0.06	-0.08	-0.39	0.06	0.24	-0.03	0.16	-0.19	-0.31	-0.15	0.17	-0.00	-0.07	-0.29	-0.32	-0.15	0.14	0.10	0.10	-0.05	0.22	-0.06	0.24	-0.02		
37	-0.27	0.02	0.18	0.04	0.11	-0.05	0.40	0.07	0.23	0.01	0.16	-0.17	-0.31	-0.11	0.17	0.01	-0.07	-0.30	-0.30	-0.08	0.18	0.12	0.10	-0.10	0.26	-0.07	0.25	0.03		
38	-0.20	0.03	0.19	0.02	0.15	-0.03	-0.40	0.07	0.22	0.04	0.16	-0.15	-0.31	-0.09	0.16	0.02	-0.07	-0.29	-0.27	-0.02	0.21	0.14	0.09	-0.13	0.29	-0.09	0.25	0.06		
39	-0.11	0.02	0.19	-0.01	0.19	-0.01	-0.39	0.07	0.21	0.04	0.15	-0.13	-0.30	-0.06	0.18	0.03	-0.07	-0.27	-0.25	0.02	0.23	0.16	0.06	-0.17	0.30	-0.12	0.23	0.07		
40	-0.02	0.02	0.19	-0.03	0.22	0.00	-0.38	0.07	0.20	0.04	0.14	-0.12	-0.28	-0.05	0.14	0.05	-0.08	-0.22	-0.23	0.04	0.24	0.19	0.02	-0.20	0.30	-0.14	0.19	0.06		
41	0.07	0.01	0.20	-0.05	0.24	0.00	-0.37	0.07	0.19	0.03	0.13	-0.10	-0.26	-0.03	0.13	0.06	-0.10	-0.15	-0.20	0.04	0.24	0.22	-0.01	-0.21	0.29	-0.17	0.15	0.04		
42	0.14	0.01	0.20	-0.07	0.25	0.00	-0.35	0.06	0.18	0.01	0.11	-0.08	-0.23	-0.02	0.10	0.07	-0.11	-0.08	0.18	0.03	0.23	0.25	-0.04	-0.21	0.26	-0.20	0.09	0.02		
43	0.21	0.00	0.20	-0.08	0.26	0.00	-0.33	0.06	0.18	-0.02	0.09	-0.06	-0.19	-0.01	0.08	0.07	-0.11	0.00	0.16	-0.00	0.21	0.29	-0.07	-0.19	0.22	-0.22	0.03	0.01		
44	0.24	-0.01	0.19	-0.07	0.26	-0.01	-0.31	0.06	0.18	-0.04	0.06	-0.03	-0.15	-0.01	0.05	0.08	-0.12	0.07	0.13	-0.05	0.18	0.33	-0.09	-0.15	0.18	-0.24	-0.03	0.01		
45	0.26	-0.03	0.17	-0.06	0.25	-0.03	-0.29	0.05	0.18	-0.06	0.04	0.01	-0.11	0.01	0.02	0.08	-0.12	0.11	0.10	-0.10	0.15	0.36	-0.10	-0.09	0.13	-0.26	-0.08	0.02		
46	0.25	-0.05	0.15	-0.04	0.24	-0.05	-0.26	0.05	0.19	-0.08	0.02	0.05	-0.06	0.02	-0.01	0.09	-0.12	0.12	0.07	-0.13	0.10	0.38	-0.09	-0.02	0.08	-0.27	-0.12	0.04		
47	0.22	-0.08	0.11	-0.01	0.22	-0.07	-0.24	0.05	0.21	-0.09	0.00	0.08	-0.01	0.04	-0.04	0.09	-0.11	0.12	0.04	-0.16	0.06	0.40	-0.08	0.05	0.03	-0.27	-0.14	0.04		
48	0.17	-0.12	0.06	0.02	0.20	-0.09	-0.02	0.05	0.23	-0.09	0.02	0.12	0.03	0.06	-0.07	0.09	-0.10	0.11	0.02	-0.18	0.01	0.40	-0.06	0.12	-0.01	-0.26	-0.15	0.02		
49	0.10	-0.15	0.00	0.06	0.18	-0.10	-0.02	0.05	0.25	-0.09	0.03	0.15	0.08	0.09	-0.10	0.08	-0.09	0.10	0.05	-0.19	-0.02	0.39	-0.02	0.17	-0.04	-0.26	-0.15	-0.00		
50	0.05	-0.18	-0.05	0.10	0.16	-0.09	-0.02	0.05	0.27	-0.09	0.05	0.19	0.01	0.12	-0.09	0.07	-0.07	0.09	0.02	-0.18	-0.05	-0.37	0.01	0.21	-0.06	-0.25	-0.14	-0.05		

VALUES OF LAG

AUTOCORRELATION VALUES FOR VARIOUS LAGS

ND SUB-INTERVALS
ECOND INTERVAL

S.D.

RVAL S.D.

TABLE 1.
SUMMARY OF AUTOCORRELATION FUNCTIONS

		PING 5						PING 6						PING 7						PING 8						PING 9						PING 10					
e	f	a	b	c	d	e	f	a	b	c	d	e	f	a	b	c	d	e	f	a	b	c	d	e	f	a	b	c	d	e	f	a	b	c	d	e	f
				56.5						60.8						57.5						67.9						73.5						61.1					
48.5	58.2	6.28	72.8	79.7	68.5	64.4	50.5	56.4	71.5	66.7	63.8	53.4	53.2	40.9	48.4	61.1	61.8	66.1	66.9	53.7	60.2	86.9	72.9	68.2	65.5	72.6	81.4	62.6	75.6	63.8	85.0	72.2	77.9	93.9	48.6	60.0	49.9
				33.9						37.7						31.5						33.4						41.9						32.9			
22.7	23.1	3.28	39.9	39.2	30.0	30.5	30.7	33.3	38.4	34.5	35.0	27.6	27.3	23.6	26.8	29.1	35.0	36.0	38.4	27.2	35.9	34.2	34.1	32.1	36.8	44.8	52.0	30.5	47.9	35.8	40.1	39.1	33.2	51.5	20.8	28.8	23.8
0.97	0.98	0.98	0.99	0.98	0.96	0.98	0.98	0.97	0.97	0.98	0.98	0.98	0.97	0.99	0.97	0.97	0.98	0.97	0.98	0.98	0.96	0.94	0.96	0.96	0.98	0.98	0.99	0.98	0.98	0.97	0.99	0.98	0.95	0.98	0.95	0.98	0.97
0.87	0.91	0.92	0.95	0.93	0.85	0.89	0.93	0.91	0.88	0.93	0.91	0.91	0.90	0.95	0.90	0.90	0.92	0.90	0.93	0.92	0.86	0.79	0.84	0.87	0.92	0.94	0.95	0.92	0.93	0.88	0.94	0.92	0.83	0.92	0.81	0.92	0.88
0.72	0.82	0.83	0.89	0.86	0.69	0.78	0.84	0.81	0.77	0.85	0.82	0.81	0.78	0.89	0.79	0.78	0.83	0.79	0.87	0.83	0.71	0.59	0.68	0.73	0.84	0.88	0.89	0.83	0.86	0.75	0.88	0.84	0.65	0.83	0.61	0.82	0.75
0.55	0.70	0.71	0.82	0.77	0.50	0.64	0.74	0.69	0.63	0.76	0.70	0.69	0.63	0.82	0.65	0.64	0.73	0.66	0.78	0.73	0.52	0.36	0.48	0.57	0.73	0.80	0.82	0.73	0.76	0.59	0.80	0.74	0.44	0.71	0.40	0.71	0.59
0.37	0.56	0.58	0.75	0.67	0.32	0.49	0.62	0.57	0.50	0.64	0.56	0.56	0.48	0.74	0.51	0.48	0.61	0.51	0.69	0.62	0.33	0.16	0.29	0.41	0.61	0.72	0.73	0.63	0.66	0.41	0.72	0.62	0.25	0.58	0.21	0.60	0.43
0.21	0.43	0.45	0.67	0.58	0.17	0.34	0.51	0.45	0.38	0.53	0.42	0.42	0.32	0.67	0.38	0.32	0.49	0.36	0.59	0.51	0.15	0.00	0.11	0.27	0.50	0.63	0.64	0.53	0.55	0.22	0.64	0.51	0.09	0.45	0.05	0.48	0.27
0.07	0.30	0.32	0.60	0.49	0.05	0.21	0.40	0.35	0.29	0.41	0.29	0.30	0.17	0.59	0.26	0.17	0.37	0.22	0.50	0.40	-0.24	-0.08	-0.05	0.16	0.39	0.55	0.55	0.44	0.44	0.06	0.56	0.40	-0.04	0.33	0.06	0.38	0.14
-0.04	0.19	0.19	0.54	0.40	-0.02	0.09	0.31	0.27	0.22	0.31	0.17	0.19	0.04	0.51	0.15	0.03	0.26	0.10	0.42	0.31	-0.11	-0.11	-0.17	0.08	0.29	0.47	0.46	0.36	0.34	-0.08	0.49	0.30	-0.12	0.22	-0.12	0.30	0.04
-0.11	0.10	0.09	0.49	0.33	-0.05	-0.01	0.23	0.21	0.18	0.21	0.07	0.10	-0.05	0.44	0.06	-0.08	0.17	-0.01	0.35	0.21	-0.19	-0.08	-0.25	0.04	0.21	0.39	0.38	0.31	0.25	-0.17	0.44	0.21	-0.16	0.12	-0.14	0.23	-0.03
-0.15	0.04	-0.00	0.44	0.28	-0.06	-0.09	0.17	0.17	0.17	0.12	-0.02	0.03	-0.12	0.38	-0.00	-0.17	0.09	-0.09	0.28	0.13	-0.23	-0.03	-0.30	0.02	0.15	0.32	0.31	0.27	0.17	-0.24	0.40	0.13	-0.17	0.04	-0.13	0.18	-0.08
-0.16	0.01	-0.07	0.41	0.23	-0.05	-0.15	0.13	0.15	0.17	0.05	-0.08	-0.01	-0.15	0.33	-0.06	-0.22	0.02	-0.15	0.23	0.05	-0.24	0.02	-0.33	0.02	0.11	0.26	0.25	0.25	0.10	-0.26	0.37	0.05	-0.17	-0.03	-0.11	0.14	-0.10
-0.14	-0.03	0.12	0.38	0.20	-0.04	-0.20	0.10	0.14	0.16	-0.02	-0.12	-0.04	-0.15	0.28	-0.10	-0.25	-0.03	-0.20	0.18	-0.03	-0.23	0.05	-0.33	0.02	0.09	0.20	0.20	0.24	0.04	-0.26	0.36	-0.02	-0.16	-0.08	-0.10	0.12	-0.11
-0.11	-0.04	-0.15	0.36	0.17	-0.04	-0.23	0.09	0.13	0.16	-0.07	-0.14	-0.04	-0.12	0.24	-0.14	-0.26	-0.07	-0.22	0.14	-0.11	-0.21	0.04	-0.31	0.03	0.10	0.16	0.16	0.25	-0.00	-0.24	0.35	-0.09	-0.15	-0.11	-0.12	0.11	-0.11
-0.07	-0.04	-0.15	0.34	0.16	-0.05	-0.25	0.10	0.13	0.14	-0.12	-0.15	-0.03	-0.07	0.21	-0.16	-0.24	-0.10	-0.22	0.19	-0.19	-0.18	-0.02	-0.27	0.04	0.12	0.32	0.34	0.26	-0.04	-0.20	0.34	-0.14	-0.14	-0.13	-0.15	0.11	-0.12
-0.03	-0.03	-0.15	0.32	0.16	-0.07	-0.27	0.10	0.13	0.12	-0.16	-0.14	-0.00	-0.00	0.18	-0.18	-0.21	-0.12	-0.21	0.07	-0.27	-0.14	-0.12	-0.23	0.05	0.18	0.09	0.12	0.27	-0.07	-0.15	0.33	-0.18	-0.14	-0.14	-0.20	0.13	-0.12
0.01	-0.02	-0.14	0.30	0.17	-0.09	-0.26	0.12	0.14	0.10	-0.19	-0.12	0.03	0.07	0.15	-0.18	-0.16	-0.12	-0.18	0.05	-0.34	-0.10	-0.24	-0.17	0.06	0.22	0.07	0.12	0.29	-0.08	-0.11	0.32	-0.21	-0.13	-0.13	-0.25	0.15	0.13
0.03	-0.01	-0.12	0.28	0.19	-0.10	-0.24	0.13	0.14	0.08	-0.22	-0.09	0.06	0.14	0.13	-0.18	-0.10	-0.12	-0.14	0.03	-0.39	-0.05	-0.36	-0.10	0.07	0.29	0.07	0.12	0.30	-0.09	-0.07	0.31	-0.21	-0.11	-0.11	-0.28	0.17	-0.13
0.04	0.00	-0.10	0.25	0.20	-0.10	-0.19	0.15	0.14	0.07	-0.25	-0.06	0.11	0.21	0.11	-0.17	-0.04	-0.12	-0.09	0.02	-0.44	-0.00	-0.44	-0.01	0.08	0.36	0.24	0.12	0.31	-0.08	-0.03	0.30	-0.20	-0.08	-0.08	-0.28	0.19	-0.13
0.02	0.01	-0.09	0.22	0.22	-0.07	-0.13	0.16	0.14	0.06	-0.26	-0.03	0.15	0.27	0.10	-0.15	0.03	-0.11	-0.03	0.01	-0.47	0.06	-0.48	0.08	0.10	0.43	0.09	0.13	0.30	-0.07	-0.01	0.28	-0.18	-0.04	-0.02	-0.25	0.21	-0.11
-0.01	0.01	-0.09	0.20	0.23	-0.02	0.05	0.17	0.14	0.06	-0.27	-0.01	0.18	0.31	0.10	-0.11	0.09	-0.09	0.03	0.01	-0.49	0.12	-0.48	0.18	0.12	0.50	0.11	0.14	0.28	-0.06	-0.00	0.25	0.14	0.01	0.04	-0.19	0.22	-0.09
-0.05	0.00	-0.09	0.17	0.23	0.04	0.03	0.19	0.13	0.06	-0.29	0.01	0.21	0.34	0.09	-0.06	0.13	-0.07	0.10	0.01	-0.50	0.18	-0.43	0.27	0.14	0.56	0.13	0.15	0.25	-0.04	-0.15	0.21	-0.10	0.07	0.11	-0.13	0.21	-0.06
-0.10	-0.00	-0.11	0.14	0.23	0.09	0.13	0.20	0.12	0.07	-0.29	0.01	0.22	0.35	0.09	-0.01	0.17	-0.06	0.17	0.00	-0.49	0.24	-0.35	0.33	0.15	0.59	0.14	0.15	0.20	-0.02	-0.06	0.16	-0.05	0.12	0.18	-0.07	0.20	-0.02
-0.15	-0.01	-0.13	0.12	0.22	0.13	0.22	0.23	0.10	0.07	-0.30	0.00	0.23	0.34	0.09	0.05	0.18	-0.05	0.23	-0.00	-0.47	-0.29	-0.27	0.35	0.15	0.60	0.15	0.14	0.14	0.00	-0.02	0.12	-0.01	0.16	0.25	-0.04	0.16	0.02
-0.20	-0.02	-0.16	0.09	0.20	0.13	0.31	0.25	0.06	0.06	-0.29	-0.02	0.22	0.31	0.09	0.11	0.18	-0.04	0.29	-0.01	-0.44	0.34	-0.20	0.33	0.13	0.59	0.15	0.13	0.07	0.02	-0.03	0.07	0.03	0.18	0.31	-0.04	0.12	0.06
-0.24	-0.02	-0.18	0.06	0.19	0.10	0.38	0.29	0.03	0.04	-0.29	-0.05	0.20	0.27	0.09	0.17	0.15	-0.04	0.32	-0.01	-0.40	0.37	-0.16	0.28	0.10	0.56	0.15	0.11	-0.01	0.04	-0.05	0.01	0.06	0.18	0.36	-0.07	0.07	0.08
-0.27	-0.02	-0.20	0.04	0.17	0.03	0.44	0.32	0.02	0.00	-0.27	-0.09	0.17	0.23	0.09	0.21	0.11	-0.04	0.34	-0.01	-0.35	0.38	-0.15	0.19	0.07	0.50	0.14	0.07	-0.08	0.05	-0.06	-0.04	0.08	0.16	0.39	-0.12	0.03	0.10
-0.27	-0.01	-0.21	0.02	0.16	-0.05	0.48	0.36	-0.07	-0.04	-0.25	0.14	0.14	0.18	0.08	0.23	0.06	-0.05	0.34	-0.02	-0.31	0.37	-0.17	0.08	0.03	0.42	0.12	0.04	-0.13	0.05	-0.06	-0.08	0.09	0.13	0.41	-0.19	-0.02	0.10
-0.26	-0.00	-0.21	0.02	0.15	0.13	0.50	0.40	-0.13	-0.09	-0.22	-0.20	0.11	0.13	0.07	0.24	-0.01	-0.06	0.31	-0.02	-0.26	0.33	-0.21	-0.04	-0.01	0.34	0.10	-0.01	-0.18	0.05	-0.05	-0.12	0.08	0.10	0.41	-0.25	-0.06	0.09
-0.23	0.01	-0.19	-0.01	0.14	-0.21	0.49	0.43	-0.18	-0.14	-0.18	-0.25	0.08	0.10	0.06	0.24	-0.08	-0.08	0.26	-0.02	-0.22	0.27	-0.25	-0.16	-0.05	0.26	0.08	-0.06	-0.21	0.04	-0.03	-0.16	0.07	0.08	0.39	-0.30	-0.10	0.07
-0.19	0.03	-0.15	-0.02	0.14	-0.25	0.47	0.46	-0.24	-0.17	-0.14	-0.29	0.05	0.07	0.04	0.22	-0.14	-0.10	0.19	-0.03	-0.17	0.21	-0.28	-0.26	-0.08	0.18	0.04	-0.11	-0.22	0.02	0.02	-0.19	0.05	0.07	0.37	-0.33	-0.13	0.05
-0.13	0.03	-0.10	-0.03	0.15	-0.27	0.43	0.49	-0.28	-0.19	-0.09	-0.31	0.02	0.06	0.03	0.19	-0.21	-0.12	0.11	-0.04	-0.13	0.15	-0.28	-0.34	-0.12	0.12	0.01	-0.15	-0.21	-0.01	0.07	-0.22	0.02	0.08	0.33	-0.33	-0.15	0.02
-0.06	0.04	-0.04	-0.03	0.17	-0.25	0.38	0.50	-0.32	-0.20	-0.04	-0.32	0.00	0.06	0.00	0.15	-0.26	-0.14	0.03	-0.05	-0.09	0.10	-0.24	-0.39	-0.15	0.08	-0.04	-0.19	-0.19	-0.05	0.14	-0.25	-0.00	0.10	0.28	-0.30	-0.17	-0.00
-0.35	0.03	0.03	-0.04	0.19	-0.21	0.33	0.51	-0.35	-0.19	0.01	-0.31	-0.03	0.06	-0.02	0.11	-0.30	-0.17	-0.06	-0.06	-0.05	0.07	-0.16	-0.41	-0.19	0.06	-0.09	-0.23	-0.15	-0.09	0.21	-0.27	-0.03	0.13	0.24	-0.24	-0.18	-0.02
0.05	0.01	0.09	-0.04	0.21	-0.15	0.26	0.49	-0.36	-0.17	0.06	-0.29	-0.06	0.07	-0.05	0.07	-0.32	-0.19	-0.14	-0.08	-0.01	0.04	-0.05	-0.40	-0.24	0.05	-0.13	-0.25	-0.11	-0.12	0.29	-0.28	-0.05	0.15	0.18	-0.17	-0.19	-0.04
0.09	-0.02	-0.16	-0.05	0.23	-0.08	0.19	0.47	-0.35	-0.15	0.10	-0.26	-0.09	0.08	-0.08	0.03	-0.32	-0.23	-0.21	-0.10	0.04	0.03	0.07	-0.35	-0.28	0.07	-0.18	-0.27	-0.06	-0.15	0.35	-0.29	-0.08	0.15	0.13	0.09	-0.20	-0.06
0.10	-0.05	0.22	-0.06	0.24	-0.02	0.12	0.43	-0.34	-0.12	0.14	-0.21	-0.12	0.08	-0.12	-0.00	-0.31	-0.26	-0.26	-0.12	0.07	0.02	0.17	-0.29	-0.32	0.10	-0.22	-0.28	-0.00	-0.18	0.39	-0.30	-0.09	0.14	0.08	-0.01	-0.21	-0.08
0.10	-0.10	0.26	-0.07	0.25	0.03	0.05	0.38	-0.31	-0.09	0.17	-0.15	-0.15	0.08	-0.15	-0.03	-0.28	-0.29	-0.31	-0.15	0.11	0.01	0.25	-0.21	-0.36	0.14	-0.26	-0.28	0.04	-0.20	0.42	-0.30	-0.11	0.12	0.02	0.07	-0.22	-0.09
0.09	-0.13	0.29	-0.09	0.25	0.06	-0.01	0.32	-0.28	-0.07	0.19	-0.08	-0.19	0.07	-0.19	-0.06	-0.23	-0.32	-0.33	-0.18	0.14	-0.01	0.28	-0.13	-0.39	0.18	-0.28	-0.28	0.07	-0.20	0.42	-0.29	-0.11	0.08	-0.04	0.12	-0.22	-0.10
0.06	-0.17	0.30	-0.12	0.23	0.07	-0.08	0.26	-0.25	-0.06	0.21	-0.00	-0.22	0.05	-0.22	-0.08	-0.18	-0.34	-0.35	-0.21	0.16	-0.04	0.25	-0.04	-0.41	0.23	0.30	-0.27	0.09	-0.20	0.39	-0.29	-0.12	0.04	-0.09	0.16	-0.22	-0.12
0.02	-0.20	0.30	-0.14	0.19	0.06	-0.13	0.20	-0.21	-0.04	0.21	0.08	-0.24	0.02	-0.25	-0.09	-0.12	-0.35	-0.36	-0.23	0.17	-0.09	0.18	0.05	-0.41	0.26	-0.32	-0.26	0.09	-0.18	0.34	-0.28	-0.11	0.00	-0.15	0.19	-0.22	-0.13
-0.01	-0.21	0.29	-0.17	0.15	0.04	-0.18	0.14	-0.17	-0.04	0.21	0.15	-0.26	-0.02	-0.28	-0.10	-0.06	-0.35	-0.36	-0.25	0.17	-0.14	0.08	0.13	-0.39	0.29	-0.32	-0.24	0.07	-0.15	0.27	-0.27	-0.11	-0.04	-0.20	0.19	-0.22	-0.15
-0.04	-0.21	0.26	-0.20	0.09	0.02	-0.22	0.10	-0.14	-0.03	0.21	0.23	-0.27	-0.06	-0.29	-0.10	0.00	-0.33	-0.36	-0.27	0.17	-0.20	-0.02	0.21	-0.36	0.31	-0.32	-0.23	0.05	-0.11	0.19	-0.27	-0.09	-0.07	-0.24	0.17	-0.22	-0.16
-0.07	-0.19	0.22	-0.22	0.03	0.01	-0.25	0.06	-0.10	-0.02	0.19	0.29	-0.27	-0.11	-0.30	-0.10	0.06	-0.29	-0.37	-0.28	0.17	-0.24	-0.10	0.27	-0.31	0.32	-0.32	-0.21	0.01	-0.07	0.10	-0.27	-0.07	-0.08	-0.27	0.14	-0.21	-0.16
-0.09	-0.15	0.18	-0.24	-0.03	0.01	-0.26	0.04	-0.06	-0.02	0.18	0.33	-0.27	-0.15	-0.31	-0.10	0.11	-0.24	-0.37	-0.28	0.16	-0.26	-0.15	0.33	-0.27	0.31	-0.31	-0.19	-0.03	-0.01	0.00	-0.27	-0.05	-0.09	-0.30	0.10	-0.21	-0.16
-0.10	-0.09	0.13	-0.26	-0.08	0.02	-0.26	0.03	-0.01	-0.01	0.16	0.36	-0.25	-0.18	-0.30	-0.08	0.15	-0.18	-0.37	-0.28	0.16	-0.26	-0.15	0.36	-0.22	0.29	-0.29	-0.18	-0.06	0.05	-0.08	-0.29	-0.03	-0.09	-0.31	0.05	-0.21	-0.15
-0.09	-0.02	0.08	-0.27	-0.12	0.04	-0.24	0.03	0.04	0.00	0.14	0.37	-0.22	-0.20	-0.29	-0.05	0.18	-0.12	-0.36	-0.28	0.16	-0.21	-0.11	0.37	-0.18	0.26	-0.26	-0.17	-0.09	0.11	-0.16	-0.30	-0.00	-0.09	-0.30	0.01	-0.21	-0.13
-0.08	0.05	0.03	-0.27	-0.14	0.04	-0.20	0.04	0.10	0.02	0.12	0.37	-0.20	-0.21	-0.27	-0.02	0.20	-0.07	-0.34	-0.28	0.15	-0.14	-0.04	0.37	-0.16	0.21	-0.23	-0.16	-0.11	0.16	-0.22	-0.32	0.03	-0.09	-0.29	0.05	-0.22	-0.11
-0.06	0.12	-0.01	-0.26	-0.15	0.02	-0.14	0.05	0.14	0.03	0.10	0.36	-0.17	-0.21	-0.23	0.02	0.21	-0.02	-0.31	-0.28	0.14	-0.03	0.07	0.33	-0.15	0.14	-0.19	-0.16	-0.12	0.20	-0.26	0.34	0.06	-0.11	-0.26	0.09	-0.23	-0.08
-0.02	0.17	-0.04	-0.26	-0.15	-0.00	-0.06	0.09	0.17	0.03	0.07	0.34	-0.15	-0.18	-0.19	0.06	0.21	0.02	-0.27	-0.29	0.12	0.09	0.18	0.27	-0.16	0.07	-0.15	-0.16	-0.12	0.24	-0.28	-0.35	0.09	-0.13	-0.23	0.11	-0.24	-0.06
0.01	0.21	-0.06	-0.25	-0.14	-0.05	0.03	0.12	0.18	0.03	0.05	0.31	-0.13	-0.14	-0.14	0.09	0.19	-0.06	-0.22	-0.30	0.10	0.21	0.28	0.18	-0.18	-0.01	-0.12	-0.16	-0.11	0.27	-0.28	-0.36	0.12	-0.17	-0.18	0.11	-0.25	-0.03

pings	1 - 34	16.0 - 17.5 seconds
pings	1 - 34	14.5 - 16.0 seconds
pings	35 - 61	12.0 - 13.5 seconds
pings	35 - 77	9.0 - 10.5 seconds
pings	78 - 123	13.5 - 15.0 seconds
pings	124 - 200	14.5 - 16.0 seconds

The interval sampled for some of the pings included the target return. This occurred for the following intervals: (1) pings 17 - 34; 16.0 - 17.5 seconds, and (2) pings 51 - 61; 12.0 - 13.5 seconds.

These intervals are not included in the results presented here. An analysis of the statistical data for each ping indicated the following.

The mean and the standard deviation varied from ping to ping: however, there appeared to be a linear relation between them. Noting that for a Rayleigh Distribution the ratio of the standard deviation to the mean is a constant; i.e., ρ/μ equals 0.52, we plot the line

S.D. = 0.52 mean

In our earlier report the relationship of the mean to the standard deviation was obtained from a free-hand fit, using the initial results from 61 surface duct pings, (see Reference 1, page 51/52). In order to generalize this result to both surface duct and bottom bounce, and to obtain a more objective fit, a least-squares linear regression line was computed for a subset of the data, consisting of a random sample of 62 pings taken from surface duct and bottom bounce intervals. The relationship obtained was

S.D. = 0.645 mean - 11.27

The corresponding line for a Rayleigh distribution is

S.D. = 0.523 mean*

and the equation of the free hand fit was

S.D. = 0.429 mean + 10.95

The difference between the free-hand fit and the least-squares can be in part explained by the fact that they are not based on exactly the same data, and that the free-hand fit did

* A typographical error in the original report incorrectly stated the coefficient as 0.423.

not include any bottom bounce pings. It is of interest to note that, if the average of the estimated slopes and intercepts is calculated, we obtain

S.D. = 0.537 mean - 0.16

which is close to the theoretical values for a Rayleigh distribution. All three lines fit the data quite well. If this point is pursued further, a regression analysis should be made based on all the data. This should include confidence bounds about the regression line.*

The coefficient of correlation between the mean and standard deviation for the data used in the least-squares regression was 0.89; i.e., 79 percent of the variation in the standard deviation could be attributed to the variation in the mean. The average value of the mean and standard deviation was 104.4 and 56.0 (all numbers have been divided by 10^3). It was noted (Figure 35) that the points representing no signal return are closely clustered about the plotted line and generally fall in the region (mean < 80). The majority of intervals which contained the target did not necessarily fall near the line and most are off the scale of the plot and hence are not shown. Thus, the ratio of the mean to the standard deviation over a 1.5-second interval might be used as part of a scheme to differentiate intervals with targets from target-free intervals.

The above result indicates that the mean and standard deviation are highly correlated; that is, for no-target intervals, the higher the output level the larger the spread of the values. This result applies to both surface duct and bottom bounce returns. In fact, the location along the line was more a function of the day of the recording than it was the mode of transmission. Pings 1 to 34 (16.0 to 17.5 seconds) which represented one day's recordings, were generally grouped at the low end of the line in Figure 35 below a mean of 10.5 (after elimination of the pings with targets in the intervals) while pings 36 to 72, which were recorded on another day, were clustered in the upper region above 100. The bottom bounce pings (78 to 123), which were all recorded on the same day, also generally fell at the low end of the scale, while pings 124 to 200 were at the high end.

The distribution of the correlator output was positively skewed for every interval; thus, the distribution was asymmetrical with a long tail at the high end of the distribution. The values of

$$\sqrt{b_1} = \frac{\sqrt{n}\ \Sigma (x_i - \bar{x})^3}{[\Sigma (x_i - \bar{x})^2]^{3/2}} = \text{standard measure of skewness}$$

* As a matter of fact, since both the mean and standard deviation are random variables, appropriate techniques for such cases should be used rather than assuming that the means are fixed as was done above.

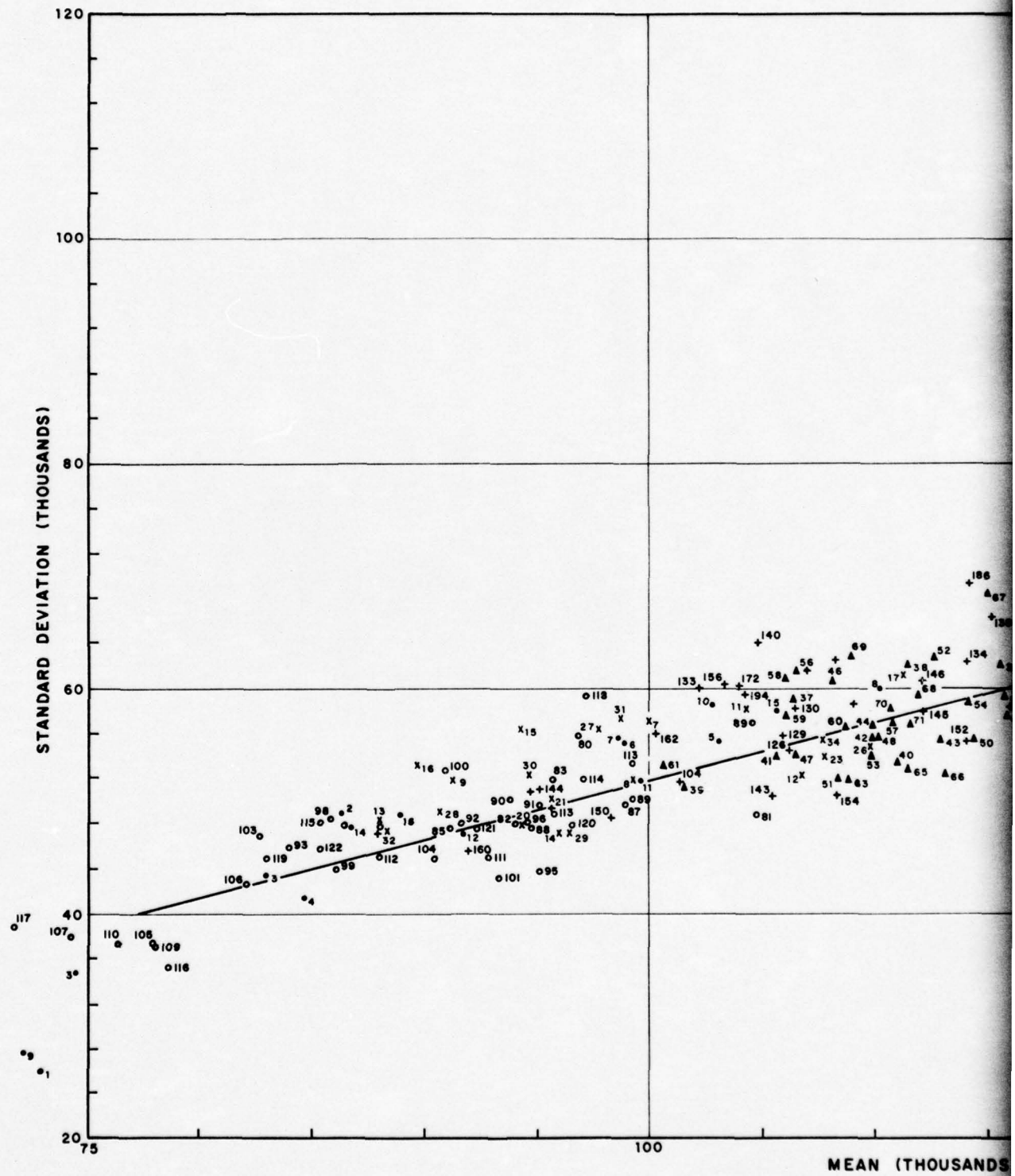
120
100
80
60
40
20
75
100
STANDARD DEVIATION (THOUSANDS)
MEAN (THOUSANDS

A2304

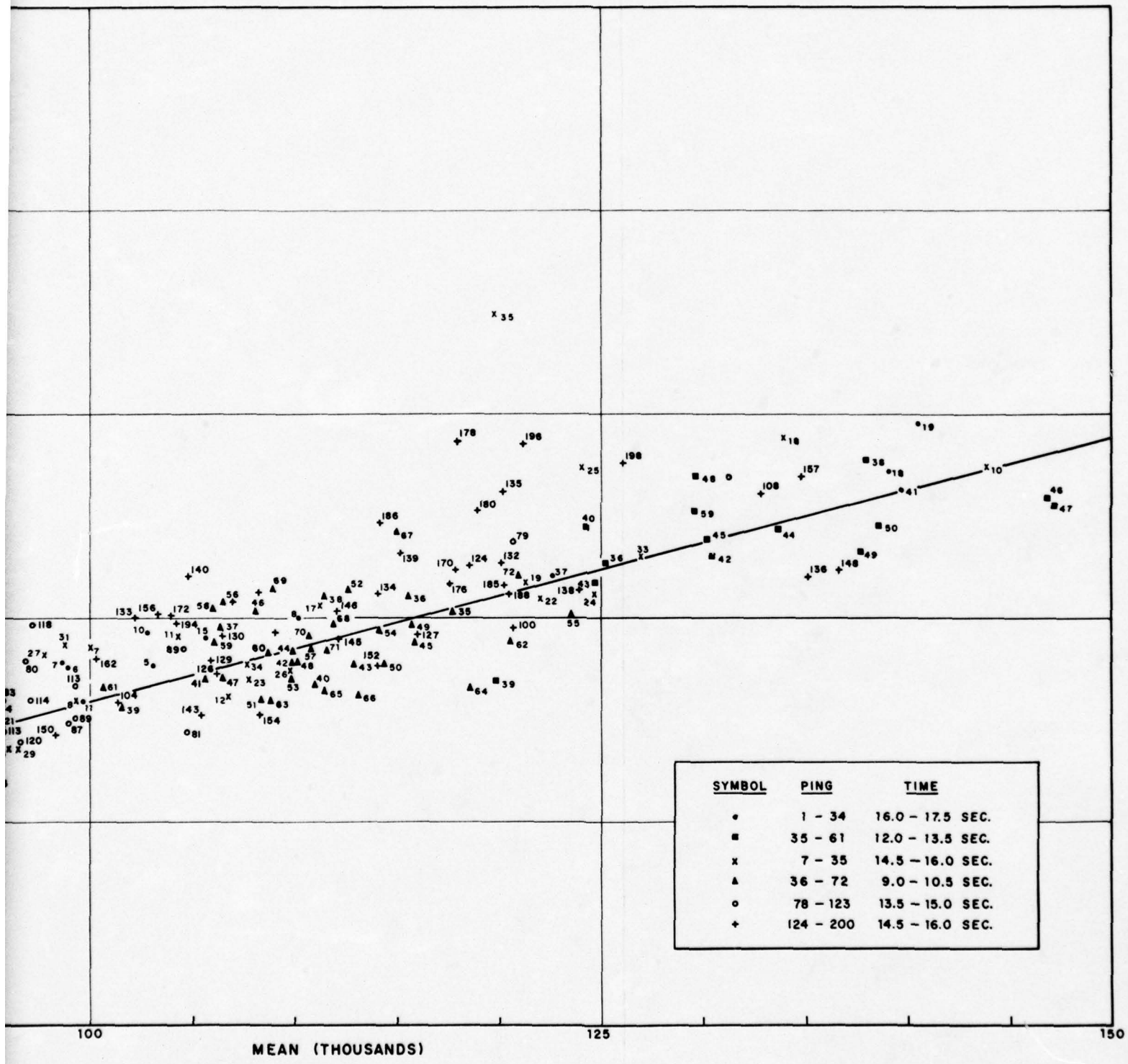

Figure 35. Standard Deviation vs. Mean

were generally less than 1.0, although several exceptions were noted. There was no apparent difference in the $\sqrt{b_1}$ values for the surface duct and bottom bounce transmissions. The values of

$$b_2 = \frac{n \Sigma (x_i - \bar{x})^4}{[\Sigma (x_i - \bar{x})^2]^2} = \text{standard measure of kurtosis}$$

which measures the relative peakedness of the distribution were generally less than 4.0, although there were numerous exceptions. There was an apparent linear relationship between $\sqrt{b_1}$ and b_2 which is illustrated in the plot of Figure 36. The estimate of the relationship based on the free-hand fit of the line is

$$\sqrt{b_1} = 0.368\, b_2 - 0.568$$

The line was drawn on the basis of pings 1 to 61, however, it appears to fit the subsequently plotted data. There does not appear to be any difference in the surface duct and bottom bounce modes.

A least-squares regression line has been computed based on a random sample of 62 pings from the surface duct and bottom bounce modes. The relationship obtained was

$$\sqrt{b_1} = 0.288\, b_2 - 0.280$$

The coefficient of correlation was 0.89; i.e., 0.79 percent of the variation in b_2 could be explained by the variation in $\sqrt{b_1}$. The average value of $\sqrt{b_1}$ and b_2 was 0.69 and 3.28 compared to the Rayleigh values for $\sqrt{\beta_1}$ and β_2 of 0.63 and 3.26.

Based on these results, one can tentatively hypothesize that the distribution of 1.5-second intervals of target-free returns have the same properties in both modes of transmission. This hypothesis must be substantiated by further investigations.

The theoretical values of $\sqrt{b_1}$ and b_2 for a Rayleigh distribution are 0.63 and 3.26 which fall on the plotted line of Figure 36.

Care must be exercised in using these standardized moments for evaluation purposes, because they are quite sensitive to one or two extreme values; thus, these statistics should be evaluated in conjunction with a probability plot. In most cases where extreme values of $\sqrt{b_1}$ and b_2 were obtained, it was due to one very high value.

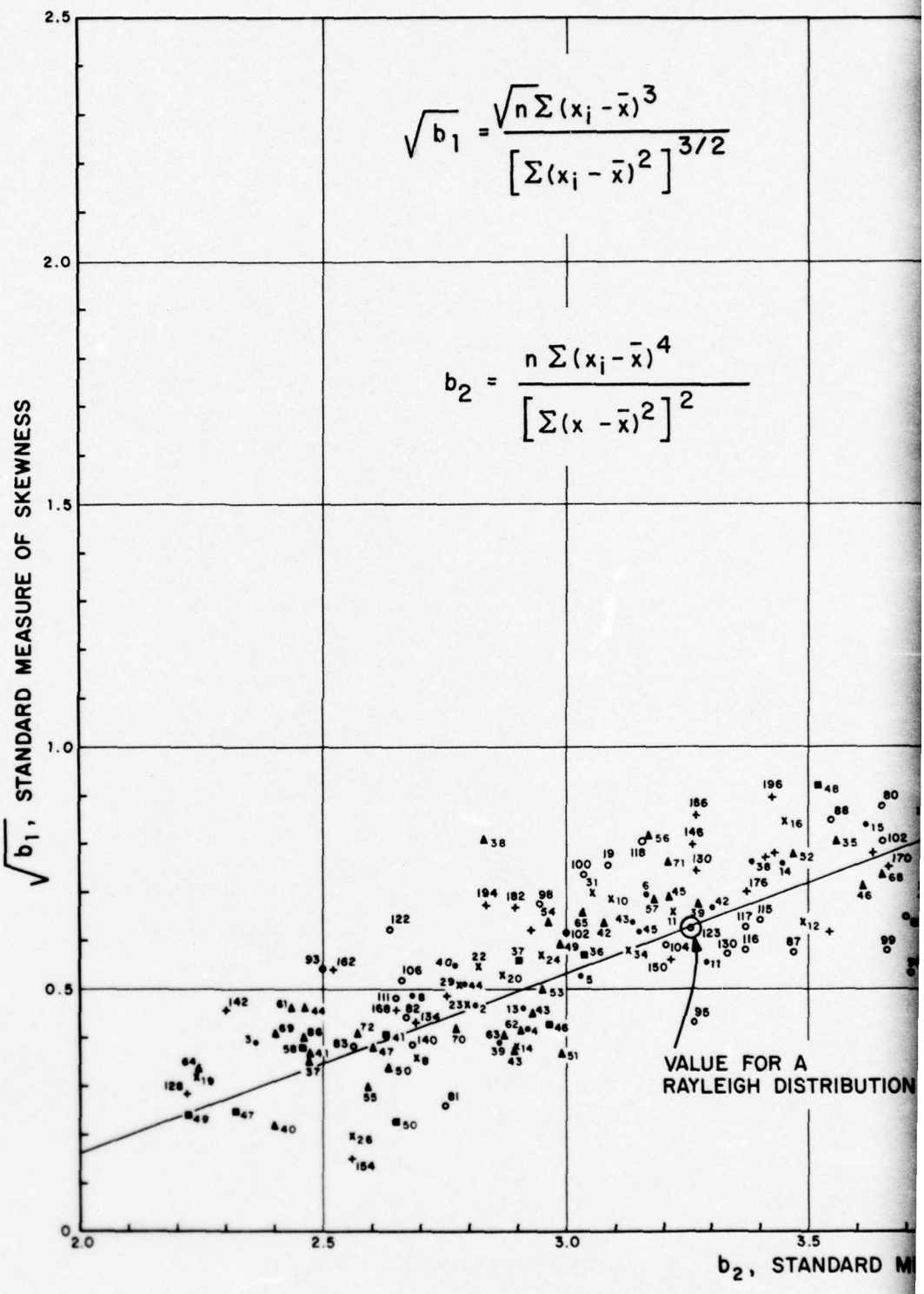

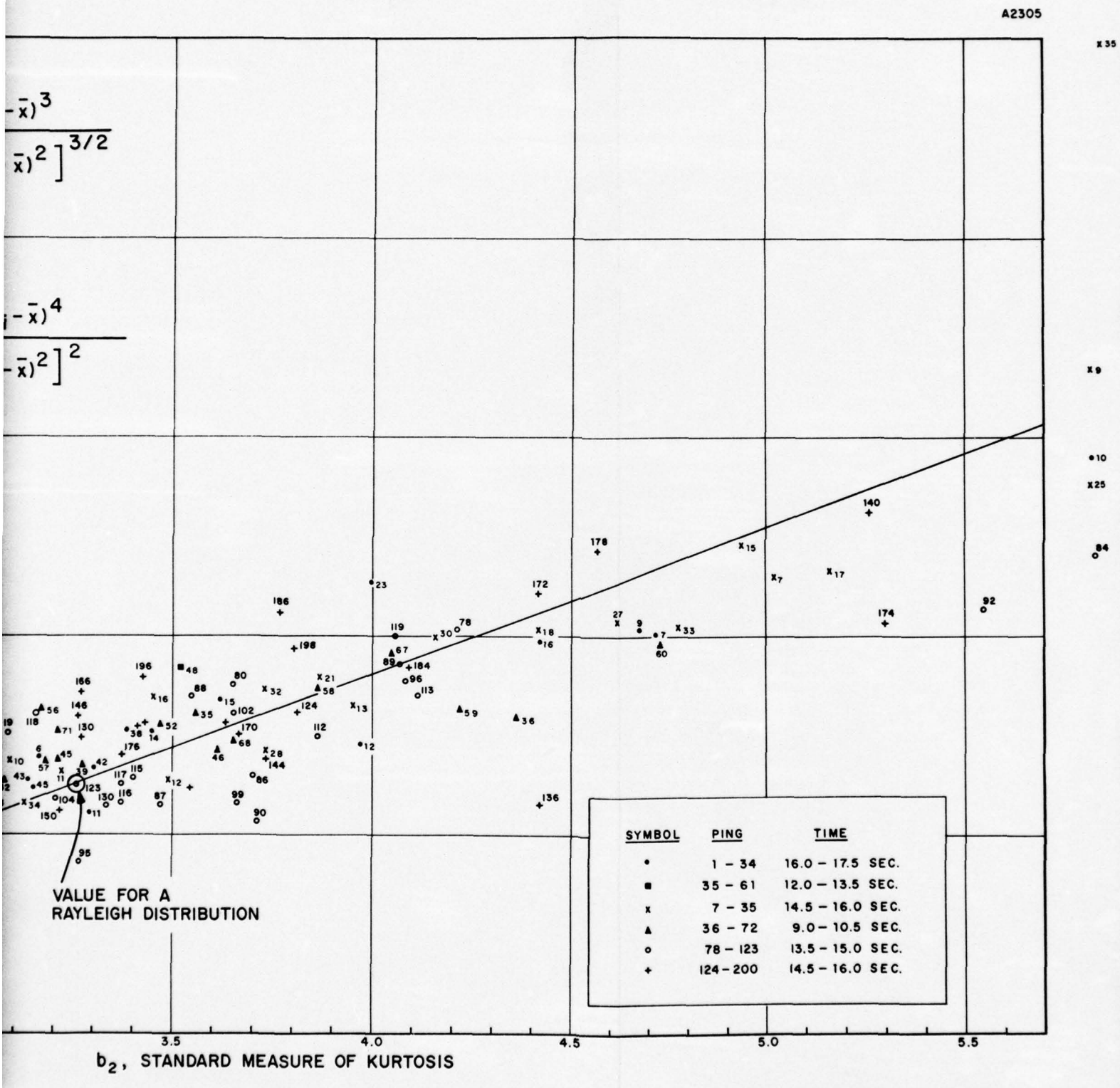

Figure 36. Standard Measure of Kurtosis vs. Standard Measure of Skewness

D. ANALYSIS OF HISTOGRAMS

Histograms plotted for intervals from some of the earliest pings studied are shown in Figure 37. The purpose of the histograms was to convey a general idea of the shape of distribution from which the data were taken and to allow a visual comparison of the various pings and intervals within a ping. An examination of the histogram showed that the shapes for similar intervals from adjacent pings are similar, but the shape varies over time. An attempt was made to relate the shape of the histogram to characteristics of the power plots. The plots can be categorized as follows (although there is a continuum of shapes).

1. Noise Interval -- No Specific Feature

These plots are generally concentrated about the modal value and the right-hand tail drops sharply. See pings 29 to 32 (14.5 to 16.0 seconds) in Figure 37. Values over 300,000 are very rare, with most values falling below 200,000.

2. Noise Interval -- Includes Lesser Reverberation Maximum

These plots are not as concentrated about the modal value. See pings 45 to 48 (12.0 to 13.5 seconds) in Figure 37. The right-hand tail contains a relatively higher percentage of values than the pings in the above category. The occurence of values over 300,000 are still not common but values over 200,000 are quite prevalent.

3. Noise Interval -- Includes Dominant Reverberation Maximum

These plots are more diffuse (flatter) than those in the second category above. See pings 57 to 60 (12 to 13.5 seconds) in Figure 37. There is a fair percentage of values greater than 300,000 and values over 200,000 are common.

4. Interval Containing Target Echo Arrival

These plots are quite flat with a high right-hand tail. These distributions generally have high values of $\sqrt{b_1}$ due to the long right-hand tail. See pings 29 to 32 (16.0 to 17.5 seconds) in Figure 37. There is a large percentage of values over 300,000.

The above results suggest that for intervals of noise input, the correlator output has an average output between 90,000 and 100,000, and its upper tail drops rapidly so that most of the observations are below 200,000. If the relative reverberation level increases, this distribution becomes more diffuse with the right-hand tail getting longer. When a signal return is present, the distribution becomes more diffuse and the proportion of high correlator outputs increases.

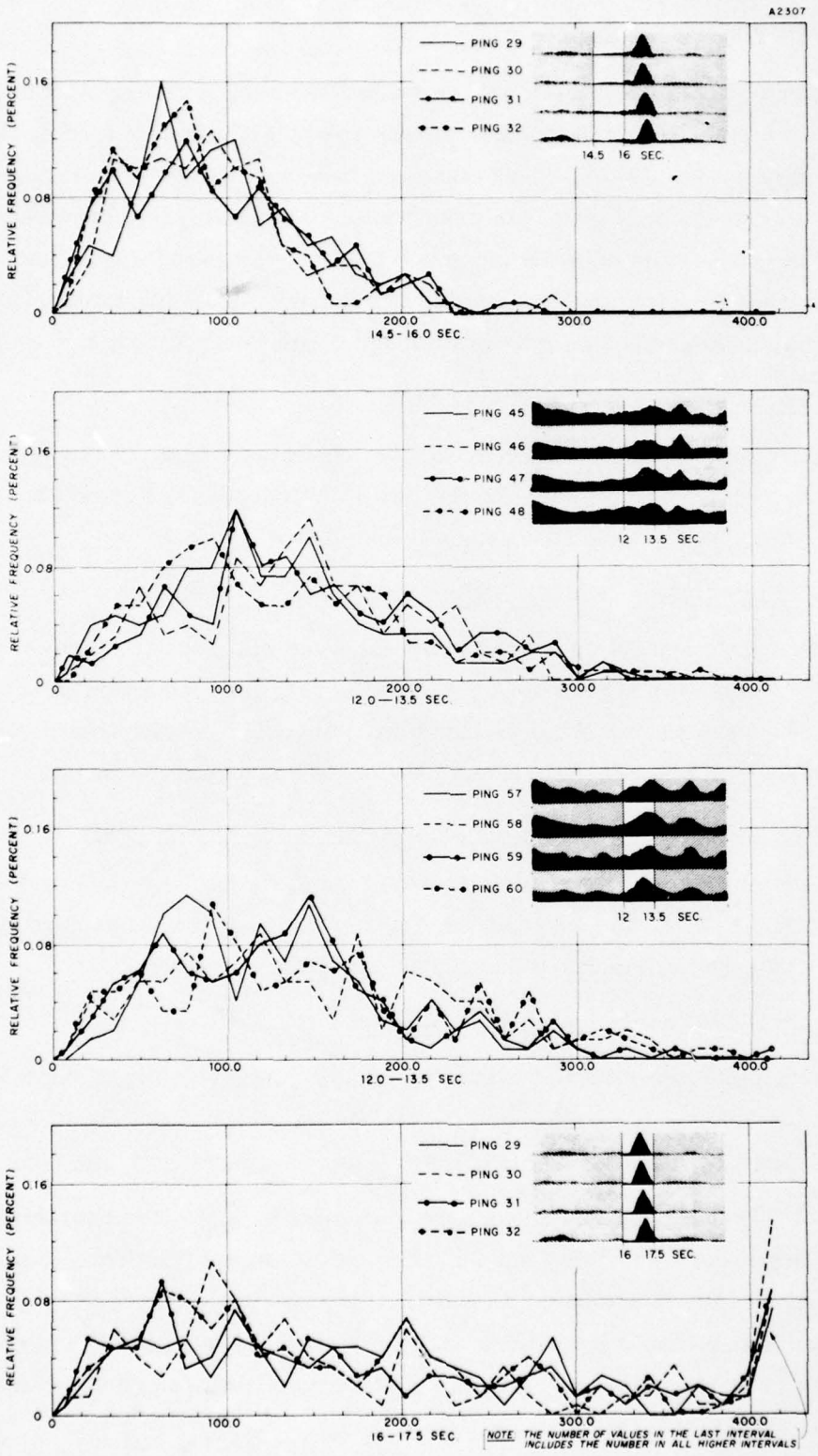

Figure 37 Histograms of Correlator Output Samples

SECTION IV

STATISTICAL MODELING OF CORRELATOR OUTPUT

A. GENERAL DISCUSSION

One of the major objectives of the study of the correlator output was to determine if a probabilistic model could be used to describe the behavior of a target-free interval; however, there were several difficulties which came up immediately. First (as was noted in the studies of the serial correlation matrix, the mean, and the standard deviations) for subdivisions of a single interval, the return was nonstationary in both mean and covariance. Secondly, as described earlier, the serial correlation function behaved erratically; thus the sample values are neither independent nor uncorrelated. Hopefully, for most intervals, the serial correlation will be low.

In order to reduce the effect of any correlation between sample values, a probability plotting technique was used to evaluate the samples. If the sample size is large and the correlation small, the effective sample size will not be too far from the actual sample size (the effect of the correlation is to reduce the amount of information in the sample) and the plotting points will not be radically affected by the correlation. In addition, only every fifth value will be plotted (except for the lowest 5 and highest 10) so that small irregularities due to the correlation will be less pronounced.

Initially, several common statistical models were fitted to a subset of the pings. The models included the normal, log normal, extreme value, Weibull, and Chi-squared distributions. The only model which appeared to be at all useful was the Weibull with an estimated shape parameter close to 2.0. Since the Rayleigh distribution is a special case of the Weibull with shape parameter 2.0, it seemed to be a reasonable model to investigate since it agreed with theoretical expectations. However, one difficulty in using the typical Weibull probability paper to test the Rayleigh assumption is that is exagerates the lower tail (small values) of the distribution and compresses the upper tail. While this is desirable in using the Weibull distribution for lifetime models, it is not useful in this case, since we are interested in getting a model which is adequate for describing the high values of correlator output. In order to overcome this problem, Rayleigh probability paper was used to examine the reasonableness of using a Rayleigh model.

Before proceeding with this discussion, it is important to note the following. In using the technique of probability plotting or any other statistical test, we are attempting to determine if the proposed model can be used to adequately describe the population from which the sample was drawn. It is, of course, possible that a set of data can appear as if

it came from several different distributions; thus, the fact that a given model is reasonable to describe a given sample is neither sufficient nor conclusive evidence that the sample came from the hypothesized model. In fact in the real world there is no such thing as a Rayleigh distribution, this is just an idealized model which is useful for approximating certain types of phenomena. Secondly, with probability plotting there is no objective way to reject or accept a given model. An individual must subjectively make up his own mind as to whether a given plot is adequately linear or not. Thus, the categorization of the plots in this report is somewhat arbitrary. If the Rayleigh model was appropriate, a straight line plot would be obtained which would appear to pass through the origin. It would be expected that the higher values in the upper tail would have a higher variation about this line than the values in the remainder of the distribution; therefore, in assessing the linearity of these points a straight line was drawn by hand, based on the lower 50 to 60 percent of the plotted observations. If this line adequately represented the entire set of data, then the Rayleigh model was assumed to be adequate. (If the data fitted all but the highest value, it was still classified as adequate.) If the data systematically departed from the straight line then the model was classified as inadequate.

In addition, it should be remembered that it is always possible to find a better representation of a set of data by using models with more parameters; however, in this case such models cannot be related to the physical phenomena being observed as is possible with the Rayleigh. Since the Rayleigh model will be shown to be inadequate for more than 50 percent of the intervals, another model -- the Johnson S_B distribution -- will be fitted to the data and compared to the Rayleigh fit.

B. SURFACE DUCT MODE, PINGS 1 TO 34

Pings 1 to 30, 14.5 to 16.0 seconds, zero doppler
Pings 1 to 6, 16.0 to 17.5 seconds, zero doppler

A total of 36 samples from the first set of surface duct returns (all same day) were plotted on Rayleigh paper. Fourteen, or 39 percent, of the pings could be adequately described by a Rayleigh distribution, 16 did not appear to be Rayleigh, and six were classified as marginal.

The pings for which the Rayleigh was an adequate model were:

14.5 to 16.0 -- ping number 1, 5, 8, 9, 10, 12, 13, 20, 22, 24
16.0 to 17.5 -- ping number 2, 4, 5, 6

Ping 9 had one extreme value which was much too high but the remaining points plotted in a straight line. The range of $\sqrt{b_1}$ and b_2 values for these pings (with the exception of ping 9, whose $\sqrt{b_1}$ and b_2 values were inflated by the one high observation) was 0.36 to 0.90 and 2.69 to 4.08. The values for a Rayleigh are 0.63 and 3.26.

The 16 pings for which the Rayleigh was not an adequate model, broken down by whether the highest values were too high or too low were:

Too high: 14.5 to 16.0 -- ping number 3, 6, 7, 15, 16, 17, 18, 21, 25, 27, 30
Too low: 14.5 to 16.0 -- ping number 14, 19, 26
16.0 to 17.5 -- ping number 1, 3

The range of $\sqrt{b_1}$ and b_2 values for the high group was 0.86 to 1.47 and 3.45 to 6.0. In fact, all but two of the b_2 values were above 4.0; thus, this group of samples have longer tails and are more skewed than the Rayleigh group. The theoretical Rayleigh values for $\sqrt{b_1}$ and b_2 are outside the range of values of this group. The range of $\sqrt{b_1}$ and b_2 for the low group was 0.20 to 0.39 and 2.24 to 2.89. Here again, the Rayleigh values do not fall in these intervals. These distributions are less skewed and have lower tails than the Rayleigh. The six marginals pings were:

14.5 to 16.0 — ping numbers 2, 4, 11, 23, 28, 29

It should be noted that pings 1 to 6, which has two time intervals represented in the above study, did not necessarily fall in the same category, indicating that the distributional form may not be stationary within a ping. This will be investigated at greater length below. Also, it should be noted that successive pings for the same time interval tended to fall in the same classification.

An attempt was made to determine why, statistically, certain pings appeared to be approximately Rayleigh and others were not. It was reasoned that if the correlator output is represented as

$$z_i = \sqrt{x_i^2 + y_i^2} \qquad i = 1, 2, \ldots, 150$$

then if the x_i and y_i are independently normally distributed with zero means and the same variance, then z_i should be Rayleigh. Likewise, if the z_i's are independent (or approximately so) the plotted results should lie in a straight line. In order to investigate these properties, a selection of pings was made from the above and the following was done.

1. The ping interval was divided into three samples of 50 each and the mean of each component (x and y) for each sample was obtained; in addition, a test for normality (W test) was performed on the x's and y's for each segment. This will be denoted below as the interval check.
2. The means and variances (of x and y) were computed for the entire interval. Statistical tests were run to check if the mean of the interval for each component was zero (t test), whether the variance of each component was the same (F test), and whether the x's and y's were correlated. This is the combined interval test.
3. A sample of every third observation, 50 in all, was selected from the interval. This corresponds to a sampling rate of 1/30. The means, variances, normality, and correlation were checked as above. This is called the overall test.

The results of the above checks are given in Table 2. There were no apparent differences between the adequate pings and other pings; thus, the factors investigated do not account for the non-Rayleigh behavior. One remaining factor which will be investigated is the differences in the serial correlation for adequate and inadequate pings.

C. SURFACE DUCT MODE, PINGS 35 TO 77

Pings 36 to 72 (even only), 9.0 to 10.5 seconds

There were a total of 19 pings examined from this group. Of these, six (or 32 percent) were classified adequate Rayleigh's, 11 (or 58 percent) were inadequate and two were marginal. Ping numbers 36, 42, 44, 54, 70, and 72 could reasonably described by Rayleigh models, although ping 36 had two high values. The $\sqrt{b_1}$ and b_2 values for these pings ranged between 0.42 to 0.65 and 2.46 to 3.09 except for ping 36 whose values were 0.80 and 4.37. These values are somewhat lower than those for Day 1 surface duct transmission, for which the Rayleigh was an adequate model.

Ping numbers 38, 46, 56, 58, and 60 had values which were relatively higher than could be expected from a Rayleigh model. The $\sqrt{b_1}$ and b_2 values ranged from 0.73 to 0.89 and 2.82 to 4.73. Again we note a difference in the $\sqrt{b_1}$ and b_2 from the Rayleigh class above. It was noted in addition that no values of $\sqrt{b_1}$ were above 1.0 and only three values of b_2 were above 4.0 for pings 36 to 72 including the odd numbered ones. Thus, it would appear that for this time interval, the pings are less skewed and do not have as many relatively large values as for Pings 1 through 34, 14.5 to 16.0 seconds.

Ping numbers 40, 48, 50, 62, 64, and 66 had values which were relatively smaller than could be expected from a Rayleigh model. The $\sqrt{b_1}$ and b_2 values ranged between 0.22 to 0.42 and 2.24 to 2.91, which agrees closely with the results for Pings 1 through 34. The marginal pings were 52 and 68.

TABLE 2

RESULTS OF STATISTICAL TEST OF PING INTERVALS

Pings 1 to 19, 25 to 27, 29 to 30; 14.5 to 16.0 Seconds
(Significant tests have been run at the five percent level
for F and R and ten percent for W and t)

Ping	Classification	Interval Check	Combined Interval	Overall Test
1	Adequate	1-W (10%)	ATP	W (10%)
2	Marginal	2-W (10%)	ATP	ATP
3	Inadequate	ATP	ATP	ATP
4	Marginal	1-W (10%)	ATP	ATP
5	Adequate	ATP	ATP	ATP
6	Inadequate	ATP	ATP	ATP
7	Inadequate	1-W (1%)	ATP	W (5%), F (5%)
8	Adequate	ATP	ATP	ATP
9	Adequate (1 large value)	1-W (1%), 1-W (5%)	R (5%)	W (10%)
10	Adequate	1-W (5%)	R (1%)	ATP
11	Marginal	1-W (5%)	ATP	ATP
12	Adequate	1-W (5%)	F (5%)	ATP
13	Adequate	1-W (10%)	ATP	ATP
14	Inadequate	1-W (5%)	F (1%)	ATP
15	Inadequate	ATP	F (5%), R (1%)	W (5%)
16	Inadequate	ATP	ATP	W (5%), W (10%)
17	Inadequate	ATP	R (1%)	ATP
18	Inadequate	ATP	ATP	W (10%), t (10%)
19	Inadequate	ATP	ATP	ATP
25	Inadequate	ATP	R (1%)	ATP
26	Inadequate	ATP	ATP	W (10%)
27	Inadequate	ATP	ATP	ATP
29	Marginal	ATP	ATP	2-W (5%)
30	Inadequate	1-W (5%)	ATP	t (10%)

The results for the two day's surface duct pings would seem to indicate that the Rayleigh model could possibly be used to represent the data if $\sqrt{b_1}$ falls between 0.40 and 0.80 and b_2 falls between 2.50 and 3.50. The error in using such a criteria would have to be further investigated and perhaps a more optimum selection can be found.

D. BOTTOM BOUNCE MODE, PINGS 78 TO 122

A total of 19 bottom bounce pings were selected for study from pings 86 to 122. Of these, a total of nine (or 47 percent) were classified as adequate, seven were inadequate, and three were marginal.

Pings 86, 92, 94, 98. 102, 104, 110, 112, and 114 could adequately be described by a Rayleigh model, although ping 92 had one extremely high value. The values of $\sqrt{b_1}$ and b_2, with the exception of those of ping 92, ranged from 0.37 to 0.80 and 2.67 to 3.79, which agrees closely with the surface duct results of Pings 1 through 34. Ping 92 had corresponding values of 1.09 and 5.52.

Pings 96, 108, and 118 had values which were higher than would be expected from a Rayleigh model. The $\sqrt{b_1}$ and b_2 values were 0.89, 0.77, and 0.81 and 4.07, 3.32, and 3.15 respectively. These values agree with the result for the corresponding group in the surface duct mode of Pings 36 through 76.

The highest values for pings 90, 120, and 122 were lower than would be expected from a Rayleigh model. The $\sqrt{b_1}$ and b_2 values were 0.51, 0.59, and 0.63 and 3.69, 3.31, and 2.62, respectively. These results did not agree with the surface duct returns. There was also one ping -- number 100 -- which was erratic and could not be classed as either too high or too low.

The marginal pings were 88, 106, and 116. There was some indication that the overall appearance of the bottom bounce plots was somewhat different than the surface duct plots in that many in the adequate class were on the borderline of being marginal, and that some of the inadequate plots looked different than those in the surface duct mode. This supposition may be investigated at a later time.

E. BOTTOM BOUNCE MODE, PINGS 124 TO 200

A total of 26 pings (every third ping) from this group was selected for study. Of these, 14 (or 54 percent) were classified as adequate, nine (or 35 percent) were classified as inadequate, and three (or 11 percent) were classified as marginal.

Pings 124, 127, 130, 133, 139, 145, 157, 163, 166, 181, 187, 190, 193, and 199 were adequately described by a Rayleigh model. (Ping 181 had one very high value.) The values of $\sqrt{b_1}$ and b_2 for these pings ranged from 0.45 to 0.82 and 2.66 to 3.81, with the exception of ping 181, which had values of 0.91 and 4.22. These results agree closely with those from the bottom bounce returns from the first sequence.

Pings 172 and 178 were classified inadequate high. The $\sqrt{b_1}$ and b_2 values were 1.09 and 1.20, and 4.42 and 4.57, respectively. Pings 142, 148, 151, 160, and 175 were classified inadequate low. Their $\sqrt{b_1}$ and b_2 values ranged from 0.39 to 0.61 and 2.29 to 3.52. There were two pings which were erratic and were classified as inadequate odd. Their $\sqrt{b_1}$ values were 0.58 and 0.16, and b_2 values were 4.41 and 2.54. The marginal pings were 169, 184, and 196.

F. WITHIN PING VARIABILITY

Four pings were selected in order to investigate how the correlator amplitude varied within a ping: ping 4, 5, and 6 were chosen from the surface duct and ping 78 from the bottom bounce mode.

The surface duct mode pings did not include the target return. Five 1.5-second intervals were selected from these three pings covering 11.5 to 19.0 seconds. The statistical results are shown in Table 3. It would appear that the $\sqrt{b_1}$ and b_2 values vary almost as much within a ping as they do between pings for the same time interval. Likewise there is a large variation in the mean and standard deviation, in fact almost as much variation within a ping as between pings for the same time interval on the same day. A further demonstration of the nonstationarity within these three pings is given by the Rayleigh plots for each interval. For ping 3, the second interval 13.0 to 14.5 and the last 17.5 to 19.0 could be adequately described by a Rayleigh model while the other three could not. In fact, for some intervals the extreme points were too big for a Rayleigh model and for others they were too small. Similar results were obtained for ping 4 where one interval was adequate, three were marginal and one was inadequate and ping 5, where three were adequate and two were inadequate.

Ping 78 was studied in two doppler channels (291, 301) for six 1,5-second intervals (13.5 to 22.5) which included several target returns. These results are given in Table 3. The variation in the means and standard deviations are directly traceable to the occurrence of the target signal. Likewise, the variations in $\sqrt{b_1}$ and b_2 can be tied to the occurrence of one or two high values, again probably coming from the target return. The average,

TABLE 3

CORRELATOR STATISTICS WITHIN A SINGLE PING

	Time				
Ping 3	11.5-13.0	13.0-14.5	14.5-16.0	16.0-17.5	17.5-19.0
$\bar{x}$	82.50	89.70	79.60	69.50	90.80
s	44.20	48.40	48.40	35.70	47.80
$\sqrt{b_1}$	0.746	0.60	1.47	0.393	0.556
b_2	3.50	2.65	6.14	2.37	3.00
$\bar{x}/s$	1.87	1.85	1.64	1.95	1.90
Classification	Marginal	Adequate	Inadequate	Inadequate	Adequate
Ping 4					
$\bar{x}$	126.70	107.10	74.50	84.60	113.10
s	61.10	77.40	41.00	41.80	67.70
$\sqrt{b_1}$	0.44	1.90	0.74	0.43	1.17
b_2	2.71	7.31	3.19	2.93	4.46
$\bar{x}/s$	2.07	1.38	1.82	2.02	1.67
Classification	Marginal	Inadequate	Marginal	Adequate	Marginal
Ping 5					
$\bar{x}$	117.90	105.70	109.90	103.20	104.00
s	73.40	67.90	60.10	55.50	60.50
$\sqrt{b_1}$	2.50	1.35	0.72	0.54	0.83
b_2	15.57	5.76	3.41	3.04	3.44
$\bar{x}/s$	1.61	1.56	1.83	1.86	1.72
Classification	Adequate	Inadequate	Adequate	Adequate	Inadequate

TABLE 3 (concluded)

Ping 78(291)	13.5-15.0	15.0-16.5	16.5-18.0	18.0-19.5	19.5-21.0	21.0-22.5
$\bar{x}$	87.80	117.80	135.80	115.00	128.50	106.20
s	44.90	59.80	67.70	66.70	76.90	52.40
$\sqrt{b_1}$	0.436	0.645	0.662	0.533	0.878	0.273
b_2	2.60	3.39	3.23	2.64	3.41	2.53
$\bar{x}/s$	1.96	1.97	2.01	1.72	1.67	2.03
Classification	Adequate	Adequate	Adequate	Adequate	Inadequate	Marginal
Ping 78(301)						
$\bar{x}$	102.90	129.20	162.60	122.30	131.00	113.00
s	54.80	75.90	92.40	74.80	73.40	59.00
$\sqrt{b_1}$	0.65	0.944	1.801	2.221	0.708	0.479
b_2	3.18	3.59	11.04	15.45	2.97	2.66
$\bar{x}/s$	1.88	1.70	1.76	1.64	1.78	1.92
Classification	Adequate	Inadequate	Inadequate	Adequate (1 high value)	Adequate	Adequate

standard deviation, $\sqrt{b_1}$ and b_2 appear to be systematically higher for the 301 channel. The difference in doppler channels is investigated below. The Rayleigh distribution appeared to be adequate for four of the six intervals from both channels, although one of the intervals in the 301 channel had one very high value.

G. ESTIMATION OF THE ADEQUACY OF THE RAYLEIGH MODEL

A study was made to determine if the ratio of the standard deviation to the mean could be used to indicate the adequacy of a Rayleigh model. The adequacy of the model was determined subjectively by an examination of the Rayleigh probability plots. Pings were classified as adequate (A), marginal (M), inadequate low (INL) (high values were too small for a Rayleigh model), or inadequate high (INH) (high values were too large for a Rayleigh model). Surface duct and bottom bounce pings were analyzed separately.

The data which are given in Table 4 show that, for surface duct pings, the average of the ratio of the standard deviation to the mean was lowest (0.488) for the INL category, was 0.529 for the A category, 0.539 for the M category, and 0.577 for the INH category. A statistical analysis showed that there was less than one out of 100 chances that this difference was due to random fluctuations. Two inconsistent observations were dropped from the analysis (see Table 4). The inadequate odd values were not included in the above analysis. Note that the average for the A group was close to the theoretical Rayleigh value of 0.523 and there was little overlap between the A, INH, and INL groups. In fact, if one uses the range 0.50 to 0.55 for the A group, there are only two out of 22 members of this group below this range and three above it. On the other hand only two out of 18 of the INH group are below 0.55 and three out of 11 of the INL group above 0.50.

The results for the bottom bounce pings are not as clear-cut as the one for surface duct due to the significantly higher variation of the ratio within each of the categories. The average within variance for the bottom bounce mode ratios was 0.0015 compared to 0.00087 for surface duct. There was less than a one in 20 probability that this difference was due to chance. The lowest average for the ratio of the standard deviation to the mean was 0.506 for the INL category; it was 0.534 for the A category, 0.547 for the M category, and 0.563 for the INH category. There was approximately a one in 10 chance that these differences were due to random fluctuations. Due to the higher within-category variances, there was no clear-cut separation of the categories as was the case for the surface duct pings; however, the ordering of the means for the bottom bounce was the same as for the surface duct and the magnitudes were close to each other.

TABLE 4

THE RATIO OF STANDARD DEVIATION TO MEAN FOR VARIOUS CATEGORIZATIONS OF 1.5-SECOND INTERVALS FOR SURFACE DUCT AND BOTTOM BOUNCE PINGS

Surface Duct Standard Deviation/Mean				
	Adequate	Marginal	Inadequate Low	Inadequate High
	0.501	0.576	0.462	0.608
	0.273*	0.536	0.514	0.642
	0.539	0.482	0.723	0.582
	0.494	0.550	0.523	0.606
	0.622	0.599	0.499	0.570
	0.547	0.557	0.482	0.601
	0.538	0.504	0.508	0.594
	0.561	0.542	0.483	0.555
	0.525	0.494	0.477	0.581
	0.572	0.557	0.452	0.526
	0.522	0.529	0.463	0.601
	0.490		0.491	0.576
	0.548			0.558
	0.510			0.557
	0.507			0.560
	0.500			0.577
	0.538			0.572
	0.505			0.519
	0.517			
	0.520			
	0.525			
	0.526			
	0.528			
Mean	0.529	0.539	0.488	0.577
Variance	0.00088	0.00124	0.00047	0.00089

* These points were dropped since they were "odd" values.

TABLE 4 (concluded)

Bottom Bounce Standard Deviation/Mean					
	Adequate	Marginal	Inadequate Low	Inadequate High	Inadequate Odd*
	0.540	0.505	0.532	0.517	0.580
	0.503	0.523	0.498	0.547	0.470
	0.549	0.453	0.535	0.603	0.429
	0.590	0.602	0.512	0.585	0.648
	0.573	0.583	0.460		
	0.514	0.616	0.513		
	0.518		0.498		
	0.527				
	0.535				
	0.628				
	0.551				
	0.487				
	0.534				
	0.486				
	0.531				
	0.538				
	0.555				
	0.542				
	0.502				
	0.497				
	0.514				
	0.528				
Mean	0.534	0.547	0.507	0.563	0.532
Variance	0.00112	0.00405	0.00064	0.00149	--

* This column of data was not included in the analysis.

The above results indicate that for the surface duct pings, it may be possible to categorize the pings into one of three classes: adequate, inadequate high, or inadequate low, based on the ratio of the standard deviation to the mean. The value of such a classification scheme for bottom bounce pings is questionable

H. DOPPLER CHANNEL INVESTIGATION

One of the questions studied in this project was: How does the correlator output vary in the different doppler channels? The present study was limited to 11 surface duct pings, numbers 7 to 17. Samples were selected from the interval 14.5 to 16.0 seconds after transmit at a sampling rate of 1 in 10 from doppler channels 280, 290, 300, 310, and 320 Hz. Hence, a sample of 150 observations was taken from each channel for each ping. The time period chosen was free of the main target return. For each channel from each ping, the mean, standard deviation, $\sqrt{b_1}$, b_2, and a Rayleigh plot were obtained. In addition the pair-wise correlation between doppler channels for each ping was computed.

Both the average correlator output and the standard deviation of the correlator output were significantly different for the five doppler channels. The probability that the observed difference was due to chance was less than 0.0001. The results for the average and standard deviation shown in Table 5 are similar, since these two measures are highly correlated as pointed out previously. The highest value of these two statistics occurred in the zero doppler (300 Hz) channel and monotonically decreased as the cycles increased or decreased; however, the falloff was more rapid as the cycles increased. The mean decreased 10.3 percent -- from 102.4 to 91.8 -- and the standard deviation decreased 10.7 percent -- from 55.9 to 49.9 -- as the frequency decreased to 280, while the mean decreased 16.9 percent from 102.4 to 85.1, and the standard deviation 19.0 percent from 55.9 to 45.2 as the frequency increased to 320 Hz. Thus, the 300 Hz channel has a higher mean and larger variability than the other channels, and both these quantities decrease monotonically as we move up and down doppler. It is also noted that both the mean and standard deviation vary from ping to ping. In addition, pings that had a high average correlator output, tended to be high in all channels while those with a low average tended to be low in all channels. For example, pings 10 and 17 had the highest averages in all the channels, while pings 9, 13, 14, and 16 were the lowest.

The standardized measures of skewness ($\sqrt{b_1}$) and kurtosis (b_2) (the third and fourth standardized moments) are recorded in Table 6. The statistical significance of the differences noted are not as positive as in the case of the means and standard deviations. This

TABLE 5

CORRELATOR OUTPUT AS A FUNCTION OF DOPPLER CHANNEL

Means and Standards Deviations,
Pings 7 to 17, 14.5 to 16.0 Seconds

Doppler Channel Means*						
Ping	280	290	300	310	320	Mean
7	90.0	102.8	100.1	98.6	83.8	95.06
8	89.6	104.3	99.3	101.7	86.7	96.32
9	81.4	82.4	91.4	76.9	75.7	91.56
10	125.4	132.7	144.1	122.4	110.9	127.10
11	98.0	112.6	104.5	96.9	84.9	99.38
12	92.7	92.9	106.8	93.9	86.8	94.62
13	84.9	93.6	88.1	86.5	78.9	86.40
14	88.4	84.5	96.1	82.3	74.2	85.10
15	87.2	89.9	94.4	89.7	84.8	89.20
16	74.2	85.4	89.7	88.5	80.5	83.66
17	98.3	109.7	111.3	98.4	88.7	101.28
Mean	91.83	99.16	102.35	94.16	85.08	94.52
Doppler Channel Standard Deviation*						
7	47.9	51.9	57.0	52.5	44.5	
8	50.1	58.2	52.1	52.7	46.8	
9	48.0	51.5	52.3	45.2	43.2	
10	64.0	73.6	75.2	68.6	62.7	
11	50.1	54.1	58.2	48.9	43.7	
12	52.3	46.5	52.3	46.3	43.9	
13	45.1	58.8	48.3	43.3	38.8	
14	43.3	43.2	47.2	40.9	40.9	
15	46.8	47.1	56.7	40.8	45.2	
16	43.8	43.4	53.3	44.5	42.3	
17	57.5	58.7	61.8	55.9	45.6	
Mean	59.90	52.45	55.85	49.05	45.24	

* Values given have been divided by 1000.

TABLE 6

CORRELATOR OUTPUT AS A FUNCTION OF DOPPLER CHANNEL

Standardized Third and Fourth Moments
Pings 7 to 17, 14.5 to 16.0 Seconds

Doppler Channel $\sqrt{b_1}$						
Ping	280	290	300	310	320	Mean
7	0.405	0.492	1.159	0.489	0.763	0.662
8	0.642	0.718	0.363	0.525	0.776	0.605
9	0.931	1.132	1.672	1.007	1.269	1.202
10	0.337	0.416	0.697	0.923	0.462	0.567
11	0.375	0.200	0.661	0.616	0.817	0.512
12	0.717	0.598	0.646	0.225	0.375	0.512
13	0.515	0.644	0.831	0.518	0.372	0.576
14	0.339	0.380	0.389	0.451	0.557	0.423
15	0.528	0.440	1.234	0.276	0.544	0.604
16	0.929	0.892	0.859	0.703	0.665	0.810
17	0.947	0.663	1.174	0.800	0.480	0.813
Mean	0.606	0.598	0.880	0.594	0.644	
Doppler Channel b_2						
7	3.01	2.39	5.02	2.79	3.42	
8	3.10	3.14	2.69	3.15	3.86	
9	3.95	4.82	8.92	4.52	5.74	
10	2.70	2.40	3.09	4.16	2.38	
11	2.54	2.43	3.23	2.68	3.68	
12	3.11	3.24	3.49	2.83	2.86	
13	2.64	2.99	3.96	2.89	2.56	
14	2.42	2.58	2.89	2.23	2.90	
15	3.10	2.48	4.95	2.58	3.07	
16	3.76	4.16	3.45	2.92	3.61	
17	3.84	3.03	5.16	3.48	2.64	
Mean	3.11	3.06	4.26	3.11	3.34	

TABLE 7

RATING OF RAYLEIGH PLOTS OF CORRELATOR OUTPUT
AS A FUNCTION OF DOPPLER CHANNEL

Pings 7 to 17, 14.5 to 16.0 Seconds

	Doppler Channel Rating					
Ping	280	290	300	310	320	Total A's
7	NA	NA	NA	A	NA	1
8	A	NA	A	NA	A	3
9	NA	NA	A	A	NA	2
10	NA	NA	A	NA	NA	1
11	NA	NA	A	A	A	3
12	NA	A	A	NA	NA	2
13	A	NA	A	A	NA	3
14	NA	NA	NA	NA	A	1
15	A	A	NA	NA	A	3
16	NA	A	NA	A	NA	2
17	NA	A	NA	NA	A	2
Total A's	3	4	6	5	5	

A = Adequate

NA = Not Adequate

is in part due to the much higher variances for these statistics. The zero doppler channel (300 Hz) had the highest average $\sqrt{b_1}$ value -- 0.880 -- compared to 0.611 for the other four channels. This difference was significant at a five percent level test; i.e., there was less than five percent chance that the differences observed were due to chance. Likewise, the highest average b_2 value occurred in the zero doppler channel -- 4.26 -- compared to an average of 3.16 for the other four channels. Again, we note as indicated earlier that the $\sqrt{b_1}$ and b_2 values are highly correlated; thus, one concludes that there is an indication that the correlator output is more skewed and has a higher kurtosis (fourth moment) measure. These higher measurements are apparently due to the occurrence of more extreme values (relatively further away from the mean in terms of standard units) in the 300 Hz channel. It should be noted that the theoretical values for a Rayleigh distribution of the standardized third and fourth central moments are 0.63 and 3.26, respectively, which are close to the average values of the four doppler channels excluding the 300 Hz channel.

The Rayleigh plots for each of the 11 pings and five channels were examined and arbitrarily classified as adequate or inadequate. These ratings are given in Table 7. The adequate classification, A, contains all those plots for which the writer felt that the plotted points fell close enough to a straight line to consider the Rayleigh as an adequate model. All other plots were assigned to the inadequate or NA class. It should be understood that the fact that a given sample was classified as adequate does not imply that the Rayleigh represents the "actual" distribution.

The results in Table 7 are not clear-cut nor may even be meaningful. Every ping had at least one doppler channel for which the correlator output could be modeled by the Rayleigh distribution, but no ping had as many as four channels where it was adequate. This would indicate that the distribution of the correlator output is not stable from channel to channel or that the Rayleigh is a poor model or both.

Another factor investigated in this study was the correlation between the correlator output in pairs of doppler channels. These results are given in Table 8. While some of the correlation coefficients are significantly different than zero (all values over 0.159 for five percent test) the highest coefficient was 0.22; hence, any correlation which does exist is relatively small. Thus, a high correlator output in one channel does not cause either a high or low output in the other channels. This is, of course, limited to regions with no target return as defined above.

TABLE 8

DOPPLER CHANNEL CORRELATION

Channel Coefficient of Correlation						
Ping	280-300	280-320	300-320	290-300	290-310	300-310
7	0.05	0.05	0.16	0.02	-0.05	-0.123
8	0.07	0.11	-0.01	0.129	—	-0.02
9	0.01	0	0.158	0.133	0.10	0.12
10	0.07	0.18	-0.04	0.167	-0.005	0.10
11	-0.07	-0.01	0.05	-0.01	0.03	-0.02
12	0.02	0.04	-0.04	0.03	-0.14	0.09
13	0.13	0.03	0.146	0.127	-0.112	0.171
14	-0.04	0.04	-0.02	0.05	0.01	0.01
15	0.10	-0.03	0.06	0.06	-0.184	-0.03
16	0.15	-0.02	-0.06	0.09	0.172	0.02
17	0.22	0.11	0.11	0.08	0.08	0.10

J. COMPARISON OF MODELS

In an attempt to find a more flexible model to use instead of the Rayleigh, the Johnson S_B family was investigated. Initial investigation indicated that the Johnson S_B family would be appropriate since the plot of $\sqrt{b_1}$, b_2 in Figure 36 could correspond to members of the S_B family. An initial study of 1.5-second intervals from seven surface duct pings was made comparing the S_B and Rayleigh approximations. In fitting the S_B curve, it was assumed that the minimum possible value was zero and a three-parameter model was used. The S_B model was chosen so that the sample data and Johnson S_B approximation had the same 5, 50, and 95 percent points. The maximum likelihood estimator of the Rayleigh model parameter was used.

The results of this study are shown in Table 9, which gives a comparison of the estimated quantiles from the sample with those estimated from the S_B and Rayleigh distributions. The percentages corresponding to the quantiles are shown at the top of the table; thus, the column heading 0.925 gives the 92.5 percentage point of the distribution. An examination of the results indicates that the Rayleigh model does not fit the data. This is in part due to the method of estimating the parameter. The maximum likelihood estimator is very sensitive to extreme values and, thus, if there is one large value in the data, it will give a too high estimate of the parameter, resulting in a poor fit.

A second comparison was made, this time using a two-parameter Johnson S_B distribution with the Rayleigh distribution for pings 7 to 16. The Johnson S_B distribution, in its general form, can be defined by

$$z = \gamma + \delta \ell n \left(\frac{y - \epsilon}{\epsilon + \lambda - y} \right) \qquad \epsilon \leq y \leq \epsilon + \lambda$$

where z is a standard normal variate and y is the Johnson S_B variate. The greek symbols represent the fourth parameters of the distribution. The parameters ϵ and λ define the range of the variable. In the two-parameter fit used below, ϵ was assumed to be zero and λ to be 10^6; thus, only the parameters γ and δ were allowed to vary. These parameters were estimated by matching percentage points. A one-parameter Rayleigh defined by

$$f(y) = 2\lambda y \, e^{-\lambda y^2} \qquad 0 \leq y \leq \infty$$

was used in the comparison. The parameter λ was estimated from the slope of the line drawn to the plotted points on Rayleigh probability paper.

The resulting fits for the interval 14.5 to 16.0 seconds for pings 7 to 16 is shown in Table 10. The results indicate that the Rayleigh model fit the data for those pings which were classified adequate (9, 10, 12, and 13) with the exception of ping 8. The Johnson S_B curve provided a poor fit for all pings except number 7.

These results indicate that the two-parameter Johnson S_B with $\epsilon = 0$ and $\lambda = 10^6$ does not provide an adequate model for the data. No doubt better fits can be obtained if λ is not fixed; i.e., a three-parameter S_B model is used. The Rayleigh model will be adequate for those ping intervals which were classified adequate. A large improvement in fit was obtained by estimating the Rayleigh parameter from the probability plot rather than the method of maximum estimation.

K. INVESTIGATION OF INTERVALS LESS THAN 1.5 SECONDS

One of the questions noted in an earlier discussion was: What should be the size of the sampling interval? Previously all ping intervals studied were 1.5 seconds; however, it was felt that due to the nonstationarity of the return, a smaller interval would be more reasonable a time period to work with in order to evaluate the underlying model for the noise. Of course, if too small an interval is chosen, it will be difficult to assess what is a good model and the serial correlations will have an even greater effect in distorting this evaluation.

It was decided to investigate ping intervals of 0.5 and 1.0 second, using pings 3, 4, and 5 with time interval 11.5 to 19.0 seconds after transmit, and ping 78 channels 291 and 301 with time interval 13.5 to 22.5 seconds. A probability plot for each interval was prepared and used to classify the interval as adequate (A), inadequate high (INH), inadequate low (INL), marginal (M), and inadequate odd (INO). The latter classification covers those plots which did not fall into the previous two inadequate categories. The results are shown in Tables 11 and 12.

An attempt was made to relate the above classifications as shown in Table 13. The returns are divided into 0.5-second intervals and the probability plot classification is shown above the intervals. The classifications for 1.0- and 1.5-second intervals are also included. For many of the inadequate pings, it was obvious that there were too many high spikes, or too high a spike, or not enough high spikes as compared to the intervals classified as Rayleigh. There are large differences in the intervals; for example the interval 17.5 to 18.0 seconds for ping 3 is a good deal smoother than the proceding or succeeding intervals. In fact, the $\sqrt{b_1}$ and b_2 values (-0.1 and 3.05) indicate that a normal distribution

TABLE 11

CLASSIFICATION OF PING INTERVALS OF DURATION 0.5 SECONDS

Time	Ping 3 Category	Ping 4 Category	Ping 5 Category	Ping 78(291) Category	Ping 78(301) Category
11.5-12.0	A - 2 high values	A	A		
12.0-12.5	A - 1 high value	A	A		
12.5-13.0	A	INL	INH		
13.0-13.5	A	INH	INH		
13.5-14.0	M	INO	INH	INO	A
14.0-14.5	INO	A	A	INL	INL
14.5-15.0	A	A	A	A	A
15.0-15.5	INH	A	A	A	A
15.5-16.0	INO	INH	M	A	INH
16.0-16.5	INH	INO	A	INL	INH
16.5-17.0	A	A	INO	INH	INL
17.0-17.5	A	A	M	A	A
17.5-18.0	INO	A	A	INL	INH
18.0-18.5	A	INH	INH	A	A
18.5-19.0	A	INO	A	INH	INL
19.0-19.5				INL	A
19.5-20.0				INH	A
20.0-20.5				A	A
20.5-21.0				A	A
21.0-21.5				INO	A
21.5-22.0				INL	A
22.0-22.5				INL	A

TABLE 12

CLASSIFICATION OF PING INTERVALS OF DURATION 1.0 SECONDS

Time	Ping 3 Category	Ping 4 Category	Ping 5 Category	Ping 78(291) Category	Ping 78(301) Category
11.5-12.5	A - 2 odd	A	INL		
12.5-13.5	A	INH	INH		
13.5-14.5	INO	A - 2 odd	A	A	INL
14.5-15.5	INH	INH	A	A	A
15.5-16.5	INO	INO	A	A	INH
16.5-17.5	INL	A	A	M	INL
17.5-18.5	INL	INH	INH	INL	INH
18.5-19.5				A	INO
19.5-20.5				A	A
20.5-21.5				A	A
21.5-22.5				INL	A

TABLE 13

INTERVAL CLASSIFICATION

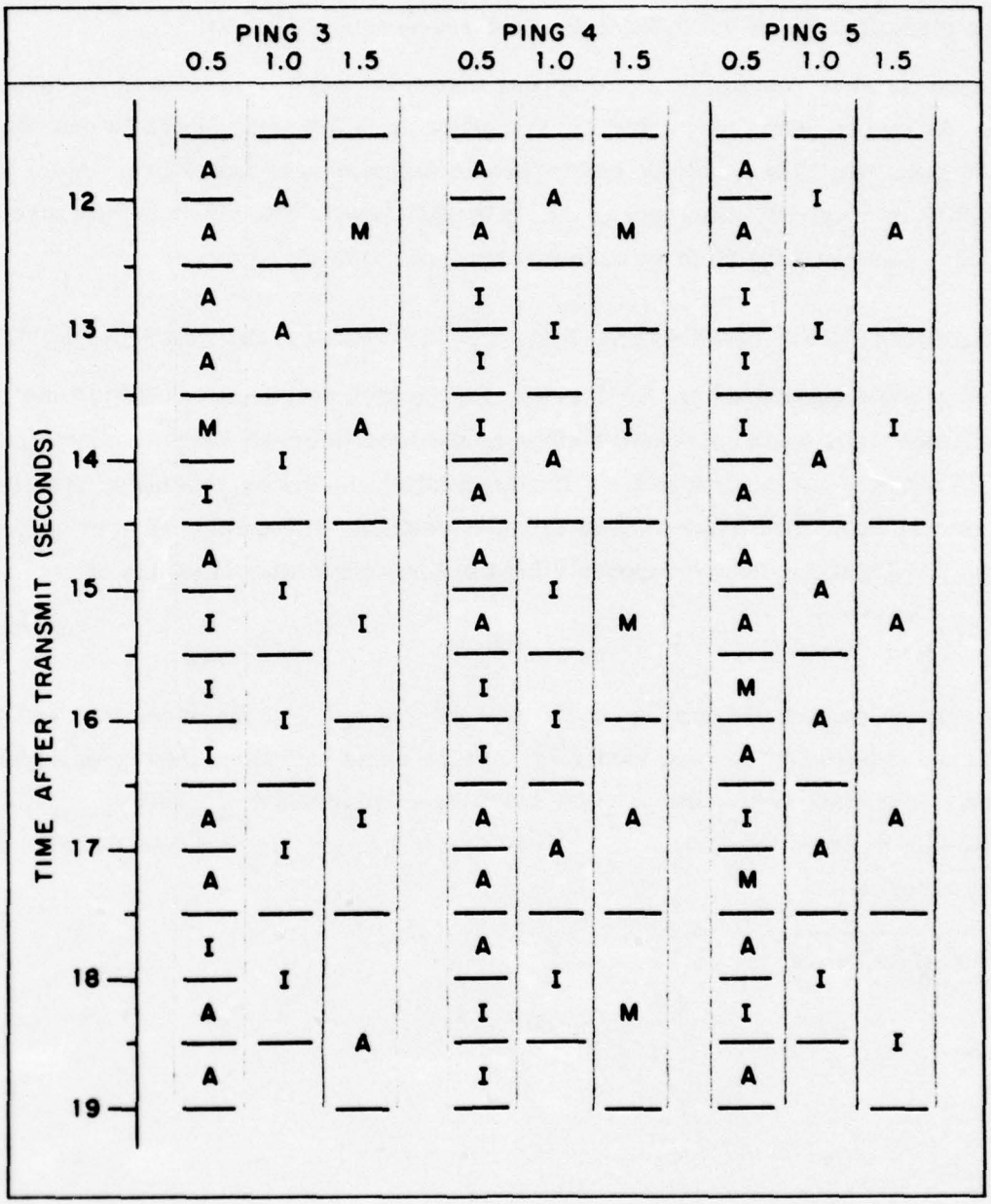

would be a good model for this interval. The probability plot in Figure 38 confirms this hypothesis.

The correlator output plots for two frequencies are illustrated in Figure 39, together with the classification of the 0.5-, 1.0-, and 1.5-second intervals.

Based on these results, it would appear that a 0.5-second interval is a reasonable one to use. As can be seen from Table 13, two adequate 0.5-second intervals can combine into an inadequate one. This could be due to the nonstationarity of the return. Also, using a 0.5-second interval, it would appear that it is often possible to pinpoint the cause of the inadequate classification from an examination of the correlator output.

L. ELIMINATION OF CONSISTENT PING-TO-PING HIGH CORRELATOR OUTPUTS

One of the suppositions put forth to explain the high percentage of inadequate Rayleigh models, especially when consecutive pings (same time interval) were so classified, was the occurrence of bottom return from fixed nontarget objects or sidelobes. The following rationale was developed to investigate this phenomenon. If the returns were truly noise, then subtracting the x and y components for the same time after transmit of

$$z_j = \sqrt{x_j^2 + y_j^2} \qquad j = 1, 2, \ldots 150$$

for successive pings will not affect the distribution of z_j. For instance, if x_j and y_j are zero mean, independent normal variables with the same variance, then z_j is Rayleigh distributed. Likewise, if $x_{i,j}$ and $y_{i,j}$ are from the i^{th} ping and $x_{i+1,j}$ and $y_{i+1,j}$ are from the next ping in time, then $\Delta x_j = x_{i+1,j}$ and $\Delta y_j = y_{i,j} - y_{i+1,j}$ are both normal, zero mean random variates and

$$z_j^* = \sqrt{\Delta x_j^2 + \Delta y_j^2}$$

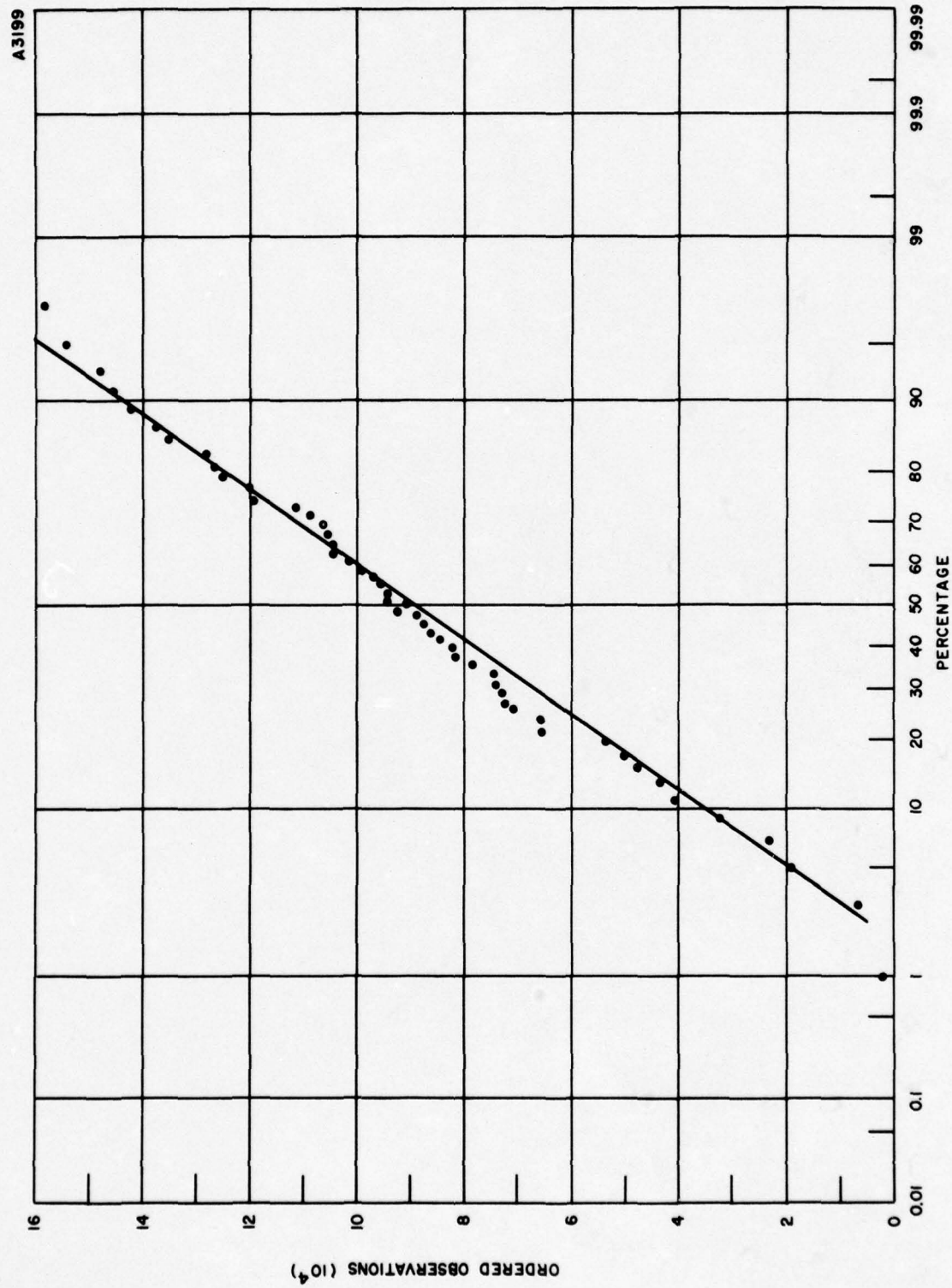

Figure 38. Probability Plot

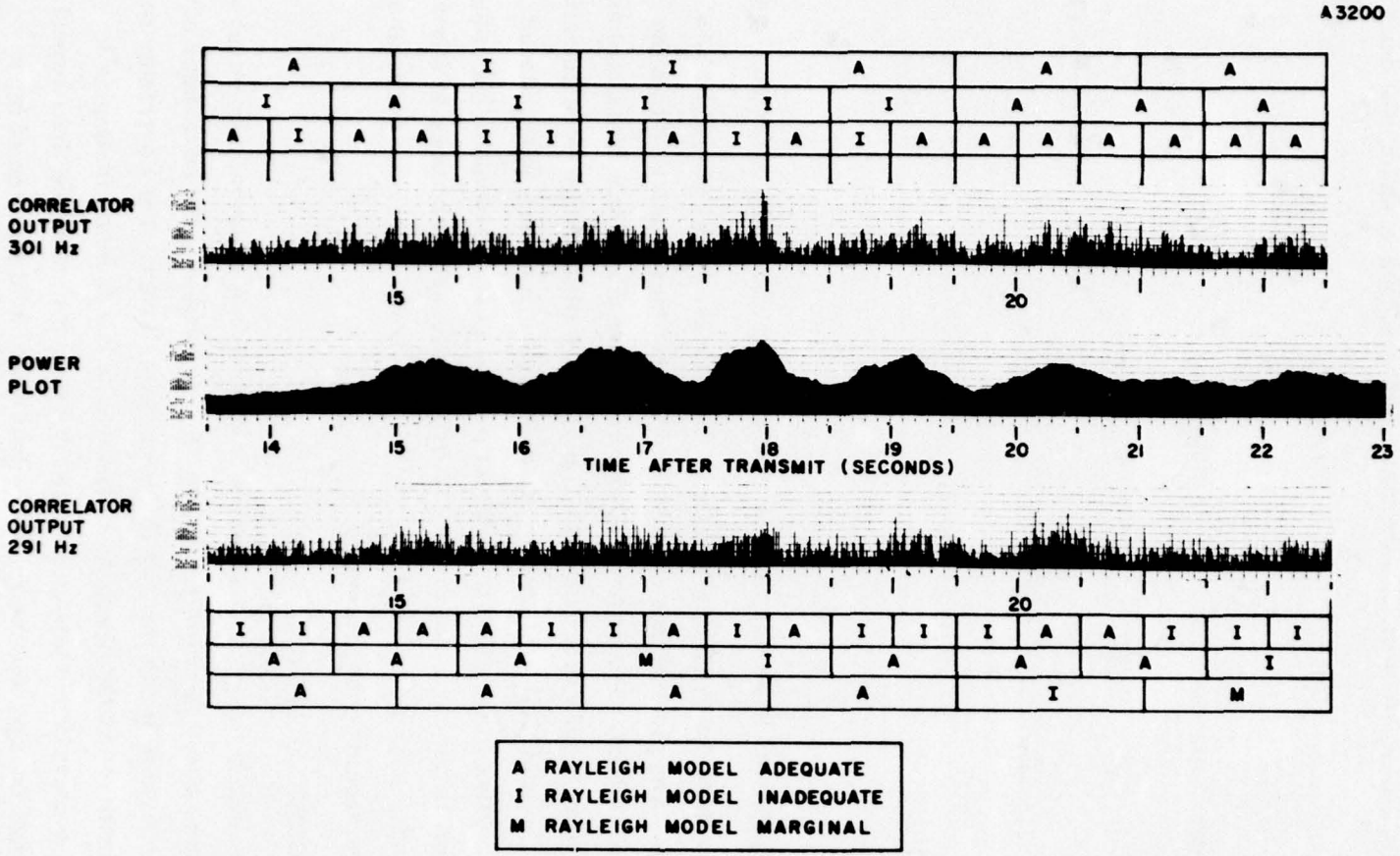

Figure 39. Correlator Output, Ping 78

is still Rayleigh (although its parameter will have changed). On the other hand if $x_j = x'_j + a_j$ and $y_j = y'_j + b_j$, where x'_j and y'_j are normal zero mean variates, and a_j and b_j are constants, then

$$z_j = \sqrt{x_j^2 + y_j^2}$$

is not Rayleigh. However, if for the i^{th} and $i^{th} + 1$ pings

$$\Delta x_j = x'_{i,j} + a_j - x'_{i+1,j} - a_j = x'_{i,j} - x'_{i+1,j} \text{ and}$$

$$\Delta y_j = y'_{i,j} + b_j - y'_{i+1,j} - b_j = y'_{i,j} - y'_{i+1,j}$$

then

$$z_j^* = \sqrt{\Delta x_j^2 + \Delta y_j^2}$$

will be Rayleigh.

The effect of the subtraction is the elimination of constant peaks in the correlator output.

This subtraction was done for the following pings: 6-7, 14-15, 15-16, 16-17, 17-18, 18-19, 25-26, and 26-27. The plots of five of these eight "new" pings indicated that the Rayleigh was a reasonable model. Previously, all the individual pings were classified as inadequate. It is interesting to note that four out of the five new pings which were classified as adequate arose from the subtraction of an inadequate high ping from an inadequate low. Also, all of the new inadequate pings came from the difference of two inadequate high pings. The meaning of this result is not clear at present. Further work should be done in this area by examining the correlator plots to see what is actually occurring. Also, the correlation between successive pings should be determined.

M. INPUT - OUTPUT CORRELATION

Where we have been able to compare reasonably long stretches of correlator output with the power plot for the same time, as shown in Figure 18, for example, the correlator output appears to vary in a manner similar to the way the power plot varies. The correlator output is a very spikey thing compared to the power plot, and one has to do some imagining to follow a mean value in the correlator output. It does not seem unreasonable that, especially in the absence of any target energy, the correlator output would be a function of input amplitude -- it is a linear correlator.

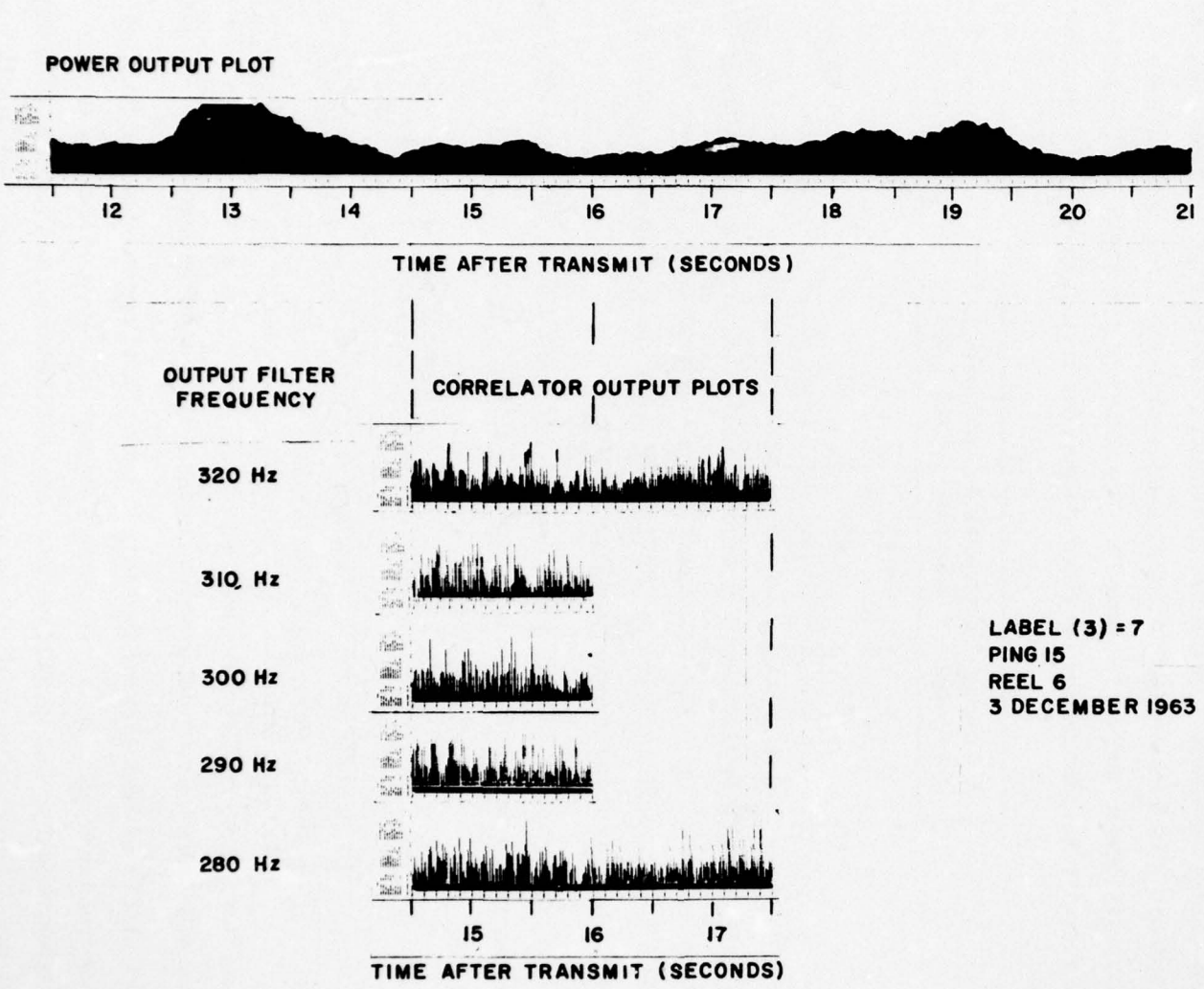

Figure 40. Correlator Outputs and Power Plot, Ping 7

CONFIDENTIAL

If this is the case, some measure of the correlator output samples from the different doppler channels should correlat significantly. We know from the past work that there is no significant pairwise correlation between samples taken at the same time from two different doppler channels. A measure or statistic of the correlator output which might be more likely to show some correlation from channel to channel is the average or mean value over some time interval. We have numbers for the means over 1.5-, 1.0-, and 0.5-second intervals for two frequency outputs for ping 78. The values of correlation coefficients for the pairwise correlation of the means for similar times for various averaging times are shown below.

Averaging Time (sec)	Correlation Coefficient	Number of Data Used
1.5	0.93	6
1.0	0.52	9
0.5	0.75	18

The few data on which the 1.5- and 1.0-second calculations are based tends to discredit them somewhat; however, the 0.5-second value is probably significant, i.e., the likelihood of measuring a value of 0.75 or higher from sets of samples selected from independent gaussian distributions is less than one chance in a thousand.

The rest of the question is: Do the means of the correlator outputs correlate with the means of the power plot outputs? They do. The values are:

	Correlation Coefficient
Power Plot vs. 301 Hz Output	0.74
Power Plot vs. 291 Hz Output	0.67

It appears that, with significance, the means of the power plot and the means of these two frequency outputs of the correlator are related (at least, for this ping).

The work which was done showing the independence of the doppler channels (for individual samples) was done using data from pings 7 through 17. Plots of the data on hand for ping 7 were mounted so that it could be seen if the suspected correlation was obvious (Figure 40). The 1.5-second intervals do not show this correlation very dramatically, but it does appear obvious in the three-second interval.

Because the input amplitude varies with time, especially during one ping, the correlator output samples must be drawn from Rayleigh distributions with different means or scale factors. When we look at the distribution of these samples, collected over a long interval, we are looking at the distribution of samples selected from a continuum of Rayleigh distributions. This collection is not supposed to have a Rayleigh distribution.

Prior work has established that the histograms for the same time intervals in consequtive pings are quite similar. This would be the case if, for example, the power plots were quite similar. We have already observed that the dominant features of the power plots are quite stable from ping to ping.

As a further complication, we observe that a replica of the transmitted signal would, if it arrived during one of these intervals, cause disproportionately high correlator outputs and, hence, distort the output distributions. We have observed output spikes which are much higher than usually occur during noise times, and speculate that they may result from some coherent bottom scattered (reflected) energy arriving at these times.

We would prefer, for some purposes, to have the correlator output more independent of input amplitude. It would for example, allow simple amplitude thresholds to be used to separate more important output samples from those of less importance. As it is now, the output amplitude is a function of both:

1. The amount of correlation with the reference, and
2. The input power level.

Such a system could be implemented in a variety of ways, such as a clipper correlator and an energy detector or, instead of a clipper correlator, a normalized linear correlator. There could perhaps be some advantage to using such a dual channel and combining the outputs using a detection function which could be formulated to take advantage of an understanding of the statistics of the outputs of both processors.

N. CONCLUSIONS (STATISTICAL STUDY)

The modeling of the target-free portion of the correlator amplitude has just begun. We have been able to show that about 40 percent of the pings can be reasonably described by a Rayleigh model, and that a rough guide to the appropriateness of the model can be obtained from examination of the $\sqrt{b_1}$, b_2 values. However, we are not completely satisfied with our determination of why the majority of plots do not follow a Rayleigh model. One of the possible reasons might be a high serial correlation for those pings whose plots were poor, or possibly the nonstationarity of the ping in the 1.5-second interval. Perhaps a smaller

interval should be used or perhaps a higher sampling rate. These questions will have to be investigated in order to refine the present results.

The conclusions which can be drawn to date are as follows:

1. The returns are nonstationary in mean, covariance, and possibly distributional form.
2. The variability within a ping is as high as between 1.5-second intervals of pings taken in the same period of time sampled at the same time after transmit.
3. There is a strong linear relationship between the mean and the standard deviation which appears to be invariant to day-to-day fluctuations and mode of transmission; this property may be useful for classification of targets.
4. There is a linear relationship between $\sqrt{b_1}$ and b_2.
5. Approximately 40 percent of the intervals studied could be resonably fit by a Rayleigh distribution.
6. The zero doppler channel appears to have higher correlator values, higher variability, and is more skewed with higher tails than the other doppler channels.
7. The output values in one channel are not correlated with those in the other channels.
8. The amplitudes fall off faster as the frequency increases than when it decreases for the pings studied.

SECTION V

TARGET ECHOES

A. GENERAL

We are particularly interested in the target echoes. It is these target echoes which, in the long term, we want to help the operator to detect. We are not very far along with either processing or understanding of target echo data. To some extent, we have been waiting for success with the noise model of the correlator output before starting a major effort on target echoes. What has been done is to look at some of the echoes from the first two data reels to obtain an idea of the complexity of the upcoming problem. Many of the following illustrations are presented to describe the features that have been noticed, rather than an attempt to explain them.

The data that has been collected are summarized in Tables 14 and 15; the data are shown in graph form in Figures 41 and 42. The words are used as follows:

Ping Numbers

The new ping number is a consecutive sequence of numbers on our new data tape.

The old ping number is the number assigned to the ping during the original experiment.

Target Range

This is the time of arrival of the echo as represented by the peak correlator output.

Frequency

The frequency (to the nearest Hz) of the correlator output peak.

Nominally, the 300 Hz output channel is zero doppler and lower frequencies result from closing range.

Peak Correlator Output

Typically, it is the largest amplitude correlator output sample we found in the area. The area was a relatively short time interval, usually from 0.2 to 0.4 seconds, and from 5 to 10 Hz wide. This interval was centered about the power plot peak time.

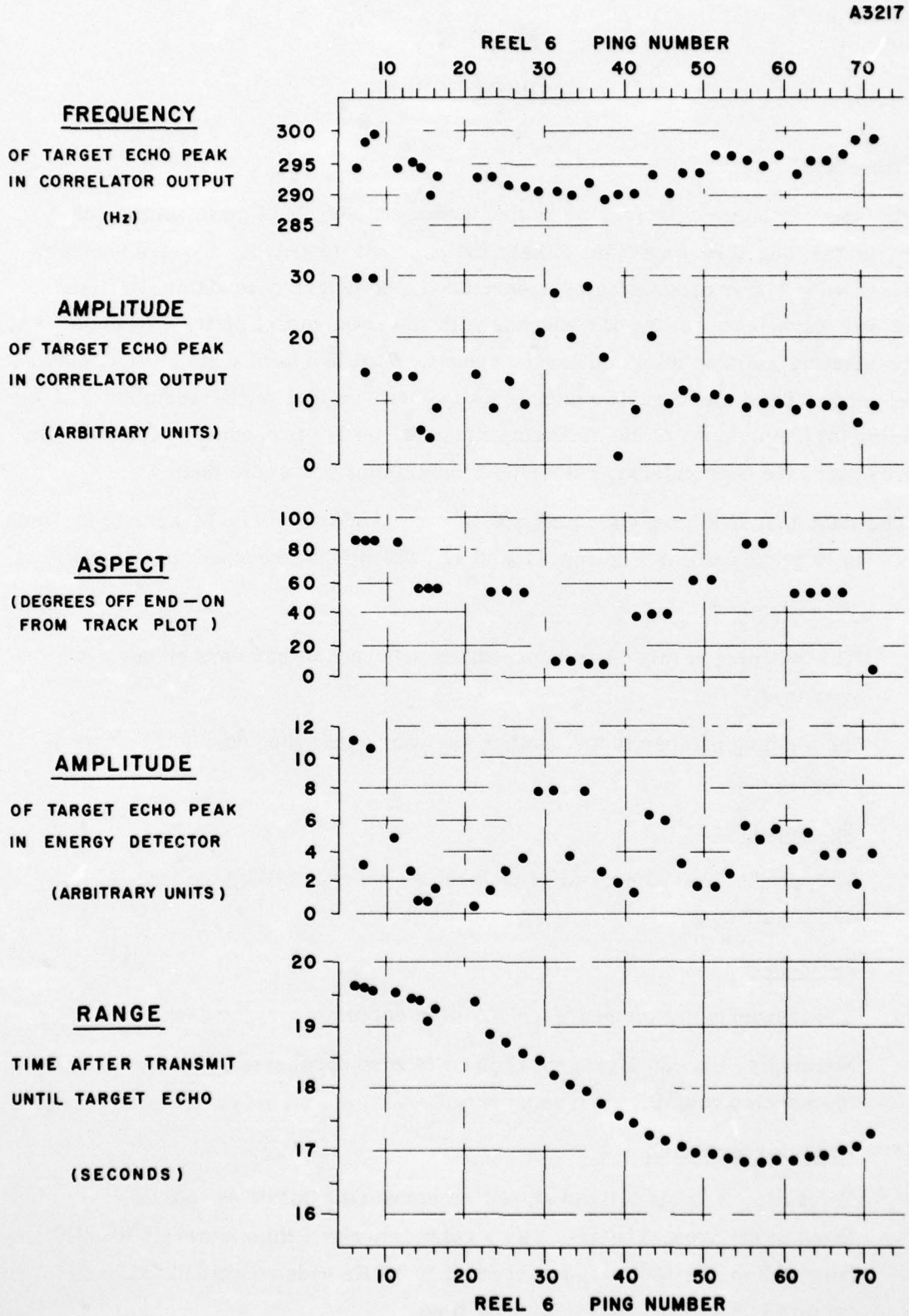

Figure 41. Plots of Target Echo Data, Reel 6

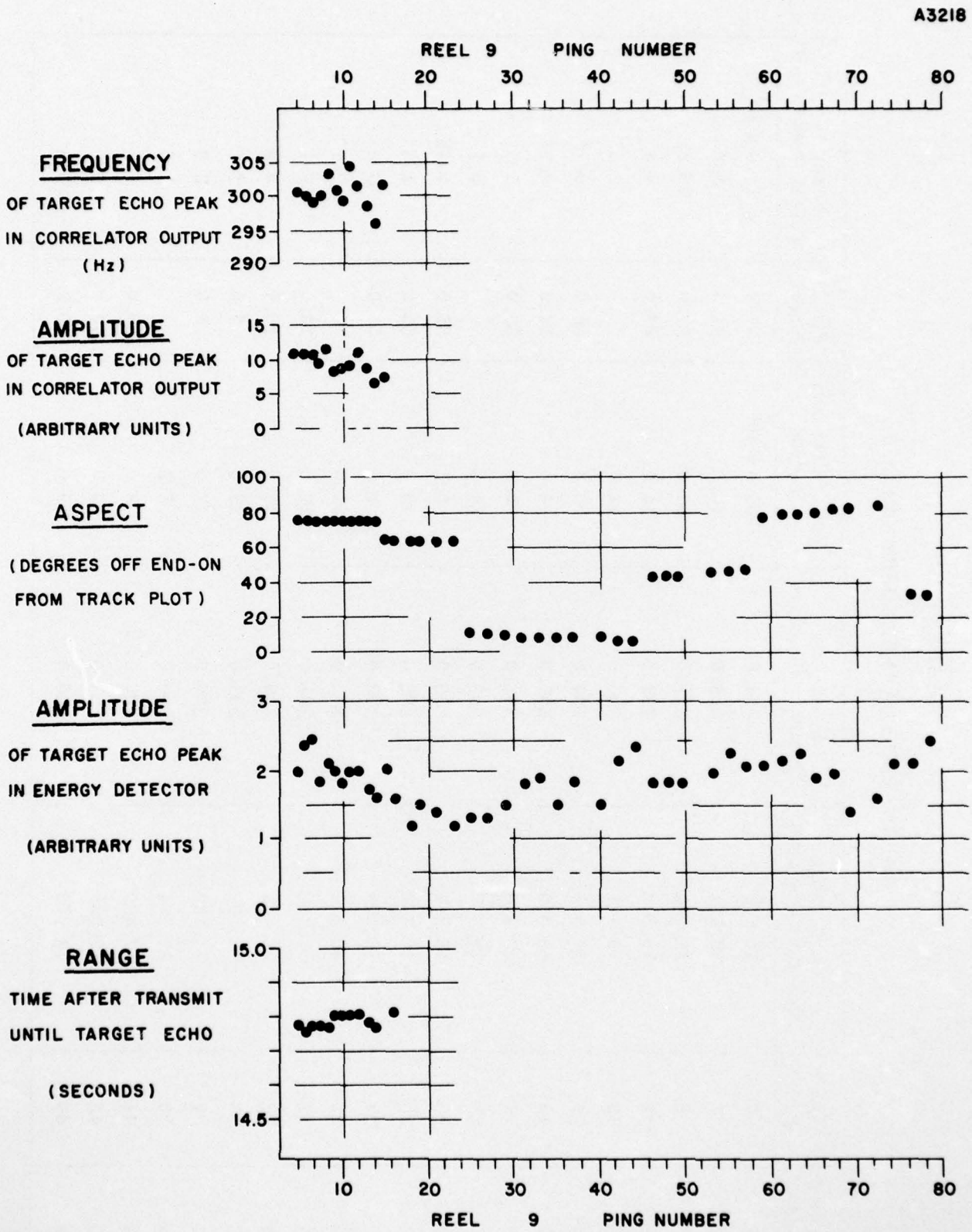

Figure 42. Plots of Target Echo Data, Reel 9

TABLE 14

TARGET ECHO DATA SUMMARY - REEL 6

New Ping Number	Reel 6 Ping No.	Target Range (secs after transmit)	Peak Echo Frequency Chamber	Peak Correlator Output	E.O.* Aspect	Power Plot** Target Peak Output
1	6	19.642	294.0	30.0×10^5	87.0	11.0×10^6
2	7	19.614	298.0	15.0	87.0	3.0
3	8	19.584	299.0	30.0	87.0	10.5
4	11	19.520	294.0	14.0	87.0	4.4
5	13	19.444	295.0	14.0		2.5
6	14	19.396	294.0	5.3	56.0	0.77
7	15	19.080	290.0	4.0	56.0	0.71
8	16	19.270	295.0	9.3	56.0	1.6
9	21	19.373	295.0	14.0		0.3
10	23	18.834	295.0	8.2	55.0	1.45
11	25	18.710	292.0	13.0	55.0	2.6
12	27	18.576	292.0	9.6	55.0	3.3
13	29	18.414	291.0	21.0		7.7
14	31	18.216	291.0	27.0	10.0	7.7
15	33	18.062	290.0	20.0	10.0	3.3
16	35	17.908	292.0	28.0	9.0	7.7
17	37	17.738	289.0	17.0	8.0	2.3
18	39	17.574	290.0	1.2		1.8
19	41	17.460	290.0	8.0	39.0	1.1
20	43	17.258	293.0	20.0	40.0	6.0
21	45	18.216	290.0	9.0	40.0	5.8

TABLE 14 (concluded)

New Ping Number	Reel 6 Ping No.	Target Range (secs after transmit)	Peak Echo Frequency Chamber	Peak Correlator	E.O.* Aspect	Power Plot** Target Peak Output
22	47	17.122	293.0	12.0×10^5		3.0×10^6
23	49	16.998	293.0	10.0	61.0	1.5
24	51	16.946	296.0	11.0	62.0	1.4
25	53	16.886	296.0	10.0		2.1
26	55	16.814	295.0	8.5	85.0	5.2
27	57	16.812	294.0	9.3	86.0	4.4
28	59	16.808	296.0	9.0		5.0
29	61	16.834	293.0	7.7	54.0	3.8
30	63	16.908	295.0	9.2	54.0	4.7
31	65	16.928	295.0	8.7	54.0	3.6
32	67	17.080	296.0	8.8	54.0	3.8
33	69	17.110	298.0	5.7		1.5
34	71	17.360	298.0	8.6	4.0	3.6

* Aspect is shown as degrees off end-on. Values are not given for pings nearest each course change.

** These values are rescaled to agree with the current program. New values equal old value x 27.5.

CONFIDENTIAL

TABLE 15

TARGET ECHO DATA SUMMARY - REEL 9

New Ping Number	Reel 9 Ping No.	Target Range (secs after transmit)	Peak Echo Frequency Chamber	Peak Correlator Output	E.O. Aspect	Power Plot Target Peak Output
35	4	14.785	301.0	11.0×10^5	77	2.0×10^6
36	5	14.774	300.0	11.0	77	2.4
37	6	14.788	299.0	11.0	77	2.5
38	7	14.786	300.0	9.6	77	1.8
39	8	14.788	303.0	12.0	77	2.1
40	9	14.802	301.0	8.1	77	2.0
41	10	14.804	299.0	8.4	77	1.8
42	11	14.804	304.0	9.3	77	2.0
43	12	14.806	302.0	11.0	77	2.0
44	13	14.790	298.0	8.4	77	1.7
45	14	14.770	296.0	6.8		1.6
46	15	14.808	302.0	7.6	63	2.0
47	16				63	1.6
48	18				63	1.2
49	19				63	1.5
50	21				63	1.4
51	23				63	1.2
52	25				11	1.3
53	27				11	1.3
54	29				10	2.0
55	31				10	1.8
56	33				10	1.9

TABLE 15 (concluded)

New Ping Number	Reel 9 Ping No.	Target Range (secs after transmit)	Peak Echo Frequency Chamber	Peak Correlator Output	E.O. Aspect	Power Plot Target Peak Output
57	35				9	1.5×10^6
58	37				9	1.8
59	40				8	1.5
60	42				7	2.2
61	44				6	2.4
62	46				43	1.8
63	48				44	1.8
64	50				45	1.8
65	53				46	2.0
66	55				47	2.3
67	57				48	2.1
68	59				78	2.1
69	61				79	2.2
70	63				80	2.3
71	65				81	1.9
72	67				83	2.0
73	69				84	1.4
74	72				85	1.6
75	74					2.2
76	76				37	2.2
77	78				37	2.5

CONFIDENTIAL

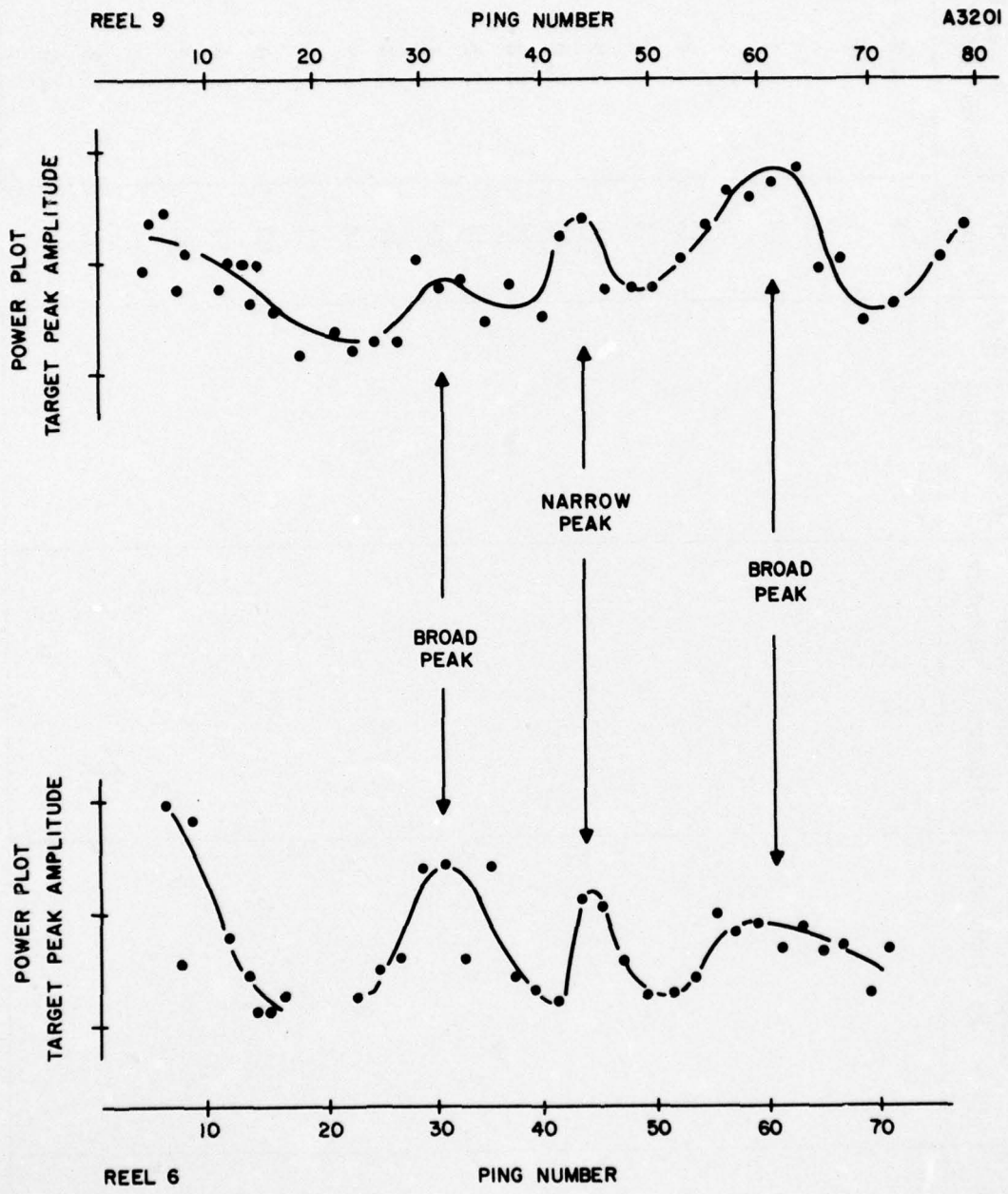

Figure 43. Target Echo Amplitude Comparison

E.O. Aspect

This is a measure of aspect which we used. It is the number of degrees off end-on which we measured on the track plots.

It was used to try to show that problems arise as the aspect varies either way from a beam aspect. It is not supposed to suggest the bow and stern aspects are similar; they do not appear to be.

Power Plot Target Peak Output

The output of the 0.5-second integrator at a peak which appears, from looking at several pings, to be the target echo.

B. TARGET PEAKS IN THE POWER PLOTS

The energy detector output plots, or power plots, for the data which have been digitized are presented in Appendix A. The first two figures illustrate the two surface duct sequences that have been studied. In both of these records the targets are quite obvious. In the Reel 6 (Figure A-1) sequence the target is obvious in all but a few pings by its very size. In the Reel 9 (Figure A-2) sequence, although the target gets lost in the reverberation for a few pings in the middle, it is otherwise easy to find. One observes that it is a great help, when attempting to identify the target, to be able to see a string of pings. The several bumbs in many of the Reel 9 plots would be difficult to interpret with reliability without reference to at least several of the neighboring plots.

It was observed earlier, and it is obvious from Figure 8, that the ping-to-ping variation in target amplitude is much greater for the Reel 6 data. This is true until toward the end where it seems to settle down to about the same amplitude as the Reel 9 targets. We do not know why it occurs this way.

The way that the target peaks vary is even more interesting when the two runs are considered together. Plots of both the Reel 6 and Reel 9 data versus ping number are shown in Figure 43. The vertical scales are different. The ping-to-ping times are a little different so that these plots versus time would not line up quite so well. It is quite interesting that they are so similar.

One of the questions that was asked about the target data was; "How well does it correlate with our measure of aspect?" In order to find out, a number was invented for this measure of aspect: E.O. aspect; is the number of degrees off end-on. Thus, a beam target is 90^{o} (a large number) and a bow target is 0^{o} (a small number).

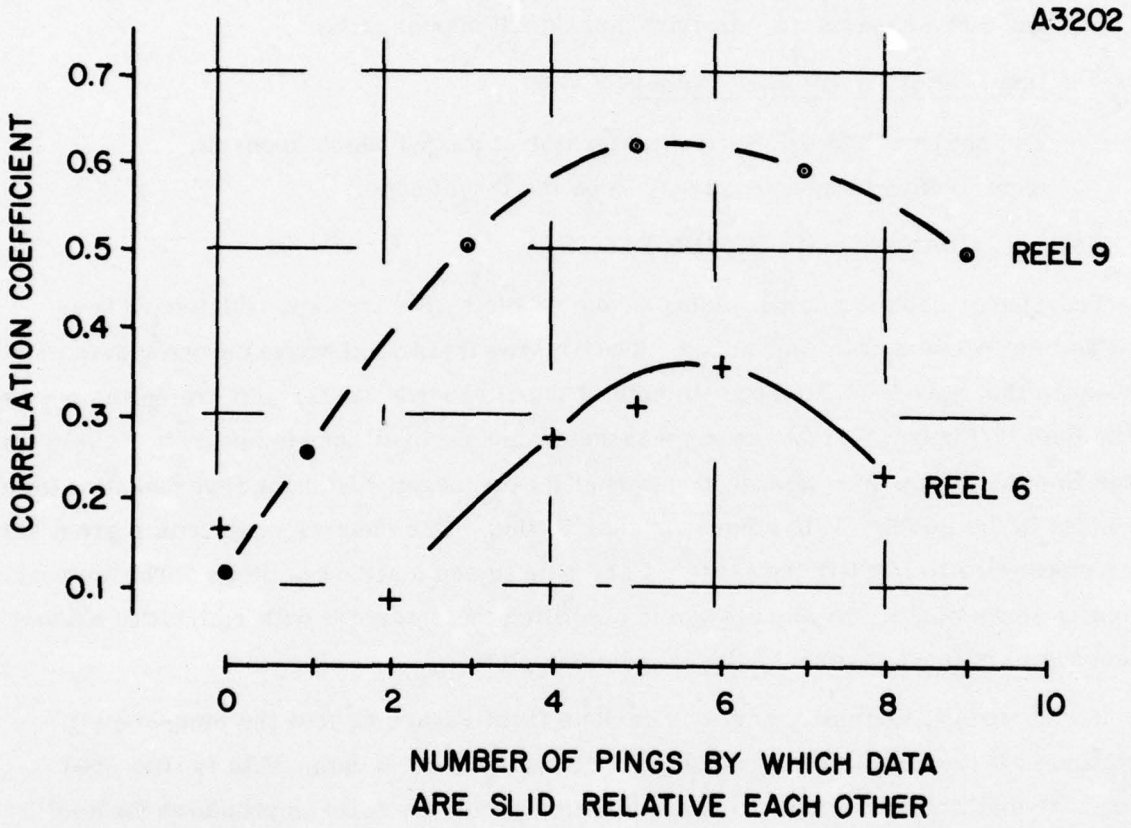

Figure 44. Correlation of Target Echo Peak and E.O. Aspect

This gives a set of numbers that is large when big echoes are expected, and small when problems are expected. This does not indicate that we think that bow and stern target echoes are the same; for the moment, however, we want to see how things look on the basis of this fairly simple concept of aspect.

Calculations showed no significant correlations between the power plot target peaks and E.O. aspect--this was a surprise. We knew that we were not observing the 10 or 20 dB difference that we could have believed, but it did seem like there should be some correlation. Perhaps the experiment plots are so wrong that our measure of aspect is no good.

Based upon the observation that the power plot target data and E.O. aspect data for Reel 9 seemed to have the same sort of shape, but that they did not seem to go through their minimums at the same ping we calculated correlation coefficiencies for instances when the data were slid with respect to ping number. The results, presented in Figure 44, show the spectacular increase in correlation coefficient as a shift of five or six pings is approached. It looked like it should happen but when faced with the fact that it does, we do not know how to interpret it. We did not expect the Reel 6 data to display this same feature, but it does.

It just has to be that our measure of aspect is in error.

Our interest in the effect of aspect is sparked by the experiences of those who lose targets whenever they change from beam aspect. They, of course, are using the correlator outputs.

For the Reel 6 data we have calculated the correlation between the power plot peaks and the correlator output peaks and find it to be about 0.5. This is quite significant because there are 34 samples. (It would happen less than one time in 200 experiments if samples were selected from two independent gaussian distributions.) Figure 45 is a plot of the correlator output target peaks versus the power plot target peaks.

The calculated correlation between the correlator output peaks and E.O. aspect was small, and we did not pursue a slid version. We ought to try this again when we obtain a good measure of aspect.

C. TARGET PEAKS IN THE CORRELATOR OUTPUT

In Reference 1, pages 23 to 26, some observations about targets in the correlator output and some samples are shown. These are simple plots of the output of one doppler filter with time.

AD-A031 506 GENERAL ELECTRIC CO SYRACUSE N Y HEAVY MILITARY ELEC--ETC F/G 17/1
COMPUTER-AIDED DETECTION STUDY.(U)
JUL 66

UNCLASSIFIED

NOBSR-93298

NL

2 OF 2
ADA031506

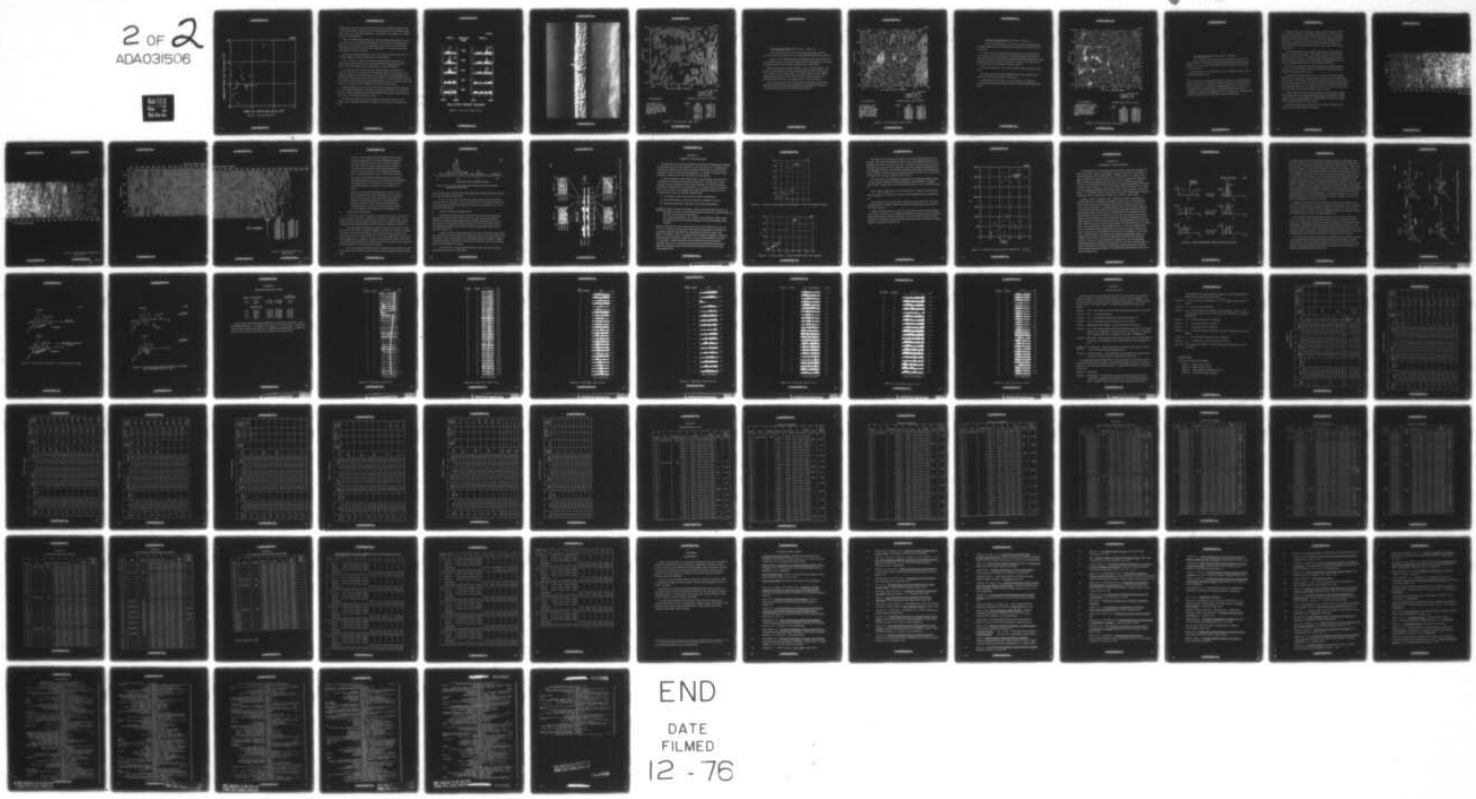

END

DATE
FILMED
12 - 76

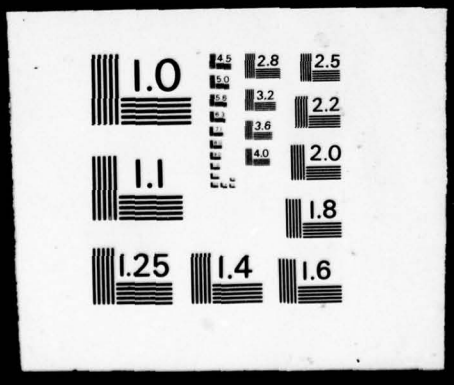

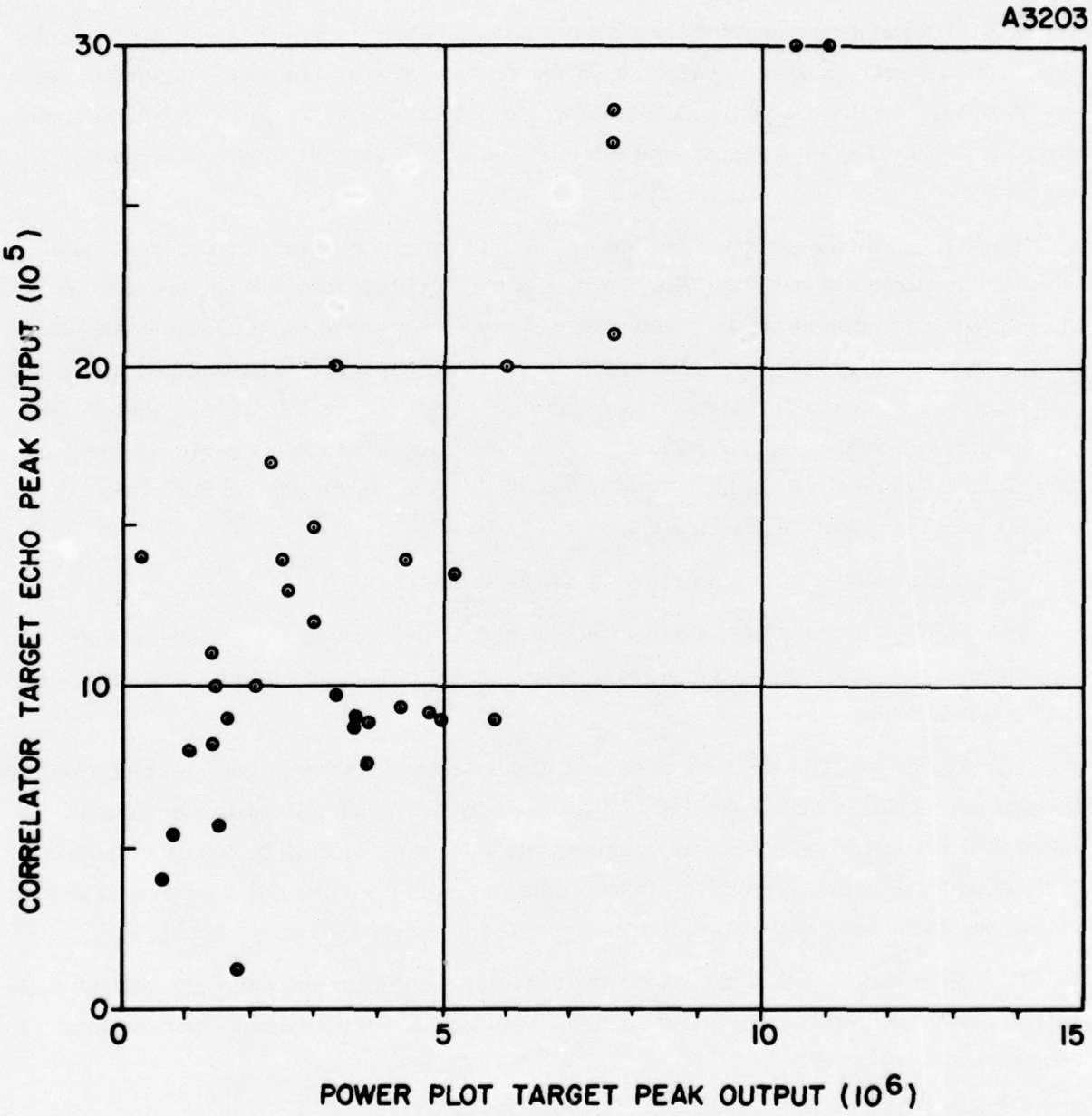

Figure 45. Plot of Target Peaks

Although these plots are good and useful when the signal-to-background ratio is high, it is somewhat difficult to figure out what is going on when it is not. Problems can be due to noise (or reverberation) background, multipath due to propagation, or multiple echoes due to target extent.

Figure 46 illustrates these difficulties. Observe that the peaks marked 1, 2, and 3 are each located at a different output frequency. It is possible that only the highest peak, shown as 2, should be used to detect the target, but then it would seem that additional echo pulses could provide useful information. It is a function of how they were caused or what they represent.

This gets us interested in finding out how to look at the echo arrivals to see if we can piece together a plausable explanation of what is going on.

Figure 47 shows a model of the correlator output surface for Ping 6 Reel 6. This is a particularly good return in terms of high SNR and one simple echo peak. Other views of this model are shown in Reference 1, pages 37 through 39.

All of the pings of Reel 6 have been processed like pings 10 and 11 shown in Figure 46, namely, for some time interval, typically about 0.2 seconds and for five frequency channels. From these plots come the times of arrival and frequencies, for both the Reel 6 data and for the first few pings of Reel 9, we observed that the plot was not smooth. It appeared that the target submarine had to move in an erattic manner with respect to the ship in order to satisfy the plot; that did not seem likely.

Another possibility is that the echo which is best in each ping is not the same one; i.e., the target highlight which causes the echo peak moves about on the submarine. Either as another possibility or as a complicating factor the specific path used by the echo return can be different from ping to ping.

In order to get a better look at the correlator output plane, we have moved toward contour map-like presentations. Figures 48, 49, and 50 show some of these plots.

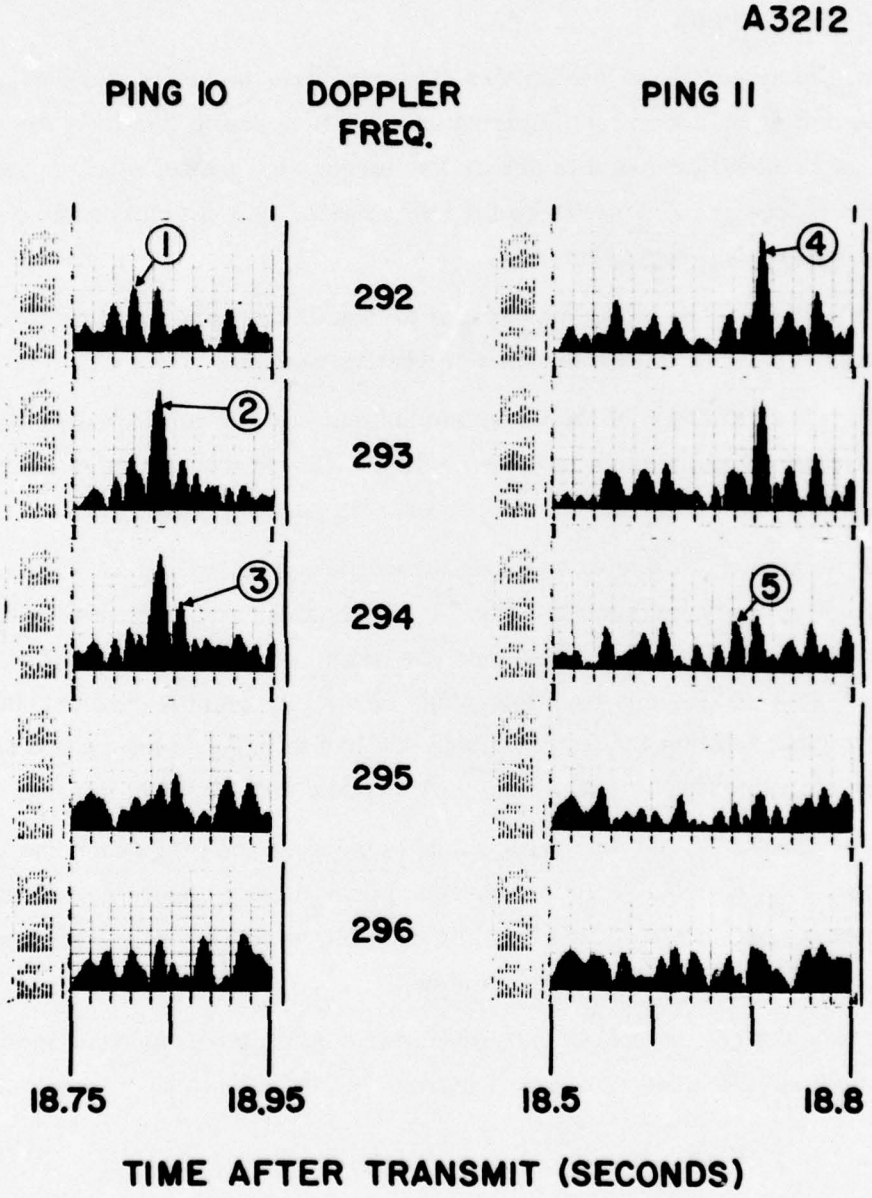

Figure 46. Echo Time, Pings 10 and 11

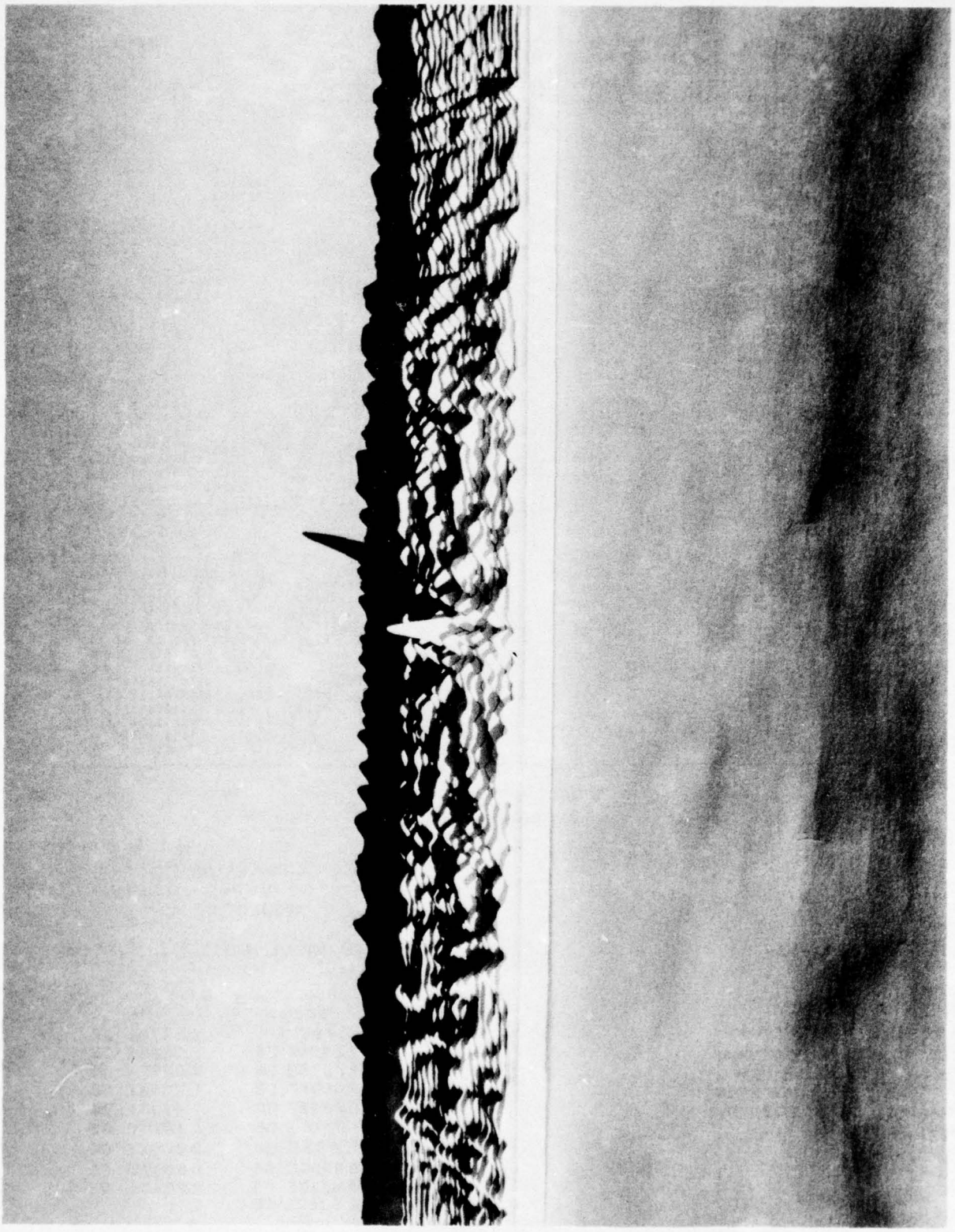

Figure 47. Target Echo Surface Model, Ping 6, Reel 6

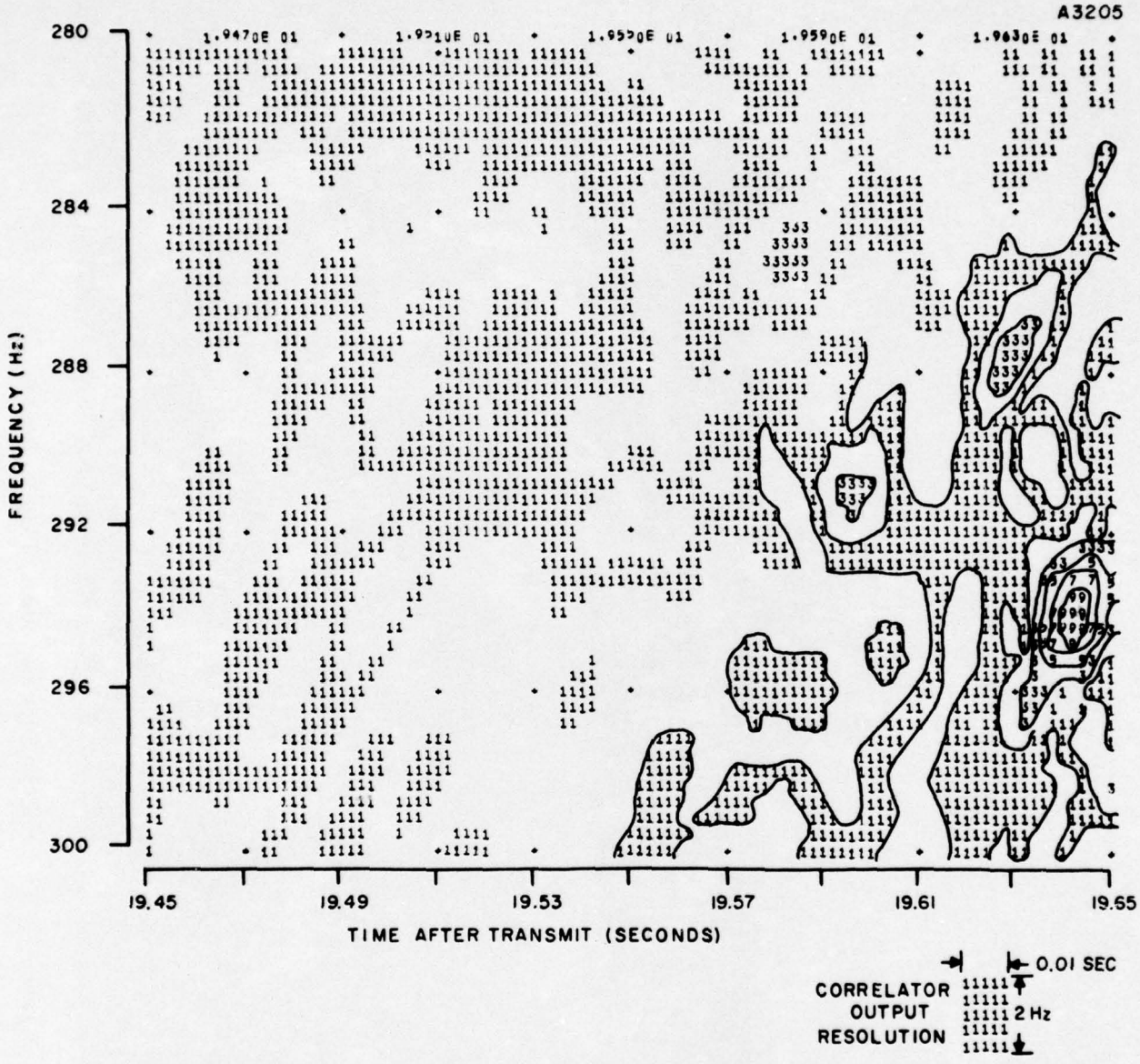

SIFT CONTOUR MAP

MAXIMUM VALUE IN PLOT IS 2.49E 06

THE NUMBERS THAT ARE PLOTTED IN EACH REGION ARE PROPORTIONAL TO THE PEAK VALUE. SOME CONTOUR LINES HAVE BEEN DRAWN IN THE AREA OF THE OUTPUT PEAK.

SYMBOL	FROM	TO
9	ABOVE	2.6478E 06
	2.6478E 06	2.3536E 06
7	2.3536E 06	2.0594E 06
	2.0594E 06	1.7652E 06
5	1.7652E 06	1.4710E 06
	1.4710E 06	1.1768E 06
3	1.1768E 06	8.8259E 06
	8.8259E 05	5.8839E 05
1	5.8839E 05	2.9420E 05
	2.9420E 05	0.

Figure 48. Sift Contour Map, Ping 6, Reel 6

Correlator Output Surface, Ping 6, Reel 6, Figure 48

This is the first ping and it is a particularly good return. There is one great peak in the correlator output at 19.642 seconds and 294 Hz (see Figure 47).

This sort of a contour map shows the peak very well and shows that there are hills nearby that are 30 per cent as high (3 means in the thirties) as the peak. One observes that far away from the peak there are no hills shown.

This plot is relative or percent amplitude, which is a little deceptive. This is the very highest peak that we have seen and hence, the contour intervals are very wide (only 10 intervals are used). The contour interval is almost 300,000 which is higher than most of the correlator outputs in the noise region. It is interesting that there are so many outputs which exceed this high level.

Some contour lines are drawn to show how they would look. They are well-behaved and smooth because correlator outputs are calculated five times per resolution increment in both range and frequency direction.

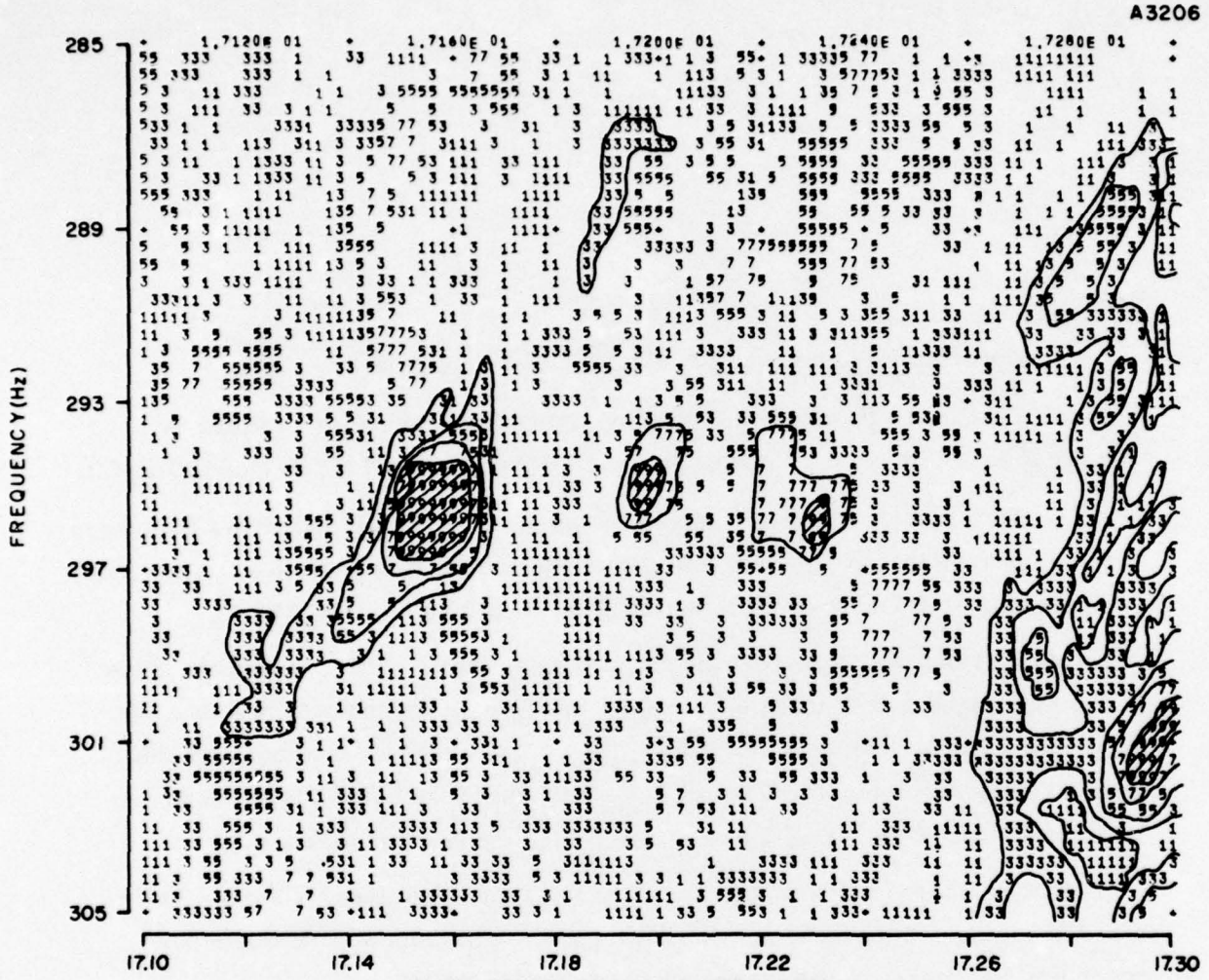

SIFT CONTOUR MAP

MAXIMUM VALUE IN PLOT IS 1.89E 06

THE NUMBERS PLOTTED IN EACH REGION ARE THE ARRAY AMPLITUDES TRUNCATED TO HUNDRED THOUSANDS. ONLY ODD NUMBERS ARE PLOTTED. PEAKS AT THE HIGHEST SIFT LEVEL ARE SHADED GREY.

SYMBOL	FROM	TO
9	ABOVE	9.0000E 05
	9.0000E 05	8.0000E 05
7	8.0000E 05	7.0000E 05
	7.0000E 05	6.0000E 05
5	6.0000E 05	5.0000E 05
	5.0000E 05	4.0000E 05
3	4.0000E 05	3.0000E 05
	3.0000E 05	2.0000E 05
	2.0000E 05	1.0000E 05
1	1.0000E 05	7.8125E 03

Figure 49. Sift Contour Map, Ping 45, Reel 6

Correlator Output Surface, Ping 45, Reel 6, Figure 49

This is a strong looking echo on the power plot but confusing on the correlator output plots. The submarine is closing and the aspect is probably bow-quarter.

It is quite clear from this type of plot that there are several high peaks. This plot sifts the data into intervals of 100,000 and prints the odd numbers. Only the odd numbers are printed with the hope that the blank regions will enhance the illusion that it is some sort of contour map. Again, only 10 intervals are used and all regions over 900,000 are filled in with 9's.

This kind of clipping is not too serious because values that high are quite rare.

Drawing contour lines is more difficult because of the smaller contour interval and because of the surface complication.

Having this plot shows exactly why it was difficult to interpret the correlator output plot, and convinces us that we do not know which peak is the target.

A3207

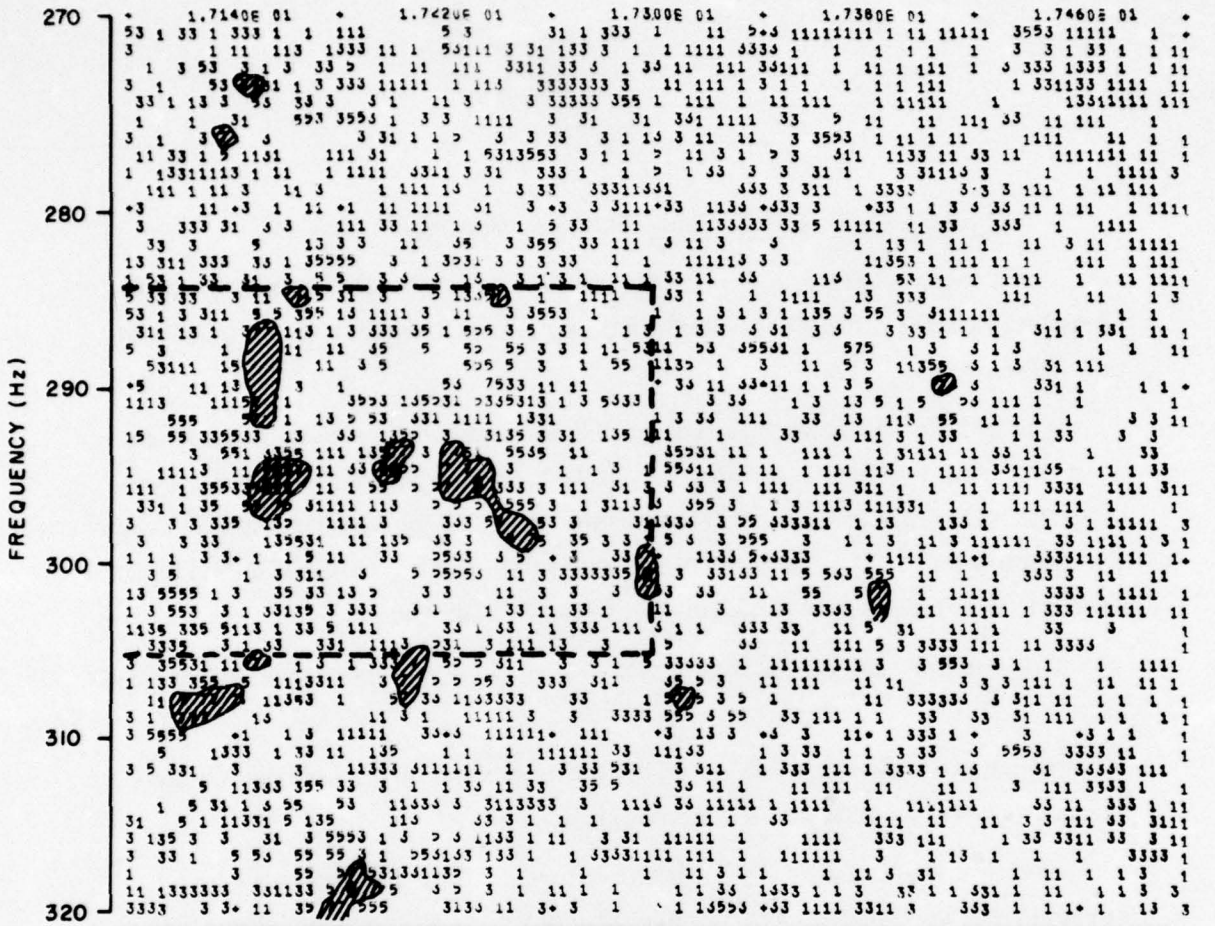

SIFT CONTOUR MAP

MAXIMUM VALUE IN PLOT IS 1.72E 06

THESE NUMBERS ARE HUNDRED THOUSANDS LIKE THELAST ONE. THE DIFFERENCE IS THE NUMBER OF CORRELATOR OUTPUTS PER RESOLUTION ELEMENT. NINES ARE BLACKENED AND SEVENS ARE CIRCLED AND GREY.

SYMBOL	FROM	TO
9	ABOVE	9.0000 E 05
	9.0000 E 05	8.0000 E 05
7	8.0000 E 05	7. 0000 E 05
	7.0000 E 05	6.0000 E 05
5	6.0000 E 05	5.0000 E 05
	5.0000 E 05	4.0000 E 05
3	4.0000 E 05	3.0000 E 05
	3.0000 E 05	2.0000 E 05
1	2.0000 E 05	1.0000 E 05
	1.0000 E 05	7.8125 E 03

Figure 50. Sift Contour Map, Ping 45, Reel 6

Correlator Output Plot, Ping 45, Reel 6, Figure 50

This is another look at correlator output surface for ping 45. This time the number of calculations per resolution increment is reduced to two in frequency and 2.5 in range. The extent of the last plot, Figure 49, is shown by the dashed lines.

Although the plot is still quite useful, it is very difficult to make a good looking set of contour lines.

The contour lines are important because they emphasize any overall geometric features which occur; for example, we suspect that much of the minor relief shows a tendency to run parallel to a diagonal from lower left to upper right. This tendency was noticed strongly in a plot of the foot hills near but not including any peaks from this ping's data. We do not know how to interpret such an effect, but it seems as if it would be a good one to track down.

We have recently tested a program to make a (real) contour map of the array of numbers that are the correlator output. Figure 51 is such a map of the output surface for ping 6 Reel 6. This is the same surface, incidentally, that is shown in the model of Figure 47. Only the overall appearance is the same, that is, because the strips are not in the model in the right order. (This is a mistake we noticed while trying to see why it didn't agree with the contour map.)

In this map the contours are relatively clear and the overall geometric patterns are quite well presented. It is difficult to determine with certainty whether a given "bull's-eye" is a hole or a hill. Perhaps we can find some way to mark one or the other. A grid of numbers in the background of the plot shows the magnitude of the indicated array sample in thousands.

Figure 52 is a sift-map of the array which prints a number quantizing the array values into hundred thousands. Presumably most questions can be answered by referring to this array.

The target time outputs of the first 10 or 12 pings in the second surface duct sequence are particularly interesting because the range to the target does not change much from ping to ping. The ship and sub seem to be on near parallel courses. This sequence gives us a chance to look at a set of consecutive echoes (no interspersed FM) to see what echoes look like under relatively simple conditions. We expect them to be quite similar, one to the next.

We have sift-contour plots of these pings and have made simple contour maps of each of them on transparent (acetate) sheets. Each sheet is a contour map of an area 0.4 second (range) by 50 Hz (frequency) and shows by contour lines the highest peak and some lower peaks.

It is interesting to stack the sheets of various pings in different orders and look at the resultant picture; for example:

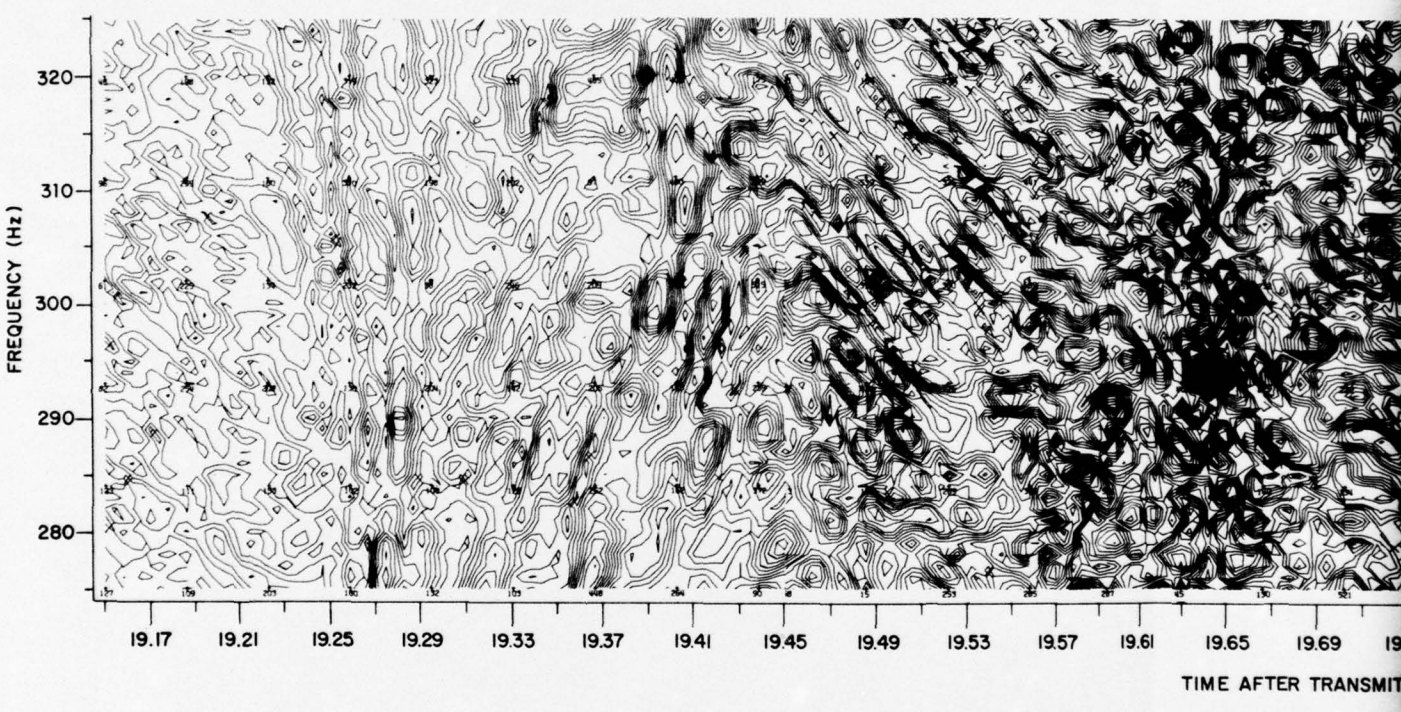
FREQUENCY (Hz)
320
310
300
290
280
19.17
19.21
19.25
19.29
19.33
19.37
19.41
19.45
19.49
19.53
19.57
19.61
19.65
19.69
TIME AFTER TRANSMIT

CONFIDENTIAL

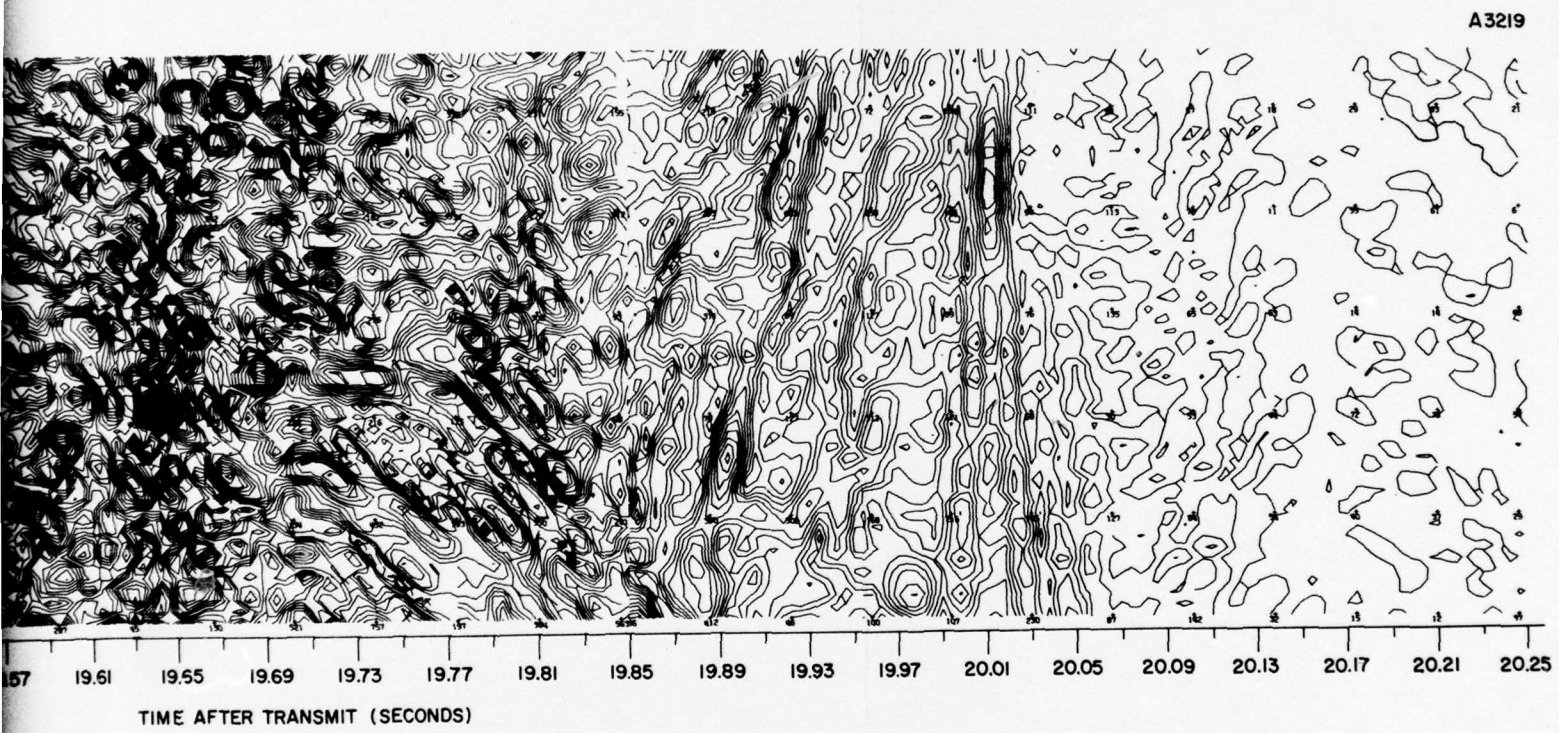

Figure 51. Correlator Output Contour Map, Ping 6, Reel 6

CONFIDENTIAL


TIME AFTER TRANSMIT (SECONDS)
19.17
19.21
19.25
19.29
19.33
19.37
19.41
19.45
19.49
19.53
19.57
19.61
19.65
19.69
FREQUENCY (Hz)
280
290
300
310
320

SYMBOL	FROM		TO	
9	ABOVE		1.0000E	06
8	1.0000E	06	9.0000E	05
7	9.0000E	05	8.0000E	05
6	8.0000E	05	7.0000E	05
5	7.0000E	05	6.0000E	05
4	6.0000E	05	5.0000E	05
3	5.0000E	05	4.0000E	05
2	4.0000E	05	3.0000E	05
1	3.0000E	05	2.0000E	05
0	2.0000E	05	1.0000E	05
	1.0000E	05	0.0	

KEY TO SYMBOLS

Figure 52. Correlator Output Array, Ping 6, Reel 6

If the six with the highest peaks are stacked so that the peaks are lined up (vertically), it is quite startling that a large percent of the bumps on each plot are also lined up vertically. The places where there are no bumps also line up quite well. It is obviously the ambiguity surface showing through and obviously it should show best for the echoes that are largest (but it is quite reassuring to have it work out so dramatically).

If the others (those without the highest peaks) are compared to this collective picture, to see which of several likely peaks might fit the pattern best, it is obvious that one is better than others even though peaks aren't available to cover all those of the pattern.

If they are lined up with time and frequency correct, it is a four-dimensional model of the ping sequence. We can see that targets from successive pings can be at the same range and be noticably spread in frequency. We can imagine that the targets are groups at several discrete ranges instead of a continuous smear or spread. If present, this effect might be due to propagation mode switching or target highlights, etc.

D. TARGET PEAK STATISTICS

If we are to be able to complete the correlator model which we seek, we will have to have some sort of a probability distribution for target peaks. In this respect we have no idea yet about how similar the Reel 6 and Reel 9 data will look. The output samples from the Reel 6 data are plotted as a histogram in Figure 53.

The most serious impediment to progress in this area is our lack of a good set of rules to tell what is a target; for example, the histogram of Figure 53 contains one sample from each of the 34 pings. Even in those cases--ping 45 Reel 6, for example--where we are quite sure that there are several target peaks, we have used only the highest one. Is it right to use more than one peak from a given ping? How can we identify target peaks? For example, how many target peaks show on Figure 50? To these questions we do not yet have good answers.

But even the questions presented above are biased toward a specific approach to obtain the target statistics. Implicit in them is that an ensemble approach is to be used.

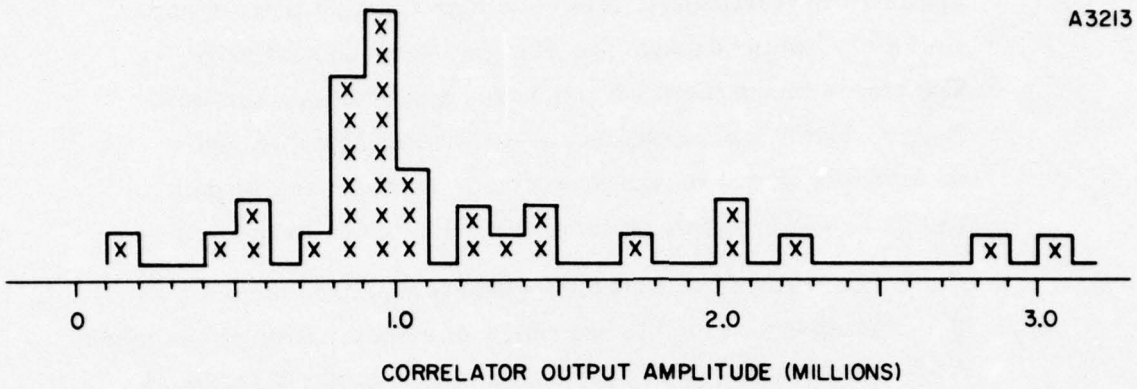

Figure 53. Grey Maps of Correlator Output Surface for Times of Possible Returns Via Bottom Path

There are those who recommend that target statistics be collected from time-sampling the target echo region of many pings.

So far, we have not tried to make a decision. The best answer is probably a function of how the data look, what for and how the data are to be used, and how well we understand the data. We plan to look at the echoes in more detail to see if we can improve our understanding.

E. TARGET PEAKS VIA BOTTOM PATH

Because they come at about the right time, some pairs of bumps following the target on the power plots of some of the pings in the second half of the Reel 6 sequence are suspect of being triangular path and bottom bounce echoes. If this is true, it gives us an opportunity to look at echoes under fairly poor signal-to-noise (reverberation) conditions, but in the enviroment of an experiment about which we are trying to learn a lot.

Figure 54 illustrates the portion of the return under consideration and presents grey maps of the correlator output plane. These grey maps are sift contour maps which use symbols in order of blackness to fill the amplitude intervals--blackest is highest. An interesting feature of the maps is that they can be reduced so much and yet present about all the information they contain.

One can observe a distinct diagonal pattern in most of the plots; we do not understand the significance of this pattern.

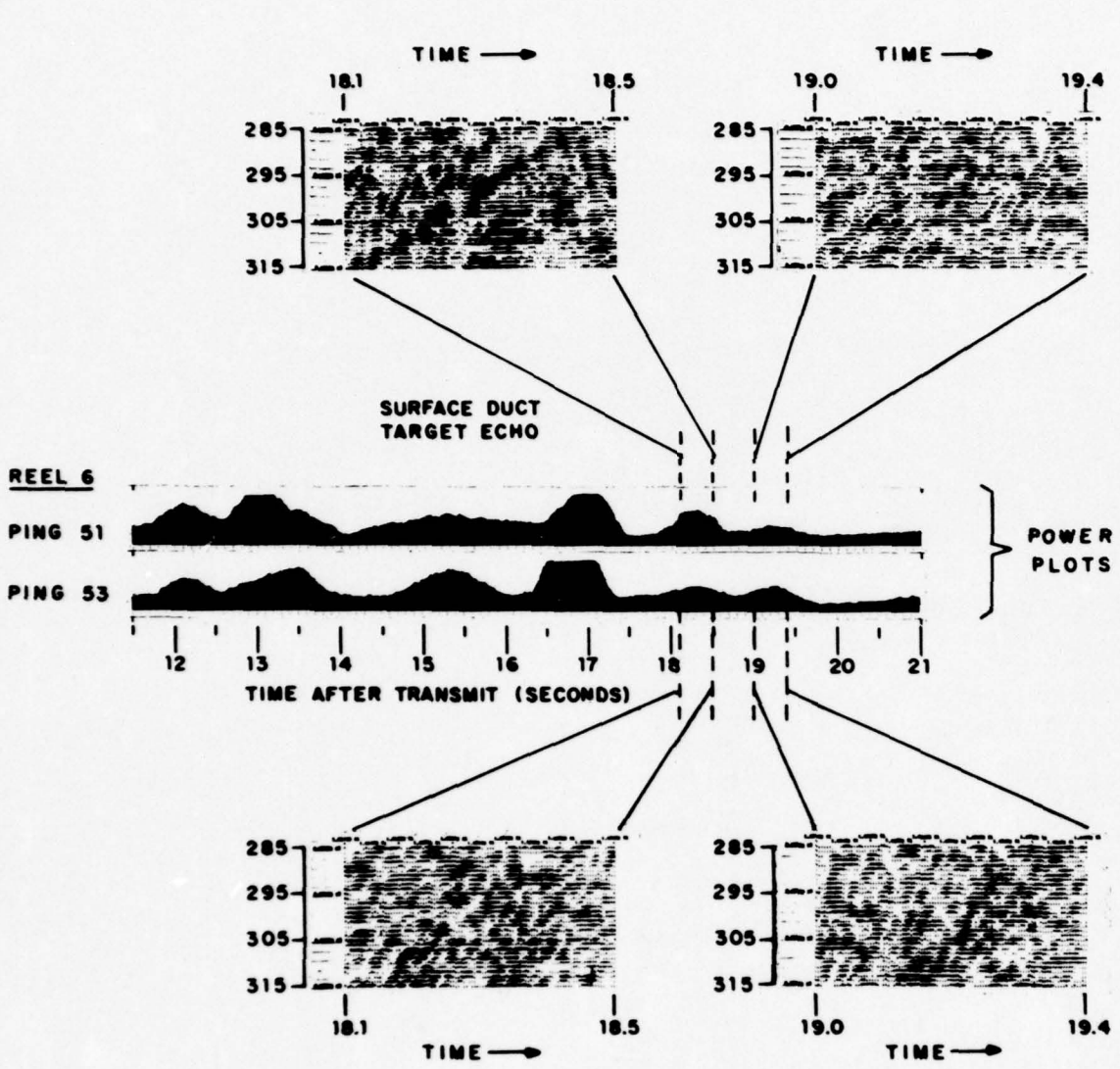

Figure 54. Grey Maps of Correlator Output Surface for Times of Possible Target Returns Via Bottom Path

CONFIDENTIAL

SECTION VI

WINDOW VECTOR STATISTICS

The statistical study of the noise provides a sound basis for establishing a threshold on correlator output for detection based on a given false alarm rate. The high signal-to-noise-ratio (SNR) for most of the pings studied indicates that an exercise (using available test data) in showing detection capability, on this basis, would show a good probability of detection but would not furnish any useful results.

A limited investigation of the target regions in several pings was made to see if clustering type techniques look promising for detection. The basic data studied were the computer calculated correlator output amplitude over intervals (windows) of 120ms; a correlation index of 2 was used (i.e., a correlator output was calculated every 2 ms). An event was considered as an output exceeding a threshold of 180 k correlator output units. The variables considered were:

N the number of events within the 120-ms window (60 Maximum)

A_p the peak amplitude by which the threshold was exceeded by an event

$\bar{A}$ the average amplitude by which the events exceeded the threshold

$\frac{N}{N_{+1}+N_{-1}}$ the number of events in the doppler channel of interest divided by the sum of the number of events in the next higher frequency channel (N_{+1}) and the number in the next lower frequency channel (N_{-1}).

The channel spacing used is 1 Hz. (Based on the preliminary results shown, this probably is not the best channel spacing to look for discriminants in this variable.)

The data used were from target intervals from Reel 9 ping numbers 39, 42, 43, 44, 45, 46, 47. The target intervals were those with peak target outputs--not windows in all doppler channels at the target time. Representative (of noise) windows were chosen from adjacent regions of available data for comparison purposes. Values are plotted for pairs of variables in Figures 55, 56, and 57. Since relatively few points were calculated, density distributions of the individual variables are not shown separately; they can be visualized from the spread of plotted points along one axis. Similarly, the general nature of pairwise joint distributions are obvious from the plotted sample points.

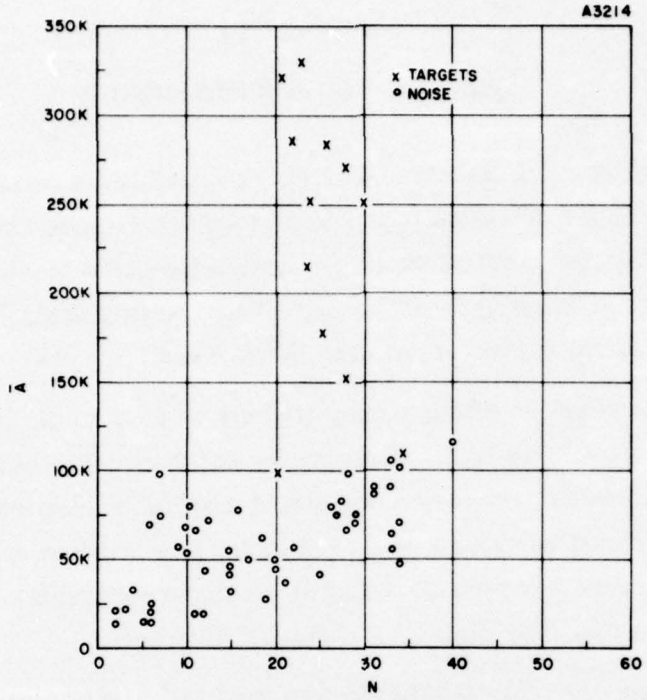

Figure 55. Correlator Average Excess Over Threshold vs. Number of Threshold Crossing

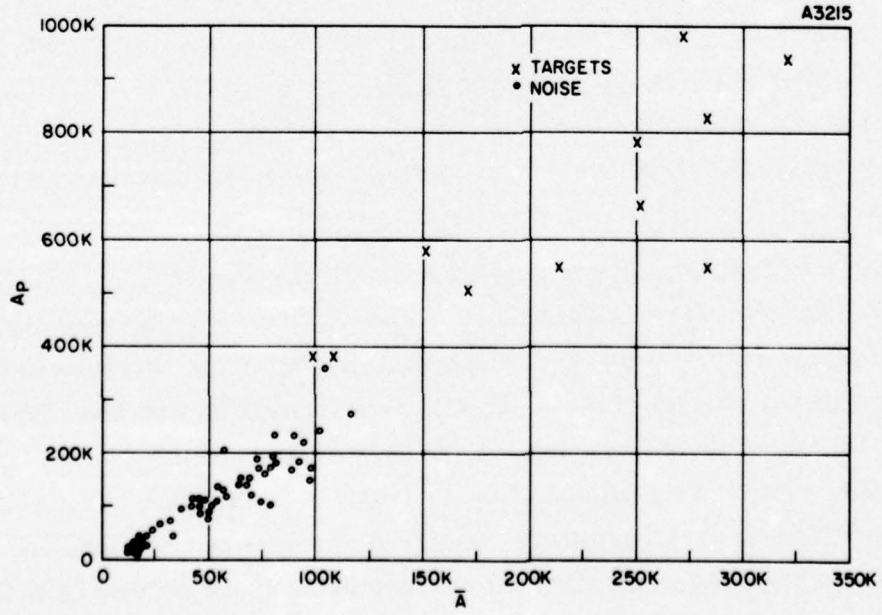

Figure 56. Correlator Peak vs. Average Amplitude Excess Over Threshold

The tendancy of N to decrease with higher $\bar{A}$ in the high $\bar{A}$ region (Figure 55) is an example of the unexpected dependencies which this type of presentation discloses; this particular one, however, may not be of value as a linear discriminant since it does not extend down into the low $\bar{A}$ region. Otherwise, N and $\bar{A}$ are apparently independent for the target data. $\bar{A}$ alone is a very good discriminant for these data. Some improvement could be added by using the discriminating feature that the values of N for target returns are spread over a narrower band than those for noise.

The values of A_p and $\bar{A}$ (Figure 56) are positively correlated for targets and also for noise; there is relatively little discrimination in their dependency characteristics. Either variable alone is a good discriminant; however, A_p is a little better than $\bar{A}$.

The $\bar{A}$ versus $\frac{N}{N_{+1}+N_{-1}}$ values are plotted in Figure 57. Note that the target distribution of $\frac{N}{N_{+1}+N_{-1}}$ is restricted to a relatively narrower band than was the distribution of N.

The distribution of A_p with the other variables is similar to that of $\bar{A}$, for both targets and noise, as might be expected from the strong correlation of A_p and $\bar{A}$ with each other (Figure 56).

Based on the data observed, it appears more promising to look for better discriminants which will hold up in lower SNR conditions than to evaluate any specific detection function based on the available discriminants. Direct evaluation of specific detection functions is complicated by the fact that the distributions of these variables are strongly affected by changes in threshold levels.

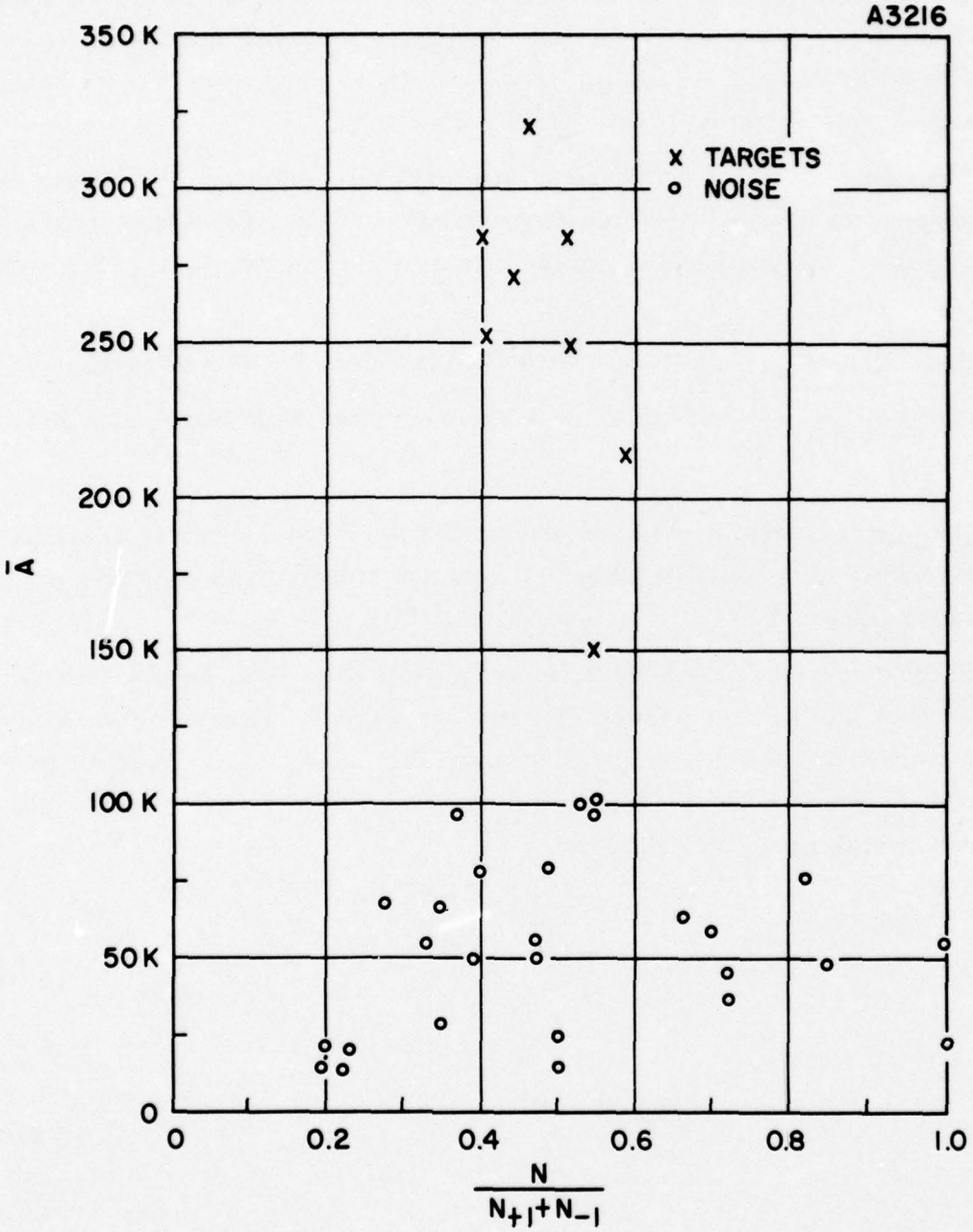

Figure 57. Correlator Average Excess Over Threshold vs. $\frac{N}{N_{+1} + N_{-1}}$

SECTION VII

DISCRIMINANT CHARACTERISTICS

A discriminant is a characteristic which can be used to help detect the difference between data which contain a target (Signal + Noise) and data which do not (Noise). A simplified example of the probability density distribution $P(X_1)$ of a measure (X_1) of such a characteristic is shown in Figure 58 (a), (b), and (c). The density distribution $P(X_2)$ of another discriminant (X_2) whose "S+N" and "N" distribution completely overlap, even in the high SNR case (but which still contains discrimination information), is shown in Figure 58 (d), (e), and (f). The detection thresholds indicated in the sketch for such variables (X_1 and X_2) are particularly easy to apply and, thus, such discriminants, or combinations of them, are the best to use if their performance [probability of detection, P(D), and probability of false alarm, P(FA)], is good enough.

Usually, however, especially in the low SNR cases, better performance is desired. When there is additional discrimination (between S+N and N) information in the joint distribution relationships among the measured variables, it can be used to improve their performance. A simplified example of the joint distribution $P(X_3, X_4)$ of two variables (X_3 and X_4) where positive correlation exists in both the S+N and N distributions is shown in Figure 59 (a). A different display (two-dimensional) of the same distribution is shown in Figure 59 (b), where the areas inside the plane figures include some percentage (say, 95 percent) of their respective distributions; this presentation method is used to eliminate confusion in showing distributions for lower SNR cases. Figure 59 (c) shows a case where the positive correlations between two variables have no discrimination value when the SNR gets very low; the discrimination values of the two individual variables deteriorate in about the same manner. Figure 59 (d) shows a case where the discrimination value of X_4 does not disappear as fast as that of X_3, in which case the joint distribution provides an excellent discriminant even though the two variables are positively correlated for both S+N and N and neither variable, by itself, is a good discriminant. Algebraically, this joint distribution discriminant could be considered as the quantity $(X_4 - X_3)$ whose threshold value lies along the threshold line indicated in Figure 59 (d); values greater than K indicate S+N and values less than K indicate N. The distribution of this quantity is like the one shown in Figure 58 (a).

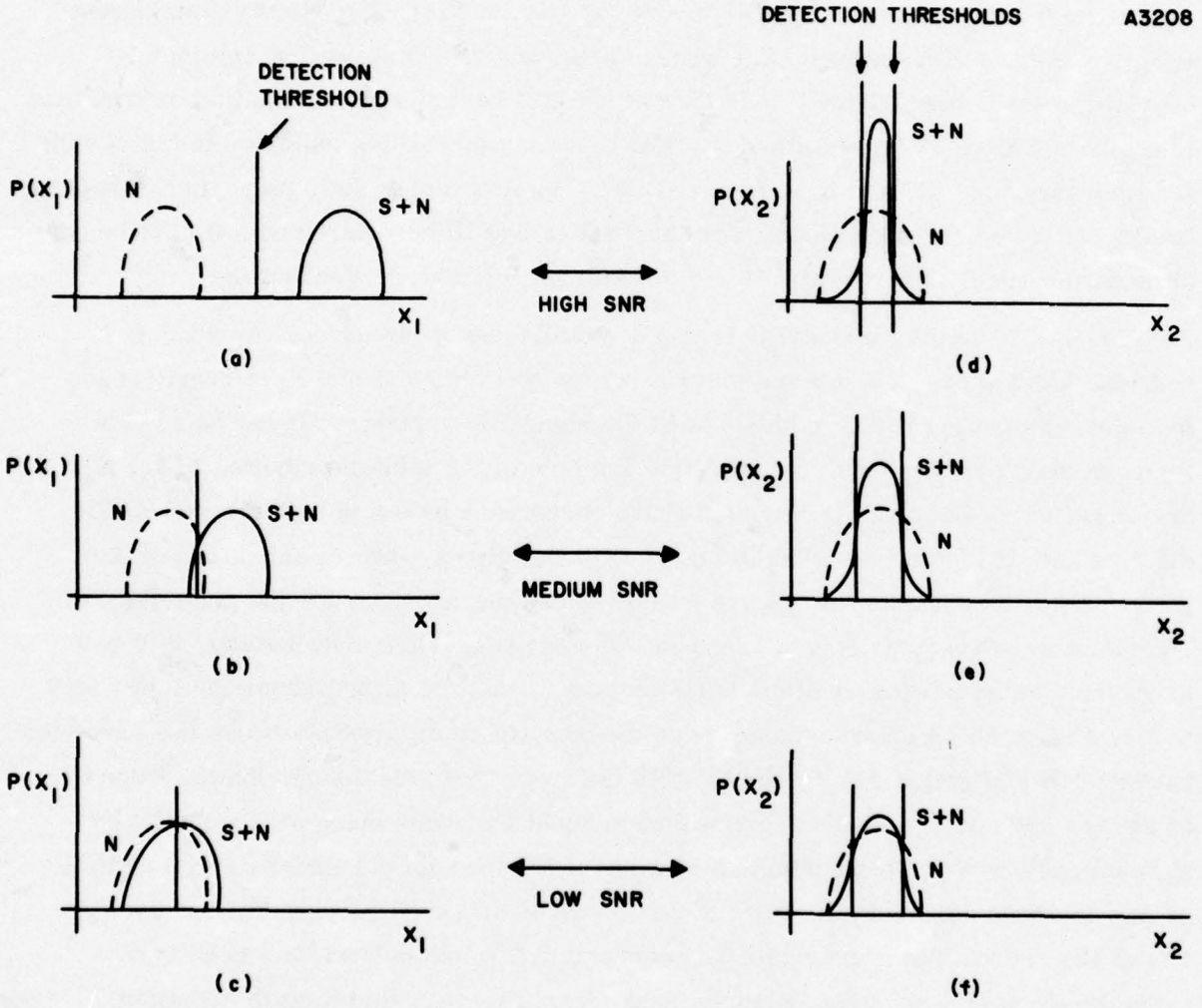

Figure 58. Typical Distributions of Single Variable Discriminants

A similar case where the joint distribution retains discrimination information while that of the individual variables deteriorates with poorer SNR is shown in Figure 60; in this case the two variables are negatively correlated for both S+N and N. Another case is shown in Figure 61, where the two variables are positively correlated for S+N but uncorrelated for N. If the discriminant based on correlation in this example (Figure 61) were considered algebracally $(X_8 - X_7)$, it would have a distribution like that shown in Figure 58 (d). The distributions shown in these sketches are simplified to point out the general characteristics of discrimination information to be searched for; in the practical case these distributions will often be multivariate, nonlinear, and much more difficult to recognize and use. Many of them will be multimodal, which further complicates practical use of the information. Eventually, more complicated detection functions, using n-dimensional space concepts, will probably be required to effectively combine the information in the various discriminants. A premature attempt to use such complicated techniques as a data analysis tool could, however, hide the very cause and effect relationships for which we are looking.

Generally, these distributions will change with time; thus, the measure of any distribution depended upon as a basis for detection must be adaptive. This requirement is one of the reasons for studying the basic statistics of noise and the effects of time varying parameters. Normally, the noise distribution (rather than an expected distribution of S+N) will be the basis for setting threshold levels.

The search for discriminants is based primarily on measuring characteristics which are suspected of varying with known physical causes. A secondary method is the analysis of data taken for the primary method in the hope of discovering unexpected relationships. This includes the time variation of each measured quantity as well as cross-correlation (based on time) and the previously discussed joint distributions. This secondary method is, essentially, an attempt to discover characteristics that would have been measured in the first place if they had been recognized as discriminants.

The value of discriminants for general use will depend upon how well their behavior can be predicted from a given practical situation and how well they hold up as SNR decreases; thus, some discriminants found to be good from some particular set of sea data may not be generally useful if their behavior cannot be accurately predicted for different operating conditions and SNR levels.

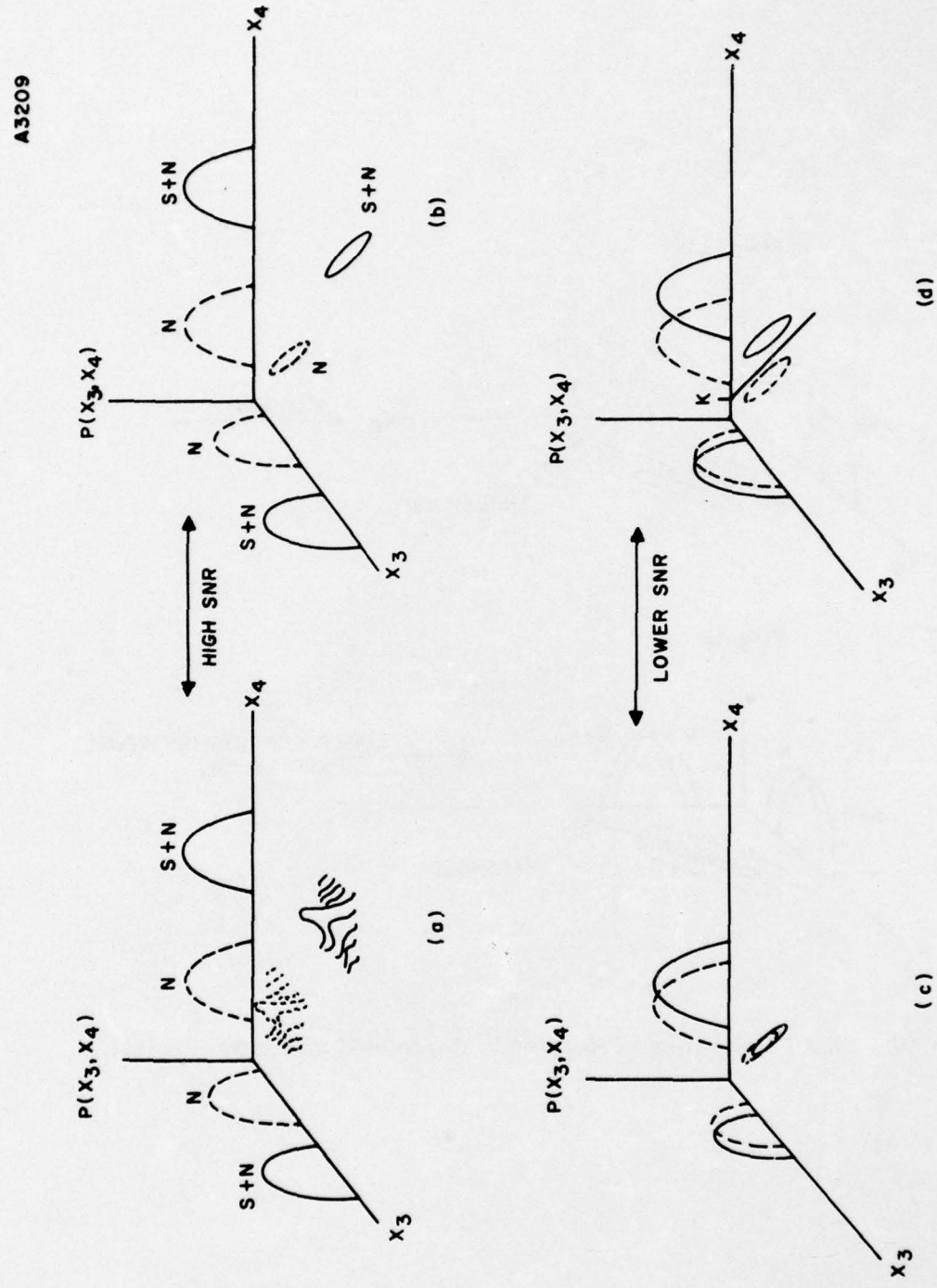

Figure 59. Joint Distribution of Positively Correlated Measured Variables

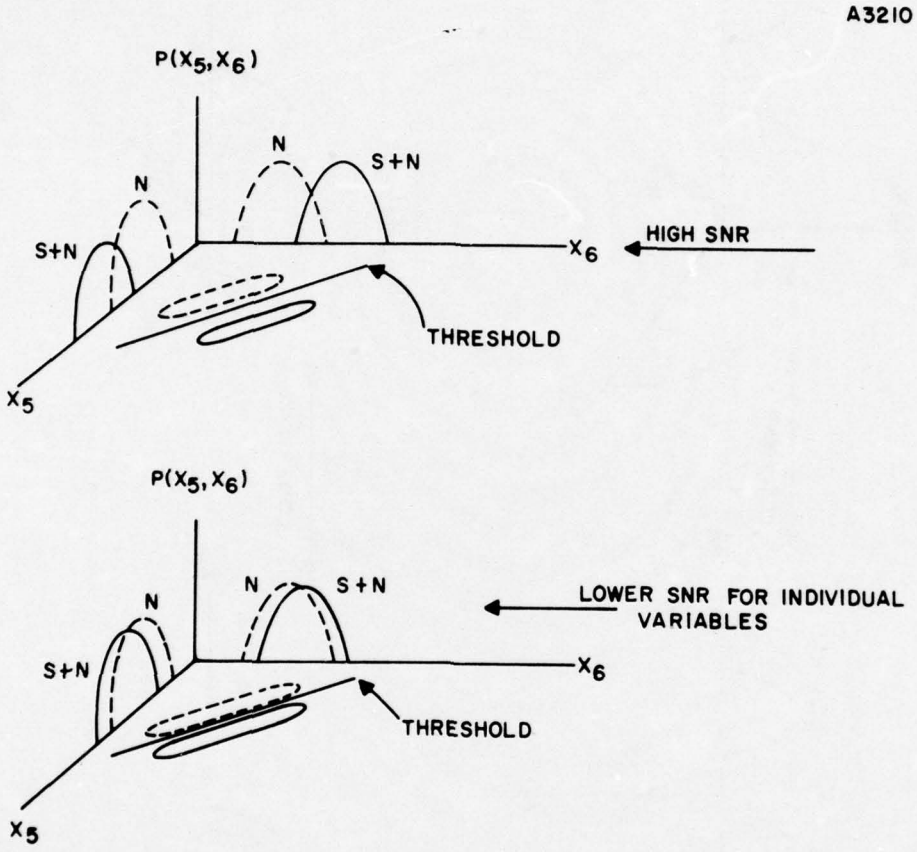

Figure 60. Joint Distribution of Negatively Correlated Measured Variables

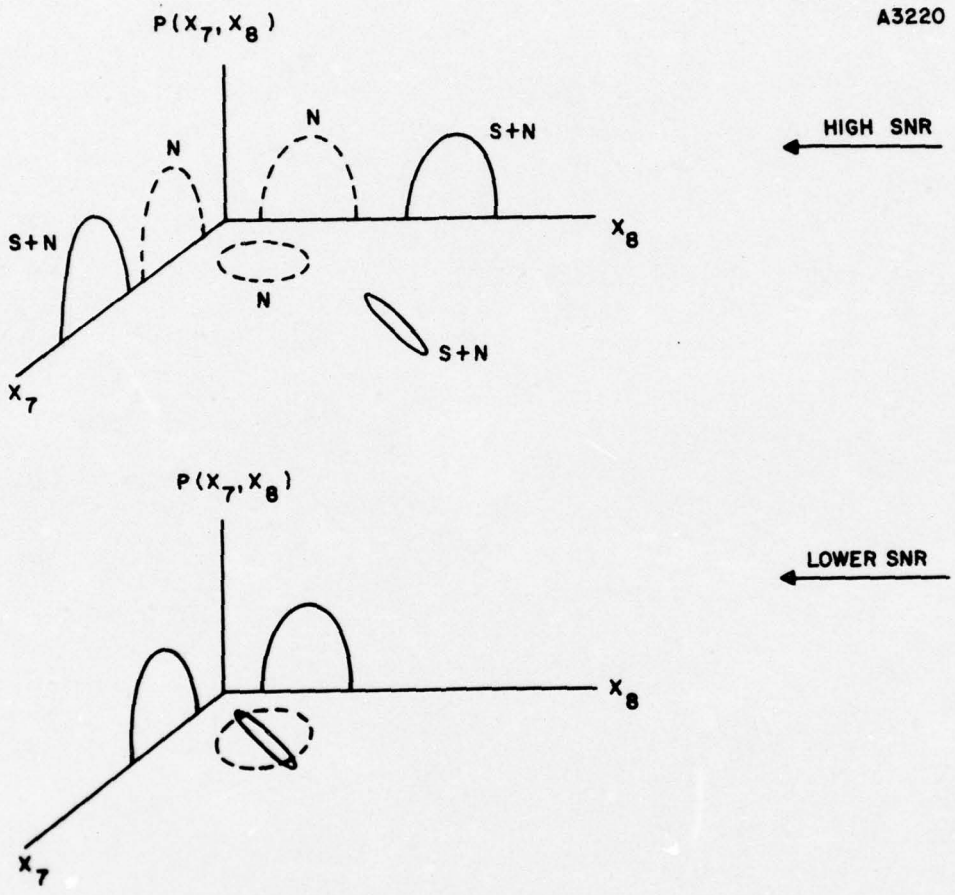

Figure 61. Joint Distribution of Measured Variables with Different Types of Distribution for S + N and N

APPENDIX A

DIGITIZED SONAR DATA, PRFM

Figure	Surface Duct			New Ping Numbers
A-1	Reel 6	12-3-63	34 Pings	1-34
A-2	Reel 9	12-5-63	43 Pings	35-77
	Bottom Bounce			
A-3	Reel 5	1-25-65	28 Pings	78-105
A-4	Reel 6	1-25-65	18 Pings	106-123
A-5	Reel 7	1-26-65	26 Pings	124-149
A-6	Reel 8	1-26-65	21 Pings	150-170
A-7	Reel 9	1-26-65	30 Pings	171-200

These computer-generated plots (see Reference 1 for program) are like the A-scope presentation of the sonar. The ordinate is the energy in a 0.5-second filter. The plots are scaled so that the highest peak is full scale. Although this scaling optimizes the dynamics of the plot, one loses a lot of feel for how conditions vary from ping to ping.

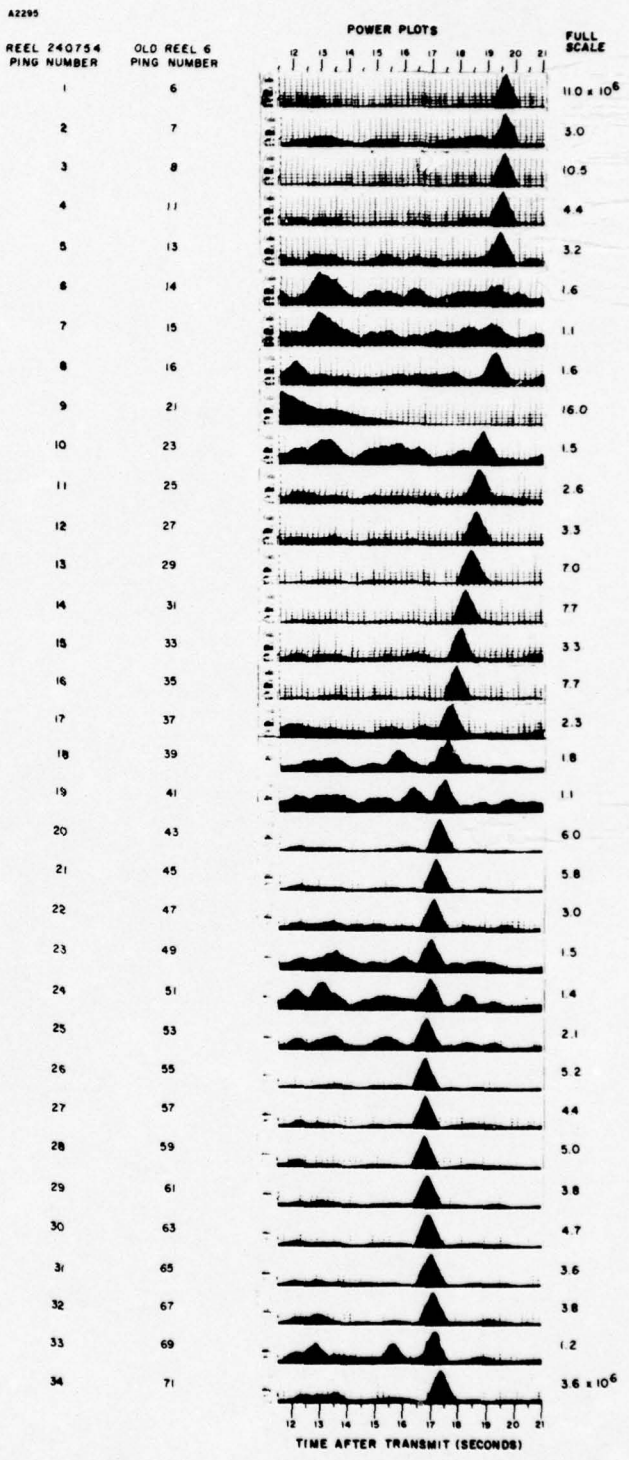

Figure A-1. Power Plots, Pings 1 to 34

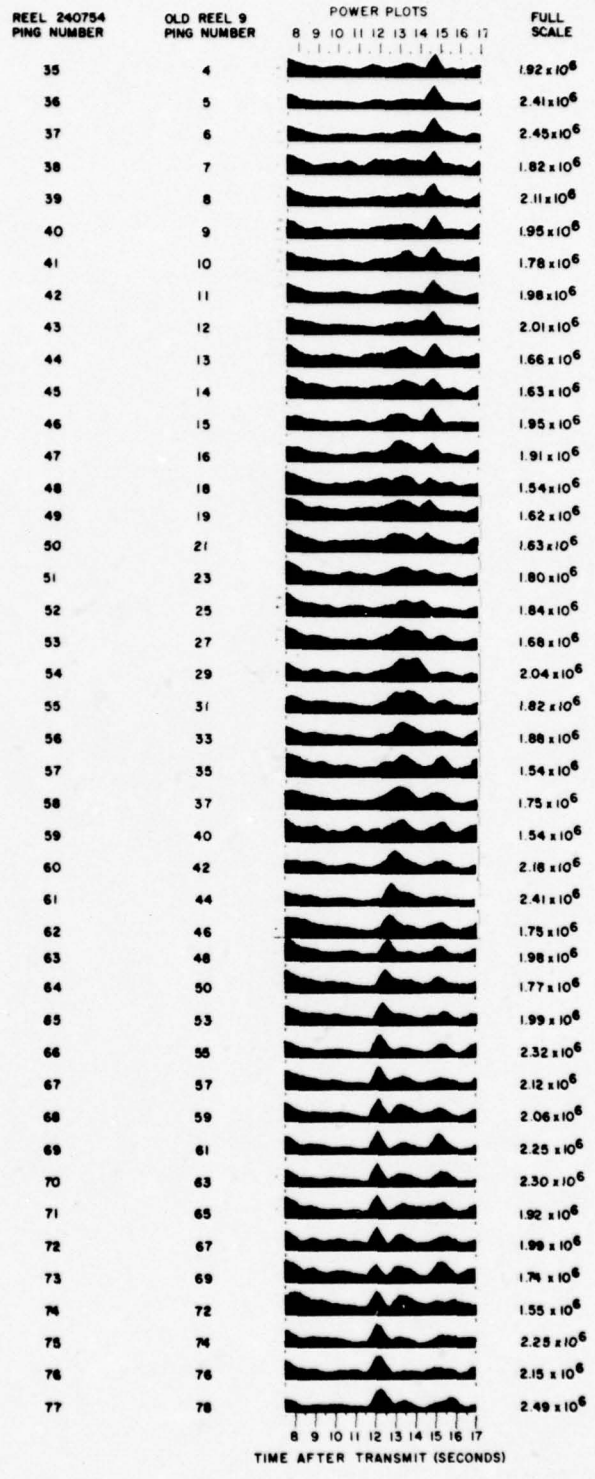

Figure A-2. Power Plots, Pings 35 to 77

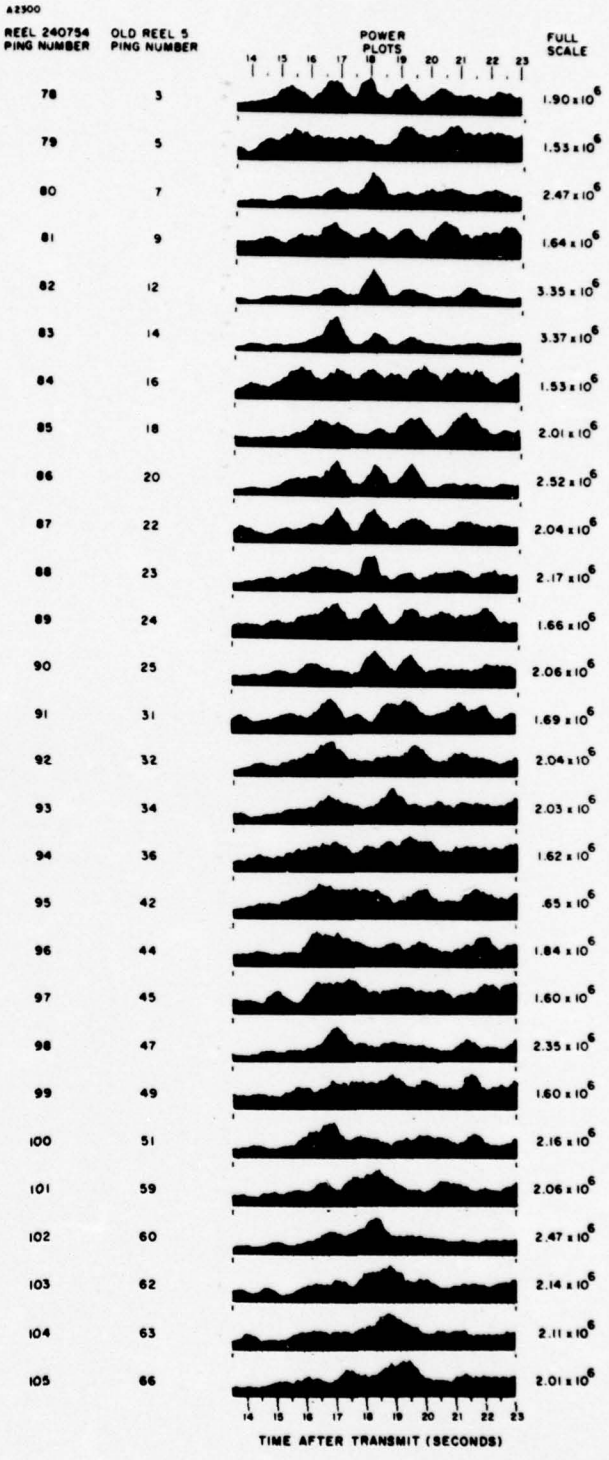

Figure A-3. Power Plots, Pings 78 to 105

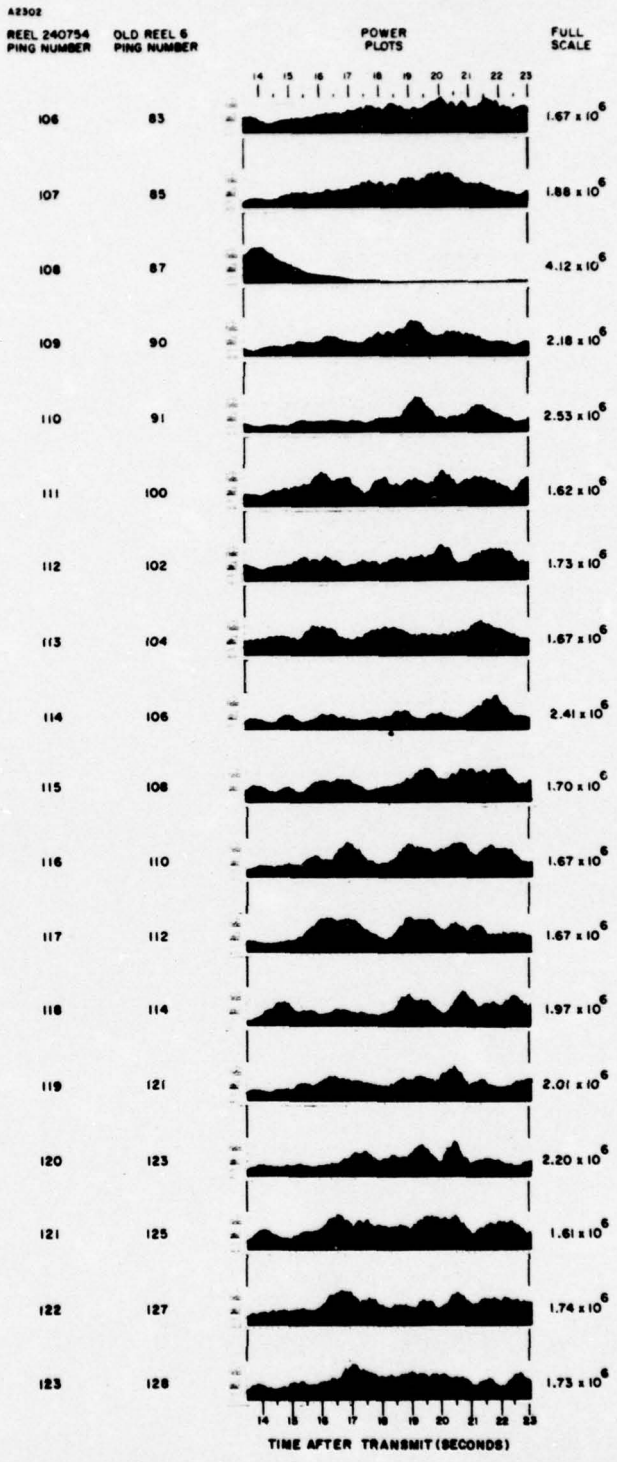

Figure A-4. Power Plots, Pings 106 to 123

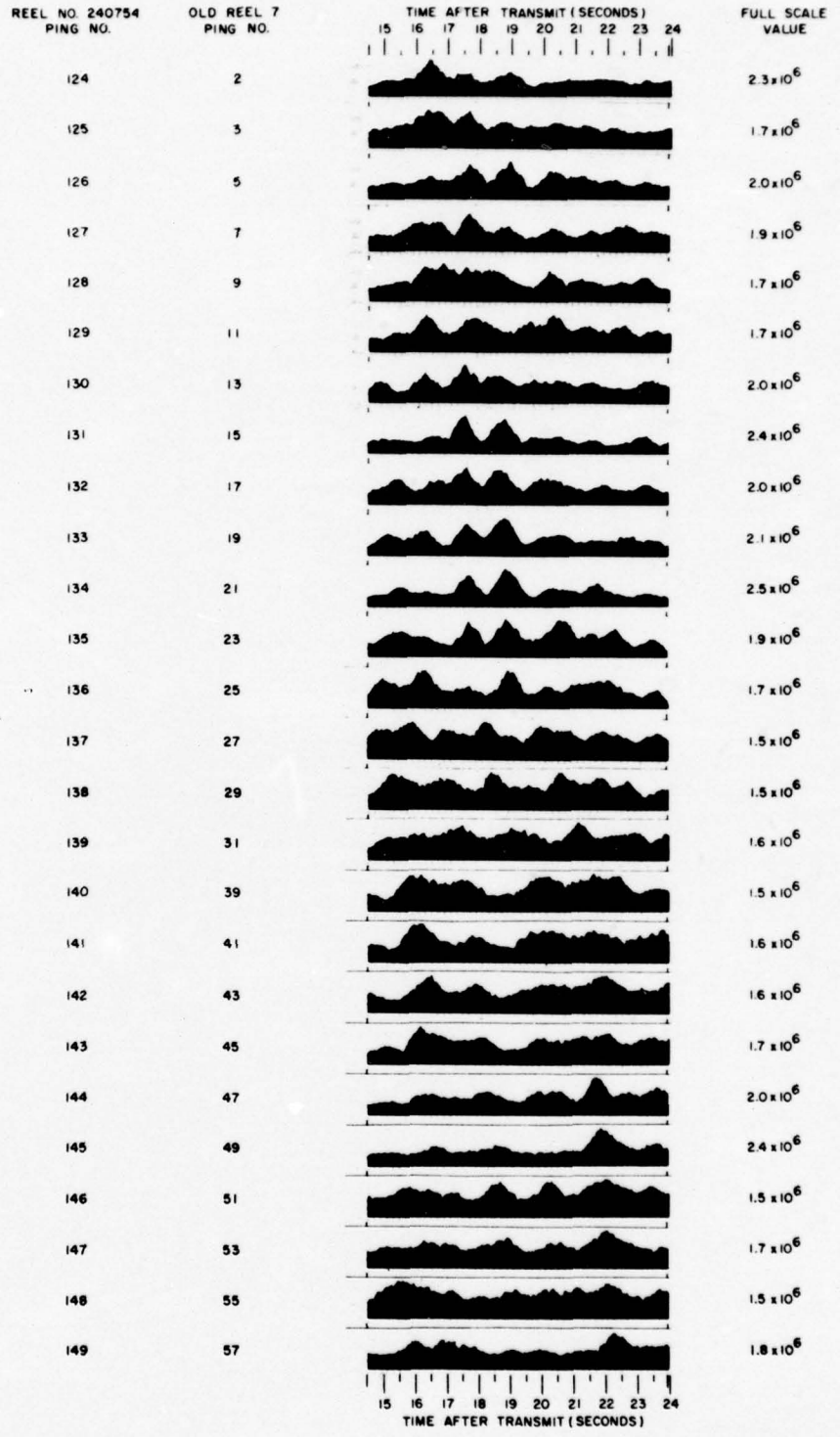

Figure A-5. Power Plots, Pings 124 to 149

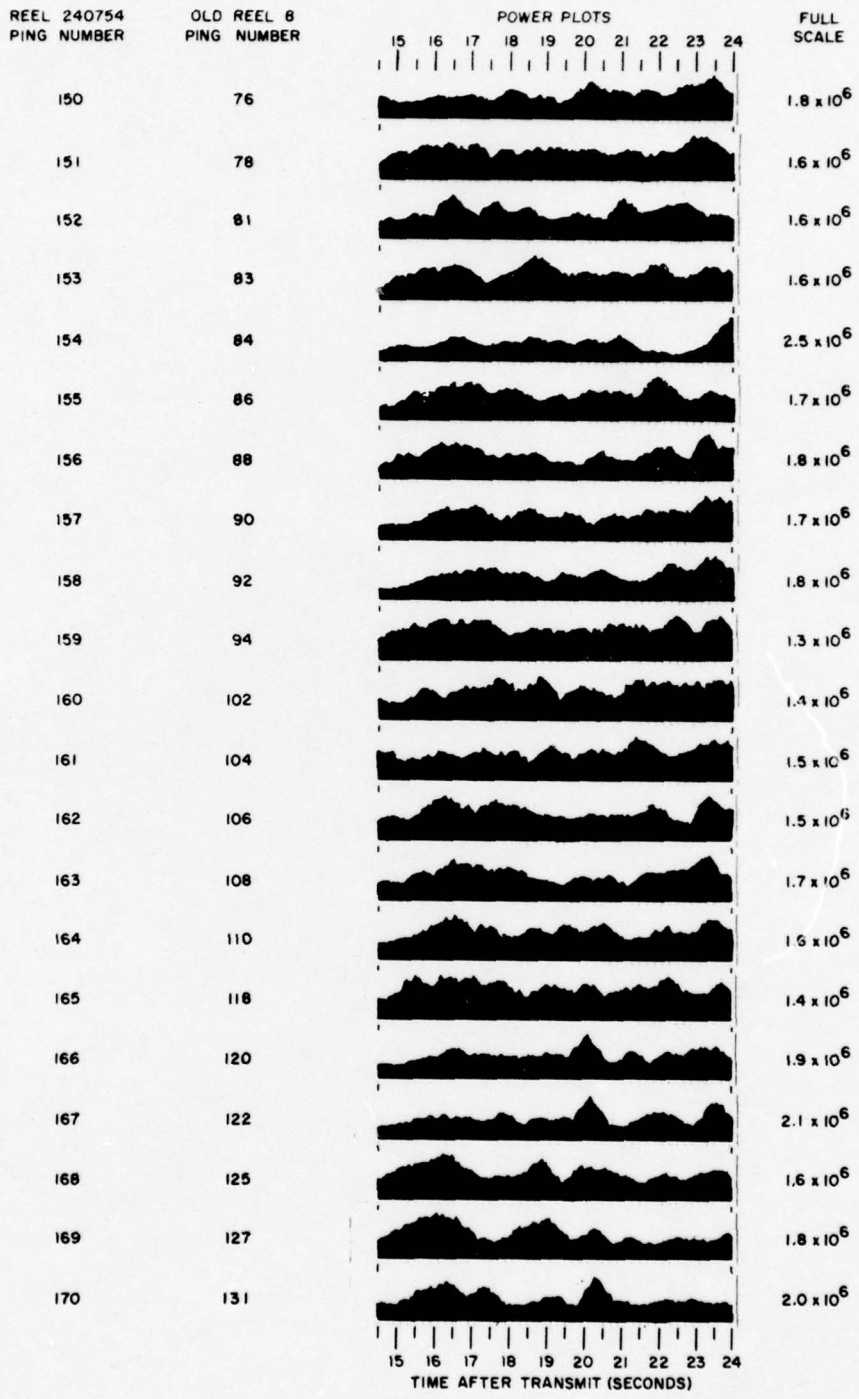

Figure A-6. Power Plots, Pings 150 to 170

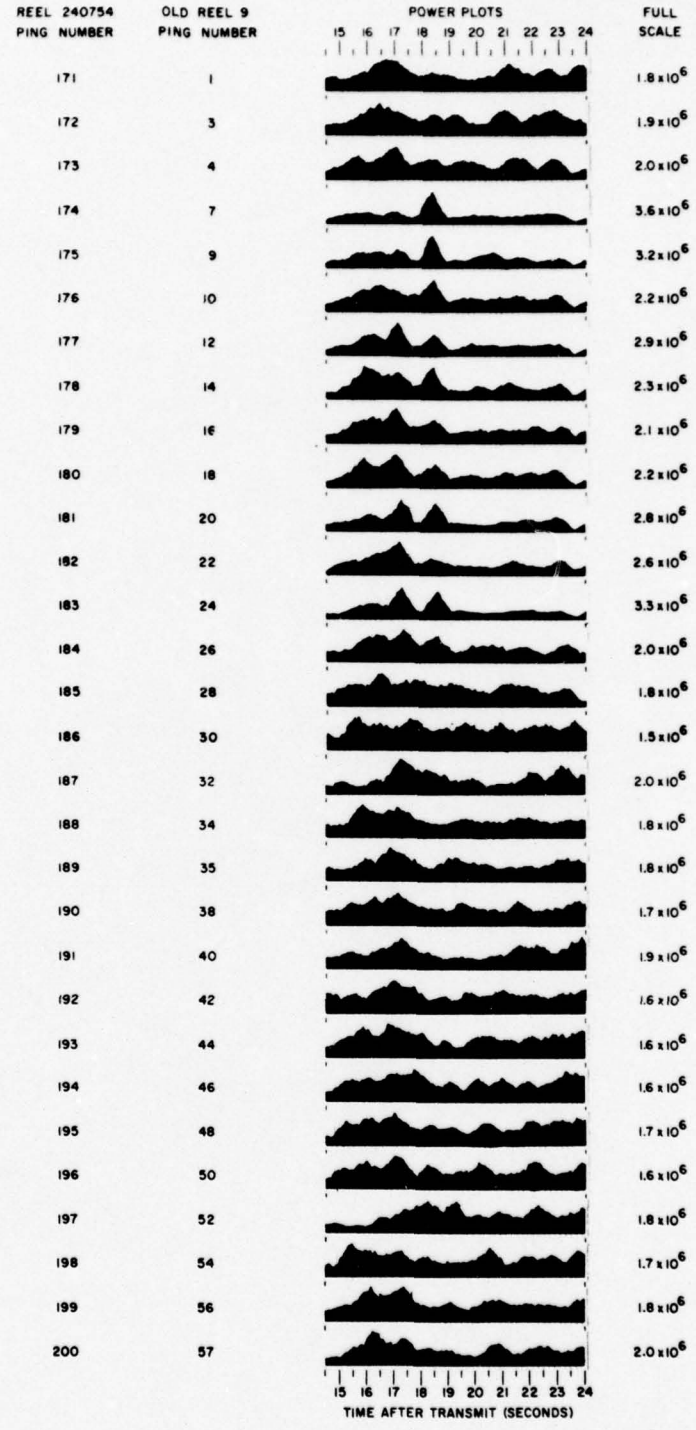

Figure A-7. Power Plots, Pings 171 to 200

APPENDIX B

CATALOG OF PINGS

In order to summarize the information obtained on each ping-time interval-doppler channel combination, a catalog has been prepared (see Section 1 of this appendix). The first three columns of the catalog contain a description of the ping, i.e., the ping number, the time interval, and doppler channel. The following additional information is also included.

Column 4: Mean -- the average value of the sampled correlator outputs for the intervals.

Column 5: S.D. -- the standard deviation.

Column 6: $\sqrt{b_1}$ -- the standardized measure of skewness for the interval.

Column 7: b_2 -- the standardized measure of kurtosis for the interval.

Column 8: (Standard Deviation)/(Mean) -- the ratio of Column 5 to Column 4.

Column 9: Plot -- this column indicates whether a Rayleigh plot was made and into which category it was classified. The codes used are: A - adequate, M - marginal, INH - inadequate high, INL - inadequate low, and INO - inadequate odd.

Column 10: Ray. Slope -- this column gives the slope of the line drawn on the Rayleigh plot corrected for the scaling of the paper; these numbers must be multiplied by 10^4.

Columns 11 and 12: S_B Parameters -- these columns give, respectively, the estimates of δ and λ for the two-parameter S_B distributional fit.

Column 13: Power Plot Target -- this column shows what proportion of the target return (if known) was in the interval as indicated by the power plot.

A listing of information obtained for the x and y component of the correlator output is contained in Section 2 of this appendix. This includes the means, variances, and correlation for x and y and various summary statistics. The following information is contained in each column.

Column 1: Ping number.

Column 2: Identification -- in this analysis a ping was broken into three parts, and statistics were gathered on each subinterval as well as the entire interval. Also, a composite interval of 50 observations comprised of every third

observation from the entire interval was analyzed. This column identifies to which of the sets of data the entries refer.

Column 3: $\bar{y}$ -- the mean of the y component of $z = \sqrt{x^2 + y^2}$ where z is the correlator output.

Column 4: $\bar{x}$ -- the mean of the x component.

Column 5: W_y -- the W statistic for normality for the y component. The 10, 5, and 1 percent values of W are 0.955, 0.947, and 0.930, respectively. Low values nonnormality.

Column 6: W_x -- the W statistic for the x component.

Column 7: V_y -- the variance of the y component.

Column 8: V_x -- the variance of the x component.

Column 9: t_y -- the value of the student t statistic, a test for zero mean, for the y component.

Column 10: t_x -- the value of the t statistic for the x component.

Column 11: r_{xy} -- the coefficient of correlation between x and y.

Column 12: The value of the F statistic -- a test for equality of variances of the x and y components.

1. Catalog of Pings

The section consists of four listings:

Table B-1. Surface Duct, 300 Hz

Table B-2. Bottom Bounce, 300 Hz

Table B-3. Pings with Intervals Smaller Than 150

Table B-4. Up and Down Doppler Channels

TABLE B-1

SURFACE DUCT, Hz

Ping	Time	Channel	(000) Mean	(000) S.D.	$\sqrt{b_1}$	b_2	S.D./ Mean	Plot	(10^4) Ray Slope	2-Par. Fit S_B Param. δ	2-Par. Fit S_B Param. λ	Power Plot Target
1	14.5-16.0	300	78.2	39.2	0.90	4.07	0.501	A	8.4			
	16.0-17.5		54.6	25.2	0.37	2.43	0.462	INL				
2	14.5-16.0		101.6	58.5	0.84	3.64	0.576	M	12.2			
	16.0-17.5		86.3	23.6	0.48	2.82	0.273	A				
3	11.5-13.0		82.5	44.2	0.75	3.50	0.536	M				
	13.0-14.5		89.7	48.4	0.60	2.65	0.539	A				
	14.5-16.0		79.6	48.4	1.47	6.14	0.608	INH	8.85			
	16.0-17.5		69.5	35.7	0.39	2.37	0.514	INL				
	17.5-19.0		90.8	47.8	0.56	3.00	0.526	A				
4	11.5-13.0		126.7	66.1	0.44	2.71	0.482	M				
	13.0-14.5		107.1	77.4	1.90	7.31	0.723	INL				
	14.5-16.0		74.5	41.0	0.74	3.19	0.550	M	8.7			
	16.0-17.5		84.6	41.8	0.43	2.93	0.494	A	9.6			
	17.5-19.0		113.1	67.7	1.17	4.46	0.599	M				
5	11.5-13.0		117.9	73.4	2.50	15.57	0.622	A(2 High)				
	13.0-14.5		105.7	67.9	1.35	5.76	0.642	INH				
	14.5-16.0		109.9	60.1	0.72	3.41	0.547	A	12.66			
	16.0-17.5		103.2	55.5	0.54	3.04	0.538	A	12.06			
	17.5-19.0		104.0	60.5	0.83	3.44	0.582	INH				1/10

CONFIDENTIAL

TABLE B-1 (continued)

Ping	Time	Channel	(000) Mean	(000) S.D.	$\sqrt{b_1}$	b_2	S.D./ Mean	Plot	(10^4) Ray. Slope	2-Par. Fit S_B Param. δ	λ	Power Plot Target
6	14.5-16.0	300	108.5	65.8	1.10	4.20	0.606	INH	11.7			
	16.0-17.5		99.0	55.5	0.71	3.17	0.561	A	11.91			
7	14.5-16.0		100.0	57.0	1.16	5.02	0.570	INH	10.5	1.43	3.45	
	16.0-17.5		98.8	55.6	1.01	4.72	0.563					
8	14.5-16.0		99.3	52.1	0.36	2.69	0.525	A	14.4	1.16	3.13	
	16.0-17.5		110.4	60.1	0.50	2.69	0.544					
9	14.5-16.0		91.4	52.3	1.67	8.92	0.572	A	10.5	1.45	3.70	
	16.0-17.5		46.9	26.6	1.03	4.69	0.567					
10	14.5-16.0		144.1	75.2	0.70	3.09	0.522	A	16.2	1.32	2.72	
	16.0-17.5		102.7	58.4	1.45	6.06	0.569					
11	14.5-16.0		104.5	58.2	0.66	3.23	0.557	M	11.76	1.29	3.20	
	16.0-17.5		99.7	52.0	0.57	3.30	0.522					
12	14.5-16.0		106.8	52.3	0.65	3.49	0.490	A	11.76	1.37	3.34	
	16.0-17.5		91.6	47.0	0.74	3.98	0.513					
13	14.5-16.0		88.1	48.3	0.83	3.96	0.548	A	10.2	1.34	3.54	
	16.0-17.5		83.2	43.7	0.47	2.92	0.525					
14	14.5-16.0		96.1	47.2	0.39	2.89	0.491	INL	11.4	1.41	3.67	
	16.0-17.5		86.7	48.1	0.77	3.46	0.555					
15	14.5-16.0		94.4	56.7	1.23	4.95	0.601	INH	11.73	1.33	3.35	
	16.0-17.5		105.7	58.0	0.85	3.62	0.549					

CONFIDENTIAL

TABLE B-1 (continued)

Ping	Time	Channel	(000) Mean	(000) S.D.	$\sqrt{b_1}$	b_2	S.D./ Mean	Plot	(10^4) Ray. Slope	2 Par. Fit S_B Param. δ	λ	Power Plot Target
16	14.5-16.0	300	89.7	53.3	0.86	3.45	0.594	INH	9.6	1.34	3.50	
	16.0-17.5		88.9	48.9	0.99	4.42	0.550					1/10
17	14.5-16.0		111.3	61.8	1.17	5.16	0.555	INH	11.4	1.55	3.50	
	16.0-17.5		129.5	67.2	0.68	3.46	0.519					1/2
18	14.5-16.0		134.1	77.9	1.03	4.42	0.581	INH	17.7	1.46	2.87	1
	16.0-17.5		139.0	74.9	0.93	3.99	0.539					1/2
19	14.5-16.0		121.5	63.5	0.32	2.24	0.523	INL	14.28	1.25	2.99	
	16.0-17.5		140.5	79.2	0.76	3.55	0.564					2/3
20	14.5-16.0		94.4	48.1	0.53	2.87	0.510	A	10.5	1.50	3.79	
	16.0-17.5		210.7	168.5	1.56	5.07	0.800					3/4
21	14.5-16.0		95.8	50.4	0.90	3.88	0.526	INH	10.5	1.47	3.65	
	16.0-17.5		189.1	141.7	1.44	5.95	0.749					ALL
22	14.5-16.0		122.0	61.9	0.55	2.82	0.507	A	13.5	1.53	3.42	
	16.0-17.5		164.6	120.0	1.15	4.15	0.729					ALL
23	14.5-16.0		107.8	54.3	0.48	2.81	0.504	M	12.21	1.46	3.49	
	16.0-17.5		152.1	97.1	1.14	4.00	0.638					ALL
24	14.5-16.0		124.7	62.3	0.58	2.95	0.500	A	13.5	1.60	3.58	
	16.0-17.5		138.9	79.6	1.51	6.79	0.573					ALL
25	14.5-16.0		124.2	74.6	1.38	6.30	0.601	INH	13.5	1.22	2.72	
	16.0-17.5		157.1	97.4	1.00	3.46	0.620					ALL

CONFIDENTIAL

TABLE B-1 (continued)

Ping	Time	Channel	(000) Mean	(000) S.D.	$\sqrt{b_1}$	b_2	S.D./ Mean	Plot	(10^4) Ray. Slope	2 Par. Fit S_B Param. δ	λ	Power Plot Target
26	14.5-16.0	300	109.8	54.8	0.20	2.57	0.499	INL	14.28	1.37	3.39	
	16.0-17.5		176.9	183.2	4.84	39.49	1.04					ALL
27	14.5-16.0		97.7	56.3	1.04	4.62	0.576	INH	11.49	1.56	4.38	
	16.0-17.5		182.5	154.0	2.16	9.59	0.844					ALL
28	14.5-16.0		90.6	49.1	0.71	3.74	0.542	M	10.29	1.35	3.55	
	16.0-17.5		180.7	142.1	1.44	5.27	0.786					ALL
29	14.5-16.0		96.3	47.6	0.51	2.78	0.494	M	10.5	1.49	3.75	
	16.0-17.5		193.9	124.0	1.01	4.15	0.640					ALL
30	14.5-16.0		94.7	52.8	1.00	4.17	0.558	INH	10.2	1.37	3.44	
	16.0-17.5		204.7	168.0	1.56	5.52	0.821					ALL
31	14.5-16.0		98.9	57.6	0.70	3.05	0.582			1.22	2.72	
	16.0-17.5		190.1	155.5	1.41	5.23	0.818					ALL
32	14.5-16.0		88.3	47.7	0.87	3.73	0.540			1.37	3.39	
	16.0-17.5		183.3	136.7	1.13	3.93	0.746					ALL
33	14.5-16.0		127.1	66.2	1.03	4.79	0.521			1.56	4.38	
	16.0-17.5		149.6	97.5	1.12	4.17	0.652					ALL
34	14.5-16.0		107.8	55.4	0.58	3.13	0.514			1.35	3.55	
	16.0-17.5		138.3	110.8	1.38	4.89	0.801					ALL DAY 1

TABLE B-1 (continued)

Ping	Time	Channel	(000) Mean	(000) S.D.	$\sqrt{b_1}$	b_2	S.D. Mean	Plot	(10^4) Ray. Slope	2 Par. Fit S_B Param. δ	2 Par. Fit S_B Param. λ	Power Plot Target
35	14.5-16.0	300	119.8	90.0	3.50	22.02	0.751			1.49	3.75	ALL
	12.0-13.5		117.8	60.9	0.82	3.57	0.517					DAY 2
36	9.0-10.5		115.5	62.1	0.80	4.37	0.538	A		1.37	3.44	
	12.0-13.5		125.4	64.9	0.57	3.04	0.518					
37	9.0-10.5		106.3	58.4	0.36	2.47	0.549					
	12.0-13.5		122.8	64.1	0.56	2.91	0.522					
38	9.0-10.5		111.4	62.0	0.81	2.83	0.557	INH				
	12.0-13.5		138.0	75.4	0.77	3.40	0.546					
39	9.0-10.5		101.5	51.5	0.68	3.27	0.508					
	12.0-13.5		119.9	54.3	0.39	2.86	0.453					
40	9.0-10.5		111.1	53.6	0.22	2.40	0.482	INL				
	12.0-13.5		124.4	68.8	0.56	2.78	0.553					
41	9.0-10.5		105.7	54.1	0.37	2.48	0.512					
	12.0-13.5		139.8	72.7	0.41	2.63	0.520					
42	9.0-10.5		110.0	55.6	0.65	3.09	0.505	A				
	12.0-13.5		130.5	66.0	0.68	3.30	0.506					
43	9.0-10.5		113.0	55.6	0.45	2.94	0.492					
	12.0-13.5		124.8	63.4	0.64	3.14	0.508					
44	9.0-10.5		109.9	56.8	0.47	2.46	0.517	A				
	12.0-13.5		133.6	68.5	0.51	2.78	0.513					

CONFIDENTIAL

TABLE B-1 (continued)

Ping	Time	Channel	(000) Mean	(000) S.D.	$\sqrt{b_1}$	b_2	S.D./ Mean	Plot	(10^4) Ray. Slope	2 Par. Fit S_B Param. δ	2 Par. Fit S_B Param. λ	Power Plot Target
45	9.0-10.5	300	115.9	57.8	0.70	3.22	0.499					
	12.0-13.5		130.4	67.7	0.62	3.16	0.519					
46	9.0-10.5		108.1	60.5	0.73	3.62	0.560	INH				
	12.0-13.5		146.9	71.8	0.44	2.96	0.489					
47	9.0-10.5		106.4	54.0	0.38	2.60	0.508					
	12.0-13.5		147.0	71.3	0.25	2.33	0.485					
48	9.0-10.5		109.9	55.8	0.39	2.89	0.508	INL				
	12.0-13.5		129.9	74.1	0.92	3.52	0.570					
49	9.0-10.5		115.7	59.3	0.60	2.99	0.513					
	12.0-13.5		137.8	66.6	0.25	2.23	0.483					
50	9.0-10.5		114.4	55.3	0.34	2.63	0.483	INL				
	12.0-13.5		138.7	69.2	0.23	2.66	0.499					
51	9.0-10.5		108.5	51.9	0.38	3.00	0.478					
	12.0-13.5		131.0	69.3	0.69	3.08	0.529					
52	9.0-10.5		112.7	62.8	0.79	3.48	0.557	M				
	12.0-13.5		134.8	70.8	0.48	2.61	0.525					1/10
53	9.0-10.5		109.8	54.7	0.50	2.96	0.498					
	12.0-13.5		127.7	68.2	0.66	3.17	0.534					1/10
54	9.0-10.5		114.1	59.3	0.65	2.96	0.520	A				
	12.0-13.5		129.3	74.7	0.69	3.01	0.578					1/4

TABLE B-1 (continued)

Ping	Time	Channel	(000) Mean	(000) S.D.	$\sqrt{b_1}$	b_2	S.D./ Mean	Plot	(10^4) Ray. Slope	2 Par. Fit S_B Param. δ	2 Par. Fit S_B Param. λ	Power Plot Target
55	9.0-10.5	300	123.5	60.6	0.30	2.59	0.491					
	12.0-13.5		142.2	84.5	1.40	6.77	0.594					1/2
56	9.0-10.5		106.5	61.4	0.83	3.18	0.577	INH				
	12.0-13.5		141.5	75.8	0.44	2.76	0.536					3/4
57	9.0-10.5		111.0	57.1	0.68	3.19	0.514					
	12.0-13.5		127.9	64.0	0.89	3.49	0.500					3/4
58	9.0-10.5		106.0	60.6	0.87	3.86	0.572	INH				
	12.0-13.5		148.7	79.9	0.38	2.46	0.537					ALL
59	9.0-10.5		106.0	57.3	0.83	4.23	0.541					
	12.0-13.5		129.8	70.5	0.94	4.33	0.543					ALL
60	9.0-10.5		108.7	56.4	0.98	4.73	0.519	INH				
	12.0-13.5		150.2	86.7	0.54	2.53	0.577					ALL
61	9.0-10.5		100.5	53.3	0.47	2.43	0.530					
	12.0-13.5		142.0	73.8	0.20	2.13	0.520					ALL
62	9.0-10.5		120.5	57.5	0.42	2.91	0.477	INL				
63	9.0-10.5		108.9	52.2	0.41	2.87	0.479					
64	9.0-10.5		118.5	53.6	0.33	2.24	0.452	INL				
65	9.0-10.5		111.2	53.3	0.67	3.03	0.479					
66	9.0-10.5		113.1	52.4	0.41	2.46	0.463	INL				

CONFIDENTIAL

TABLE B-1 (concluded)

Ping	Time	Channel	(000) Mean	(000) S.D.	$\sqrt{b_1}$	b_2	S.D./ Mean	(10^4) Ray. Slope	Plot	2 Par. Fit S_B Param. δ	2 Par. Fit S_B Param. λ	Power Plot Target
67	9.0-10.5	300	115.3	67.5	0.96	4.05	0.585					
68	9.0-10.5		112.0	59.3	0.74	3.66	0.529	M				
69	9.0-10.5		109.1	62.6	0.41	2.41	0.574					
70	9.0-10.5		110.7	58.1	0.43	2.78	0.525	A				
71	9.0-10.5		111.4	57.1	0.76	3.22	0.513					
72	9.0-10.5		121.1	64.0	0.42	2.58	0.528	A				
73	9.0-10.5		103.6	47.6	0.39	3.52	0.459					
74	9.0-10.5		110.0	56.7	0.64	3.50	0.515					
75	9.0-10.5		123.6	63.7	0.58	3.13	0.515					
76	9.0-10.5		107.3	57.8	0.54	2.63	0.539					
77	9.0-10.5		107.9	61.5	0.97	3.77	0.570					

TABLE B-2

BOTTOM BOUNCE, 300 Hz

Ping	Time	Channel	Mean	S.D.	$\sqrt{b_1}$	b_2	S.D./ Mean	Plot	10^4 Ray. Slope
78	14.5 to 16.0	300	131.2	73.8	1.01	4.19	0.563		
79			120.2	68.7	0.73	3.08	0.572		
80			97.3	55.2	0.86	3.63	0.567		
81			105.2	48.4	0.24	2.72	0.460		
82			94.0	48.4	0.44	2.64	0.515		
83			95.8	51.2	0.39	2.55	0.534		
84			103.9	58.7	1.28	6.0	0.565		
85			91.2	47.8	0.68	3.24	0.524		
86	13.5 to 15.0	300	74.5	36.2	0.63	3.64	0.486	A	7.8
87			98.5	49.0	0.57	3.47	0.497		
88			94.3	47.6	0.83	3.52	0.505	M	10.29
89			98.5	49.6	0.51	3.69	0.504		
90			93.3	49.6	0.51	3.69	0.532	INL	9.99
91			94.4	50.4	0.54	2.76	0.534		
92			91.7	48.7	1.09	5.52	0.531	A	10.2
93			83.3	46.6	0.54	2.50	0.559		
94			87.8	47.2	0.50	2.88	0.538	A	10.2
95			94.6	43.6	0.43	3.22	0.461		
96			93.9	48.5	0.89	4.07	0.517	INH	10.2
97			91.0	48.8	0.58	2.77	0.536		
98			86.5	48.0	0.69	2.92	0.555	A	10.11
99			86.3	43.8	0.57	3.65	0.508		
100			90.7	52.6	0.74	3.01	0.580	INO	10.2
101			93.4	43.3	0.51	2.83	0.464		
102			86.1	46.7	0.80	3.66	0.542	A	10.5
103			82.3	46.7	0.62	2.98	0.567		
104			90.6	45.5	0.57	3.20	0.502	A	9.69
105			77.2	37.2	0.56	2.76	0.482		
106			81.8	42.8	0.52	2.65	0.523	M	8.73

TABLE B-2 (continued)

Ping	Time	Channel	Mean	S.D.	$\sqrt{b_1}$	b_2	S.D./ Mean	Plot	10^4 Ray. Slope
107	14.5 to 16.0	300	74.1	38.7	0.54	2.74	0.522		
108			208.8	114.3	0.77	3.32	0.547	INH	22.41
109			77.2	37.9	0.58	2.78	0.491		
110			76.4	38.0	0.37	2.67	0.497	A	7.5
111			93.0	44.5	0.49	2.64	0.478		
112			87.5	45.0	0.75	3.85	0.514	A	9.9
113			95.2	48.6	0.85	4.10	0.511		
114			96.8	51.1	0.73	3.79	0.528	A	11.10
115			85.4	47.9	0.62	3.40	0.561		
116			77.3	35.0	0.58	3.36	0.453	M	7.74
117			72.8	39.2	0.63	3.36	0.538		
118			98.0	59.1	0.81	3.15	0.603	INH	10.98
119			82.6	44.5	1.00	4.04	0.539		
120			96.5	48.1	0.59	3.31	0.498	INL	11.4
121			91.8	47.2	0.61	3.14	0.514		
122			84.9	45.4	0.63	2.62	0.535	INL	8.76
123			99.4	53.7	0.61	3.24	0.540		
124			118.2	63.8	0.79	3.80	0.540	A	13.56
125			119.9	64.2	0.49	3.09	0.535		
126			106.9	54.3	0.67	3.49	0.508		
127			116.0	58.3	0.48	2.72	0.503	A	12.99
128			110.9	55.5	0.29	2.22	0.500		
129			105.7	55.3	0.51	2.65	0.523		
130			106.6	58.5	0.72	3.25	0.549	A	12.99
131			110.6	56.4	0.47	2.59	0.510		
132			119.6	64.9	0.79	3.60	0.543		
133			101.8	60.1	0.68	3.23	0.590	A	12.99
134			114.2	62.2	0.42	2.69	0.545		
135			120.8	72.6	0.84	3.20	0.601		
136			135.7	63.8	0.58	4.40	0.470	IND	15.8
137			134.4	74.2	0.43	2.58	0.552		

TABLE B-2 (continued)

Ping	Time	Channel	Mean	S.D.	$\sqrt{b}_1$	b_2	S.D./ Mean	Plot	10^4 Ray. Slope
138	14.5 to 16.0	300	124.0	62.5	0.77	3.42	0.504		
139			115.5	66.2	0.48	2.66	0.573	A	14.10
140			105.3	64.8	1.30	5.26	0.615		
141			107.2	62.7	0.99	3.96	0.585		
142			95.9	49.1	0.46	2.92	0.512	INL	10.50
143			105.9	50.6	0.66	2.94	0.478		
144			95.1	49.8	0.69	3.72	0.524		
145			112.6	57.9	0.45	2.79	0.514	A	12.45
146			111.9	60.7	0.76	3.25	0.542		
147			111.1	57.1	0.65	2.93	0.514		
148			137.3	63.1	0.61	3.52	0.460	INL	16.11
149			107.0	55.7	0.57	2.98	0.521		
150			98.7	48.9	0.54	3.21	0.495		
151			118.7	60.9	0.53	3.08	0.513	INL	13.95
152			114.1	54.8	0.49	2.76	0.480		
153			103.8	56.7	0.67	2.68	0.546		
154			108.9	46.7	0.16	2.54	0.429	INO	10.71
155			108.6	59.3	0.54	2.82	0.546		
156			104.2	60.3	1.25	5.92	0.579		
157			100.0	51.8	0.63	2.69	0.518	A	11.34
158			94.9	49.8	0.54	3.01	0.525		
159			107.2	52.9	0.61	3.15	0.493		
160			92.7	46.2	0.47	2.91	0.498	INL	10.5
161			108.8	54.5	0.61	3.05	0.501		
162			100.6	56.9	0.55	2.52	0.566		
163			107.8	56.8	0.58	2.86	0.527	A	10.26
164			101.6	50.9	0.54	2.77	0.501		
165			122.9	70.4	0.92	3.97	0.573		
166			88.4	47.3	0.82	3.24	0.535	A	10.29
167			98.8	57.0	0.64	3.03	0.577		
168			133.1	72.5	0.46	2.64	0.545		
169			130.9	78.8	0.97	4.23	0.602	M	15.51

TABLE B-2 (concluded)

Ping	Time	Channel	Mean	S.D.	$\sqrt{b_1}$	b_2	S.D./ Mean	Plot	10^4 Ray. Slope
170	14.5 to 16.0	300	118.1	64.4	0.76	3.62	0.545		
171			103.2	53.8	0.63	3.17	0.521		
172			103.5	60.5	1.09	4.42	0.585	INH	12.42
173			125.0	75.2	0.84	3.50	0.602		
174			108.7	61.7	1.03	5.30	0.568		
175			114.4	54.7	0.39	2.33	0.478	INL	12.30
176			117.7	62.8	0.70	3.37	0.534		
177			119.7	64.8	0.81	3.81	0.541		
178			118.3	76.6	1.20	4.57	0.648	INH	12.69
179			115.3	66.9	2.05	10.54	0.580		
180			118.8	70.9	1.42	6.52	0.597		
181			111.3	69.9	0.91	4.22	0.628	A	12.96
182			118.8	64.8	0.68	2.89	0.545		
183			106.9	60.7	0.69	3.37	0.568		
184			114.1	66.5	0.93	4.03	0.583	M	14.31
185			118.2	65.9	0.97	4.18	0.558		
186			114.5	68.8	1.05	3.78	0.601		
187			86.1	47.4	0.70	3.59	0.551	A	10.44
188			120.6	63.2	0.53	2.82	0.524		
189			111.1	54.6	0.82	4.34	0.491		
190			120.8	58.8	0.62	2.93	0.487	A	10.26
191			104.7	55.4	0.91	3.57	0.529		
192			108.7	58.4	0.75	3.42	0.537		
193			112.2	59.9	0.73	3.81	0.534	A	12.81
194			104.6	59.5	0.69	2.85	0.569		
195			123.2	71.7	0.54	2.99	0.582		
196			121.7	75.0	0.90	3.43	0.616	M	15.0
197			73.7	42.6	0.71	3.06	0.578		
198			126.2	73.4	0.95	3.82	0.582		
199			109.5	55.2	0.56	2.93	0.504	A	11.97
200			104.2	58.6	0.85	3.78	0.562		

TABLE B-3

PINGS WITH INTERVALS SMALLER THAN 150

Ping	Time	Channel	Mean	S.D.	b_1	b_2	S.D./ Mean	Plot
3	11.5-12.0	300	74.4	38.9	0.94	4.87	0.523	A(2 High)
	12.0-12.5		74.4	37.8	0.86	3.75	0.508	A(1 High)
	12.5-13.0		98.6	50.2	0.30	2.65	0.509	A
	13.0-13.5		91.2	49.5	0.84	2.84	0.543	A
	13.5-14.0		107.7	50.7	0.12	2.21	0.471	M
	14.0-14.5		70.3	36.2	0.33	1.92	0.515	INO
	14.5-15.0		80.3	41.6	0.49	2.81	0.518	A
	15.0-15.5		96.8	62.7	1.15	4.06	0.648	INH
	15.5-16.0		61.5	27.1	0.64	3.81	0.441	INO
	16.0-16.5		75.6	39.0	0.55	2.20	0.516	INH
	16.5-17.0		58.8	34.2	0.29	2.07	0.582	A
	17.0-17.5		74.1	30.8	0.23	2.07	0.416	A
	17.5-18.0		91.3	40.5	-0.01	3.05	0.444	INO
	18.0-18.5		79.3	43.01	0.47	2.45	0.542	A
	18.5-19.0		101.8	55.8	0.60	2.44	0.548	A
	11.5-12.0	300	123.1	66.1	0.64	2.55	0.537	A
	12.0-12.5		121.9	63.3	0.64	3.17	0.519	A
	12.5-13.0		135.0	52.2	0.04	2.37	0.387	INL
	13.0-13.5		159.3	100.8	0.08	3.38	0.633	INH
	13.5-14.0		91.9	44.0	1.15	5.57	0.479	INO
	14.0-14.5		70.0	39.3	0.40	2.25	0.561	A
	14.5-15.0		60.3	34.3	0.49	2.31	0.569	A
	15.0-15.5		83.4	43.4	0.73	2.81	0.520	A
	15.5-16.0		79.9	40.8	0.73	3.28	0.511	INH
	16.0-16.5		89.5	40.2	0.22	2.97	0.449	INO
	16.5-17.0		86.7	48.8	0.48	2.53	0.563	A
	17.0-17.5		77.6	34.1	0.22	2.59	0.439	A
	17.5-18.0		91.0	46.7	0.84	3.73	0.513	A
	18.0-18.5		123.4	80.2	1.26	4.37	0.650	INH
	18.5-19.0		124.9	66.3	0.52	2.16	0.531	INO

TABLE B-3 (continued)

Ping	Time	Channel	Mean	S.D.	b_1	b_2	S.D./ Mean	Plot
5	11.5-12.0	300	121.9	47.9	0.20	2.34	0.393	A
	12.0-12.5		82.8	49.9	0.68	2.59	0.603	A
	12.5-13.0		149.1	95.7	2.56	11.75	0.642	INH
	13.0-13.5		144.2	82.8	0.95	4.04	0.574	INH
	13.5-14.0		92.7	50.6	0.78	2.98	0.546	INH
	14.0-14.5		80.3	46.0	0.61	2.81	0.573	A
	14.5-15.0		102.2	53.9	0.44	2.79	0.527	A
	15.0-15.5		129.6	72.2	0.56	2.55	0.557	A
	15.5-16.0		97.9	46.2	0.21	2.71	0.472	M
	16.0-16.5		88.0	50.5	0.79	3.12	0.574	A
	16.5-17.0		92.2	55.5	1.29	5.74	0.602	INO
	17.0-17.5		131.9	64.5	0.35	2.47	0.489	A
	17.5-18.0		105.4	55.8	0.38	2.23	0.529	A
	18.0-18.5		114.4	57.5	0.42	3.76	0.503	INH
	18.5-19.0		89.9	50.2	0.80	3.11	0.558	A
78	13.5-14.0	291	79.4	38.2	0.56	3.02	0.481	INO
	14.0-14.5		92.3	45.4	0.20	2.21	0.492	INL
	14.5-15.0		91.6	49.1	0.42	2.52	0.536	A
	15.0-15.5		136.0	71.7	0.51	2.69	0.527	A
	15.5-16.0		108.7	50.1	0.54	3.09	0.461	A
	16.0-16.5		108.7	50.7	0.08	2.36	0.466	INL
	16.5-17.0		136.5	77.9	1.01	3.62	0.571	INH
	17.0-17.5		125.9	58.0	0.50	2.60	0.461	A
	17.5-18.0		145.1	64.3	0.06	2.26	0.443	INL
	18.0-18.5		110.6	61.9	0.63	2.66	0.560	A
	18.5-19.0		95.8	55.0	0.68	2.51	0.574	INH
	19.0-19.5		138.6	74.6	0.09	2.49	0.538	INL
	19.5-20.0		95.4	48.3	1.01	4.17	0.506	INH
	20.0-20.5		174.6	83.8	0.35	2.74	0.480	A
	20.5-21.0		115.4	70.6	0.77	2.99	0.612	A
	21.0-21.5		109.7	51.7	0.45	3.19	0.471	INO

TABLE B-3 (continued)

Ping	Time	Channel	Mean	S.D.	b_1	b_2	S.D. / Mean	Plot
78	21.5-22.0	291	88.6	46.6	0.14	1.95	0.526	INL
	22.0-22.5		120.2	53.8	0.06	2.09	0.448	INL
78	13.5-14.0	301	82.5	45.4	0.55	2.60	0.550	A
	14.0-14.5		104.3	45.9	0.26	2.42	0.440	INL
	14.5-15.0		121.8	63.9	0.51	2.65	0.525	A
	15.0-15.5		152.9	83.9	0.69	3.07	0.549	A
	15.5-16.0		121.9	77.5	0.90	3.06	0.636	INH
	16.0-16.5		112.6	57.9	1.04	4.42	0.514	INH
	16.5-17.0		163.5	77.6	0.04	1.90	0.475	INL
	17.0-17.5		130.2	66.6	0.20	2.47	0.512	A
	17.5-18.0		194.0	114.6	2.26	10.27	0.591	INH
	18.0-18.5		97.0	55.6	0.66	3.19	0.573	A
	18.5-19.0		118.6	59.6	0.01	1.88	0.503	INL
	19.0-19.5		151.5	93.0	2.72	14.68	0.614	A(1 High)
	19.5-20.0		99.5	60.8	1.21	5.89	0.611	A(1 High)
	20.0-20.5		138.2	69.3	0.50	2.42	0.501	A
	20.5-21.0		155.2	77.6	0.48	2.31	0.5	A
	21.0-21.5		127.4	60.1	0.16	2.17	0.472	A
	21.5-22.0		82.3	44.6	0.76	3.12	0.542	A
	22.0-22.5		129.3	58.5	0.37	3.03	0.452	A
3	11.5-12.5	300	74.4	38.4	0.90	4.35	0.516	A (2 ODD)
	12.5-13.5		99.9	50.0	0.56	2.67	0.501	A
	13.5-14.5		89.0	47.8	0.47	2.50	0.537	INO
	14.5-15.5		88.6	53.8	1.20	4.87	0.607	INH
	15.5-16.5		68.5	34.3	0.77	3.03	0.501	INO
	16.5-17.5		66.4	33.5	0.18	2.12	0.505	INL
	17.5-18.5		85.3	42.2	0.22	2.59	0.495	INL
4	11.5-12.5	300	122.5	64.8	0.64	2.84	0.529	A
	12.5-13.5		147.2	81.2	1.28	4.98	0.552	INH
	13.5-14.5		81.0	43.2	0.84	4.63	0.533	A (2 High)

TABLE B-3 (continued)

Ping	Time	Channel	Mean	S.D.	b_1	b_2	S.D./ Mean	Plot
4	14.5-15.5	300	71.8	40.8	0.77	3.16	0.568	INH
	15.5-16.5		84.7	40.8	0.47	3.01	0.482	INO
	16.5-17.5		82.2	42.4	0.54	2.98	0.516	A
	17.5-18.5		107.2	67.6	1.53	5.95	0.631	INH
5	11.5-12.5	300	102.4	52.7	0.33	2.26	0.515	INL
	12.5-13.5		146.6	89.5	1.95	9.28	0.611	INH
	13.5-14.5		86.5	48.8	0.73	3.03	0.564	A
	14.5-15.5		115.9	65.2	0.68	3.04	0.563	A
	15.5-16.5		101.6	51.3	0.36	2.52	0.505	A
	16.5-17.5		102.1	55.3	0.62	3.47	0.542	A
	17.5-18.5		90.1	53.1	1.09	4.78	0.589	INH
78	13.5-14.5	291	85.9	42.4	0.40	2.52	0.494	A
	14.5-15.5		113.8	65.3	0.75	3.31	0.574	A
	15.5-16.5		108.7	50.4	0.31	2.72	0.464	A
	16.5-17.5		131.2	68.9	0.95	3.83	0.525	M
	17.5-18.5		127.9	65.4	0.32	2.26	0.511	INL
	18.5-19.5		117.2	68.9	0.48	2.60	0.588	A
	19.5-20.5		135.0	79.0	0.89	3.40	0.585	A
	20.5-21.5		112.5	62.0	0.74	3.39	0.551	A
	21.5-22.5		104.4	52.7	0.20	2.20	0.505	INL
78	13.5-14.5	301	93.4	47.0	0.37	2.44	0.503	INL
	14.5-15.5		137.3	76.2	0.77	3.41	0.555	A
	15.5-16.5		117.3	68.6	1.02	3.74	0.585	INH
	16.5-17.5		146.7	74.2	0.15	2.15	0.506	INL
	17.5-18.5		145.5	102.3	2.32	12.23	0.703	INH
	18.5-19.5		135.1	79.8	2.40	15.84	0.591	INO
	19.5-20.5		118.9	68.0	0.80	3.45	0.572	A
	20.5-21.5		141.3	70.8	0.50	2.66	0.501	A
	21.5-22.5		105.8	57.1	0.65	3.15	0.540	A

TABLE B-4

UP AND DOWN DOPPLER CHANNELS

Ping	Time	Channel	Mean	S.D.	$\sqrt{b_1}$	b_2	S.D./ Mean	Power Plot Target
7	14.5 to 16.0	280	90.0	47.8	0.41	3.01	0.531	
8			89.6	50.1	0.64	3.10	0.559	
9			81.4	48.0	0.93	3.95	0.590	
10			125.4	64.0	0.34	2.70	0.510	
11			98.0	50.1	0.38	2.54	0.511	
12			92.7	52.3	0.72	3.11	0.564	
13			84.9	45.1	0.52	2.64	0.531	
14			88.4	43.3	0.34	2.42	0.490	
15			87.2	46.8	0.53	3.10	0.537	
16			74.2	43.8	0.93	3.76	0.590	
17			98.3	57.5	0.95	3.84	0.585	
7	14.5 to 16.0	320	83.8	44.5	0.76	3.42	0.531	
8			86.7	46.8	0.78	3.86	0.540	
9			75.7	43.2	1.27	5.74	0.571	
10			110.9	62.7	0.46	2.38	0.565	
11			84.9	43.7	0.82	3.68	0.515	
12			86.8	43.9	0.38	2.86	0.506	
13			78.9	38.8	0.37	2.56	0.492	
14			74.2	40.9	0.56	2.90	0.551	
15			84.8	45.2	0.54	3.07	0.533	
16			80.5	42.3	0.67	3.61	0.525	
17			88.7	45.6	0.48	2.64	0.514	
1	16.0 to 17.5	280	52.4	30.8	1.06	4.47	0.588	
2			86.7	47.3	0.69	3.12	0.546	
3			59.3	28.4	0.41	2.57	0.479	
4			75.4	38.8	0.56	2.92	0.515	
5			97.9	46.8	0.68	3.65	0.478	
6			99.4	51.1	0.63	3.31	0.514	
7			91.2	50.4	1.08	4.11	0.553	

TABLE B-4

UP AND DOWN DOPPLER CHANNELS (continued)

Ping	Time	Channel	Mean	S.D.	$\sqrt{b_1}$	b_2	S.D./ Mean	Power Plot Target
8			89.6	43.7	0.74	3.46	0.488	
9			42.1	19.6	0.71	3.39	0.466	
10			98.9	48.2	0.60	3.00	0.487	
1	16 to 17.5	320	51.0	24.3	0.20	2.49	0.476	
2			75.4	39.9	0.41	2.64	0.529	
3			60.4	28.6	0.71	3.78	0.474	
4			68.8	35.7	0.64	3.29	0.519	
5			83.2	45.7	0.72	3.38	0.549	
6			83.8	47.0	0.69	3.12	0.561	
7			82.7	41.2	0.25	2.35	0.498	
8			84.2	47.8	0.84	3.81	0.568	
9			40.3	21.3	0.60	3.12	0.529	
10			93.6	50.6	0.81	3.69	0.541	
78	13.5 to 15	291	87.8	44.9	0.44	2.60	0.511	
78		301	102.9	54.9	0.65	3.18	0.536	
78	15 to 16.5	291	117.8	59.7	0.65	3.39	0.507	
78		301	129.2	75.9	0.94	3.59	0.587	1.00
78	16.5 to 18	291	135.8	67.7	0.66	3.23	0.499	
78		301	162.6	92.4	1.80	11.04	0.568	1.00
78	18 to 19.5	291	115.0	66.7	0.53	2.64	0.58	
78		301	122.4	74.8	2.22	15.45	0.611	1.00
78	19.5 to 21	291	128.5	76.9	0.88	3.41	0.598	
78		301	131.0	73.4	0.71	2.97	0.560	0
78	21 to 22.5	291	106.2	52.4	0.27	2.53	0.493	
78		301	113.0	59.0	0.48	2.66	0.522	
7	14.5 to 16	310	98.6	52.4	0.49	2.79	0.531	
8			101.7	52.7	0.53	3.15	0.518	
9			76.9	45.2	1.01	4.52	0.588	
10			122.4	68.6	0.92	4.16	0.560	
11			96.9	48.9	0.62	2.68	0.505	
12			93.9	46.3	0.23	2.83	0.493	

TABLE B-4

UP AND DOWN DOPPLER CHANNELS (concluded)

Ping	Time	Channel	Mean	S.D.	$\sqrt{b_1}$	b_2	S.D./ Mean	Power Plot Target
13			86.5	43.3	0.52	2.89	0.501	
14			82.3	40.9	0.45	2.23	0.497	
15			89.7	40.8	0.28	2.58	0.455	
16			88.5	44.5	0.70	2.92	0.503	
17			98.4	55.9	0.80	3.18	0.568	
7	14.5 to 16	290	102.8	51.9	0.49	2.39	0.505	
8			104.3	58.2	0.72	3.14	0.558	
9	14.5 to 16	290	82.4	51.5	1.13	4.82	0.625	
10			132.7	73.6	0.42	2.40	0.555	
11			112.6	54.1	0.20	2.43	0.481	
12			92.9	46.5	0.60	3.24	0.501	
13			93.6	48.8	0.64	2.99	0.521	
14			84.5	43.2	0.38	2.58	0.511	
15			89.9	47.1	0.44	2.48	0.524	
16			85.4	43.4	0.89	4.16	0.508	
17			109.7	58.7	0.66	3.03	0.535	
*6-7	14.5 to 16	300	144.0	91.5	0.88	3.53	0.635	
14-15			135.1	66.6	0.74	4.35	0.493	
15-16			130.7	73.2	1.08	5.11	0.560	
16-17			149.6	82.8	1.21	5.24	0.553	
17-18			167.6	107.3	1.16	4.71	0.640	
18-19			179.2	99.1	0.49	2.71	0.553	
25-26			186.9	92.0	0.65	3.01	0.492	
26-27			142.4	79.5	0.55	2.74	0.558	

*May have different scaling

2. Statistical Summary of Analysis of the Sine and Cosine Components of Correlator Output. (Interval 14.5 to 16.0 seconds)

Ping	Ident.	$\bar{y}$	$\bar{x}$	W_y	W_x	V_y	V_x	t_y	t_x	r_{xy}	F
1	1st 50	0.01	0.02	0.977	0.977						
	2nd 50	-0.05	0.04	0.971	0.981						
	3rd 50	0.01	-0.02	0.954	0.979						
	Ent. Inter.					0.41	0.40	-0.18	0.24	0.03	1.04
	Every 3rd	-0.03	0.01	0.952	0.971	0.45	0.47	-0.27	0.12	0.03	0.96
2	1st 50	-0.04	-0.02	0.981	0.955						
	2nd 50	0.00	0.02	0.981	0.976						
	3rd 50	-0.08	-0.05	0.953	0.985						
	Ent. Inter.					0.73	0.72	0.15	-0.22	-0.13	1.02
	Every 3rd	0.09	-0.03	0.966	0.975	0.71	0.62	0.78	-0.30	-0.20	1.14
3	1st 50	-0.01	0.00	0.986	0.986						
	2nd 50	0.05	0.02	0.977	0.988						
	3rd 50	-0.02	0.04	0.984	0.970						
	Ent. Inter.					0.41	0.51	0.17	0.40	-0.03	0.80
	Every 3rd	0.06	-0.07	0.988	0.976	0.44	0.44	0.65	-0.80	-0.01	1.01
4	1st 50	-0.05	0.05	0.974	0.984						
	2nd 50	0.07	0.07	0.982	0.963						
	3rd 50	0.03	-0.05	0.951	0.979						
	Ent. Inter.					0.36	0.40	0.30	0.41	0.04	0.89
	Every 3rd	-0.03	-0.02	0.971	0.978	0.30	0.46	-0.25	-0.25	-0.17	0.66
5	1st 50	0.03	0.07	0.983	0.982						
	2nd 50	-0.01	-0.16	0.984	0.981						
	3rd 50	-0.09	0.10	0.978	0.976						
	Ent. Inter.					0.85	0.80	0.53	0.04	0.11	1.06
	Every 3rd	0.13	-0.03	0.977	0.970	0.63	0.88	1.12	-0.22	0.20	0.72
6	1st 50	0.06	0.09	0.976	0.966						
	2nd 50	0.08	-0.05	0.971	0.962						
	3rd 50	0.12	0.07	0.973	0.979						
	Ent. Inter.					0.85	0.83	1.15	0.46	0.02	1.02
	Every 3rd	-0.06	0.01	0.977	0.961	0.74	0.83	-0.52	0.04	-0.17	0.89

Ping	Ident.	$\bar{y}$	$\bar{x}$	W_y	W_x	V_y	V_x	t_y	t_x	r_{xy}	F
7	1st 50	-0.02	0.07	0.971	0.981						
	2nd 50	0.01	0.01	0.979	0.974						
	3rd 50	0.00	0.06	0.908	0.972						
	Ent.Inter.					0.73	0.66	-0.06	0.71	-0.03	1.09
	Every 3rd	-0.08	0.11	0.938	0.961			-0.69	1.12	0.19	1.62
14	1st 50	-0.03	0.06	0.967	0.971						
	2nd 50	0.00	-0.08	0.975	0.973						
	3rd 50	0.07	-0.02	0.978	0.947						
	Ent.Inter.					0.45	0.76	0.28	-0.17	-0.15	0.60
	Every 3rd	0.13	0.09	0.975	0.959	0.48	0.75	1.32	-0.73	-0.27	0.64
15	1st 50	0.06	-0.02	0.972	0.971						
	2nd 50	-0.09	-0.03	0.976	0.981						
	3rd 50	0.03	0.08	0.981	0.962						
	Ent.Inter.					0.74	0.55	1.03	0.27	-0.21	1.33
	Every 3rd	-0.04	0.04	0.979	0.951	0.66	0.65	-0.32	0.34	-0.19	1.02
16	1st 50	0.06	-0.01	0.982	0.968						
	2nd 50	-0.11	0.02	0.973	0.969						
	3rd 50	-0.06	0.00	0.970	0.976						
	Ent.Inter.					0.59	0.55	-0.51	0.16	0.00	1.07
	Every 3rd	-0.11	-0.03	0.935	0.950	0.45	0.61	-1.13	-0.26	-0.09	0.74
17	1st 50	0.01	-0.06	0.970	0.961						
	2nd 50	-0.03	0.03	0.978	0.965						
	3rd 50	-0.02	-0.12	0.971	0.976						
	Ent.Inter.					0.86	0.83	-0.35	-0.62	0.22	1.04
	Every 3rd	0.11	-0.02	0.977	0.973	0.94	0.64	0.79	-0.17	0.15	1.48
18	1st 50	0.08	0.11	0.972	0.974						
	2nd 50	0.09	-0.07	0.973	0.983						
	3rd 50	-0.14	0.16	0.964	0.981						
	Ent.Inter.					1.15	1.38	-0.69	0.53	0.03	0.83
	Every 3rd	-0.15	0.30	0.952	0.963	1.04	1.45	-1.02	1.72	0.01	0.72

Ping	Ident.	$\bar{y}$	$\bar{x}$	W_y	W_x	V_y	V_x	t_y	t_x	r_{xy}	F
19	1st 50	0.02	-0.07	0.968	0.973						
	2nd 50	-0.14	0.11	0.966	0.967						
	3rd 50	0.07	-0.09	0.964	0.967						
	Ent.Inter.					0.92	1.05	-0.50	0.05	0.08	0.88
	Every 3rd	-0.01	-0.23	0.978	0.974	0.91	0.96	-0.09	-1.64	0.20	0.95
25	1st 50	0.09	0.06	0.993	0.981						
	2nd 50	-0.07	-0.10	0.978	0.972						
	3rd 50	-0.03	0.09	0.977	0.980						
	Ent.Inter.					1.03	1.19	-0.20	0.20	-0.26	0.86
	Every 3rd	0.11	-0.72	0.960	0.974	1.10	1.43	0.73	-0.42	-0.18	0.77
26	1st 50	0.10	0.06	0.967	0.976						
	2nd 50	-0.11	-0.13	0.964	0.975						
	3rd 50	-0.03	0.08	0.963	0.970						
	Ent.Inter.					0.90	0.69	-0.03	0.13	0.02	1.29
	Every 3rd	0.04	-0.03	0.954	0.975	0.94	0.70	0.30	-0.26	0.22	1.34
27	1st 50	-0.01	0.05	0.965	0.967						
	2nd 50	0.05	-0.05	0.978	0.980						
	3rd 50	0.09	0.05	0.981	0.984						
	Ent.Inter.					0.70	0.64	-0.25	0.28	-0.02	1.10
	Every 3rd	0.09	0.00	0.982	0.978	0.54	0.60	0.81	0.00	-0.03	0.90
30	1st 50	0.10	-0.13	0.944	0.980						
	2nd 50	0.07	0.15	0.983	0.976						
	3rd 50	-0.05	0.02	0.966	0.980						
	Ent. Inter.					0.70	0.54	0.55	0.32	-0.07	1.29
	Every 3rd	0.24	0.05	0.968	0.959	0.70	0.60	1.97	0.48	-0.01	1.16

APPENDIX C

BIBLIOGRAPHY

Computer-aided detection is a broad subject embracing a wide range of techniques which have been developed in other contexts and independently. We have, during the course of our work, made reference to many documents, books, and reports. So many, in fact, that any attempt to cite references for many of the ideas presented would be impractical. We have chosen not to reference* the reports in that way but rather to provide an organized bibliography.

The first list is an accession number listing; that is, the items are listed in order by an arbitrarily assigned accession number. This list is also in alphabetic order for authors' last names.

The second list is a Key Word In Context (KWIC) list of the same documents. In this type of list the titles are printed once for each word in the title and then arranged in alphabetic order. A column near the center of the page is used to align the various entries. Authors' names are included in this listing.

The idea behind the KWIC listing is that the words of the title contain subject information and this sort of list is something like a subject catalog. The numbers to the right are the accession numbers mentioned above. In some cases we have taken liberties with the author's idea of the title.

---

* We have made several references to our earlier report in order to avoid the need to reproduce figures and text contained therin.

ACCESSION NUMBER LISTING

1. Computer-Aided Detection Study, Technical Information Series Report R65EMH36, General Electric Company, Syracuse, N.Y., This is a report covering the first four months effort on this contract.

2. Atlantic Basin - I, Introduction, Oceanography & Marine Climate, National Intelligence Survey, NIS 104-1, Nov. 1951, Central Intellegence Agency, Washington, D.C., (Confidential).

3. Wide-Band DIMUS Study, Section V, Advanced Sonar Development, General Electric Company, Syracuse, N.Y., 1965.

4. Ambient Noise Studies, NEL Report 1260, (AD362-504), (Confidential).

5. Aiken, C.D., Becker, P.W., Pfeifer, G.F., Application of Pattern Recognition Techniques To Malfunction Detection via Sonic Analysis, Technical Information Series Report R65ELS18, General Electric Company, June 1965.

6. Akers, S.B., Techniques of Adaptive Decision Making, Technical Information Series Report R65ELS12, General Electric Company, October 1965.

7. Arabadjis, C., An Investigation of Linear Finite Optimum and Frequency Constrained Digital Filters for Random and Deterministic Signals, Technical Information Series Report R62DSD56, General Electric Company, Syracuse, N.Y., Rev. 2.

8. Astemborski, T.J., Linear Discrimination in Statistical Distributions, Technical Information Series Report R62EMH66, General Electric Company, Syracuse, N.Y., December 19, 1962 (Confidential).

9. Astemborski, T.J., Probabilty Distributions in Computer Aided Detection, Technical Information Series Report R63EMH39, General Electric Company, Syracuse, N.Y., December 5, 1963 (Confidential).

10. Astembroski, T.J., Probability Distribution in Computer Aided Detection, Technical Information Series Report R64EMH18, General Electric Company, Syracuse, N.Y., December, 1964 (Confidential).

11. Batchelder, L., "Sonics in the Sea", Proc. IEEE, October, 1965.

12. Bedient, H. A., and Neilon, J. R., Automatic Production of Meteorological Contour Charts, Proceedings 1962 ACM National Conference.

13. Bell, T.J., Cole, B.F., Hay, W.C., Phelps, Jr., H.N., White, Jr., F.S., Five Studies Concerning AN/SQS-26 Equipment and Echo-Ranging Performance (U), USL RPT 725, U.S. Navy Underwater Sound Laboratory, February 10, 1966, (Confidential).

14. Bendat, J.S., Thrall, G.P., Spectra of Nonstationary Random Processes, Technical Report AFFDL-TR-64-198, Measurement Analysis Corporation, March, 1965.

15. Blackman, R.B., and Tukey, J.W., The Measurement of Power Spectra, Dover Publications, Inc., New York, 1958.

16. Brown, R.L., Precision Contour Plots Using a Modified False Position Isolation Scheme, Unpublished Memorandum, January, 1966.

17. Burrington, R.S., May D.C., Jr., Handbook of Probability and Statistics with Tables, Handbook Publishers, Inc., Sandusky, Ohio, 1958.

18. Capon, J., Hilbert Space Methods for Detection Theory and Pattern Recognition, IEEE Transations on Information Theory, April, 1965.

19. Chin, John E., Cook, Charles E., "The Mathematics of Pulse Compression-A Problem in System Analysis," Sperry Engineering Review, October, 1959.

20. Clayden, D.O., Clowes, M.B., and Parks, J.R., "Letter Recognition and the Segmentation of Running Text."

21. Costas, J.P., Computer Simulation Study of the AN/SQS-26 (XN-2) Sonar System, Technical Information Series Report R64EMH22, General Electric Company, Syracuse, N.Y., May 11, 1964 (Confidential).

22. Costas, J.P., Some Notes on Sonar System AN/SQS-26 (XN-2) Sea Data Analysis, Technical Information Series Report R65EMH13, General Electric Company, Syracuse, N.Y., May 21, 1965 (Confidential).

23. Costas, J.P., Medium Constraints on Sonar Design and Performance, Technical Information Series Report R65EMH33, General Electric Company, Syracuse, N.Y., November 2, 1965.

24. Costas, J.P., Bauer, L.W., Computer Analysis of Sonar System AN/SQS-26 (XN-2) Sea Data, Technical Information Series Report R64EMH32, General Electric Company, Syracuse, N.Y., October 29, 1964 (Confidential).

25. David, F.N., Tables of the Correlation Coefficient, issued by the Biometrika Office, University College, London, 1954 (1938).

26. Dayhoff, M.O., A Contour-Map Program for X-Ray Crmstallography, Communications of the ACM, Vol. 6, Number 10, October 1965.

27. D'Ortenzio, Remo J., "Introductory Statistics and Sampling Concepts Applied to Radar Evaluation," RCA Review, March 1964.

28. Donegan, J.H., Dowell, W.B., Constant Variance AGC and Time Constant Effects for the AN/SQS-26 Preformed Beam, Technical Information Series Report R65EMH21, General Electric Company, Syracuse, N.Y., July 21, 1965 (Confidential).

29. Douglas, R.T., Auto Correlation and Power Spectrum (with Automatic Plotting), Program GD* 50-06-2, General Electric Company, Syracuse, N.Y.

30. Fisher, Sir Ronald A., Cornish, E.A., "The Percentile Points of Distributions Having Known Cumulants," Technometrics, May, 1960.

31. Garber, S.M., Deltic Correlators for Signal Reception, Technical Information Series Report R57ELS102, General Electric Company, Syracuse, N.Y., October 14, 1957 (Confidential).

32. Garber, S.M., "Display Systems for Sonars with Large Numbers of Receiving Arrays", General Electric Company, October 28, 1964.

33. Garber, S.M., Response of Correlation Receivers to Distorted Signals, General Electric Company, Syracuse, N.Y.,
Preliminary Results Nov. 9, 1965 (Unpublished Technical Memo.)
Continuing Results Dec. 29, 1965 (Unpublished Technical Memo.)

34. Hahn, G., Reference Notes on Basic Statistics and Probability, Technical Information Series Report 63GL78, General Electric Company, Advanced Technology Laboratories, Schenectady, N.Y., May 29, 1963.

35. Holt, J.F., Auto - And Cross Correlation Function Generator, Program RWACZF (704 SAP), Oct. 20, 1958.

36. Holt, J.F., Power Spectral Density Function, Program RW PS2F, (704 SAP) Nov. 5, 1958.

37. IBM, Catalog of Programs for IBM Data Processing Systems, IBM Systems Reference Library Form C20-8090-3, Sept. 1963.

38. Jacobson, Melvin, J., The Output Probability Distribution of a Correlation Detector with Signal Plus Noise Inputs, Rensselaer Polytechnic Institute, Department of Mathematics, Troy, N.Y., June 1, 1962.

39. Jagger, C.E., and McLaughlin, R.H., An Oscilloscope Technique for Displaying Ambiguity Surfaces, Technical Information Series Report RQ65EE30, Canadian General Electric Company Limited, Toronto, Canada, August 20, 1965.

40. Jagger, C.E., and McLaughlin, R.H., A Compilation of Photographs of Ambiguity Surfaces of Same Short Codes, Technical Information Series Report RQ65EE32, Canadian General Electric Company Limited, Toronto, Canada, August 30, 1965.

41. Johnson, N.L., On an Extension of the Connexion Between Poisson and X^2 Distributions, University College, London.

42. Johnson, N.L., Systems of Frequency Curves Generated by Methods of Translation.

43. Johnson, N.L., An Approximation to the Multinomial Distribution: Some Properties and Applications, University College, London.

44. Johnson, N.L., Welch, B.L., Applications of the Non-Central t-Distribution.

45. Johnson, N.L., and Young, D.H., Some Applications of Two Approximations to the Multinomial Distribution, University College, London.

46. Kenworthy, D.J., PhD, Program to Plot One Line of a Contour Map of a Function of Two Variables, McMaster University, Hamilton, Ontario, May 10, 1966.

47. Kohler, T.P., Hildebrant, H., Statistical Distribution Analyzer, Technical Information Series Report R63EMH32, General Electric Company, Syracuse, N.Y., August 27, 1963.

48. Lavallee, R. L., Effect of Sampling Rate and Smoothing on Output S/N Ratios for Analog and Deltic Correlators, Technical Memo, June 23, 1965.

49. Lavallee, R. L., Effect of Pulse Length on Processing Gain for an Analog Correlator (Sea Data), General Electric Company, Syracuse, N. Y., October 21, 1965 (Technical Memorandum).

50. Le Cam, L., ET. AL., On the Distribution of Sums of Independent Random Variables, University of California, Berkeley, ASTIA AD 627,129, 1965.

51. Litton, Industries Inc., Interim Development Report for Target Recognition by Extraction of Statistical Invariants, Litton Systems, Inc., October 31, 1961 (Confidential).

52. Litton Industries, Inc., "Final Development Report for TRESI (Target Recognition by Extraction of Statistical Invariants)" (Confidential).

53. Lurin, Ely, S., Digital Radar Techniques.

54. Mann, H. B., and Whitney, D. R., "On a Test of Whether One or Two Random Variables is Stochastically Larger than the Other," Annals of Math. Statistics, Ohio State University, 1947.

55. March, H. Wysor, Schulkin M., and Kneale, S. G., "Scattering of Underwater Sound by the Sea Surface," Journal of Acoustical Society of America, Vol. 33, March, 1961.

56. Mason, Robert E., The Digital Approximation of Contours, Journal of the Association for Computing Machinery, Vol. 3, 1956.

57. Mason, S., Flow Chart for a Highly Automatic System, Informal Correspondance, Spring 1966.

58. Mellen, R. H., Doppler Shift of Sonar Backscatter from the Sea Surface, AVCO Marine Electronics Office, JASA - Letter.

59. Monroe, Alfred, J., Digital Processes for Sampled Data Systems, Space Technology Laboratories.

60. Moroney, M.J. Facts From Figures, Penguin Books, A236 First Published 1951.

61. R. Mosher and R. Southworth, Auto-Correlation and Power Spectrum Analysis, Program NY CP1, April 25, 1957.

62. C. Murray, P. Schuls and S. Adams, Computer Aided Detection for the SQS-26 Sonar System, Technical Information Series Report R63EMH30, General Electric Company, Syracuse, N.Y., July 25, 1963 (Confidential).

63. Norris, A.B., A Ray Tracing Program for High Speed Digital Computers, Bell Telephone Labs, Inc., Whippany, N.J., May 7, 1962.

64. Palmieri, Chester A., Radar Waveform Design.

65. Pearson, Egon S., D. Sc., "The Percentage Limits for the Distribution of Range in Samples from a Normal Population (n = 100)."

66. Pine, T.G., A Delay Line Time Compressor (DELTIC) System for Correlation Detection of Sonar Signals, NEL Report 658, February 9, 1956 (Confidential).

67. Pratt, J.R., Laboratory Simulation of Coded Pulse Processing System for AN/SQS-26(XN-2), Technical Information Series Report R64EMH19, General Electric Company, Syracuse, N.Y., July 22, 1964 (Confidential).

68. Price, R. and Hofstetter, E.M., "Bounds on the Volume and Height Distributions of the Ambiguity Function, "IEEE Transactions on Information Theory, 1965.

69. Pryce, R.A., "Computer Programs for the AN/SQS-26 Preselector Evaluation", NEL Report 1247, (Confidential), (AD362-503).

70. Remley, W.R., Doppler Dispersion Effects in Matched Filter Detection and Resolution, Proceedings of the IEEE, January 1966.

71. Roe, G.M. and White, G.M., Probability Density Functions for Correlators with Noisy Reference Signals, General Electric Company, Syracuse, N.Y.

72. Sebestyen, George S., Classification Decisions in Pattern Recognition, MIT, Technical Report 381, April 25, 1960.

73. Shapiro, S.S., Dr., Testing for Distributional Assumptions with Small Samples, Technical Information Series Report 64GL161, General Electric Company, Schenectady, N.Y., October 5, 1964.

74. Shapiro, S.S., Probability Plotting, General Electric Company, Technical Information Series Report R65GL23, February 1, 1965.

75. Sims, W.E. and Bostick, F.S., Jr., An Analysis of Dynamic Power Spectra, EE ResLab, University of Texas, Auxtin, Texas, Report No. 139, December 31, 1965.

76. Southerland, GL and Chaitin, LJ, Computer Routine for Power Spectral Density Analysis by the MEB-PSD Method, Stanford Research Institute, Menlo Park, Calif., Memo Report 8, April 1964, Astia No. AD440-888.

77. Swinnerton-Dyer, H.P F., The Calculation of Power Spectra, COMPUTER JOURNAL, Volume 5, April 1962.

78. Tanner, Wilson P., Jr., and Birdsall, T.G., "Definitions of d' and η as Psychophysical Measures," Journal of Acoustical Society of America, University of Michigan, October, 1958.

79. "Analysis of Signal Processing and Related Topics Pertaining to the AN/SQS-26 Sonar Equipment - A Summary Report, II" October 16, 1964 -- Tracor Report -- (Confidential).

80. "Processing Gain Achievable by Ping-to-ping Integration" October 22, 1964 -- Tracor Report -- (Confidential).

81. "Analysis of Signal Processing and Related Topics Pertaining to the AN/SQS-26 Sonar Equipment - A Summary Report, III" October 11, 1965 -- Tracor Report -- (Confidential).

82. Warr, R.E., Device Clustering, General Electric Company, Technical Information Series Report R65ELS19, February, 1965.

83. White, F.S., Jr., Area Alpha Test Data, Usnusl Letter Ser. 932-071, April 4, 1966 to General Electric Company, Syracuse, N.Y., (Confidential).

84. Wilks, S.S., Mathematical Statistics, Princeton University, 1950.

85. Winfield, D.W., "Time Spreading in One-way Bottom Bounce Transmission Progress Report", General Electric Company, Technical Information Series Report R65EMH34, November 15, 1965 (Confidential).

86. Zetler, B.D., Schuldt, M.D., Whipple, R.W. and Hicks, S.D., "Harmonic Analysis of Tides from Data Randomly Spaced in Time," Journal of Geophysical Research, U.S. Coast & Geodetic Survey, June 15, 1965.

KWIC LISTING

DISPLAY SYSTEMS FOR SONARS WITH MANY	RECEIVING ARRAYS • GARBER,SM	32
DELTIC CORRELATORS FOR SIGNAL	RECEPTION • GARBER,SM	31
ER PFEIFER PATTERN	RECOGNITION FOR MALFUNCTION DETECTION • AIKEN BECK	05
.R. LETTER	RECOGNITION • CLAYDEN,D.O. • CLOWES,M.B. • PARKS,J	20
CLASSIFICATION DECISIONS IN PATTERN	RECOGNITION • SEBESTYEN,GS	72
RT SPACE METHODS FOR DETECTION THEORY AND PATTERN	RECOGNITION HILBE	18
LITY DENSITY FUNCTIONS FOR CORRELATORS WITH NOISY	REF SIGS PROBABI	71
DISPERSION EFFECTS IN MATCHED FILTER DETECTION •	REMLEY,WR DOPPLER	70
TRACOR SUMMARY	REPORT 2, OCT 1964 SQS-26 SIG PROCESSING, ETC	79
TRACOR SUMMARY	REPORT 3, OCT 1965 SQS-26 SIG PROCESSING, ETC	81
INTERIM DEVELOPMENT	REPORT FOR TRESI • LITTON	51
FINAL DEVELOPMENT	REPORT FOR TRESI • LITTON	52
• GARBER,SM	RESPONSE OF CORRELATION RCVRS TO DISTORTED SIGNALS	33
HERLAND COMPUTER	ROUTINE FOR POWER SPECTRAL DENSITY ANALYSIS • SOUT	76
DIGITAL PROCESSES FOR	SAMPLED DATA SYSTEMS • MONROE,AJ	59
DISTRIB. OF RANGE OF	SAMPLES FROM A NORMAL POPULATION • PEARSON,E.S.	65
TESTING FOR DISTRIBUTIONAL ASSUMPTIONS WITH SMALL	SAMPLES • SHAPIRO	73
STATISTICS AND	SAMPLING APPLIED TO RADAR EVALUATION • DEORTENZIO	27
LAVALLEE EFFECT OF	SAMPLING RATE AND SMOOTHING ON CORRELATOR OUTPUT,	48
WAVE	SCATTERING BY IRREGULAR SURFACES • MARSH,H.W.	55
CONTOUR PLOTS USING AN ITERATIVE	SCHEME • BROWN,RL	16
HARMONIC ANALYSIS OF TIDES • ZETLER,BD	SCHULTZ,MB WHIPPLE,RW HICKS,S	88
CAD FOR THE AN/SQS-26 • R63EMH30 • MURRAY,C. •	SCHULS,P. • ADAMS,S.	62
NOTES ON AN/SQS-26(XN-2)	SEA DATA ANALYSIS • COSTAS,JP	22
COMPUTER ANALYSIS OF AN/SQS-26(XN-2)	SEA DATA • COSTAS,JP BAUER,LW	24
SONICS IN THE	SEA • BATCHELDER,L.	11
CLASSIFICATION DECISIONS IN PATTERN RECOGNITION •	SEBESTYEN,GS	72
R DISTRIBUTIONAL ASSUMPTIONS WITH SMALL SAMPLES •	SHAPIRO TESTING FO	73
PROBABILITY PLOTTING • R65GL23 •	SHAPIRO,S.S.	74
DOPPLER	SHIFT OF SURFACE BACKSCATTER • MELLEN,R.H.	58
PHOTOS OF AMBIGUITY SURFACES OF SOME	SHORT CODES • JAGGER MCLAUGHLIN	40
DELTIC CORRELATORS FOR	SIGNAL RECEPTION • GARBER,SM	31
INVESTIGATION OF DIGITAL FILTERS FOR ..	SIGNALS • ARABADJIS,C	07
RESPONSE OF CORRELATION RCVRS TO DISTORTED	SIGNALS • GARBER,SM	33
A DELTIC FOR DETECTION OF SONAR	SIGNALS • PINE,TG	66
DENSITY FUNCTIONS FOR CORRELATORS WITH NOISY REF	SIGS PROBABILITY	71
ANALYSIS OF DYNAMIC POWER SPECTRA •	SIMS,WE BOSTICK,FS	75
TT,JR LAB	SIMULATION OF CODED PROCESSING FOR AN/SQS-26 • PRA	67
P	SIMULATION STUDY OF THE AN/SQS-26(XN-2) • COSTAS,J	21
TESTING FOR DISTRIBUTIONAL ASSUMPTIONS WITH	SMALL SAMPLES • SHAPIRO	73
EFFECT OF SAMPLING RATE AND	SMOOTHING ON CORRELATOR OUTPUT, LAVALLEE	48
A DELTIC FOR DETECTION OF	SONAR SIGNALS • PINE,TG	66
DISPLAY SYSTEMS FOR	SONARS WITH MANY RECEIVING ARRAYS • GARBER,SM	32
	SONICS IN THE SEA • BATCHELDER,L.	11
TER ROUTINE FOR POWER SPECTRAL DENSITY ANALYSIS •	SOUTHERLAND COMPU	76
ORRELATION AND POWER SPECTRUM ANALYSIS • MOSHER,R	SOUTHWORTH,R AUTO-C	61
OGNITION HILBERT	SPACE METHODS FOR DETECTION THEORY AND PATTERN REC	18
COMPUTER ROUTINE FOR POWER	SPECTRAL DENSITY ANALYSIS • SOUTHERLAND	76
POWER	SPECTRAL DENSITY FUNCTION • HOLT,JF	36
T,JS THRALL,GP	SPECTRA OF NONSTATIONARY RANDOM PROCESSES • BRENDA	14
THE MEASUREMENT OF POWER	SPECTRA • BLACKMAN,RB TUKEY,JW	15
ANALYSIS OF DYNAMIC POWER	SPECTRA • SIMS,WE BOSTICK,FS	75
THE CALCULATION OF POWER	SPECTRA • SWINNERTON-DYER,HPF	77
AUTO-CORRELATION AND POWER	SPECTRUM ANALYSIS • MOSHER,R SOUTHWORTH,R	61
AUTO-CORRELATION AND POWER	SPECTRUM • DOUGLAS,RT	29
WINFIELD,DW TIME	SPREADING IN ONE-WAY BOTTOM BOUNCE TRANSMISSION •	85
ET AL THE	SQS-26 AND ITS ECHO-RANGING PERFORMANCE • BELL,TG	13
PROGRAMS FOR AN/	SQS-26 PRESELECTOR EVALUATION • PRYCE,RA	69
LAB SIMULATION OF CODED PROCESSING FOR AN/	SQS-26 • PRATT,JR	67
S. CAD FOR THE AN/	SQS-26 • R63EMH30 • MURRAY,C. • SCHULS,P. • ADAMS,	62
SIMULATION STUDY OF THE AN/	SQS-26(XN-2) • COSTAS,JP	21
NOTES ON AN/	SQS-26(XN-2) SEA DATA ANALYSIS • COSTAS,JP	22
COMPUTER ANALYSIS OF AN/	SQS-26(XN-2) SEA DATA • COSTAS,JP BAUER,LW	24
EBRANDT,H	STATISTICAL DISTRIBUTION ANALYZER • KOHLER,TP HILD	47
LINEAR DISCRIMINATION IN	STATISTICAL DISTRIBUTIONS • ASTEMBORSKI,T.J	09
BASIC	STATISTICS AND PROBABILITY • HAHN,G	34
N • DEORTENZIO	STATISTICS AND SAMPLING APPLIED TO RADAR EVALUATIO	27
MATHEMATICAL	STATISTICS • WILKS,S.S.	84
HANDBOOK OF PROBABILITY AND	STATISTICS WITH TABLES • BURRINGTON,RS	17
AMBIENT NOISE	STUDIES • NEL	04
SIMULATION	STUDY OF THE AN/SQS-26(XN-2) • COSTAS,JP	21
COMPUTER AIDED DETECTION	STUDY	01
WIDE BAND DIMUS	STUDY	03
ETC TRACOR	SUMMARY REPORT 2, OCT 1964 SQS-26 SIG PROCESSING,	79
ETC TRACOR	SUMMARY REPORT 3, OCT 1965 SQS-26 SIG PROCESSING,	81
ON THE DISTRIBUTION OF	SUMS OF INDEPENDENT RANDOM VARIABLES, LECAM,L	50
DOPPLER SHIFT OF	SURFACE BACKSCATTER • MELLEN,R.H.	58
PHOTOS OF AMBIGUITY	SURFACES OF SOME SHORT CODES • JAGGER MCLAUGHLIN	40
OSCILLOSCOPE TECH. FOR DISPLAYING AMBIGUITY	SURFACES • JAGGER,CE	39
WAVE SCATTERING BY IRREGULAR	SURFACES • MARSH,H.W.	55
THE CALCULATION OF POWER SPECTRA •	SWINNERTON-DYER,HPF	77
FLOW CHART FOR HIGHLY AUTOMATED	SYSTEM • MASON,S	57
RBER,SM DISPLAY	SYSTEMS FOR SONARS WITH MANY RECEIVING ARRAYS • GA	32
	SYSTEMS OF FREQUENCY CURVES • JOHNSON,N.L.	42